THE UNIVERSITY OF WARWICK

A TRANSLATIONAL STUDY OF THE MECHANISMS FOR METABOLIC RECOVERY AFTER BARIATRIC SURGICAL INTERVENTION: FROM ADIPOSE MITOCHONDRIA TO PATIENT BENEFIT

By

Lucia Martinez de la Escalera Clapp, R.D.

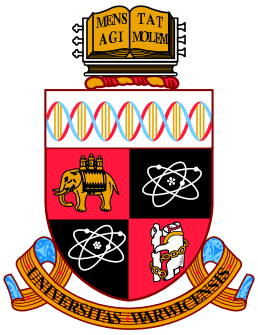

Warwick Medical School

THE UNIVERSITY OF WARWICK

A dissertation submitted for the degree of DOCTOR OF PHILOSOPHY

November 2017

Contents

List of Tables

List of Figures

Acknowledgements

I would like to thank all the patients and staff associated with the study that generously gave their support to achieve the outcomes of this research. In particular I would like to thank Dr. Philip McTernan, Dr. Milan Piya and Dr. Gyanendra Tripathi for their supervision, guidance and support. I would also like to thank to the staff of the Warwickshire Institute for the Study of Diabetes, Endocrinology and Metabolism (WISDEM) at UHCW, for allowing me access to learn about their service, their clinical insight and their patients, without which this research would not have been possible. In particular, I wish to extend my gratitude to Neha Shah (Bariatric Dietitian), Jenny Abraham (Bariatric Nurse), Dr. Milan Piya (Consultant Endocrinologist) and Mr. Vinod Menon (Consultant Surgeon), for their contribution to data gathering and research discussion.

Much of this research was also supported by the EFSD through the New Horizons Collaborative Research Initiative (EFSD New Horizons research grant). I am also extremely grateful to my home country of México, and its National Council for Science and Technology (CONACyT), for the funding and generous opportunity to learn about the obesity crisis accross international borders.

Finally, on a personal note, I wish to thank my family for their love and support. Thank you to my parents and my sister for their encouragement, pep-talks and

advice. To my husband, Nigel, for cleaning the house, and bringing me toasted cheese sandwiches while I worked. Thank you also to my research family: Laura, Alice, Maaike, Sahar, Anoud, Jinus, Farrah, Philip V, Philip M, and Adaikala, for all the research tips, help around the lab, and enjoyable lunch times.

Declaration

All sentences or passages quoted in this project dissertation from other people's work have been specifically acknowledged by clear cross referencing to author, work and page(s). I understand that failure to do this amounts to plagiarism and will be considered grounds for failure in this module and the degree examination as a whole.

This thesis is submitted to the University of Warwick in support of my application for the degree of Doctor of Philosophy. It has been composed by myself and has not been submitted in any previous application for any degree. The work presented (included data generated and data analysis) was carried out by the author, except in the cases outlined below:

All patient data outlined in Chapter 7 was collected between 2011 and 2016 by staff at UHCW Specialist Weight Management Service, in particular Neha Shah (Bariatric Dietitian), Jenny Abraham (Bariatric Nurse), Dr. Milan Piya (Consultant Endocrinologist) and Mr. Vinod Menon (Consultant Surgeon). A full list of staff who participated in the care and data gathering of patients during their treatment is acknowledged by the author and may be found in Apendix 1 (Table 7.5). Ms Alanoud Aladel collated the patient data from the electronic records into a workable database during the auditing process, and the Multidisciplinary

Team at the Warwickshire Institute for the Study of Diabetes, Endocrinology and Metabolism (WISDEM) contributed in the intellectual discussion that allowed the author to frame the research questions.

Parts of this thesis have been published by the author and include the data presented in Chapter 3 and Chapter 4 as follows:

- L. Martinez de la Escalera, I. Kyrou, J. Vrbikova, V. Hainer, P. Sramkova, M. Fried, M. K. Piya, S. Kumar, G. Tripathi, P.G. McTernan. 2017. Impact of gut hormone FGF-19 on type-2 diabetes and mitochondrial recovery in a prospective study of obese diabetic women undergoing bariatric surgery. BMC Medicine. 15(1):34. doi: 10.1186/s12916-017-0797-5.

Other publications:

- X. Ruiz-Herrera, E.A. de los Ríos, J.M. Díaz, R.M. Lerma-Alvarado, L. Martínez de la Escalera, F. López-Barrera, M. Lemini, E. Arnold, G. Martínez de la Escalera, C. Clapp and Y. Macotela. 2016. Prolactin Promotes Adipose Tissue Fitness and Insulin Sensitivity in Obese Males. Endocrinology. Early release DOI: 10.1210/en.2016-1444 **F1000Prime Recommended.

- C. Clapp, L. Martinez de la Escalera, G. Martinez de la Escalera. 2012. Prolactin and blood vessels: A comparative endocrinology perspective. Gen Comp Endocrinol. DOI:10.1016/ j.ygcen.2011.12.033

Name: Lucia Martinez de la Escalera Clapp

Signed:

Date:

Synopsis

The obesity pandemic is one of the greatest challenges facing public health worldwide. With epidemiological projections forecasting only its acceleration, it is clear that the current anti-obesity approach has not been effective. This thesis seeks to outline, through a translational approach, the various reasons for which the obesity crisis continues to grow and to provide further insight into which modifiable factors may contribute to more effective anti-obesity strategies. From the basic science perspective, this thesis investigated through cutting-edge laboratory technology some of the more novel and promising molecular mediators of metabolic recovery (namely gut-hormone FGF-19 and gut-derived bacterial LPS). In particular, this study contributes to a more in-depth understanding of adipose tissue mitochondria, and their role in buffering excess nutrients to maintain systemic metabolic health. From the clinical angle, this thesis explored through clinical audit some of the environmental barriers to metabolic recovery of patients undergoing treatment at a specialist bariatric service of a major NHS hospital. As a result of this translational approach, it was possible for the author to develop a profound appreciation of the complexities involved in developing an effective solution to the obesity crisis, which is rooted in two distinct (and sometimes opposite) concepts: (1) the medical and surgical treatment of obesity, targeting the physiological disorder through pharmacotherapy and/or surgery, and (2) the environmental management of obesity, targeting the dietetic, psychological, socio-economic and political causes through weight management and community development programs, industry regulation and public policy. Though often treated as separate, neither concept need be in conflict with the other. If the objective is truly to develop an effective solution to the obesity crisis, it is paramount to develop a trans-discipline community coordinated approach that addresses not just the cellular targets, but the environmental contributors to obesity.

List of Abbreviations

BMI	Body mass index
BPD	Bilio-pancreatic diversion
COX4I1	Cytochrome c oxidase subunit 4 isoform 1 (Complex IV)
DRP1	Dynamin related protein 1
ECAR	Extra-cellular acidification rate
EWL	Excess weight loss
FCCP	Carbonyl cyanide-p-trifluoromethoxyphenylhydrazone
FGF-19	Fibroblast growth factor 19
FIS1	Mitochondrial fission 1 protein
HbA1c	Glycosylated haemoglobin
HDL	High-density lipoprotein
HOMAIR	Homeostatic assessment model of insulin resistance
IRS1	Insulin receptor substrate 1
LAGB	Laparoscopic adjustable gastric banding
LDL	Low-density lipoprotein
LGCP	Laparoscopic Greater Curvature Plication
LPS	Lipopolysaccharide (bacterial endotoxin)
MFN2	Mitofusin 2
MMP	Mitochondrial membrane potential
mtATP6	mtDNA-encoded ATP synthase subunit 6 (Complex V)
MT-CO1	MtDNA-encoded cytochrome c oxydase subunit 1
mtDNA	Mitochondrial DNA
mtND6	mtDNA-encoded NADH-ubiquinone oxidoreductase chain 6 (Complex II)
OCR	Oxygen consumption rate
OPA1	optic atrophy type 1
PGC1α	Peroxisome proliferator-activated receptor γ coactivator 1 α
POLG	Mitochondrial DNA polymerase gamma
SDHA	Succinate dehydrogenase complex II subunit A
SOD1	Superoxide dismutase 1
SOD2	Superoxide dismutase 2
TFAM	Mitochondrial transcription factor A
TNF-α	Tumor necrosis factor α
UCP2	Uncoupling protein 2
WHR	Waist hip ratio

Chapter 1

Introduction and Aims

1.1 The Obesity Pandemic

Obesity Diagnosis and Classification

The terms "overweight" and "obesity" describe medical conditions characterised by the excess accumulation of body fat endangering health [1]. The most accepted and widespread method for diagnosis in adults is the use of the Body Mass Index (BMI), a ratio of weight-for-height. In adults, a BMI between 25 and $29.9\,\mathrm{Kg/m^2}$ designates the person as overweight, and above $30\,\mathrm{Kg/m^2}$ as obese (Table 1.1). The National Institute for Health and Care Excellence (NICE) recommends the use of BMI in tandem with waist circumference for the diagnosis and risk assessment (Table 1.2) of overweight, obesity, which may help differentiate between those with elevated BMI due to high fat versus muscle mass [1].

Table 1.1: Obesity Classification

Classification	BMI
Underweight	$< 18.5\,\mathrm{Kg/m^2}$
Normal weight	$18.5 - 24.9\,\mathrm{Kg/m^2}$
Overweight	$25.0 - 29.9\,\mathrm{Kg/m^2}$
Obese: Class I	$30.0 - 34.9\,\mathrm{Kg/m^2}$
Obese: Class II	$35.0 - 39.9\,\mathrm{Kg/m^2}$
Obese: Class III	$\geq 40\,\mathrm{Kg/m^2}$

Obesity classification by Body Mass Index (BMI) as defined by NICE Guidelines [1].

For adults with a BMI of $35\,\mathrm{Kg/m^2}$ or over, cardio-vascular disease risks are assumed to be very high with any waist circumference [1].

Table 1.2: Assessment of health risk using BMI and waist circumference

BMI Classification	Waist Circumference		
Men	$< 94\,\mathrm{cm}$	$94 - 102\,\mathrm{cm}$	$> 102\,\mathrm{cm}$
Women	$< 80\,\mathrm{cm}$	$80 - 88\,\mathrm{cm}$	$> 88\,\mathrm{cm}$
Overweight	*No increased risk*	*Increased risk*	*High risk*
Obese	*Increased risk*	*High risk*	*Very high risk*

Health risk assessment by Body Mass Index (BMI) and waist circumference as defined by NICE Guidelines [1].

Obesity Prevalence: Past and Present

The prevalence of obesity world-wide has nearly tripled since 1980 (Figure 1.1). Currently, about 65% of the world´s population reside in countries where obesity and overweight cause more deaths than underweight [2, 3, 4]. My own home country of Mexico (with 33%) is second only to the United States (38%) in adult obesity, and first place world-wide in childhood obesity.

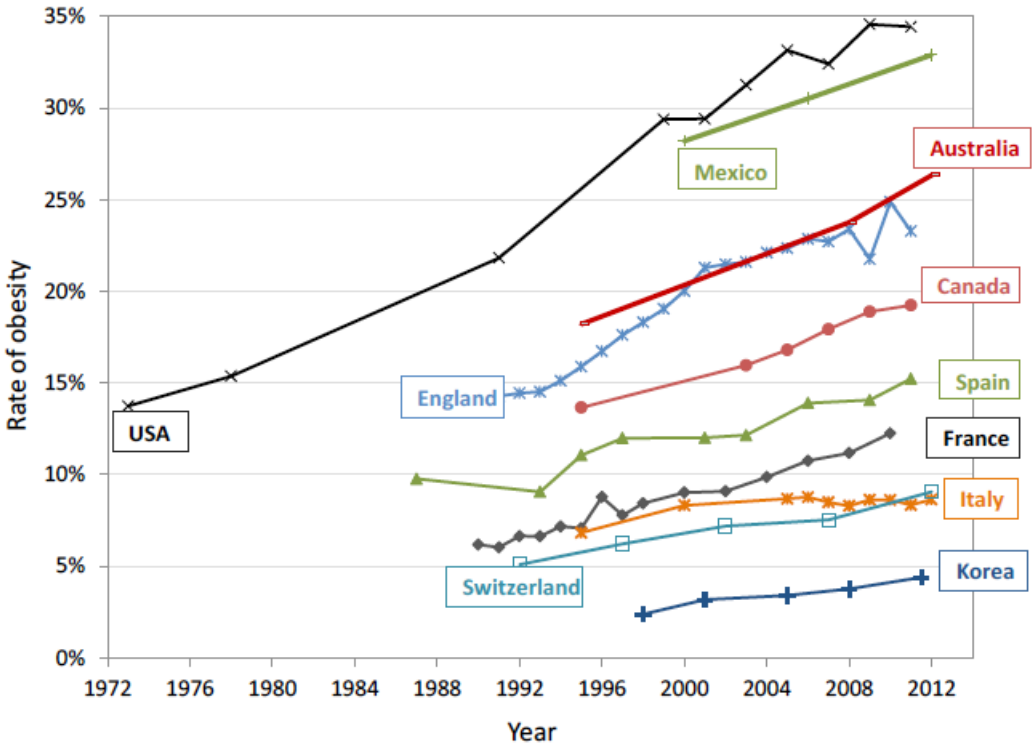

Figure 1.1: Historical trend in obesity prevalence of select countries
From the Organisation for Economic Co-operation and Development ´s(OECD) 2014 Obesity Update [2].

In the UK, 27% of adults are obese and a further 36% are overweight, making it the Western European country with the highest prevalence of obesity (Figure 1.2) [3]. The prevalence of severe obesity (BMI$\geq 40\,^{\mathrm{Kg}}/_{\mathrm{m}^2}$) in the UK has more than tripled since 1993 and is the fastest growing category of obesity [5]. Though severe obesity affected approximately just 2% of men and 4% of women in the UK in 2014, the total medical costs per capita in these severely obese individuals were

approximately 86% greater [5].

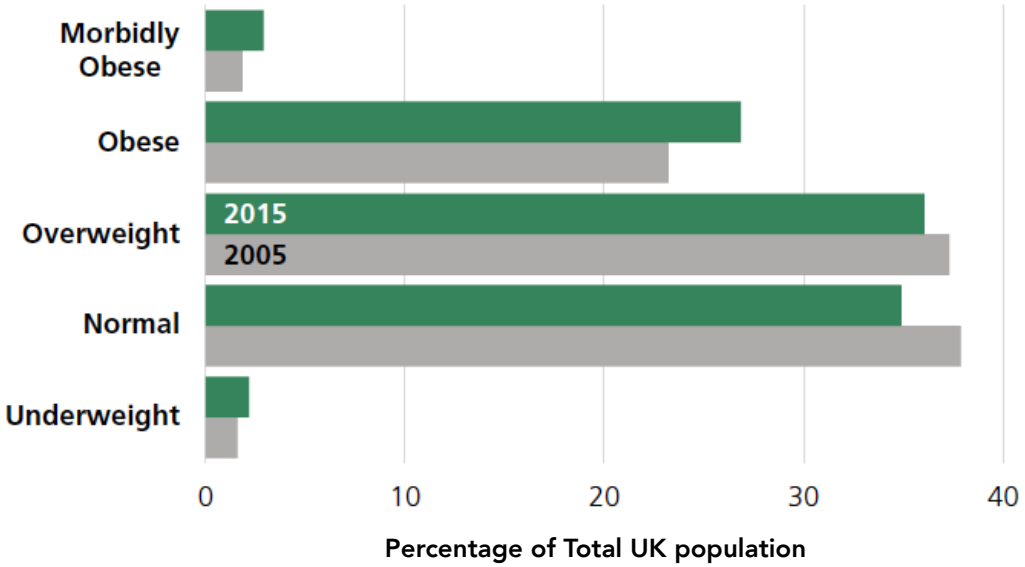

Figure 1.2: UK population distribution by BMI classification in 2005 and 2015
From House of Commons Library Obesity Statistics [6].

Obesity Prevalence: Future Projections

Recent projections, from the OECD analysis of national health survey data, show obesity rates are expected to rise steadily until at least 2030 (Figure 1.3). The United States, Mexico and England are among the countries expected to be the most affected, with 2030 obesity rates projected as 47%, 39% and 35% for each country, respectively [3]. The potential cost of overweight and obesity to the NHS is set to rise from 6.3 billion pounds per year in 2015, to 8.3 billion pounds per year in 2025 and 9.7 billion pounds per year in 2050. If including the cost of obesity-associated comorbidites, this cost is projected to increase from 27 billion pounds per year (in 2015) to 37.2 and 49.9 billion pounds per year in 2025 and 2050, respectively [7].

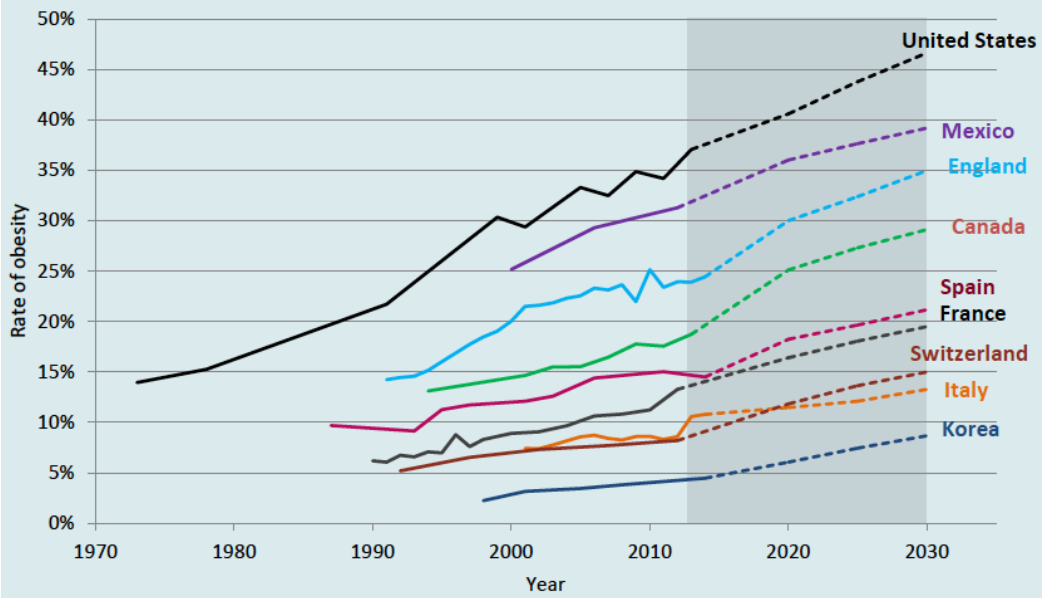

Figure 1.3: Future projected rates of obesity in select countries
From the Organisation for Economic Co-operation and Development ´s(OECD) 2017 Obesity Update [3].

1.2 The Complex Interplay between Biological, Psychological, and Socio-Economic Determinants of Obesity

At first, the cause of obesity can appear simple. As stated by the laws of thermodynamics, body fat accumulation is the net result of an unbalanced energy in, versus energy out equation. This simplistic view, widely held and often portrayed as true by the media and members of the general public, does not reflect the intricacies of what is in fact a complex and multifaceted process. In general, obesity arises from an intricate interplay between biological and environmental factors, which vary from person to person, from group to group and across a person´s lifetime [7]. From the existence of this wide variability in causes, it follows logically that there must also exist a wide array of potential solutions, which target the particular combination of each person and each group´s main barriers to change. Thus, in-depth understanding of the causes is paramount to the correct diagnosis and resolution of obesity. Evidence from the medical, life, social, economic and political sciences have produced a great deal of promising leads, however, these are not generally well integrated across disciplines, and consequently, results from trialled interventions to date have been somewhat underwhelming. In the following sections, the causes of obesity from the perspective of several disciplines are discussed in greater detail.

Causes of Obesity: Genetics and Biology

The environmental conditions throughout the process of human evolution have selected for a biology which is supremely well adapted to contend with prolonged periods of fasting, limited nutrition or even starvation. By bestowing a survival advantage to our ancestors, several (and often redundant) systems have evolved to protect the most vital aspects of our physiology (such as the constant need for energy). The result is a body which actively defends against intentional depletion of energy stores [8, 9, 10, 11]. However, the fast-pace of technological advances means that most of us now live in a drastically altered environment for which we are ill-adapted. For many, there is much interest in modifying these biological targets in such a way that health may be preserved without the need to alter the environmental factors which determine our dietary intake, and/or postpone the inevitable appearance of metabolic disease.

Much effort has gone towards trying to identify the genetics of obesity. Several genome-wide association studies have highlighted a number of genes, which when mutated may cause severe obesity within the first few weeks of life. Other genes, such as variation of the FTO gene, have been shown to contribute to weight gain, though not degree of obesity [12]. Though there is evidence to suggest adiposity is among the most heritable of human traits [13], it not yet clear whether genetic susceptibility to obesity is the result of relatively common polymorphisms with modest (but widespread) effects on risk; or multiple different rare alleles. Despite the somewhat widespread belief that such genetic pre-dispositions may affect metabolic rate or selective conversion of excess calories into fat stores, most monogenic defects associated with human obesity disturb hypothalamic pathways

controlling hunger, satiety and food intake [12]. Critical hormonal, neural pathways and feed-back loops have been identified through such research, which have facilitated a more in-depth understanding of the physiological mechanisms of food choice, weight gain and metabolic disease. Indeed, the current evidence thus far would seem to suggest that from an aetiological standpoint, obesity is more of a neurobehavioural than a metabolic disease [14].

Perhaps one of the better understood examples of molecules involved in regulation of energy intake is the adipokine, leptin [15]. The relevance of leptin was first discovered in *ob/ob* mice which due to mutations in the *ob* gene, exhibited a complete lack of the leptin protein, and were phenotypically severely obese [16]. Treatment of these mice with recombinant leptin corrected their hyperphagia, neuroendocrine and metabolic abnormalities [17]. However, in the general population, leptin levels are low in lean individuals, and heightened alongside increased adipose tissue mass. Its main role is now believed to be the stimulation of food intake when body weight is low, and obese individuals may develop a resistance to its actions [18].

In the modern world, where plentiful, energy-dense, low-cost food is ubiquitous, our intrinsic adaptations for survival must be overridden through conscious control [19, 20, 21, 22]. Recent studies employing functional resonance imaging have demonstrated how sensory factors such as sight, smell, palatability and availability of food can stimulate brain neural networks to the extent that innate control mechanisms are overwhelmed, a phenomenon termed "hedonic" hunger [23, 24].

By contrast, the innate mechanisms of satiety, which communicate to our bodies that we have had enough, are relatively weak, and easily overridden by the sight

or taste of food [25, 26]. For example, it is far easier to skip a meal than it is to avoid tasting (or finishing) a single food once it is put in front of us, despite the fact that we may already be full [25].

On the other side of the energy equation, research into the metabolic aspects of energy expenditure have yielded little to suggest this may be the cause of the rising rates of obesity. Numerous, large sample, multi-national studies have demonstrated that, after adjustment for body size and composition, energy expenditure differs little between individuals [27, 28]. Thus, there is little evidence to suggest the basic physiology of energy expenditure between lean and obese individuals is altered to protect lean individuals against weight gain.

The evidence so far would seem to negate a physiological difference between lean and obese individuals as the primary cause of obesity. Though some causative mutations affecting appetite and satiety have been identified, these have not been present in the majority of obesity cases tested [12]. More limited knowledge is available regarding genetic variants that underlie the susceptibility or resistance of an individual to obesity, and perhaps more interestingly, the interaction between the obesogenic environment and these genetic variants. In this respect, other lines of investigation have begun to show much promise, such as the role of the gut microbiota, gut hormones and the circadian rhythm [29, 30, 31, 32, 33].

Causes of Obesity: Diet and Eating Behaviours

With excessive energy intake being recognised as the primary contributor to weight gain [7, 34], what an individual eats (diet) and the context in which food is consumed (eating behaviour) are critical to the development of obesity.

Measuring dietary intake outside carefully-controlled laboratory conditions remains problematic, but a number of specific dietary risks have been consistently identified. In general, the low intake of fruits and vegetables, and their replacement with ultra-processed energy-dense foods and drinks (which are generally high in fat and/or sugar and low in dietary fibre, vitamins and minerals) are strongly associated with obesity and metabolic disease [35, 36, 37, 38, 39, 40, 41, 42, 43, 44, 45]. Unfortunately, ultra-processed foods are becoming increasingly dominant in the world diet, as cooking and food preparation habits and skills decline [46, 47]. Therefore, the current evidence suggests a healthy diet should limit (and, if possible, exclude) all but traditionally processed foods and snacks; consisting mainly of vegetables, whole grains, legumes and fruit, with limited amounts of meat, eggs and dairy. However, according to the 2013 health survey for England [5], more adults ate fewer than 3 portions of fruit and vegetables a day (45% men and 41% women), than met the recommended 5 portions.

What dictates a persons dietary choices, behaviours and preferences? The current evidence would suggest a number of points in a person´s lifetime, in which there may be critical periods of metabolic plasticity, and/or pivotal habits and attitudes are established. For instance, robust evidence suggests breast-feeding and early growth patterns are important determinants of long-term health [48, 49]. Dietary behaviours (such as preference for fruits and vegetables) are developed early in childhood and resistant to change at a later stage [50]. In young children, the most significant predictor of obesity is parental obesity (risk is increased by 10%)[22]. Even more alarmingly, whilst no amount of exercise has been found to protect against childhood obesity [51, 52, 53], proximity between fast food restau-

rants and schools was observed to be an independent predictor of BMI in children [54]. Also critical is the perimenopausal period, where a significant shift in obesity prevalence demographics is observed (over three quarters of females over the age of 45 presenting with either overweight or obesity) (UK data) [5].

The context in which a food or meal is eaten can also have a significant impact on satiety, negative habit re-enforcement and overall tendency to gain weight. Among the problem eating behaviours most commonly identified by researchers as potential contributors to obesity are: skipping breakfast, grazing, eating past satiety signals, eating when feeling bored, eating when feeling upset, eating as a reward, eating as a hobby, eating quickly, secret eating, chaotic meal patterns, avoiding meals prepared at home, eating before feeling hungry, and eating at night [55]. The characterisation of problem eating behaviours worth targeting in obesity is still at an early stage in research, and is likely to vary substantially between individuals. However, identifying and targeting these behaviours appropriately may be critical to effective obesity interventions.

Causes of Obesity: Mental Health

Higher prevalence of obesity has long been observed in several psychiatric disorders, of which the most thoroughly studied is depression [56]. This association is stronger in women and with increasing severity of obesity [57, 58, 59, 60]. Epidemiological evidence has emerged suggesting that the onset of obesity precedes that of depression in adults, whilst in children and adolescents the opposite is true [61, 62, 63].

Negative attitudes towards obese individuals have persisted even as its prevalence

has become more wide-spread. These anti-obesity biases appear early in life, but have also been uncovered in educational, occupational and health-care settings [64, 65, 66, 67, 68], and even in health professionals who specialise in obesity [69]. Thus, individuals with obesity can often encounter from their surroundings little empathy at best, and outright discrimination at worst. Thus, researchers believe that weight discrimination, encountered more often by women and individuals with higher BMI, may explain the epidemiological observations of depression prevalence in obese population [56]. Other mechanisms, such as health-related quality of life, may also explain the increased risk of depression in individuals with severe obesity [70, 71, 72, 73]. Furthermore, depending on the type of depression presentation, appetite may be either impaired or increased [74, 75], usually remaining consistent within the same person despite wide variability between individuals [76].

Other forms of mental illness have been associated with obesity. Overweight and obesity are much more prevalent in individuals with bipolar disorder (36% and 32%, respectively) than in the general population [77, 78]. A comparison of obese and non-obese individuals with bipolar disorder, highlighted that obese participants had significantly more manic and depressive episodes, and greater severity of depressive symptoms than lean counterparts [79].

The presence of schizophrenia has also been tightly associated with a higher risk of obesity [80, 81]. Schizophrenia is also associated with a 20% shorter life-expectancy, and greater prevalence of obesity co-morbidities such as type-2 diabetes, coronary heart disease, and hypertension [82, 83].

An important factor in the association between metal health and obesity is the use of antipsychotic medication, which have been shown to promote varying degrees

of weight gain, sometimes in as little as 10 weeks [84, 85] and may be linked to disturbances in hunger and satiety, though the precise mechanisms remain poorly understood. Some antidepressant and mood stabilising medications have also been associated with significant weight gain, however this varies substantially with the specific type of medication and further trials are needed [86].

Early childhood trauma resulting from abuse has also been implicated in risk of obesity. A recent meta-analysis reported childhood abuse was clearly associated with obesity as an adult, including a positive dose-response association [87].

Thus, people living with mental illness are particularly vulnerable to the risk of obesity. This relationship is often bidirectional and complex and may be at least in part, mediated by our approach to and compassion for individuals with obesity.

Causes of Obesity: Policy, Socio-economic and Cultural Factors

There is currently a lack of conclusive evidence on how and to what extent our environment encourages the obesity epidemic, however some trends and themes are emerging.

Deprivation and low socio-economic status has a strong positive association with obesity rates [88, 5]. Indeed, children in the most deprived areas of the UK are twice as likely to be obese (where obesity rates are 25%) than children in the least deprived areas (where the obesity rates at year 6 is just 12%) [5].

The amount of household income spent on food has fallen steadily since the 1960s to an average of 10%, but it is worth noting there is a wide divide between lower and higher income households. Whilst higher-income households spend below

15% of their total income on food, this spend exceeds 23% among lower-income households [89, 7]. Importantly, cheaper foods tend to be more calorie-dense, with plentiful fats and sugars and lacking in vitamins and minerals. Data from the USA show that real purchasing costs of fruits and vegetables have increased in relation to fats, oils, starches and sugars (Figure 1.4) [90]. Indeed, a positive linear correlation has been demonstrated between the prevalence of obesity across 21 countries, and the number of hours worked annually [7], though whether this is the result of socio-economic status, less cooking time or higher levels of stress is unclear.

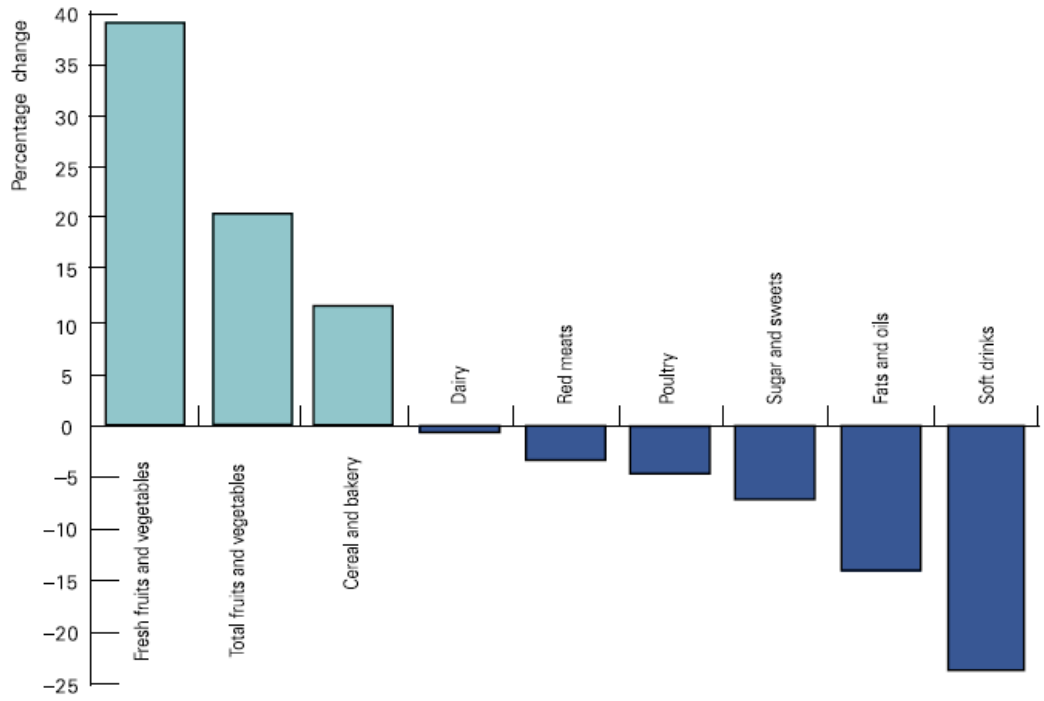

Figure 1.4: Price changes (real dollars) from 1985-2000 differentially affecting dietary components in the USA

Source: Institute of Agriculture and Trade Policy [90]

With lowered costs of non-perishable ingredients, food industry and manufacturers have developed and invested in a large range of processed foods versus raw products, which they can produce at minimal cost and sell at the price of raw

non-processed foods [91, 92]. Supermarket processed foods is one of the fastest growing category of products, particularly if marketed as "healthy" [93]. However, there is poor and lax regulation of the terminology and health benefits these foods are allowed to claim, and the result is often wide confusion and misinformation in the general public as to what is actually "healthy" [94]. Further highlighting a need for stricter regulation and government policy, is the finding that fast food outlets are more common in higher deprivation areas, where the local population have much higher risk of obesity and poor health outcomes [95, 88, 5, 96, 97].

1.3 Effectiveness of Current Obesity Treatments

Exercise Only Interventions

Exercise on its own is often discussed as a weight loss strategy. However, the evidence suggests that exercise unaccompanied by dietary changes is ineffective. A recent meta-analysis of randomised controlled trials attempting exercise-only interventions in children (which included more than 18,000 participants) concluded that no amount of exercise, even in cases where children were exercising more than ten times that of their peers, was protective against childhood obesity [51, 52, 53]. Similar conclusions can be drawn from adult studies which target weight through exercise only. One 11-year study reported that participants exercising more than 150 minutes per week gained 1.8Kg less than their sedentary peers over the period of the study [98]. A thirteen-year nurses´ study reported that in individuals with unhealthy BMI, no amount of exercise prevented weight gain over the period of the study [99]. In a twenty year study of 25,000 male participants and objectively measured exercise, men who exercised the maximum amount (more than 5 hours per week) gained 2.6Kg fewer than men who exercised a minimum of 90 minutes per week [100]. Another study, where participants were enrolled in walking programs but no dietary changes were targeted found that for every 16.9Km walked, participants lost 45g [101], such that it would take 66 to 81 hours of walking to lose 1 Kg of body weight. Thus, the evidence clearly shows that there is no realistically prescribable amount of exercise that will lead to weight loss in the absence of dietary changes.

It should be stated that exercise confers many other health benefits on mobility,

stress and cardiovascular health and should be encouraged in obese and non-obese individuals [102], however the current evidence suggests that exercise can not offset the effects of an obesogenic diet. Thus dietary changes are paramount to effective weight loss interventions.

Dietary and Lifestyle Interventions

Despite extensive research focused on the causes of obesity, research into what constitutes an effective obesity intervention is surprisingly limited. Controlled studies are finite, narrow in scope and confined to laboratory settings [103, 104, 105, 106, 1]. Few interventions have been effective in reducing prevalence of obesity. Though some are promising, they have not yet been reproduced at a larger scale. One such promising example is the Fleurbaix-Laventie Ville-Santé community-based intervention, which targets dietary choices and physical activity in children. It combines both private and public sector initiatives to generate consistent messages on select topics (*i.e.* eating more vegetables, etc...) for a 3 to 4 month duration. The lessons from this program are set to inform a much wider community-based intervention (EPODE) involving more than 130 towns in France, and two each in Belgium, and Spain, though no data is yet available for this program [107]. It is worth noting however, that interventions securing even modest amounts of weight loss have been shown to reduce healthcare costs arising from associated co-morbidities (such as type-2 diabetes) [108, 109, 110]. The North Karelia Project in Finland demonstrated that a comprehensive, determined and community-based programme can have a substantial positive effect on risk factors and eating behaviours, which were associated with favorable changes in chronic disease [111, 112, 113, 114].

Lessons From History

In the recent past, there have been repeated efforts to curb harmful behaviours such as smoking, heavy drinking, drug abuse, and safer driving. The lessons from some of these campaigns may provide valuable insight as to effective behaviour change strategies that may be used to tackle the obesity epidemic [115]. In the case of alcohol consumption and smoking, policy makers moved from basic advice provision, to facilitation of healthier options (such as nicotine patches), to active discouragement of unhealthy behaviour (through taxation, and advertising restrictions) and finally to regulatory action (such as bans on smoking in public areas) [116]. Though there is no doubt that regulation of smoking has been ultimately effective in the protection of public health, under-pressure from major tobacco corporations it took policy makers 50 years to move from evidence of harm to regulatory action [117, 116]. The food industry is no less powerful than the tobacco industry, and unlike smoking, obesity and overweight are being normalised in our society, even as the trends accelerate and the evidence grows, leaving action on diet (such as taxation of sugar-sweetened beverages and policy that would limit added sugar) far behind [94, 118, 119, 91, 120].

Lessons From Social Marketing and Behaviour Change Research

Extensive evidence from social marketing research suggest that public information campaigns instructing people to avoid certain foods, eat more fruit and vegetables, and/or exercise more frequently are unlikely to produce any real effect on the obesity problem [121, 122, 7]. Instead, interventions that go beyond informa-

tion campaigns to simultaneously inform, shift motivation, provide the necessary tools and skills are much more likely to effect meaningful behaviour change [123]. Any approach aimed at influencing behaviour, should be properly tailored to the individual and group´s specific collection of factors contributing to obesity, since evidence suggests that large behaviour change campaigns can have the opposite effect if they are not first properly tested [22].

Research shows that the interaction between the person and their environment is an important determinant of behaviour [124, 125, 126, 127], which means that some environments can make it extremely difficult to effect behaviour change [128, 129]. These studies highlight the extreme and sustained effort required to resist the temptation of the obesogenic environement [130, 131, 132], so perhaps it is not so surprising that interventions targeting individual choices within the same obesogenic environment have not proved effective. Stress [133, 21] and habit formation can further significantly undermine the individual´s ability to resist temptation [134], particularly in the case of eating behaviour [21]. Evidence suggest that people are more susceptible to information and behaviour change at times in which existing habits are temporarily broken (such as after becoming a parent, moving house, starting in a new school, surgical intervention, etc...) [22]. A person´s perception of their own vulnerability to disease (rather than severity of risk) is crucial to whether or not they will change their behaviour. However, research has shown that because people do not want to feel vulnerable, they are more likely to convince themselves that they are not at risk [135, 136], and provision of information is not likely to prove effective under these circumstances. Individuals should be encouraged to reflect and propose their own answers, as self-generated

persuasive arguments have been shown to lead to greater change, however the environmental cues should not be ignored or they will trigger old habits [22].

Bariatric Surgery

Bariatric surgery is currently the most successful treatment for obesity-related T2DM and the metabolic syndrome in morbidly obese patients [137]. Within the first two years after bariatric surgery, morbidly obese patients may often lose 50% of original weight, a figure that remains stable up to 10 years post intervention [138, 139]. Though their BMI will generally remain in the obese category (above 30), their metabolic parameters may be similar to those of lean and healthy individuals [140]. Studies comparing bariatric surgery against dietary interventions have reported that similar improvements to cardio-metabolic risk may be achieved with both [141], however maintenance of weight loss, though a challenge in both, is significantly greater after bariatric intervention [142].

However, studies comparing bariatric surgery against non-surgical programs rarely include non-surgical interventions which target all environmental causes and contributors to obesity (such as diet, stress and environmental triggers)[103, 106], so perhaps this does not necessarily reflect the true potential of non-surgical interventions, and further comparisons between surgery and comprehensive holistic non-surgical interventions are required. However, the need for robust, large-scale, multidisciplinary obesity interventions is unlikely to be met by existing funding pathways [143, 7] and is likely to require unprecedented coordination from partners outside the health sector. To ensure effectiveness, the planning of such interventions must evaluate and aim to target all causes and contributors to obesity

accordingly, either through establishing effective behaviour change strategies, new social norms, a creative and supportive environment, and engagement of community stake-holders [144, 121, 122, 22].

1.4 Provision of Weight Management Services in the UK

The current UK guidelines for treatment of obesity prioritise patients according to BMI and presence of co-morbidities (Table 1.3), the effect of which is that opportunities for meaningful intervention in patients with overweight, obesity class I and even obesity class II (without co-morbidities) are largely ignored. Despite mounting evidence that the primary causes of obesity arise exponentially from the obesogenic environment, current weight management services in the UK mostly target non-environmental causes, by prioritising obesity-associated co-morbidities whilst obese patients are simply told to lose weight. It is critical to the obesity pandemic that treatment is not divorced from prevention.

Table 1.3: UK guidelines for overweight and obesity treatment strategies

BMI Classification	**Waist Circumference**			**Co-morbidities present**
Men	$< 94\,\text{cm}$	$94 - 102\,\text{cm}$	$> 102\,\text{cm}$	
Women	$< 80\,\text{cm}$	$80 - 88\,\text{cm}$	$> 88\,\text{cm}$	
Overweight	1	2	2	3
Obesity I	2	2	2	3
Obesity II	3	3	3	4
Obesity III	4	4	4	4
Tier	**Action**			
1	General advice on healthy weight and lifestyle			
2	Diet and physical activity			
3	Diet and physical activity; consider drugs			
4	Diet and physical activity; consider drugs; consider surgery			

Source: NICE Guidelines [1]

While there are established public-private mechanisms for investment in pharmacotherapy and bariatric surgery, behavioural interventions have, historically, been poorly supported [143, 7]. Perhaps the issue lies in the many competing theories for the "main cause" of obesity, grounded in a range of disciplines (such as

dietetics, sociology, psychology, physiology, and economics) each implying different solutions, which promote both caution and confusion [143]. When combined with the multi-level nature of modern governance, the result is an intricate set of challenges for effective anti-obesity policy. In addition, if policies are developed in isolation, there is a very high likelihood that potential beneficial results from one initiative may be undermined by the well-intentioned, though opposite actions of another. Thus, there is great need for a unified, trans-discipline effort to determine and prioritise which determinants of obesity to target, and which strategies to use with reference to the evidence. As the evidence points overwhelmingly away from personal responsibility and towards the obesogenic environment [143, 7], it is illogical to continue to discuss and target the obesity crisis through person´s choices without addressing their environmental context. Attention should be refocused towards addressing the environmental contributors of obesity (such as the food industry, marketing, mental health, socio-economic deprivation and stress), and weight management interventions adequately funded to address both prevention and treatment of co-morbidities.

1.5 The Pathophysiology of Metabolic Disease

Obesity is the fourth largest risk factor for deaths in the UK (after hypertension, smoking, and high cholesterol) [5]. For individuals who fall within the obese category, the risk of disease increases sharply with BMI. With increasing body mass index (BMI), a measure of weight relative to height, there is also increasing prevalence of metabolic morbidities such as insulin resistance, type 2 Diabetes Mellitus (T2DM), hypertension, dyslipidaemia, ischaemic stroke and coronary heart disease [145, 146]. Additionally, strong associations have been observed between increasing BMI and several types of cancers such as breast, colon, kidney and pancreas [147, 148]. T2DM, ischaemic heart disease, stroke and cancer are all within the top 10 causes of death worldwide. The global average of healthcare costs for type-2 diabetes alone are projected to increase by 30-34% from 2010 to 2030, though it could be as much as 67% in developing nations [149]. Given the alarming scale of this issue, precise understanding of key cellular and systemic processes underlying adipose tissue biology and obesity-related metabolic disease are of outstanding importance.

Relevance of White Adipose Tissue in the Initiation of Metabolic Disease

Under conditions of chronic hyper-caloric supply, white adipose tissue may not be able to cope with the high demand for lipid storage, resulting in increased circulating free fatty acids and accumulation of lipotoxic metabolites such as diacylglicerol, ceramides and long-chain fatty acyl-CoA in adipose and non-adipose tissues [150].

Lipotoxic metabolites lead to direct inhibition of insulin signaling through serine phosphorylation of insulin receptor substrate (IRS) proteins and activation of inflammatory pathways [151, 152]. Further evidence to suggest cardio-metabolic disease arises from lipotoxicity can be observed in genetic conditions such as familial combined hyperlipidaemia where defects in chylomicron lipid uptake and lipolysis in white adipose tissue result in increased circulating lipid and ectopic fat deposition in organs other than white adipose tissue. Although these individuals´ BMIs are usually normal, they are insulin resistant and at high risk of cardiovascular disease [153, 154].

Within white adipose´s adaptive response to increase its lipid storage capabilities, adipogenesis is thought to play an important role, allowing white adipose tissue to grow in adipocyte number (hyperplasia) and thus store lipids innocuously in the form of triglycerides. When the pressure for increased lipid storage exceeds the adipogenic capacity of the tissue, lipid accumulates in existing adipocytes, causing them to swell (hypertrophy), develop abnormalities in lipid handling (lipotoxicity) and eventually leads to apoptosis. In both visceral and subcutaneous WATs, larger adipocyte diameter (hypertrophy) positively associates with inflammation and cardio-metabolic disease [155, 156]. Interestingly, a recent *in vitro* study showed that increased mitochondrial activity is necessary for differentiation of human preadipocytes [157], implicating mitochondria in white adipose tissue dysfunction and cardio-metabolic risk.

Apoptosis in itself is another factor that may contribute to adipose tissue dysfunction by reducing white adipose tissue mass and therefore its capacity to adequately buffer lipids. Moreover, widespread adipocyte apoptosis releases a variety of lipo-

toxic metabolites that trigger a local inflammatory response, which can directly hinder insulin sensitivity. Indeed, increased white adipose tissue apoptosis has long been observed in association with obesity and cardio-metabolic disease risk [158], though the trigger to adipocyte apoptosis itself has not yet been determined. Interestingly, mitochondria have been shown to play a signaling role in certain types of apoptosis, which are age-related and increased mitochondria-mediated apoptosis associate with higher percentage of pro-apoptotic cells in skeletal muscle [159, 160, 161].

Moreover, distribution of white adipose tissue in addition to its lipid-handling capacity is a major factor in determining cardio-metabolic risk. Lipodystrophic syndromes highlight this fact, as in these individuals loss of gluteo-femoral or subcutaneous fat (causing increased lipid deposition in visceral white adipose tissue) results in worsening metabolic and cardiovascular risk parameters [162, 163]. Although the reason behind this risk disparity remains under debate, evidence suggests this could be partially explained through tendency for inflammation. While subcutaneous white adipose tissue has higher lipid handling capacity [164, 165], visceral white adipose tissue has a high supply of innate immune cells that allow it to play a largely mechanical and protective role against external inflammatory stimuli [166]. These resident innate immune cells in visceral white adipose tissue of normal BMI and metabolically "healthy" obese individuals are mainly M2 macrophages that secrete anti-inflammatory molecules (such as IL-10 and IL-4) and serve a primarily antigen presenting role [167]. However, with increased adipocyte apoptosis, the macrophage population distribute in the tissue forming crown-like structures (CLS) and adopt an M1 phenotype, capable of secreting pro-inflammatory molecules like

IL1-ß, TNF-α and IL-6 [168, 169]. The combination of CLS, apoptotic adipocytes and circulating inflammatory cytokines during obesity are strongly associated with cardio-metabolic risk [168, 158, 170]. Interestingly, adipose tissue depot-specific differences in mitochondrial number and respiration have been identified, implicating mitochondrial functionality in cardio-metabolic risk [171].

Collectively, the evidence set out above highlights the potential role of mitochondrial alterations in adipose tissue dysfunction and the pathogenesis of obesity-associated insulin resistance and cardio-metabolic disease. In the following section, these mitochondrial alterations are examined in more detail.

1.6 Emerging Concepts in the Mechanism for Metabolic Recovery After Bariatric Surgery

Success of surgery varies from one individual to another, depending on surgical procedure, commitment to dietary and lifestyle changes, length of T2DM and metabolic disease prior to surgery, age, gender and genetics [172, 173]. However, the profound and consistent nature of weight loss following bariatric surgery was elegantly demonstrated by the Swedish Obese Subjects (SOS) trial [174], the first prospective controlled bariatric surgery intervention study and provides an instrumental opportunity to study mechanisms of metabolic health and disease. The most common surgical procedures (Figure 1.5) include:

- Laparoscopic adjustable gastric banding (LAGB): restricting the stomach using an adjustable silicone band.
- Vertical sleeve gastrectomy (VSG)/ laparoscopic greater curvature plication (LGCP): creating a smaller gastric pouch
- Bilio-pancreatic diversion (BPD): connecting the distal part of the small intestine to the ventricle, bypassing the duodenum and jejunum
- Roux-en-Y gastric bypass (RYGB): creating a smaller gastric pouch and connecting it to the distal end of the jejunum.

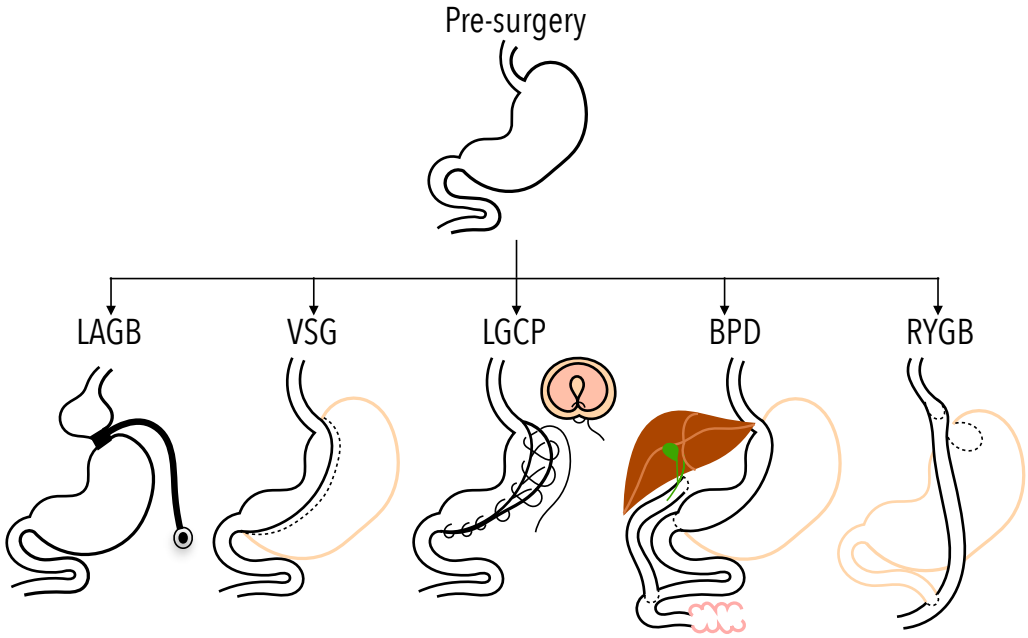

Figure 1.5: Schematics of the main types of bariatric procedures

Several In LAGB, an inflatable silicon device is wrapped around the top portion of the stomach, reducing the gastric volume which can later be adjusted in the clinic with minor invasion. In VSG, the stomach is reshaped into a tubular-like sleeve. In LGCP, the stomach is folded inward and stitched at the fold to reduce the gastric volume in a similar degree to VSG. In BPD, a VSG is performed after which the stomach is then connected to the jejunum and the duodenum to the lower part of the small intestine. In RYGB, a small gastric pouch is directly connected to the jejunum, bypassing the rest of the stomach and the duodenum.

In terms of fat loss and diabetes resolution, BPD and RYGB (which include a malabsorption component through bypass of a considerable amount of the small intestine) confer the greatest long-term improvement [137, 139, 138], but carry greater risks and side effects [175, 176]. Interestingly, patients who have undergone BPD and RYGB exhibit a pronounced improvement in diabetes within the first few days post surgery, which cannot be explained by the energy restriction or fat loss alone [177]. Thus, metabolic improvements observed post bariatric surgery are not just the result of energy restriction and malabsorption-associated fat loss, but likely involve other elements including signaling factors in the small intestine.

In the past, an overwhelming focus of those studying the mechanism of metabolic

recovery following bariatric surgery has been to examine these short-term weight-independent mechanisms, without sufficient focus on how the surgery generates weight loss in the first place. Two main hypotheses for the mechanism of metabolic improvement following bariatric surgery have been proposed: (a) the hindgut hypothesis suggests that enhanced delivery of nutrients to the small intestine trigger secretion of hindgut signals with beneficial effects on glucose homeostasis, whilst (b) the foregut hypothesis states that post-surgical metabolic improvement is the result of altered signals from the excluded segment of proximal intestine. Evidence continues to emerge that would support both possibilities, as well as several others, whilst highlighting deeper levels of complexity [178, 176, 179, 180, 181, 182]. In terms of the long-term effects of surgery however, weight loss has consistently remained as one of the main contributing factors to the metabolic advantages conferred by bariatric surgery [179].

Regulation of Energy Balance

Like many other key necessities for functional life such as temperature, blood pressure, electrolytes and glycaemia, energy stores are very carefully regulated. The complex genes-environment interaction throughout evolution has selected for highly effective processes that defend against loss of energy stores. Body fat is actively defended physiologically during periods of intentional weight loss [20], through sustained reduction of energy expenditure (resulting from loss of lean muscle) [10], more efficient muscle metabolism [9], reductions in thyroid and sympathetic activity [8], and reduced non-resting metabolic rate [11]. On the other side of the energy equation, hunger hormones (known to reduce satiation and sati-

ety) adapt to weight loss in a manner that will encourage weight regain. Diet and exercise-led weight loss efforts result in sustained reductions of leptin, insulin, peptide YY, cholecystokinin, and amylin; whilst levels of ghrelin, and pancreatic polypeptide increase. These changes are associated with elevated measures of subjective appetite [19], and altered neural activity in response to food cues in brain areas controlling enteric regulation, emotional, decision, executive functions and perception systems [11]. Following surgical weight loss, however, hunger is reduced and cognitive restraint is increased. Therefore, the most striking result of bariatric surgery, is its capacity to produce weight loss without triggering the weight-defense mechanisms that result with non-surgical means, ensuring greater probability that weight loss will be maintained.

Restriction and Malabsorption

The once popular hypotheses of food restriction and malabsorption as the main mechanisms of post-surgical weight loss have now been largely abandoned. Since the 1980s, studies have consistently confirmed that gastric-only procedures do not delay the transit of food within the foregut, and satiety signals generated with such procedures do not correspond with food transit time. Moreover, no evidence has been found that any of the most commonly performed procedures (RYGB, VSG, LAGB), with the exception of BPD, produce significant macronutrient malabsorption in sufficient amounts to influence the energy equation [183].

Gastro-Intestinal Mechanoreceptors

There is strong evidence to suggest that subtle adjustments in gastric pressure can influence satiety. A double blinded, randomised controlled trial of individuals with gastric bands, either correctly adjusted or empty demonstrated this concept. Individuals with correctly adjusted bands were less hungry, more satisfied after a meal, and satiated for longer than those whose bands were empty [184]. Neither GI hormones nor gastric emptying rate were affected by these minor mechanical adjustments, which despite this may clearly have a significant effect on weight loss.

Hormonal Changes

Insulin and the adipokines Leptin, and adiponectin, all follow the same pattern of change as with non-surgical weight loss [69, 176], and thus are unlikely to explain the enhanced effects of surgery on metabolic health. The L-cell hormones glucagon-like peptide 1 (GLP-1) and peptide YY (PYY), which reportedly deliver a rapid incretin and satiety response have been shown to increase after RYGB, BPD and VSG surgeries [185, 186]. However their contribution to weight loss efficacy of bariatric procedures remain uncertain [182]. Similarly, initial reports of the hunger hormone Ghrelin garnered much attention, as it was shown to be markedly reduced with surgery versus lifestyle weight loss interventions, however several lines of preclinical and clinical research have thrown doubt on its impact in sustained weight loss [187, 188, 189].

Bile Acid Handling

Primary bile acids are synthesised from cholesterol in the liver, stored in the gall-bladder, and secreted in the second part of the duodenum in response to a meal. They are then actively and passively absorbed in the terminal ileum and recycled via the portal vein to be secreted again (a cycle which can be completed several times a day). The nuclear farsenoid receptor X (FXR) is the primary regulator of the bile acid cycle, and may also influence hepatic effects on glucose tolerance by inhibiting gluconeogenesis, improving insulin secretion and sensitivity, and up-regulating glycogen synthesis. Bile acids may also improve glucose tolerance and satiety through intestinal stimulation of cell surface G protein-coupled bile acid receptor 5 (TGR5) and GLP-1 secretion from L-cells [190].

In humans, bile acid levels fluctuate between feeding and fasting, with robust differences detected between healthy insulin-sensitive individuals and those with type-2 diabetes [191]. Furthermore, bile acid levels are increased after RYGB, and VSG but not LAGB procedures [190]. Increased secretion of gut hormone FGF-19 (stimulated by bile acid reabsorption in the terminal ileum) is seen within days of surgery, and may be involved in increased GLP-1 and PYY secretion, improved glycaemia, and weight loss [31].

The Gastro-Intestinal Microbiome

The recent finding that fecal transplantation from bariatric subjects to germ-free animals can reproduce weight loss and mimic post-surgical metabolic improvements is extremely promising and indicative of a crucial relationship between the microbiota and metabolic disease [192]. The composition of the GI microbiome is

enormously complex, though surprisingly stable in the individual. Germ-free mice transplanted with human microbial communities were stably and heritably colonized, reproducing much of the human donor´s bacterial diversity. Mice who were then subsequently fed a high-fat, high-sugar "Western" diet had increased adiposity, a trait that was transmissible to other mice through microbiota transplantation [30]. Though true understanding of the microbiota´s role in altering metabolic and appetite signaling pathways is in a very early stage, these results are nevertheless compelling evidence of a potential physiological mechanism controlling obesity which is both related to poor diet and intrinsic to individuals with obesity.

One promising avenue for further research in this subject are gut-derived bacterial Lipopolysaccharide (LPS), also known as endotoxin, which are outer cell membrane fragments from Gram-negative bacteria, whose gut populations are encouraged by a Western diet. Due to their chemical affinity, LPS are absorbed and distributed alongside dietary fats inside chylomicrons, with circulating LPS concentrations rising in a direct proportion to dietary fats or in combination with saturated fat, high-fat or high carbohydrate meals [193, 194]. Once in circulation, LPS stimulates the innate inflammatory response in adipose tissue, and release of pro-inflammatory cytokines through the activation of TLRs and the IKK/NFkB pathway [195, 196]. As chronic, low-grade inflammation is a risk factor for the development of metabolic dysfunction [197], many studies have focused on LPS within this context. In an animal model LPS was shown to initiate obesity and insulin resistance [198], and in humans serum LPS may function as a predictive biomarker for obesity-related metabolic disease [199, 200, 201, 202].

Under normal conditions, only small amounts of LPS from gut bacteria enter the

circulation bound to dietary lipids and chylomicrons (low density lipoproteins to which they have high affinity), and are quickly eliminated by monocytes, particularly liver-resident Kupffer cells. In this way, circulating levels of LPS are dependent on dietary lipid intake and liver functionality, both of which may be altered during obesity [203]. Indeed, studies indicate that as little as one high-fat meal is sufficient to raise serum LPS levels, especially in metabolically compromised subjects and in a manner that is directly proportional to degree of insulin resistance [204]. Subjects with T2DM are reported to have higher circulating LPS levels than lean, healthy individuals [196]. Thus, meal patterns and insulin resistance can alter serum LPS, contribute to systemic inflammation and cardio-metabolic disease.

Bariatric surgery, which results in substantial weight loss and T2DM remission through gastro-intestinal remodeling, may inhibit the intestinal absorption of LPS. Indeed, in one study, RYGB was shown to decrease endotoxaemia and accompanying oxidative and inflammatory stress along with improvements of cardio-metabolic risk parameters [205]. However, the contribution of LPS to metabolic recovery following bariatric surgery remains unknown.

Portal Vein Nutrient Sensing

Neural receptors in the wall of the portal vein sense dietary protein and soluble fibre and modulate intestinal gluconeogenesis [206, 207, 208], which may influence energy and glucose homeostasis, hunger, satiety and insulin sensitivity. Glucose sensing in the portal vein influences a range of central cortical, hedonic and homeostatic regions that control food choice, and satiety [209]. Indeed, specific portal denervation in rats, resulted increased glycaemia, glucagon-like peptide 1 (GLP-1)

and insulin secretion, and reduced insulin sensitivity [210]. However, human data for a role of portal vein nutrient sensing in metabolic recovery is limited [211].

Food Preference

All effective bariatric surgeries result in reduced caloric intake through limiting hunger, improving satiation and satiety and altering food choice. However, specific food choice patterns vary with the type of surgical procedure performed. Patients who undergo LAGB typically avoid bread, pasta, and sticky rice which may generate obstructive symptoms and prefer easily digestible protein and vegetables [212, 213], whilst RYGB patients report limiting their intake of sweet and fatty foods which can cause dumping syndrome and possibly replace these with vegetables [181]. Functional MRI scans of post-surgical patients often report reduced activation of reward pathways to energy dense foods [180]. The evidence would suggest that changes in food preference involve sensory, reward and physiological taste alterations [214, 215], however the anatomical or physiological mechanisms responsible remain unknown.

1.7 The Emerging Relevance of Adipose Mitochondrial Function in the Pathophysiology of Metabolic Disease

Normal mitochondrial action is essential for maintaining physiological cellular function. Not just the main powerhouse of the cell, mitochondria are charged with many vital activities such as reactive oxygen species (ROS) production and detoxification, regulation of mitochondrial matrix and cytoplasmic calcium, metabolites synthesis and catabolism, organelle transport, some types of apoptosis, nutrient oxidation and ATP production [216]. In most instances, mitochondrial dysfunction is described as inefficient and/or insufficient ATP production [217], however an abnormality in any mitochondrial function can be termed mitochondrial dysfunction, and has the potential to produce severe metabolic alterations and contribute to insulin resistance.

The primary role of mitochondria is energy production in the form of ATP. In general terms, energy production in eukaryotic cells (primarily in the form of ATP) occurs in the mitochondrion through oxidative phosphorylation (OXPHOS) or the electron transport chain (ETC) which is comprised of several inter-membrane proteins (complex I, II, III, IV and ATP synthase) located in the inner mitochondrial membrane. In this process, reducing agents NADH and $FADH_2$ (generated from previous pathways such as glycolysis, kerb's cycle and fatty acid beta-oxidation) are oxidized to NAD and FAD, generating electrons, which are carried over from complex I of the ETC to II and so on to IV and O_2, generating H_2O. In parallel to this, protons are pumped from the matrix through to the inter-membrane space

to produce an electrochemical gradient that will become the driving force for the ATP synthase complex to produce ATP from ADP [152].

Inter-membrane proteins known as uncoupling proteins (UCPs) play an important role in lowering this electrochemical gradient, either by utilizing it to produce heat (as in the case of UCP1 in brown adipose tissue) or by facilitating proton leak to prevent excess ROS formation (UCP2 and 3). The latter is particularly relevant when there is an excess supply of electrons and low oxygen utilization (high nutrient supply and low energy demand), as the ETC complexes become saturated with electrons and excess electrons are instead pumped directly to oxygen, generating ROS. UCP2 and 3 function to reduce ROS over-accumulation by allowing excess protons to re-enter the matrix, thereby lowering the electrochemical gradient and preventing further ROS production [218, 219, 220].

Increased ROS production and reduced expression of antioxidant enzymes have long been observed in obese and type-2 diabetic patients [221, 222, 223, 224]. As ROS are extremely unstable molecules with the potential to react and alter lipids, protein and DNA leading to increased mutagenesis, inflammatory processes, decreased biogenesis [152] and further mitochondrial dysfunction, prevention of ROS overproduction is a vital matter. Indeed, ROS have been implicated in insulin resistance through activation of IκB kinase ß (IKK-ß) and various other serine kinases [225, 226, 152]. As mitochondria are the primary source of ROS within the cell, this may be a potential mechanistic link between mitochondrial dysfunction with type-2 diabetes. In support of this concept, over-expression of UCP2 or 3 *in vitro* results in lower ROS levels and enhanced metabolic rate, both protective factors against weight gain and insulin resistance [227, 228]. Conversely, UCP3

knockout mice exhibit severe oxidative damage [229]. Antioxidants, such as α-lipoic acid have been shown to oppose ROS-induced insulin resistance [230] and pharmacological compounds such as metformin [231, 232] and thiazolidinediones [233] may also improve mitochondrial function by reducing mitochondrial ROS production and stimulating biogenesis.

Mitochondrial biogenesis is the process through which old mitochondria merge (become larger through fusion) and divide (become smaller through fission) to produce new mitochondria, conserving functional and disposing of faulty mitochondrial DNA. This process is coordinated by the peroxisome proliferator-activated receptor (PPAR) co-activator 1 alpha (PGC1α) through co-activation of nuclear respiratory factor 1 (NRF-1), which in turn regulates the expression of DNA polymerase (POLG) and mitochondrial transcription factor A (TFAM) and OXPHOS genes, necessary for mitochondrial gene expression and replication [234, 220, 235]. Adequate execution of mitochondrial biogenesis protects mitochondrial DNA quality and function.

Faults in this process (which may occur in conditions of high oxidative stress and inflammation) can generate mutations in the mitochondrial genome, reduce number of mitochondria, impair oxidative capacity, further increase ROS production and adversely impact general mitochondrial function and insulin signaling [152, 236]. Indeed, inhibition of obesity-induced mitochondrial fission, rescues insulin resistance through increased p38 MAP kinase-associated IRS-1 and Akt activation [237]. Accumulation of high levels of ROS activates stress kinases [223] and pro-inflammatory signaling, which result in the inactivation of IRS proteins by their phosphorylation at serine residues [225, 226, 152]. Finally, reduced lipid oxidation

through impaired ß-oxidation results in increased intracellular build-up of lipotoxic molecules such as diacylglycerol and ceramides which stimulate pro-inflammatory signaling and directly alter insulin action [238, 239, 240, 241, 242]. Thus, mitochondrial dysfunction, through altered mitochondrial biogenesis, increased ROS production and decreased fatty acid oxidation, is a potential mechanistic link between obesity and insulin resistance.

Mitochondrial dysfunction correlates with cardiovascular risk factors such as age, physical inactivity and caloric excess. Muscle mitochondria of obese and T2DM patients have decreased mitochondrial respiration capacity, beta-oxidation, ATP production, and increased lipotoxic species and ROS, which associate with insulin resistance [217, 243, 244]. Altered mitochondrial number and morphology have also been observed in skeletal muscle and adipose tissue of obese and T2DM patients [245, 225, 246]. Moreover, pharmacological and lifestyle interventions that improve mitochondrial function also improve insulin resistance [152].

In addition to evidence that mitochondrial dysfunction may contribute to insulin resistance, there is also evidence to suggest that insulin resistance itself may contribute to mitochondrial dysfunction. One study in particular showed that, while stimulating skeletal muscle of healthy lean individuals with insulin results in increased synthesis of mitochondrial gene transcripts and proteins, the same actions on muscle from T2DM subjects produces a diminished response [247].

There are several factors known to alter PGC1α expression and by extension mitochondrial biogenesis, quality control and function such as: age, exercise, fasting and insulin, all acting in a tissue-specific manner [248, 249, 250] (Figure1.6). Indeed, factors causing increase of cellular ATP demand, such as in the case of

exercise, fasting and cold exposure have been linked with increased AMP-activated protein kinase (AMPK) and PGC1α expression [251, 252, 253, 254]. In contrast, age, insulin resistance and T2DM are associated with reduced levels of PGC1α expression [248, 255]. Pharmacological (metformin) [232, 231, 256] and lifestyle interventions (exercise [257, 258] and caloric restriction [259, 260]) that improve insulin sensitivity also stimulate mitochondrial biogenesis. Moreover, PGC1α can alter intrinsic properties of the mitochondria by elevating the expression of ROS-detoxifying enzymes like superoxide dismutase 2 (SOD2) [261] and increasing mitochondrial oxidative capacity through enhanced expression of enzymes involved in ß-oxidation, the citric acid cycle and the electron transport chain [262, 250, 263]. Thus, factors that determine cardiovascular risk are also closely involved in mitochondrial function through regulation of PGC1α.

Though several studies have highlighted a link between mitochondrial dysfunction and insulin resistance in skeletal muscle and other metabolic regulatory tissues, the contribution of mitochondria to adipose tissue dysfunction and insulin resistance is still unknown. Indeed, there is little knowledge on obesity-induced mitochondrial alterations in WAT and whether any mitochondrial alterations may be reversed via bariatric surgery.

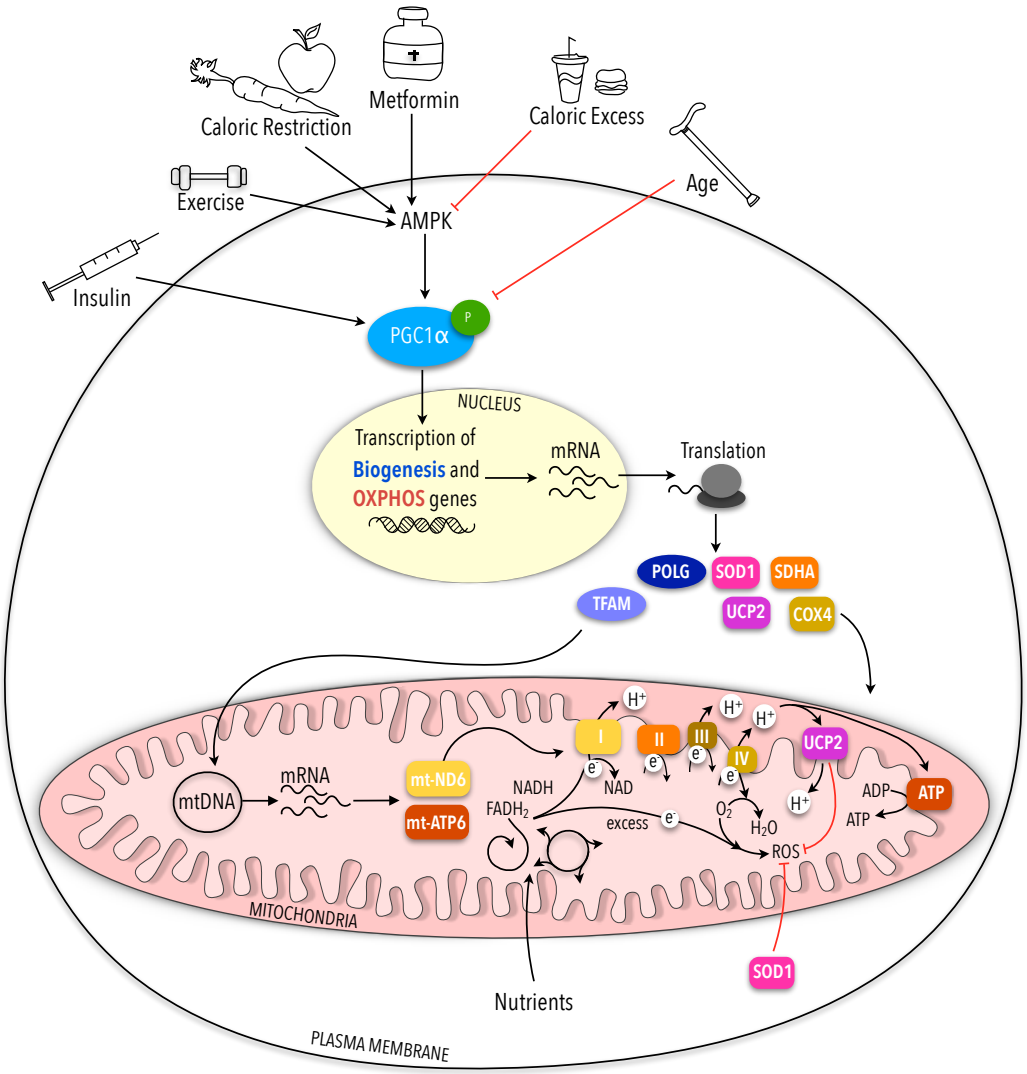

Figure 1.6: Modulation of mitochondrial function by factors which also affect metabolic disease

Several known environmental factors alter mitochondrial biogenesis and function via AMPK or PGC1α. PGC1α in turn regulates transcription of biogenesis (POLG, TFAM), OXPHOS (components of the ETC: complex I, II, III, IV, ATP) and other (SOD1, UCP2) mitochondrial function genes. TFAM regulates the transcription of mitochondrially-encoded components of the ETC, such as mt-ND6 and mt-ATP6. Nutrients are oxidised via ß-oxidation or citric acid cycle resulting in NADH and FADH2, which are subsequently further oxidised through OXPHOS to generate ATP. Electrons from NADH and FADH2 are carried over from complex I through to IV of the ETC while protons are pumped through to the inter-membrane space to provide the electrochemical gradient needed for the production of ATP from ADP by ATP synthase. Excess nutrients will result in excess electrons that are carried over to O2 to produce ROS. UCP2 and endogenous antioxidant SOD1 prevent excess accumulation of ROS. AMPK AMP-activated protein kinase, PGC1α peroxisome proliferator-activated receptor gamma co-activator 1-alpha, OXPHOS oxidative phosphorylation, POLG DNA polymerase subunit gamma, TFAM mitochondrial transcription factor A, ETC electron transport chain, UCP2 uncoupling protein 2, SOD1 superoxide dismutase 1, mtDNA mitochondrial DNA, mt-ND6 mitochondrially-encoded NADH dehydrogenase 6 (complex I), SDHA succinate dehydrogenase subunit A (complex II), COX4 cytochrome c oxidase subunit 4 (Complex IV), mt-ATP6 ATP synthase subunit 6 (Complex V), ROS reactive oxygen species.

1.8 Aims

The general aim of this thesis was to address the question of effective solutions to the obesity pandemic translationally, by investigating the range of barriers to metabolic recovery following bariatric surgery:

1. From the basic science approach, the role of:
    (a) gut-hormone FGF-19 on metabolic and mitochondrial improvement
    (b) gut-derived pro-inflammatory bacterial lipopolysaccharide (LPS) on metabolic and mitochondrial improvement, and
    (c) the direct effect of LPS on the disruption of mitochondrial function in the adipocyte
2. From the clinical approach, the environmental barriers to patient weight loss and metabolic recovery within a major UK tier 3 and 4 bariatric centre.

Chapter 2

Materials and Methods

Ethics and study design

The study was approved by the Ethics Committee of the Institute of Endocrinology (Institute of Endocrinology- Ethics Committee EC: 19/5/2009, Prague, Czech Republic). All study participants provided written and informed consent in accordance with the Declaration of Helsinki. Thirty-nine morbidly obese (BMI>35 Kg/m2), type-2 diabetic, Caucasian women undergoing either bilio-pancreatic diversion (BPD; n=12), laparoscopic greater curvature plication (LGCP; n=15), or laparoscopic adjustable gastric banding (LAGB; n=12) at the OB clinic, Prague, Czech Republic were recruited to participate in this study. Thorough biochemical and anthropometric investigations were conducted before (baseline) and six months after surgery with collection of serum samples and abdominal subcutaneous white adipose tissue (AT) biopsies at both of these time points. Patients on pharmacological treatment with incretin mimetics and/or insulin were not included in this study. All subjects included in this study were off anti-diabetic medication, including metformin.

Blood biochemistry and body composition analysis

All anthropometric and biochemical measurements were performed before and six months after surgery. Following a 10-hour overnight fast, venous blood was sampled in all patients, collected in chilled EDTA-containing tubes with and without aprotinin (for glucose and insulin measurements), aliquoted and frozen at -80ºC until assayed. Serum glucose, HbA1c and lipids were determined using the Cobas

6000 analyzer. Insulin resistance was assessed using the homeostatic model assessment of insulin resistance (HOMA-IR) according to the following equation:

$$HOMA-IR = \frac{[fasting\ glucose\,(^{\mathrm{mmol}}/_{\mathrm{L}})\ \mathrm{x}\ fasting\ insulin\,(^{\mathrm{mIU}}/_{\mathrm{L}})]}{22.5}$$

, as previously described [264]. The Friedwald formula [265] was employed to compute serum levels of LDL cholesterol. Body weight was measured to the nearest $0.5\,\mathrm{Kg}$ and height to the nearest $1\,\mathrm{cm}$. Percentage excess weight loss was calculated according to the following equation:

$$EWL\,(\%) = \frac{[Preoperative\ weight\ (\mathrm{Kg})\ -\ Postoperative\ weight\ (\mathrm{Kg})]}{[Preoperative\ weight\ (\mathrm{Kg})\ -\ Ideal\ weight\ (\mathrm{Kg})]}\ \mathrm{x}\ 100$$

with ideal body weight calculated based on a $BMI = 25\,^{\mathrm{Kg}}/_{\mathrm{m}^2}$ as follows:

$$Ideal\ weight\ (\mathrm{Kg}) = 25\ \mathrm{x}\ \left[Height\ (\mathrm{m})^2\right]$$

Body fat mass was measured using the bioimpedance method (Tanita TBF-300; Tanita corporation).

RNA isolation and qRT-PCR

For RNA extraction, $100\,\mathrm{mg}$ of frozen AT was homogenized in $500\,\mu\mathrm{L}$ Qiazol reagent (#79306 Qiagen, UK) then isolated using a column-based isolation method (RNeasy Lipid Tissue Mini Kit; #74804 Qiagen, UK) according to manufacturer´s instructions. Samples were digested with DNase I to remove potential genomic DNA contaminants (DNase I kit, #AMP-D1 Sigma-Aldrich). RNA was eluted in

$10\,\mu$L RNase-free water and $1\,\mu$L quantified in duplicate using a spectrophotometer (Nanodrop ND-1000, labtech) at $260\,$nm absorbancy. Synthesis of cDNA was performed using $200\,$ng RNA per sample and a Bioline mRNA reverse transcription kit (#BIO-65026) according to the manufacturer´s instructions. Gene expression was assayed through quantitative real-time polymerase chain reaction (qRT-PCR) using ABI 7500 standard sequence detection system (Applied Biosystems, UK). Each reaction was prepared to $25\,\mu$L final volume containing Taqman Universal PCR mastermix (#4304437 Applied Biosystems, UK), $1\,\mu$L sample cDNA and a specific commercially available Taqman gene expression assay (ThermoFisher Scientific, UK, Table 2.1). All samples were assayed in triplicate and multiplexed using 18S (ribosomal RNA) as a pre-optimised control probe. As per the manufacturer´s instructions, reactions were carried out at 50 ºC for 2 minutes, 95 ºC for 10 minutes, and then 40 cycles of 95 ºC for 15 seconds and then 60 ºC for 1 minute. For data analysis, gene expression was calculated based on the following formula:

$$mRNA\ expression = 2^{-\triangle Ct},\ \text{where}\ \triangle Ct = target\ gene\ Ct - \ 18s\ Ct$$

Table 2.1: Mitochondrial mRNA Gene Expression Taqman Assays

Gene	Assay ID
PGC1α	Hs00173304_m1
POLG	Hs01018668_m1
TFAM	Hs00273372_s1
mtND6	Hs02596879_g1
SDHA	Hs00188166_m1
COX4I1	Hs00971639_m1
mtATP6	Hs02596862_g1
UCP2	Hs01075227_m1
SOD1	Hs00533490_m1
SOD2	Hs00167809_m1
MFN2	Hs00208382_m1
OPA1	Hs01047018_m1
DRP1	Hs01552605_m1
FIS1	Hs00211420_m1
18s	4310893E

Evaluation of mitochondrial DNA (mtDNA) copy number

Total DNA was extracted from $50\,\mathrm{mg}$ frozen AT and cell culture samples using DNeasy Blood and Tissue Mini Kit (#69504 Qiagen, UK) in accordance to the manufacturer´s instructions. RNase treatment was performed to eliminate possible RNA contamination. DNA was eluted with 100 µL AE buffer and quantified using a spectrophotometer (Nanodrop ND-1000, Labtech). Relative amounts of mitochondrial DNA copy number were assessed through qPCR in an ABI Prism 7500 thermo cycler (Life Technologies) with the use of iQTM SYBR Green Supermix (#170-8880 BioRad). Mitochondrial (*mtND1*) and nuclear (*BECN1*) gene primers (Table2.2) were used to determine relative amounts of mitochondrial to nuclear DNA [266]. Each sample was measured in triplicate. Mitochondrial number was

calculated based on the following formula:

$$mtDNA\ copy\ number = 2^{\triangle Ct},\ \text{where}\ \triangle Ct = BECN1\ -\ mtND1$$

Table 2.2: Mitochondrial Copy number Primer Sequences

Gene	Forward	Reverse
mtND1	ATGGCCAACCTCCTACTCCT	GCGGTGATGTAGAGGGTGAT
BECN1	CGAGGCTCAAGTGTTTAGGC	ATGTACTGGAAACGCCTTGG

Evaluation of mitochondrial DNA integrity

Total DNA was extracted from cultured cells using DNeasy Blood and Tissue Mini Kit (#69504 Qiagen, UK) in accordance to the manufacturer´s instructions. RNase treatment was performed to eliminate possible RNA contamination. DNA was eluted with 100 µL AE buffer and quantified using a spectrophotometer (Nanodrop ND-1000, Labtech). Evaluation of mitochondrial DNA integrity was performed via qRT-PCR by comparing previously published primers [267] spanning a section of mtDNA susceptible to mutations (where 84% of known mutations occur) against a section that is not affected by any of the reported large deletions. Real-time PCR of both targets were run using a probe-based duplex qRT-PCR assay on an ABI Prism 7500 thermo cycler (Life Technologies) with the following thermal profile: 95ºC for 10 minutes, followed by 40 cycles of 95ºC for 15s, 55ºC for 15s, and 60ºC for 1 minute. The reaction components consisted of 22.5µL Taqman Universal PCR Mastermix no AmpErase® UNG (Applied Biosystems), each mitochondrial probe at 250nM (Taqman® MGB Probe, ThermoFisher Scientific,UK; shown in Table2.3) with a final reaction volume of 25µL.

Table 2.3: Mitochondrial DNA Integrity Probe Sequences

mtDNA Section	Binding Site Positions	Sequence (5´-3´)
Stable	mt 16,560-10	6FAM-CATCACGATGGATCACAGGT(NFQ)
Suceptible	mt 10,934-10,951	NED-GACCCCCTAACAACCCCC(NFQ)

Mitochondrial DNA integrity was calculated according to the following published formula [267]:

$$2^{mtDNA_{DR}}, \text{ where } mtDNA_{Deletion\ Ratio} = \frac{(Stable\ Probe\ Ct\ -\ Suceptible\ Probe\ Ct)}{Stable\ Probe\ Ct}$$

FGF-19 serum levels

For measurement of serum FGF-19 levels (pg/mL), an enzyme-linked immunosorbent assay (ELISA) kit for FGF-19 (Quantikine ELISA, R&D Systems, Minneapolis, MN) was used. All measurements were performed in duplicate according to the manufacturers instructions. This assay has a detection range of $31 - 544\ {}^{\mathrm{pg}}/_{\mathrm{mL}}$ and a coefficient of variation of $4.5\,\%$ for intra-assay and $5.5\,\%$ inter-assay precision.

LPS assay comparison and quantitation of serum levels

For serum lipopolysaccharide (LPS) determination, two methods were compared: the Limulus Amebocyte Lysate (LAL) Kinetic Chromogenic Assay (QCL-1000^{TM}, LONZA) and the EndoLISA® Elisa-based endotoxin detection assay (Hyglos). LPS concentrations of 8 human serum samples $(\mathrm{BMI}{=}21 - 38\ {}^{\mathrm{kg}}/_{\mathrm{m^2}})$ were determined in parallel with both assays. Samples were run in duplicate according to the manu-

facturers instructions. Serial sample dilution (from $1:4$ to $1:10$) and appropriate spike and negative controls were utilised to minimise enzyme-inhibitory factors in samples and confirm result validity. Results were calculated, according to manufacturers instructions, based on a LPS standard (*E. Coli* 055:B5) curve ranging from $[4 \text{ to } 0.06\,^{\text{EU}}/_{\text{mL}}]$ for the LONZA kit and from $[500 \text{ to } 0.005\,^{\text{EU}}/_{\text{mL}}]$ for the EndoLISA.

For bariatric samples, the EndoLISA® Elisa-based endotoxin detection assay (Hyglos) was used to quantify LPS serum levels. A preliminary trial of singlets was run to determine optimal dilution (1:5, 1:10; 1:20), after which samples were run at optimal dilution in duplicate. Results were calculated according to manufacturers instructions, based on a LPS standard (*E. Coli* 055:B5) curve ranging from $[500 \text{ to } 0.005\,^{\text{EU}}/_{\text{mL}}]$.

Protein extraction and Western blot

For protein extraction, $100\,\text{mg}$ of frozen human adipose tissue or $1.2 \text{ x } 10^6$ cultured adipocytes were homogenised in $200\,\mu$L Phosphosafe^{TM} Extraction Buffer (Novogen®, Merk, Germany). A Bio-Rad detergent compatible protein assay kit (Bio-Rad Laboratories, CA) and nanospectrophotometer (GeneFlow, UK) were used to quantify protein concentrations. As described previously for Western blot analyses [268], 10-20µg of protein were loaded onto a denaturing polyacrylamide gel (GeneFlow, UK), transferred on to a nitrocellulose membrane which was then incubated with a primary antibody diluted in 0.2% I-block PBS-T (IRS1 $1:250$, MT-CO1 $1:1000$, SDHA $1:1000$, ß-Actin $1:1000$) at 4ºC overnight. A chemiluminescence detection system (ECL Plus, GE Healthcare, UK) was used

to visualise protein bands, and densitometry was conducted using ImageQuant LAS 4000 Software (GE Healthcare, UK). Equal protein loading was confirmed by examining ß-actin protein expression. Primary antibodies utilised are listed in Table2.4.

Table 2.4: Primary Antibodies

1º Antibody	Supplier	Catalogue Number
IRS1	Millipore	
ß-actin	Cell Signalling	
SDHA	Cell Signalling	5839
MT-CO1	Abcam	Ab14705

Human adipocyte culture, differentiation and treatment

Human subcutaneous white adipocyte cell line ChubS7 were grown and differentiated as previously described [269]. Briefly, cells were seeded on to 6-well plates ($0.3\text{x}10^6$) unless otherwise specified, grown to $100\,\%$ confluence and differentiated for 8-10 days in DMEM/F12 with $3\,\%$ FBS and PromoCell Differentiation Supplement Mix (C-39436, PromoCell). After differentiation, cells were allowed to equilibrate in basal media for 12 hours before being treated for 24-72 hours in basal media supplemented with LPS (10 or $100\,{}^{\mathrm{ng}}/_{\mathrm{mL}}$, *E. Coli* O55:B5, Sigma, L6529), TNFα ($10\,{}^{\mathrm{ng}}/_{\mathrm{mL}}$, Sigma, H8916) or Insulin ($50\,\mathrm{nM}$, Sigma, I9278). All media were prepared with DMEM/F12 (ThermoFisher Scientific, UK, 11320033) and formulations are shown in Table 2.5.

Table 2.5: Adipocyte Culture Media Formulations

Growth Media		Differentiation Media		Basal Media	
Fetal Bovine Serum	$10\,\%$	Fetal Bovine Serum	$3\,\%$	Bovine Serum Albumin	$0.5\,\%$
Glutamine	$2\,\mathrm{mM}$	d-biotin	$8\,\mu\mathrm{g/mL}$		
		Insulin (recombinant human)	$0.5\,\mu\mathrm{g/mL}$		
		Dexamethasone	$400\,\mathrm{ng/mL}$		
		IBMX	$44\,\mu\mathrm{g/mL}$		
		L-Thyroxine	$9\,\mathrm{ng/mL}$		
		Citglitazone	$3\,\mu\mathrm{g/mL}$		

Seahorse Cell Mito Stress Test

Respiration and media acidification rate were measured using a Seahorse XF24 Extracellular Flux Analyzer (Seahorse Bioscience, Agilent Technologies). Immortalised human preadipocytes ChubS7 were seeded onto 24-well plates (Seahorse Bioscience, 100850-001) at a density of 10,000 cells/well, grown and differentiated using the standard protocol outlined above, and treated for 24 or 72 hours with or without LPS (10 or $100\,\mathrm{ng/mL}$, *E. Coli* O55:B5, Sigma, L6529). Each experimental group consisted of 5 replicates, with the experiment repeated on at least 2 separate occasions (n=10). The assay was conducted in sterile, unbuffered Assay Media prepared with Seahorse base media (Seahorse Bioscience, 102365-100) at 37ºC (pH 7.4), the formulation of which is listed in Table2.6.

Table 2.6: Seahorse Media Formulation

Reagent	Supplier	Catalog Number	Final Concentration
Sodium Pyruvate	Sigma	S8636	$1\,\mathrm{mM}$
Glutamine Glutamax®	Seahorse	Included	$2\,\mathrm{mM}$
Glucose	Sigma	G8769	$17.5\,\mathrm{mM}$

After a calibration step $(30\,\mathrm{min})$ and an equilibration step $(30\,\mathrm{min})$, the assay protocol consisted of 3 cycles of the following steps: mix $(3\,\mathrm{min})$, wait $(2\,\mathrm{min})$, measure $(3\,\mathrm{min})$, which were completed before and after each injection of Oligomycin

(Sigma, O4876), FCCP (Sigma, C2920) and combined Rotenone (Sigma, R8875) and Antimycin A (Sigma, A8674). Reagents or vehicle control were injected in the appropriate volume of a tenfold concentrated stock solution to give the following final in-well concentrations: $2\,\mu$M Oligomycin, $2\,\mu$M FCCP, $0.5\,\mu$M Rotenone/Antimycin A. Prior to experiments, reagent concentrations and seeding density were optimised as per the manufacturers instructions. Oxygen consumption rate (OCR) and extracellular acidification rate (ECAR) were calculated by the WAVE software (Seahorse Bioscience, Agilent Technologies). The basal respiration parameters were calculated from the mean of 3 individual OCR measurements as follows:

$$Basal\ Respiration = Initial\ OCR\ (\mathrm{pmol/L}) - Rotenone\ OCR\ (\mathrm{pmol/L})$$

For OCR and ECAR response to injection of each compound, data was normalised by the basal respiration of each experimental group (shown as percentage of baseline) to account for well-to-well variability in cell number.

Determination of ATP abundance

Immortalised human preadipocytes ChubS7 were seeded onto gelatin-coated 96-well white opaque cell culture plates at a density of 10,000 cells/well. Cells were grown and differentiated according to the standard protocol outlined above, and treated with or without LPS (10 or $100\,\mathrm{ng/mL}$, *E. Coli* O55:B5, Sigma, L6529) for 24 or 72 hours. Bioluminescent determination of ATP abundance was conducted using EnzyLight^{TM} ATP Assay Kit (BioAssay Systems, EATP-100) following the manufacturers instructions for adherent cells. Luminescence was read using a

PheraStar FS microplate reader (BMG Labtech), and ATP concentrations determined based on interpolation of a standard curve of known ATP concentrations ranging from $0 - 30\,\mu M$.

Determination of mitochondrial membrane potential

The dye tetramethylrhodamine ethyl ester perchlorate (TMRE, Sigma, 87917) was used to determine mitochondrial membrane potential. TMRE is a cell-permeant, positive-charged red/orange dye that is readily sequestered by polarised mitochondria (due to their negative charge) in a manner that is directly proportional to their membrane potential. Immortalised human preadipocytes ChubS7 were seeded onto a black opaque 96-well plate, differentiated and treated as described for the ATP abundance assay. Adherent cells were incubated with $300\,\mathrm{nM}$ TMRE (Sigma) diluted in basal media (described in Table 2.5) for $30\,\mathrm{min}$ at $37^{\circ}C$. Cells were then washed 3 times with warm PBS before reading fluorescence with a PheraStar FS microplate reader (BMG Labtech) at $550/590\mathrm{nM}$ excitation/emission immediately and after 10, 20 and 30 minutes. As a positive control for depolarisation, $30\,\mu M$ FCCP was added to some cells for $30\,\mathrm{minutes}$, prior to the TMRE incubation step. FCCP is an ionophore which destroys membrane potential, rendering mitochondria unable to accumulate TMRE. For background correction, cells with no TMRE and no FCCP added were used. Membrane potential was calculated using the relative

fluorescence signal of samples based on the following formula:

$$Membrane\ Potential\ (\%) = \left[\frac{(LPS\ sample - background)}{(control\ sample - background)}\right] \text{x } 100$$

Endogenous antioxidant activity assays

Activity of endogenous antioxidants SOD and Catalase was evaluated through a colorimetric method, using OxiSelect^{TM} Superoxide Dismutase Activity Assay (STA-340) and OxiSelect^{TM} Catalase Activity Assay (STA-341) Kits (Cell Biolabs). Following adipocyte differentiation and treatment, $\backsim 1.2 \text{ x } 10^6$ adherent cells were washed 3 times with ice-cold PBS, harvested with a cell scraper in $1\,\mathrm{mL}$ of cold Lysis buffer ($10\,\mathrm{mM}$ Tris, pH 7.5, $150\,\mathrm{mM}$ NaCl, $0.1\,\mathrm{mM}$ EDTA). Samples were homogenised, centrifuged and stored at -80ºC until assayed. All assays were conducted within 1 month of sample collection and were conducted in accordance to manufacturers instructions. Absorbance was read using a PheraStar FS microplate reader (BMG Labtech). SOD activity was calculated based on optical density as outlined in the following formula:

$$SOD\ activity\ (inhibition\ \%) = \left[\frac{(Blank_{OD} - Sample_{OD})}{Blank_{OD}}\right]$$

The concentration of active Catalase was determined by interpolation of a catalase standard curve. Optical density at 540nm was plotted on the "x" axis, Catalase (U/mL) on the "y" axis, and a second order polynomial equation was used to determine catalase concentrations as follows:

$$Catalase\ \left({}^{\mathrm{U}}/_{\mathrm{mL}}\right) = 174.01x^2 + 13.678x + 2.7743 \text{ where } x = optical\ density\ (540\,\mathrm{nm})$$

Quantification of total reactive oxygen and nitrogen species

Total reactive oxygen and nitrogen species were evaluated through green fluorescence using OxiSelect^{TM} *in vitro* ROS/RNS Assay Kit (STA-347, Cell Biolabs). Following adipocyte differentiation and treatment, $\backsim 1.2$ x 10^6 adherent cells were washed 3 times with ice-cold PBS, flash-frozen in dry-ice and harvested using a cell-scraper. Samples were homogenised in $200\,\mu$L PBS and stored at -80ºC and assayed within 1 month of collection. Assay was conducted according to manufacturers instructions, and fluorescence after 30 minutes was measured using a PheraStar FS microplate reader (BMG Labtech) with a $485/538$ nm filter and $530\,\mathrm{nm}$ cutoff. Total ROS/RNS were calculated by interpolation of a Hydrogen Peroxide standard curve as follows:

$$ROS/RNS\ (\mu\mathrm{M}) = 5354.5x^2 + 1043.3x + 50.496$$

where $x = relative\ flourescence\ units\ \left({}^{485}/_{538}\right)$.

2-deoxyglucose uptake

Glucose uptake in differentiated ChubS7 adipocytes was evaluated via cellular incorporation of $[^3\mathrm{H}]$-2-deoxyglucose. Following differentiation and treatment, cells were washed 3 times with warmed PBS and allowed to equilibrate in KRH buffer (containing $0.01\,\%$ BSA, $5\,{}^{\mathrm{mmol}}/_{\mathrm{L}}$ glucose) at 37ºC for 2.5 hours. Adipocytes were then incubated a further 30 minutes with KRH buffer without glucose and either no (basal control) or $100\,$µM insulin. Immediately after, $1\,{}^{\mu\mathrm{Ci}}/_{\mathrm{mL}}$ $[^3\mathrm{H}]$-2-deoxyglucose (PerkinElmer, NET328A001MC) in KRH buffer at 37ºC was added for a further10 minutes. To finalise the assay, cells were then washed 3 times with ice-cold PBS, lysed and harvested in $200\,$µL RIPA buffer and a cell scraper. Radioactivity was evaluated via scintillation counting of the lysates, diluted 1:4 in β-scintillation fluid (Beta-Plate Scint, PerkinElmer), and a scintillation Counter. Results defined as counts per minute (CPM) were normalised to total protein content and glucose uptake displayed relative to the basal control.

Analysis of mitochondrial morphology through confocal microscopy

Analysis of the mitochondrial network was performed through live cell imaging using a confocal microscope. ChubS7 cells were seeded on to gelatin-coated 35mm glass bottom culture dishes (MatTek corportation®), grown, differentiated and treated for 24 hours as described above. Upon completion of treatment, basal media was removed, replaced with $100\,\mathrm{nM}$ Mitotracker Red and cells incubated for 20 minutes at 37ºC. Cells were then washed three times with basal media and

imaged in HEPES-buffered basal media (pH 7.35) with or without LPS (10 or $100\,^{\mathrm{ng}}/_{\mathrm{mL}}$, *E. Coli* O55:B5, Sigma, L6529). The Z system attached to an inverted flourescence microscope fitted with an F-view-II cooled CCD camera (Olympus) was used to observe cells which were maintained at 37ºC throughout the imaging process. Cells were magnified 40x through an oil objective lens, and a 500 nm excitation filter was used to image the mitochondrial network.

Morphologic assessment of the mitochondrial network was conducted on confocal images using ImageJ (version 1.50i) as described by others [270]. The mitochondrial parameters assessed were mitochondrial area (μm^2) and the degree of branching, as defined by the following equation:

$$BF = \frac{MtP^2}{(4\pi MtA)}$$

where $MtP =$ length of mitochondrial outline (mitochondrial perimeter in μm) and $MtA =$ Area of mitochondria (μm^2). Four independent experiments were conducted and a minimum of 70 images were examined for each experimental group.

Statistical Analysis

Statistical analyses were performed using the SPSS 21.0 software. Data are reported as mean $\pm$ standard deviation (SD), unless otherwise specified. Data were examined for normality according to the Shapiro-Wilks criteria. Comparisons between pre- and post-surgery time-points were performed via paired two-tailed t-tests (if parametric) and the Wilcoxon signed ranks test (if non-parametric). For

categorical data, Fisher´s exact test was used. Between-group (surgery type) differences were assessed using One-way ANOVA (if parametric) and Kruskal-Wallis test (if non-parametric) using change variables, calculated as percentage change from pre-surgery values [(post/pre) x100]. For Pearson correlation analyses, change variables [(post/pre) x100] were log-transformed prior to analysis if non-parametric.

Chapter 3

Differential Effect of Bariatric Surgical Procedure on Metabolic Outcomes and Adipose Tissue Mitochondria

---

3.1 Introduction

Bariatric surgery is currently considered the most effective treatment for severe obesity, and is associated with substantial and sustained weight loss, coupled with long-term T2DM remission in the majority of cases [271, 174]. However, the type of bariatric surgical intervention also appears to be an important factor affecting the degree and spectrum of improvements in metabolic parameters [174]. Post-surgical excess weight loss ranges in degree from 15-25% after laparoscopic adjustable gastric banding (LAGB), to 30-40% after bilio-pancreatic diversion (BPD), with the degree of weight loss achieved being the strongest predictor of type-2 diabetes (T2DM) remission [272, 273, 274, 275].

Also critical to metabolic recovery are mitochondria. Established metabolic regulators [276], mitochondria are key to the adipose tissue´s (AT) ability to maintain its metabolic and endocrine functionality in the face of constant energy oversupply [277]. Mitochondria exquisitely tailor changes in energy production capacity through structural and functional modifications (fission and fusion) dependent upon supply and demand. However, in cases of chronic nutrient excess, such as obesity, the mitochondrial network is forced to sustain these adaptations (fragmentation) for the longer term, leading to severely compromised mitochondrial DNA integrity, inefficiency and metabolic stress [278, 279]. In addition, this impairment in function can further lead to an accumulation of reactive oxygen species (ROS) [236], impaired oxygen consumption and ß-oxidation [280, 281], enhanced lipotoxic species accumulation [282], pro-inflammatory cytokine production [283] and impaired insulin signaling [284, 285].

Recent studies examining mitochondria in human AT has shown that both obesity

and T2DM can lead to mitochondrial inefficiency with fewer and smaller mitochondria, and that this dysfunction is dependent upon substantial weight gain rather than adipocyte cell size [286, 287]. Beyond simple obesity, the insulin resistant state is also associated with mitochondrial dysfunction within AT [288, 289, 290], whilst studies also suggest that mitochondrial dysfunction in adipocytes itself may be causal in leading to impairment of insulin sensitivity [291, 292].

Nutrient overload, either through high-fat or high-glucose environments, has been strongly implicated in mitochondrial dysfunction, leading to increased oxidative stress and molecular mechanisms of metabolic dysfunction in AT [279, 293, 294, 295]. Therefore, interventions such as bariatric surgery that can induce substantial and sustained weight loss, may reverse the underlying cellular causes of insulin resistance by limiting over nutrition and reversing mitochondrial dysfunction in AT [271, 174, 272, 273, 274, 275].

Thus, the aims of this study were to: (1) determine whether bariatric surgery, the most effective treatment for morbid obesity to date [271, 174], can reverse mitochondrial maladaptation in AT from obese subjects with T2DM; (2) evaluate whether the type of bariatric surgery, i.e. with varying degrees of caloric restriction (as evidenced by weight loss), has a differential effect on the resulting mitochondrial health; and (3) understand which, if any, clinical or biochemical post-operative factors may be associated with a reversal in mitochondrial maladaptation.

3.2 Methods

Ethics and Study Design

All study participants provided written and informed consent in accordance with the Declaration of Helsinki. Thirty-nine morbidly obese ($BMI > 35\,{}^{\mathrm{Kg}}/_{\mathrm{m}^2}$), type-2 diabetic, Caucasian women undergoing either bilio-pancreatic diversion (BPD; n=12), laparoscopic greater curvature plication (LGCP; n=15), or laparoscopic adjustable gastric banding (LAGB; n=12) at the OB clinic, Prague, Czech Republic were recruited to participate in this study. Thorough biochemical and anthropometric investigations were conducted before (baseline) and six months after surgery with collection of serum samples and abdominal subcutaneous white adipose tissue (AT) biopsies at both of these time points. Patients on pharmacological treatment with incretin mimetics and/or insulin were not included in this study. The reader is referred to Chapter 2 Materials and Methods for greater detail.

Blood Biochemistry and Anthropometry

Anthropometric and biochemical measurements were performed before and six months after surgery, following a 10-hour overnight fast, from venous blood samples. Serum glucose, HbA1c and lipids were determined through biochemical analyses (see Chapter 2). Insulin resistance was assessed using the homeostatic model assessment of insulin resistance (HOMA-IR) [34]. The Friedwald formula [35] was employed to compute serum levels of LDL cholesterol. Body weight was measured to the nearest 0.5 Kg and height to the nearest 1 cm. Percentage excess weight loss was calculated (see Chapter 2 for equation), and body fat mass was measured

using the bioimpedance method (Tanita TBF-300; Tanita corporation).

RNA isolation and qRT-PCR

Gene expression from subcutaneous white adipose tissue biopsies before and 6 months after each bariatric surgery was determined via qRT-PCR. RNA isolation and qRT-PCR methods are detailed in Chapter 2. For detail on primer sequences of mitochondrial genes used in this study the reader is referred to Table 2.1.

Mitochondrial DNA copy number assay

Mitochondrial number was determined via analysis of relative amounts of mitochondrial to nuclear DNA [266] in subcutaneous white adipose tissue biopsies before and 6 months after each bariatric surgery. For in depth detail on this method, the reader is referred to Chapter 2.

Statistical Analysis

Statistical analyses were performed using the SPSS 21.0 software. Data are reported as mean $\pm$ standard deviation (SD), unless otherwise specified. Data were examined for normality according to the Shapiro-Wilks criteria. Comparisons between pre- and post-surgery time-points were performed via paired two-tailed t-tests (if parametric) and the Wilcoxon signed ranks test (if non-parametric). For categorical data, Fisher´s exact test was used. Between-group (surgery type) differences were assessed using One-way ANOVA (if parametric) and Kruskal-Wallis test (if non-parametric) using change variables, calculated as percentage change from pre-surgery values [(post/pre) x100]. For Pearson correlation analyses, change

variables [(post/pre) x100] were log-transformed prior to analysis if non-parametric.

3.3 Results

Differential Effect of Bariatric Procedure on Metabolic Health

The most notable difference between surgical procedures was weight loss. Though all surgical procedures resulted in significant reductions of BMI compared with pre-surgical measurements (Figure 3.1**A**), the BPD procedure produced significantly greater weight reduction (p=0.004), by a factor of approximately 30-50% on top of the other two LGCP and LAGB procedures (Figure 3.1**B**).

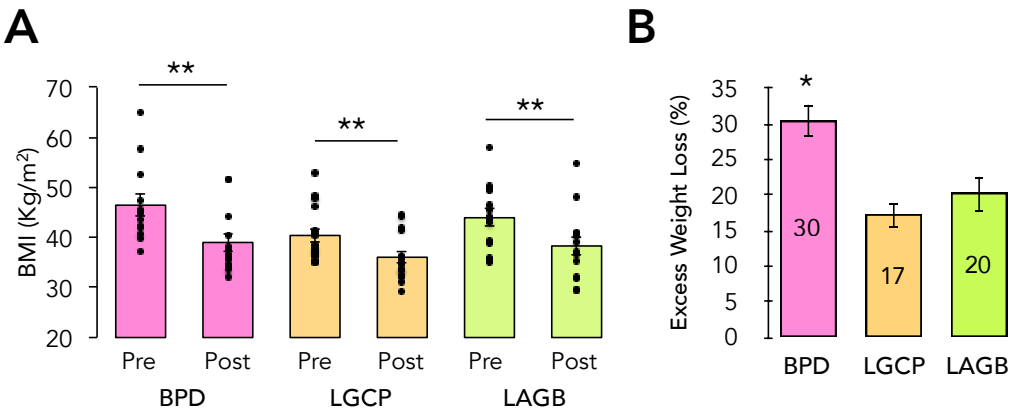

Figure 3.1: Differential effect of surgical procedure on weight loss
(A) *BMI before and 6 months after three distinct bariatric procedures: Bilio-pancreatic diversion (BPD), Laparoscopic Greater Curvature Plication (LGCP) and Laparoscopic Adjustable Gastric Banding (LAGB). Bars represent means ± standard error of the mean, with individual data points shown as dots to illustrate distribution.* ***(B)*** *Percent of the individual´s excess weight lost at 6 months post BPD, LGCP or LAGB. Pre-to-post differences were calculated using a 2-tail paired t-test, whilst one way ANOVA was used to compare change between surgeries. *p<0.05, **p<0.01.*

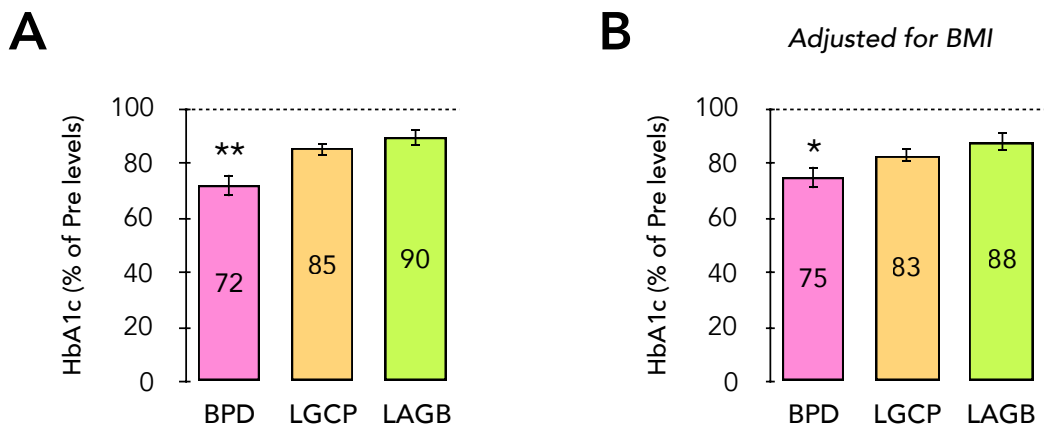

Figure 3.2: Differential effect of surgical procedure on HbA1c

(A) *Serum HbA1c before and 6 months after three distinct bariatric procedures: Bilio-pancreatic diversion (BPD), Laparoscopic Greater Curvature Plication (LGCP) and Laparoscopic Adjustable Gastric Banding (LAGB). Data is expressed as precentage of pre-surgical levels. Bars represent means ± standard error of the mean.* ***(B)*** *Serum HbA1c before and after BPD, LGCP and LAGB, showing weighted average once BMI is accounted for through ANCOVA analysis. One way ANOVA or ANCOVA was used to compare change between surgeries. *p<0.05, **p<0.01.*

The type of surgical procedure also had a significant impact on HbA1c reduction. These data is shown in Figure 3.2, as percentage of pre-surgical values. Despite similar levels of HbA1c at baseline between surgeries, the BPD procedure resulted in significantly lower circulating levels of HbA1c (a marker of long-term diabetic control), compared with LGCP (p=0.022) and LAGB (p=0.002) (Figure 3.2**A**). To clarify whether this effect could be explained by the greater weight loss shown by the BPD cohort, the analysis was repeated using ANCOVA and BMI as a covariate. As shown in Figure 3.2**B**, BPD resulted in superior HbA1c reductions, despite controlling for BMI. Indeed, further linear regression analysis revealed that inter-surgical differences in excess weight loss could account only for 30% of divergence in HbA1c, leaving the remaining 70% as the result of other, unknown factors (Table 3.1).

Table 3.1: Contribution of weight loss to surgery-induced improvements in serum HbA1c

	R square change	B Coefficient	p value
Excess weight loss	0.304	−0.776	0.0001

A linear regression analysis was performed using surgery-induced changes in serum HbA1c as the dependent variable, and excess weight loss as independent, to determine the contribution of weight loss to serum HbA1c improvements. No other variables were entered into the model.

In addition to improved diabetic control, BPD also resulted in significantly lower lipid levels. As shown in Figure 3.3**A**, total cholesterol was significantly reduced in patients who underwent BPD, but not in those who underwent LGCP, or LAGB. Subsequent ANCOVA analysis revealed that this surgery-specific difference remained unchanged after accounting for differences in BMI (Figure 3.3**B**). Indeed, further linear regression analysis revealed that inter-surgical differences in excess weight loss could account only for 12% of divergence in serum total cholesterol, leaving the remaining 88% as the result of other, unknown factors (Table 3.2). Similar results were observed in other lipids, where improvements in LDL cholesterol (29%, p=0.001) and in HDL/LDL ratio appeared greater with BPD (15% increase from pre-surgery, p=0.154) than with LGCP and LAGB procedures (2% and 4%, respectively). The aforementioned findings and all additional anthropometric, biochemical and clinical data obtained before and 6 months after bilio-pancreatic diversion (BPD; n= 12), laparoscopic greater curvature plication (LGCP; n=15) or laparoscopic adjustable gastric banding (LAGB; n=12) operations can be found in Table 3.3, to highlight comparative differences between the 3 surgeries.

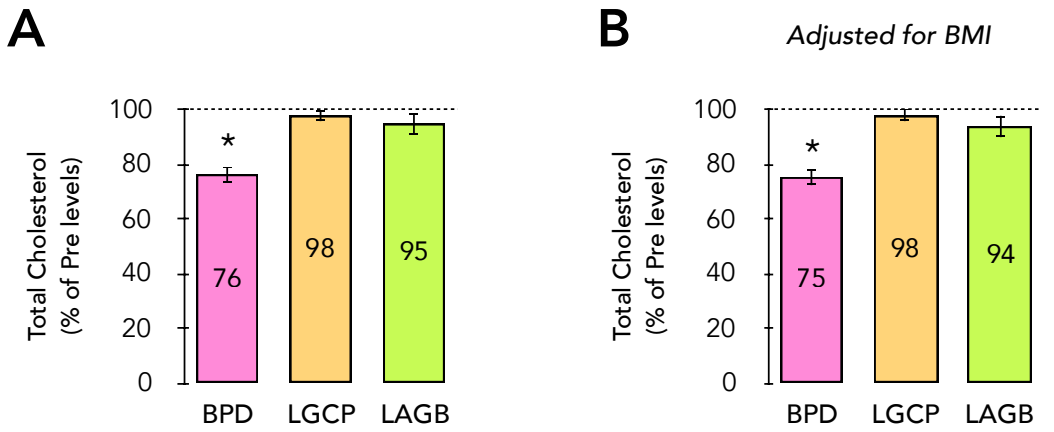

Figure 3.3: Differential effect of surgical procedure on total cholesterol
(A) *Serum Total Cholesterol before and 6 months after three distinct bariatric procedures: Biliopancreatic diversion (BPD), Laparoscopic Greater Curvature Plication (LGCP) and Laparoscopic Adjustable Gastric Banding (LAGB). Data is expressed as precentage of pre-surgical levels. Bars represent means ± standard error of the mean.* ***(B)*** *Serum Total Cholesterol before and after BPD, LGCP and LAGB, showing weighted average once BMI is accounted for through ANCOVA analysis. One way ANOVA or ANCOVA was used to compare change between surgeries. *p<0.05, **p<0.01.*

Table 3.2: Contribution of weight loss to surgery-induced improvements in total cholesterol

	R square change	B Coefficient	p value
Excess weight loss	0.127	−0.535	0.019

A linear regression analysis was performed using surgery-induced changes in serum total cholesterol as the dependent variable, and excess weight loss as independent, to determine the contribution of weight loss to serum total cholesterol improvements. No other variables were entered into the model.

Differential Effect of Bariatric Procedure on Indicators of Adipose Mitochondrial Function

Next, the impact of the different bariatric procedures on mitochondrial function in adipose tissue was examined. Transcript levels of genes associated with a range of mitochondrial functions (biogenesis, oxidative phosphorylation, uncoupling and antioxidant capacity) and dynamics (fission and fusion) were examined in adipose biopsies through qRT-PCR. Gene expression levels pre-surgery for each gene category are shown in Figures 3.4 to 3.7. Overall, transcript levels for genes involved

Table 3.3: Anthropometric, biochemical and clinical variables pre-surgery and 6-months post BPD, LGCP, and LAGB bariatric procedures

	BPD			LGCP			LAGB		
n	12			15			12		
Age (y)	50.5 ± 5.8			53.2 ± 7.5			53.6 ± 11.3		
EWL (%)	$30.7 \pm 8.4^{\dagger\dagger}$			17.4 ± 6.3			20.2 ± 9.4		
	Pre	Post	△(%)	Pre	Post	△(%)	Pre	Post	△(%)
Weight (Kg)	127.7 ± 22.6	106.9 ± 18.5**	$83.8 \pm 3.0^{\dagger}$	109.2 ± 16.5	97.6 ± 14.1**	89.5 ± 3.2	119.6 ± 19.1	105.3 ± 18.3**	88.1 ± 5.7
BMI (Kg/m^2)	46.45 ± 7.75	39.01 ± 6.37**	$84.1 \pm 3.5^{\dagger}$	40.41 ± 5.54	36.05 ± 4.62**	89.3 ± 3.4	43.95 ± 6.60	38.31 ± 7.05**	88.90 ± 4.9
WHR	0.93 ± 0.07	0.90 ± 0.07	97.7 ± 9.9	0.88 ± 0.10	0.87 ± 0.08	100.1 ± 11.1	0.90 ± 0.04	0.88 ± 0.04	98.5 ± 5.9
Body fat (%)	49.59 ± 3.70	44.68 ± 4.62**	90.2 ± 6.6	48.49 ± 3.78	44.90 ± 3.71**	92.7 ± 4.6	49.54 ± 3.44	46.39 ± 4.45*	93.6 ± 5.6
Glucose ($mmol/L$)	8.40 ± 2.57	7.01 ± 1.73	89.1 ± 30.1	8.93 ± 2.11	7.34 ± 1.64*	84.4 ± 16.9	9.30 ± 2.65	7.07 ± 1.56**	77.4 ± 8.8
Insulin ($pmol/L$)	31.48 ± 21.2	17.12 ± 12.0*	71.2 ± 73.8	26.43 ± 19.4	16.76 ± 10.9*	70.6 ± 24.7	26.20 ± 6.93	15.21 ± 5.92**	61.3 ± 26.1
HOMA IR	11.8 ± 9.74	5.3 ± 4.73*	66.1 ± 97.2	10.9 ± 9.14	5.32 ± 3.34**	61.0 ± 29.5	10.8 ± 4.13	5.07 ± 2.89**	47.1 ± 20.5
HbA1c (%)	7.1 ± 0.9	5.7 ± 0.70**	$72.1 \pm 15.1^{\dagger\dagger}$	7.3 ± 1.0	6.5 ± 0.9**	85.1 ± 8.5	7.0 ± 0.9	6.4 ± 0.6*	89.5 ± 12.5
HbA1c ($mmol/mol$)	53.84 ± 9.6	38.38 ± 7.8**	$72.1 \pm 15.1^{\dagger\dagger}$	56.33 ± 10.5	47.93 ± 10.3**	85.1 ± 8.5	52.92 ± 10.1	46.64 ± 6.2*	89.5 ± 12.5
T Chol ($mmol/L$)	4.91 ± 1.03	3.72 ± 0.86**	$75.9 \pm 9.80^{\dagger}$	4.84 ± 0.77	4.73 ± 0.82	97.8 ± 8.7	4.83 ± 0.77	4.54 ± 0.89	94.7 ± 14.9
TGL ($mmol/L$)	1.43 ± 0.66	1.59 ± 0.69	117.6 ± 51.2	1.95 ± 1.39	1.38 ± 0.71	89.2 ± 33.0	1.79 ± 0.75	1.23 ± 0.50	74.0 ± 24.4
HDL ($mmol/L$)	1.05 ± 0.21	0.81 ± 0.22**	$73.1 \pm 22.0^{\dagger\dagger}$	1.12 ± 0.33	1.15 ± 0.31	104.0 ± 15.1	1.04 ± 0.24	1.08 ± 0.25	105.0 ± 17.3
LDL ($mmol/L$)	3.19 ± 1.03	2.23 ± 0.67**	$71.4 \pm 13.2^{\dagger\dagger}$	2.82 ± 0.69	2.94 ± 0.77	107.2 ± 25.6	2.96 ± 0.65	2.90 ± 0.82	101.6 ± 33.4
HDL/LDL ratio	0.36 ± 0.14	0.40 ± 0.12	115.3 ± 28.6	0.42 ± 0.17	0.42 ± 0.18	102.0 ± 29.0	0.37 ± 0.11	0.38 ± 0.14	103.6 ± 25.6

*Data are means ± standard deviation. Within group statistical significance (pre to post-surgery) was determined using two-tailed paired t-test or Wilcoxon signed ranks test (*p<0.05; **p<0.01), whilst for between group comparisons one-way ANOVA or the Kruskal-Wallis test were used (†p<0.05; ††p<0.01). Change column (△%) denotes post-surgery values as percentage of pre-surgery values. EWL: excess weight loss, BMI: body mass index, WHR: waist-hip ratio, HOMA IR: Homeostatic assessment model of insulin resistance, HbA1c: glycosilated haemoglobin, T Chol: total cholesterol, TGL: triglycerides, HDL: High-density Lipoprotein cholesterol, LDL: low-density lipoprotein cholesterol, BPD: bilio-pancreatic diversion, LGCP: laparoscopic greater curvature plication, LAGB: laparoscopic adjustable gastric banding. All serum determinations correspond to fasting status.*

in mitochondrial biogenesis (Figure 3.4), oxidative phosphorylation (Figure 3.5), reactive oxygen species clearance (Figure 3.6), and dynamics (Figure 3.7) did not vary significantly prior to surgical intervention between the three surgical cohorts (BPD, LGCP, or LAGB) .

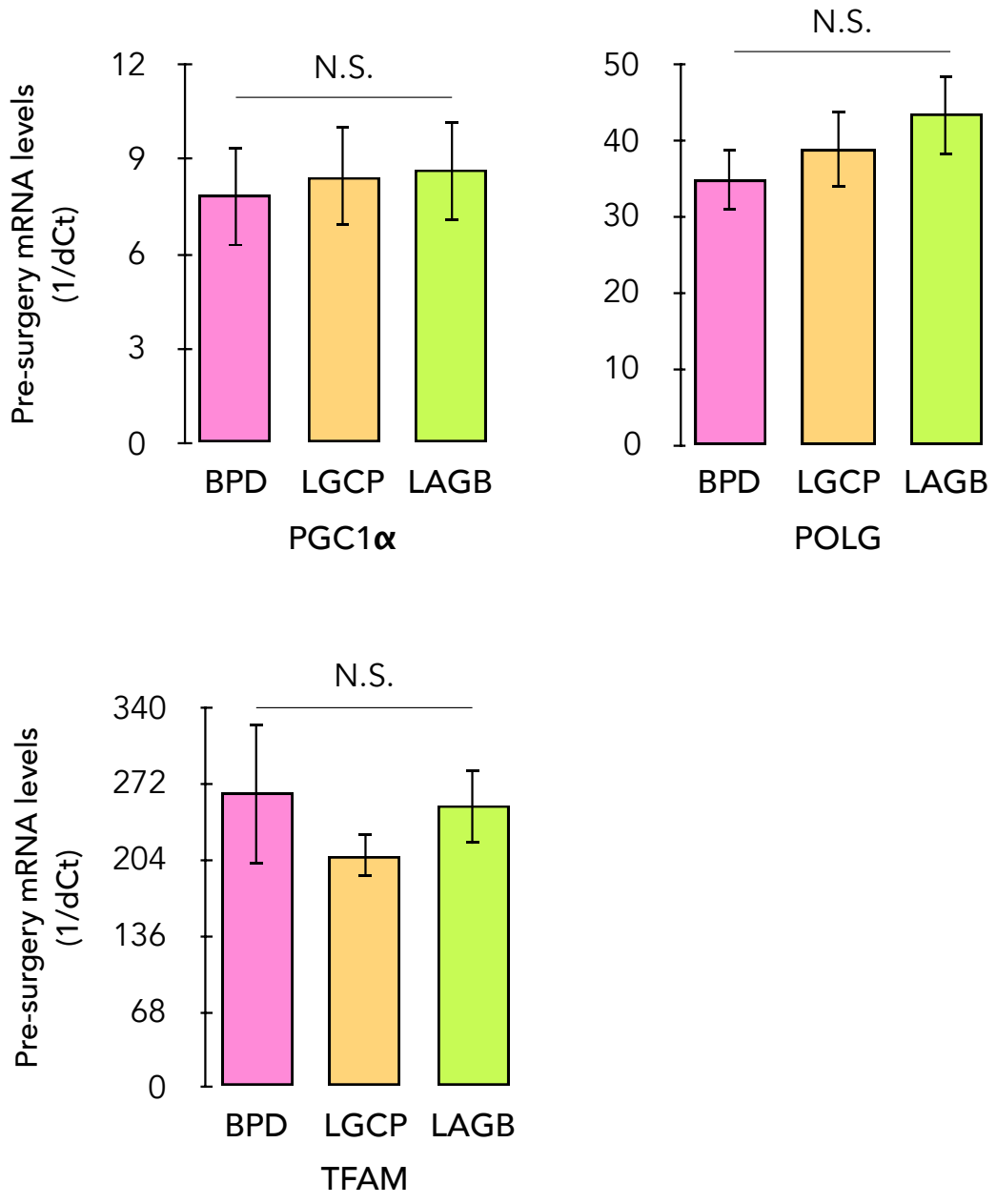

Figure 3.4: Pre-surgery comparison of genes involved in mitochondrial biogenesis
Pre-surgery adipose tissue mRNA levels of genes involved in mitochondrial biogenesis for each surgical cohort due to undergo either Bilio-pancreatic diversion (BPD), laparoscopic greater curvature plication (LGCP) or laparoscopic adjustable gastric banding (LAGB). Data is expressed as $^{1}/_{\triangle Ct}$. Bars represent means $\pm$ standard error of the mean. One way ANOVA was used to determine differences between surgeries. N.S. denotes differences shown were not statistically significant (p>0.05). PGC1α: Peroxisome proliferator-activated receptor gamma coactivator 1-alpha; POLG: mitochondrial DNA polymerase; TFAM: mitochondrial transcription factor A.

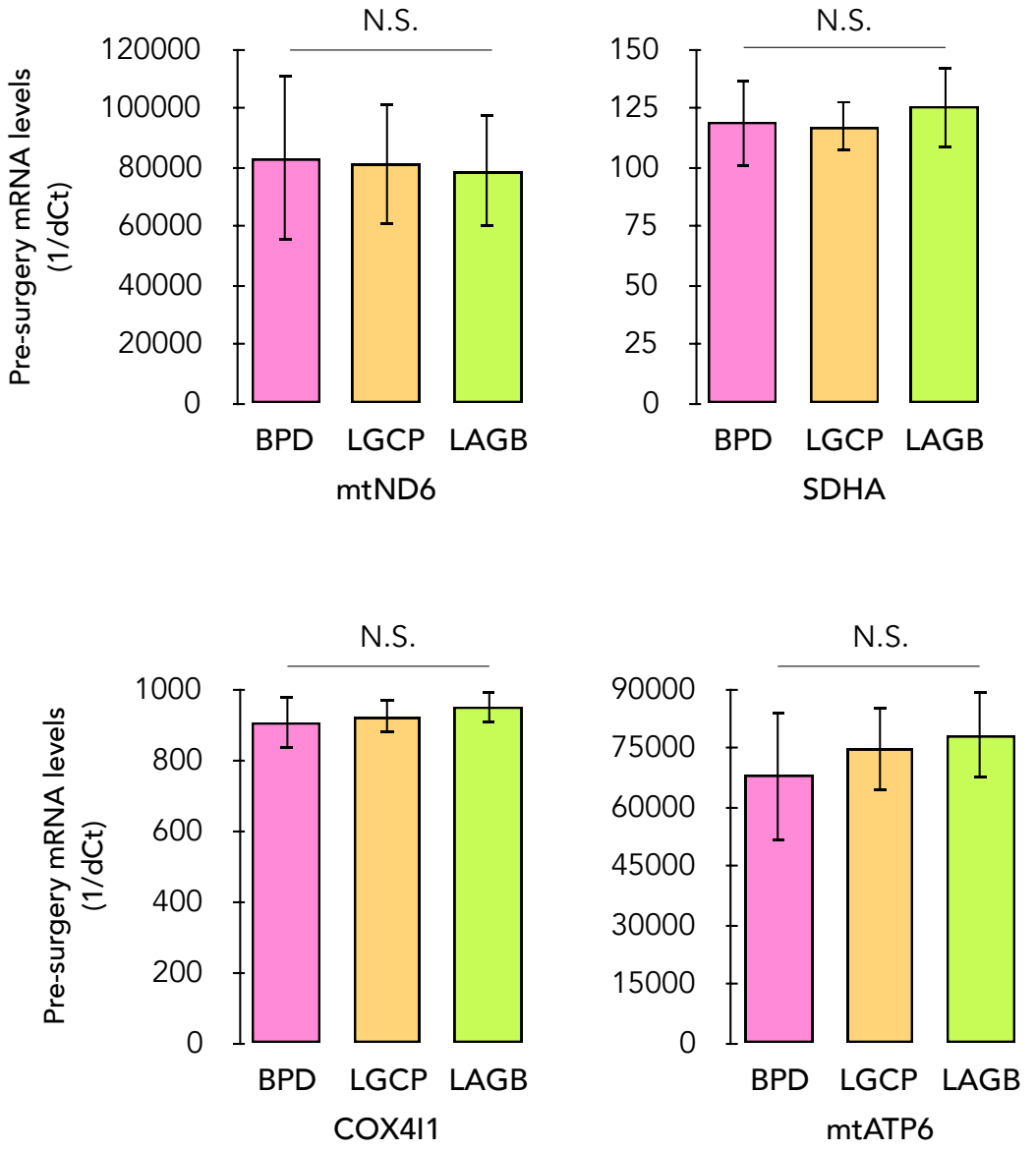

Figure 3.5: Pre-surgery comparison of genes involved in oxidative phosphorylation
Pre-surgery adipose tissue mRNA levels of genes involved in Oxidative Phosphorylation for each surgical cohort due to undergo either Bilio-pancreatic diversion (BPD), laparoscopic greater curvature plication (LGCP) or laparoscopic adjustable gastric banding (LAGB). Data is expressed as $^{1}/_{\triangle Ct}$. *Bars represent means* $\pm$ *standard error of the mean. One way ANOVA was used to determine differences between surgeries. N.S. denotes differences shown were not statistically significant (p>0.05). mtND6: mitochondrially-encoded NADH dehydrogenase 6; SDHA: Succinate Dehydrogenase Complex Flavoprotein Subunit A; COX4I1: Cytochrome c oxidase subunit 4 isoform 1; mtATP6: Mitochondrially-encoded ATP Synthase 6.*

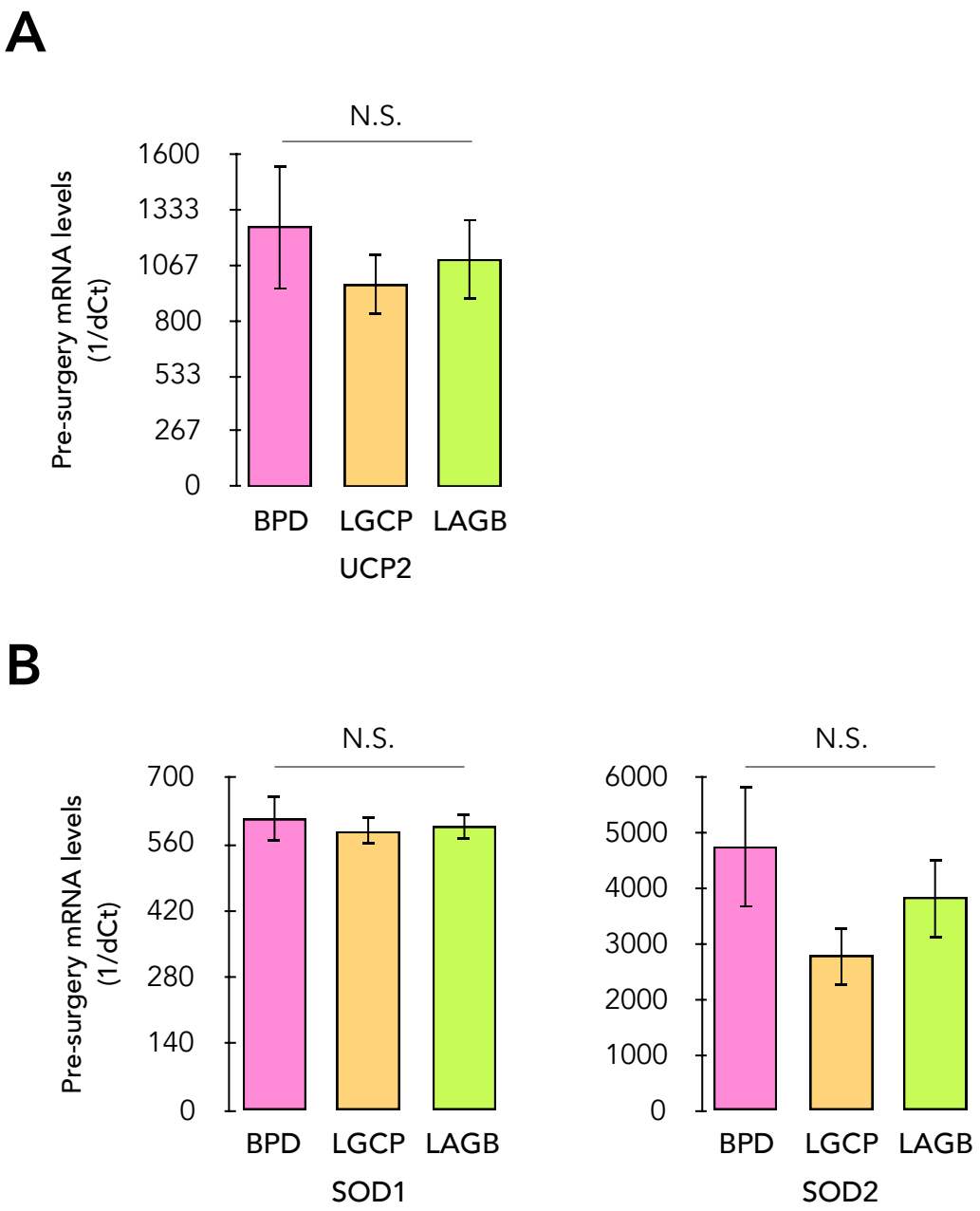

Figure 3.6: Pre-surgery comparison of genes involved in reactive oxygen species clearance

*Pre-surgery adipose tissue mRNA levels of genes involved in reactive oxygen species clearance (**A**, uncoupling and **B**, endogenous antioxidant action) for each surgical cohort due to undergo either Bilio-pancreatic diversion (BPD), laparoscopic greater curvature plication (LGCP) or laparoscopic adjustable gastric banding (LAGB). Data is expressed as $^{1}/_{\triangle Ct}$. Bars represent means $\pm$ standard error of the mean. One way ANOVA was used to determine differences between surgeries. N.S. denotes differences shown were not statistically significant (p>0.05). UCP2: Uncoupling protein 2; SOD1: Superoxide dismutase 1; SOD2: Superoxide dismutase 2.*

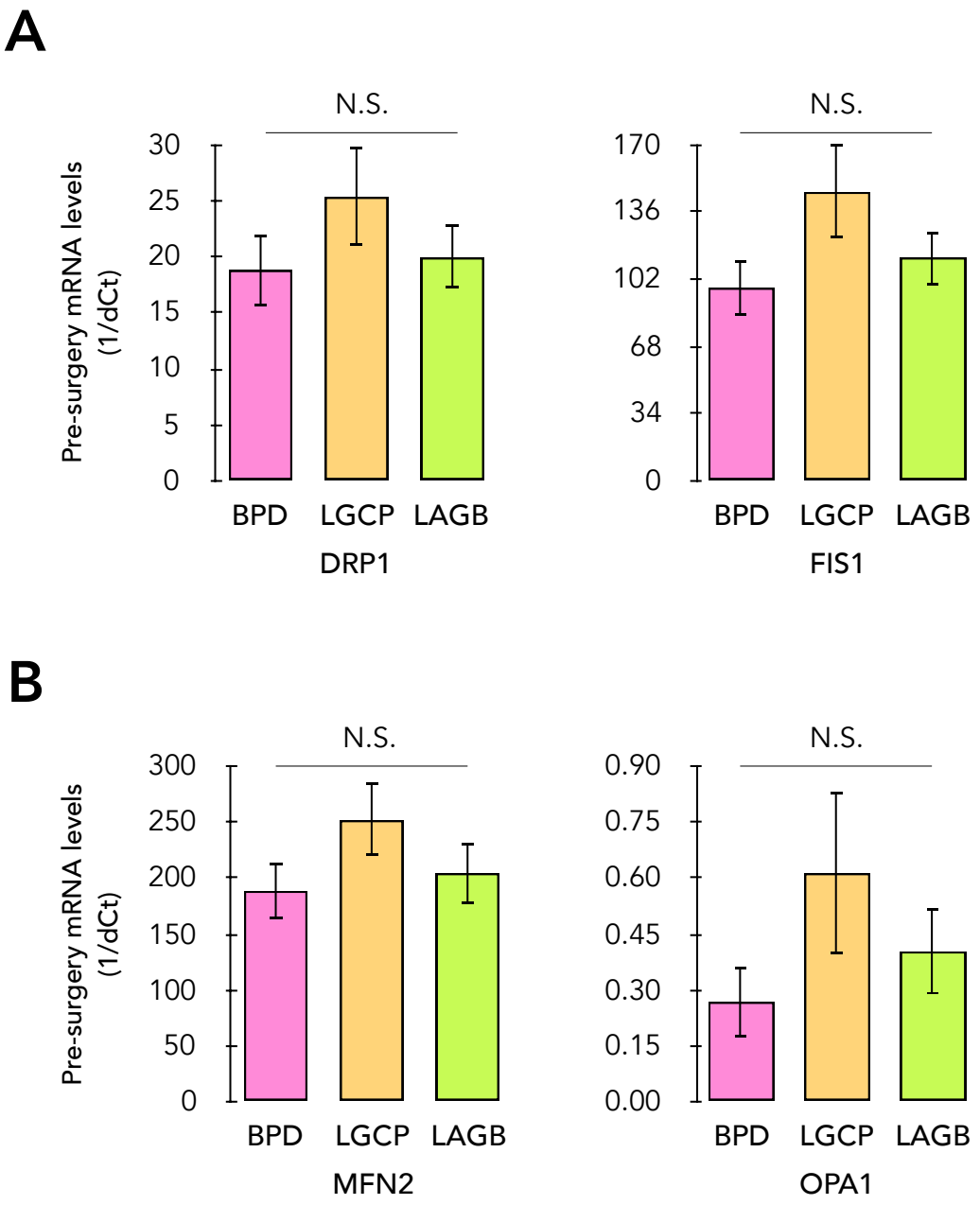

Figure 3.7: Pre-surgery comparison of genes involved in mitochondrial dynamics
*Pre-surgery adipose tissue mRNA levels of genes involved in mitochondrial dynamics (**A**, fission and **B**, fusion) for each surgical cohort due to undergo either Bilio-pancreatic diversion (BPD), laparoscopic greater curvature plication (LGCP) or laparoscopic adjustable gastric banding (LAGB). Data is expressed as $^{1}/_{\triangle Ct}$. Bars represent means $\pm$ standard error of the mean. One way ANOVA was used to determine differences between surgeries. N.S. denotes differences shown were not statistically significant ($p>0.05$). MFN2: Mitofusin 2; OPA1: mitochondrial dynamin like GTPase; DRP1: Dynamin-1-like protein; FIS1: Mitochondrial fission 1 protein.*

Gene expression levels post-surgery are shown in Figure 3.8 as fold-change of pre-surgery values. In general, mitochondrial gene mRNA levels were higher after the BPD procedure than the LGCP or LAGB operations. This was particularly

evident with oxidative phosphorylation (SDHA, COX4I1 and mtATP6), reactive oxygen species clearance (UCP2 and SOD2) and fusion (OPA1) genes, and would suggest a surgery-specific difference in bioenergetic efficiency, antioxidant capacity and mitochondrial quality control.

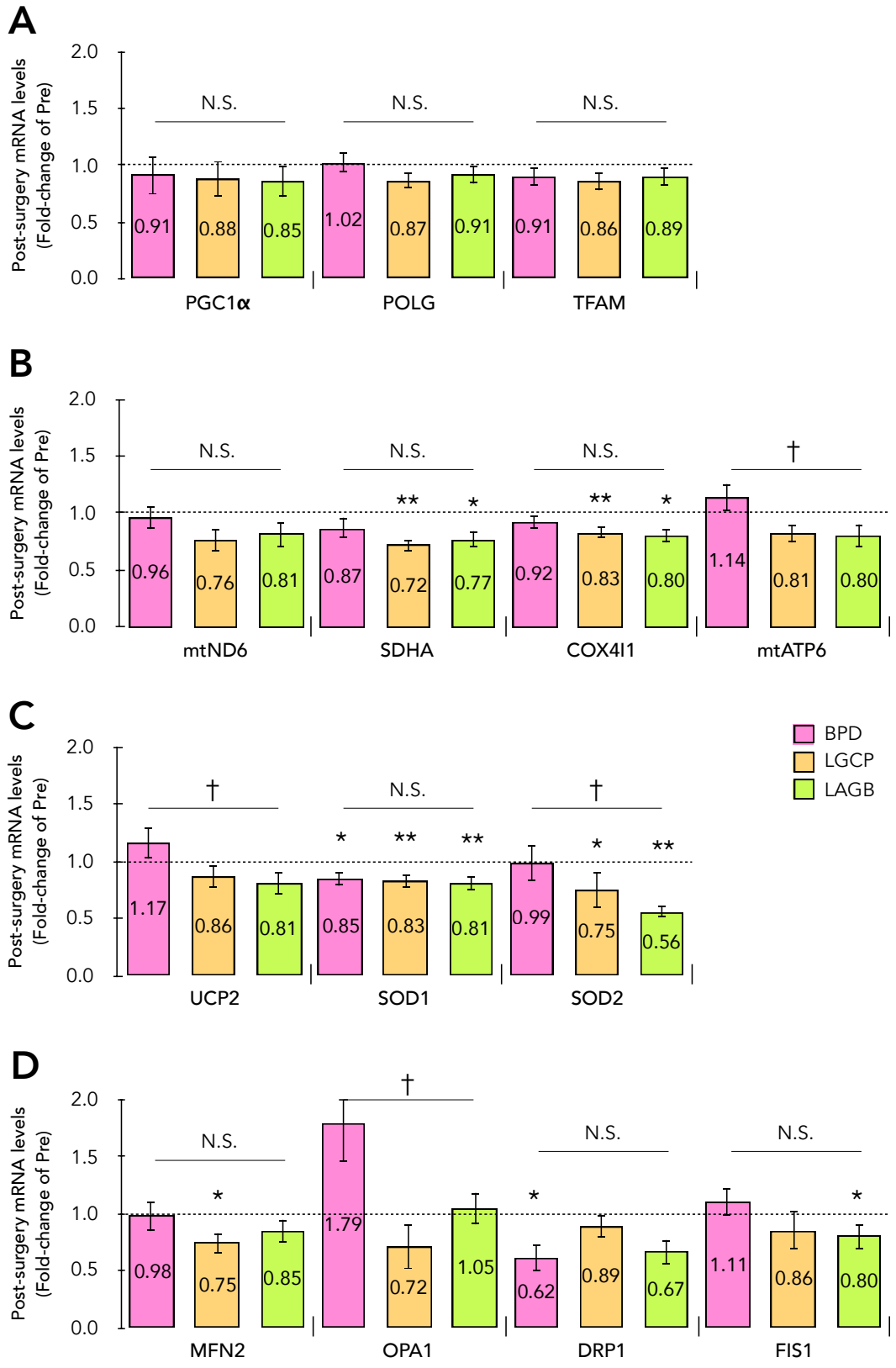

Figure 3.8: Effect of bariatric procedure on mitochondrial gene expression in adipose biopsies

*Surgery-induced changes in adipose tissue mRNA expression of genes involved in mitochondrial biogenesis (**A**), oxidative phosphorylation (**B**), reactive oxygen species clearance (**C**), and dynamics (**D**) for each surgical procedure: BPD, LGCP or LAGB. Data is expressed as fold-change of pre-surgical values (shown as dotted line). Bars represent means ± standard error of the mean. Pre-to-post surgical differences were determined via 2-tailed paired t-test (*p<0.05, **p<0.01). One way ANOVA was used to determine differences between surgeries (†p<0.05).*

The effect of each surgery on mitochondrial number in adipose biopsies was also analysed by comparing mitochondrial DNA relative to gDNA levels (Figure 3.9). Mitochondrial number did not differ significantly between cohorts prior to surgery (Figure 3.9**A**), however surgery-specific effects on mitochondrial number were observed post-surgery (Figure 3.9**B**). Whilst the LGCP and LAGB procedures seemingly lowered the number of mitochondrial DNA copies in adipose biopsies, no such effect was observed with the BPD procedure.

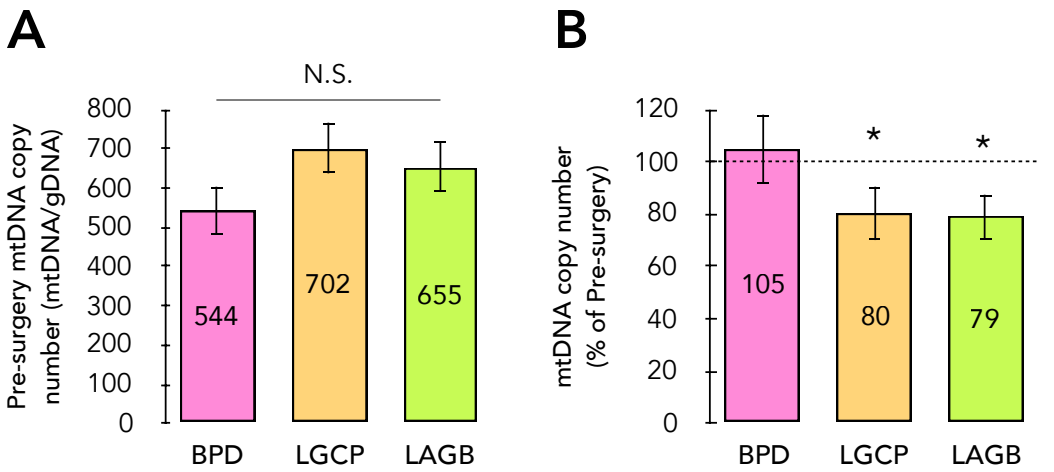

Figure 3.9: Effect of bariatric procedure on mitochondrial number in adipose biopsies

*Surgery-induced changes in adipose tissue mitochondrial DNA copy number before (**A**), and after (**B**) each surgical procedure: Bilio-pancreatic diversion (BPD), laparoscopic greater curvature plication (LGCP) or laparoscopic adjustable gastric banding (LAGB). Data is expressed as $^{1}/_{\triangle Ct}$ of mitochondrial target relative to nuclear for **A**, and as percentage change of pre-surgical values (shown as dotted line) for **B**. Bars represent means ± standard error of the mean. Pre-to-post surgical differences were determined via 2-tailed paired t-test (*p<0.05, **p<0.01). One way ANOVA was used to determine differences between surgeries (†p<0.05). N.S. denotes differences shown were not statistically significant (p>0.05).*

In order to further examine the overall impact of each surgery on adipose mitochondrial functionality, surgery-induced changes in genes involved in mitochondrial function (biogenesis, oxidative phosphorylation, uncoupling, and antioxidant capacity) and dynamics (fission and fusion) were compared to the changes observed in mitochondrial number using Pearson correlation analyses. In genes controlling function, these relationships were significantly positive after BPD surgery across 9

of 10 genes assessed, whilst significantly negative for 7 genes after LGCP surgery, and absent for all genes after the LAGB procedure (Table 3.4). Analysis of mitochondrial dynamics genes revealed significant correlations in genes involved in both fusion and fission processes within the BPD cohort. These relationships were absent in the LGCP group and present only for fusion genes in the LAGB group, indicating that the control of mitochondrial function and dynamics differed with the type of surgical procedure.

Table 3.4: Relationship of mitochondrial number to mitochondrial function and dynamics genes after BPD, LGCP and LAGB bariatric procedures

	Mitochondrial number vs.	**BPD** ($n = 12$)	**LGCP** ($n = 15$)	**LAGBP** ($n = 12$)
Function	PGC1α	0.794**	−0.688**	−0.175
	POLG	0.867**	−0.407	0.035
	TFAM	0.479	−0.560*	−0.154
	mtND6	0.758*	−0.613*	−0.153
	SDHA	0.855**	−0.600*	−0.056
	COX4I1	0.939**	−0.442	0.147
	mtATP6	0.782**	−0.547*	0.056
	UCP2	0.818**	−0.389	0.063
	SOD1	0.842**	−0.604*	0.098
	SOD2	0.696*	−0.576*	−0.017
Dynamics	MFN2	0.983**	−0.493	0.939*
	OPA1	0.808*	−0.202	0.963*
	DRP1	0.302	−0.426	0.669
	FIS1	0.871*	−0.337	0.209

*Table shows Pearson´s correlation coefficient between mitochondrial number and genes involved in mitochondrial biogenesis (PGC1α, POLG, TFAM), oxidative phosphorylation (mtND6, SDHA, COX4I1, mtATP6), uncoupling (UCP2), antioxidant function (SOD1, SOD2), fusion (MFN2, OPA1) and fission (DRP1, FIS1) processes. Correlations were calculated using change variables (pre to 6-months post-surgery percentage change). Negative correlations are shown in red. *p<0.05, **p<0.01. BPD: bilio-pancreatic diversion, LGCP: laparoscopic greater curvature plication, LAGB: laparoscopic adjustable gastric banding. PGC1α: Peroxisome proliferator-activated receptor gamma coactivator 1-alpha, POLG: mitochondrial DNA polymerase gamma catalytic subunit, TFAM: mitochondrial transcription factor A, mtND6: mitochondrially-encoded NADH dehydrogenase 6, SDHA: Succinate dehydrogenase complex subunit A, COX4I1: Cytochrome c oxidase subunit 4 isoform 1 (complex IV), mtATP6: mitochondria-DNA-encoded ATP synthase subunit 6 (complex V), UCP2: uncoupling protein 2, SOD1: superoxide dismutase 1, SOD2: Superoxide dismutase 2, MFN2: Mitofusin 2; OPA1: mitochondrial dynamin like GTPase; DRP1: Dynamin-1-like protein; FIS1: Mitochondrial fission 1 protein.*

Mapping Surgery-Specific Differences in Mitochondrial Functionality to Clinical Indicators of Metabolic Health

In order to further understand the factors contributing to the surgery-specific mitochondrial differences observed, their relationship with the metabolic variables that varied the most between surgical procedures were examined, including: excess weight loss (EWL), body mass index (BMI), serum HbA1c and serum total cholesterol (Table3.5). Most of these analyses returned non-significant relationships however, total serum cholesterol was identified to have a significant association accross all surgeries with two mitochondrial genes: mitochondrially-encoded ATP synthase 6 (mtATP6) and uncoupling protein 2 (UCP2). Shown as scatterplots in Figure 3.10, these relationships show that higher total cholesterol in serum was associated with lower expression of both mtATP6 and UCP2 genes, and that the BPD procedure generally had lower cholesterol with higher mitochondrial gene expression than the LGCP and LAGB procedures. These findings are consistent with the notion that greater lipid toxicity may be the cause of surgery-specific differences observed in mitochondrial functionality.

Table 3.5: Relationship of mitochondrial variables with clinical indicators of metabolic health

		EWL		BMI		HbA1c		Total Cholesterol	
		r	p	r	p	r	p	r	p
	mt number	−0.083	0.629	0.078	0.649	0.039	0.825	−0.120	0.486
Function	PGC1α	−0.124	0.428	0.101	0.520	0.045	0.775	−0.038	0.810
	POLG	0.072	0.647	−0.061	0.697	−0.002	0.990	−0.118	0.450
	TFAM	0.013	0.936	0.010	0.948	0.027	0.863	−0.138	0.376
	mtND6	−0.027	0.867	−0.024	0.880	0.002	0.989	−0.189	0.371
	SDHA	0.097	0.535	−0.126	0.422	−0.117	0.462	−0.089	0.571
	COX4I1	0.121	0.441	−0.157	0.315	−0.071	0.655	−0.181	0.246
	mtATP6	0.129	0.408	−0.203	0.192	−0.151	0.340	−0.318	0.038*
	UCP2	0.162	0.298	−0.200	0.198	−0.015	0.927	−0.343	0.024*
	SOD1	0.118	0.450	0.067	0.668	0.112	0.478	−0.018	0.909
	SOD2	0.131	0.404	−0.174	0.264	0.055	0.730	−0.259	0.093
Dynamics	MFN2	0.005	0.980	−0.012	0.950	−0.163	0.407	−0.085	0.662
	OPA1	−0.042	0.831	0.067	0.731	0.220	0.260	−0.198	0.303
	DRP1	−0.138	0.483	0.205	0.295	−0.005	0.980	0.192	0.327
	FIS1	0.124	0.523	−0.153	0.429	−0.016	0.935	0.067	0.728

*Table shows Pearson´s correlation coefficient (r) and p value significance (p) between metabolic and mitochondrial variables in the entire patient cohort (n=39). Correlations were calculated using change variables (pre to 6-months post-surgery percentage change). Significant correlations are shown in red. *p<0.05. EWL: excess weight loss, BMI: body mass index, HbA1c: serum glycosylated haemoglobin, PGC1α: Peroxisome proliferator-activated receptor gamma coactivator 1-alpha, POLG: mitochondrial DNA polymerase gamma catalytic subunit, TFAM: mitochondrial transcription factor A, mtND6: mitochondrially-encoded NADH dehydrogenase 6, SDHA: Succinate dehydrogenase complex subunit A, COX4I1: Cytochrome c oxidase subunit 4 isoform 1 (complex IV), mtATP6: mitochondria-DNA-encoded ATP synthase subunit 6 (complex V), UCP2: uncoupling protein 2, SOD1: superoxide dismutase 1, SOD2: Superoxide dismutase 2, MFN2: Mitofusin 2; OPA1: mitochondrial dynamin like GTPase; DRP1: Dynamin-1-like protein; FIS1: Mitochondrial fission 1 protein.*

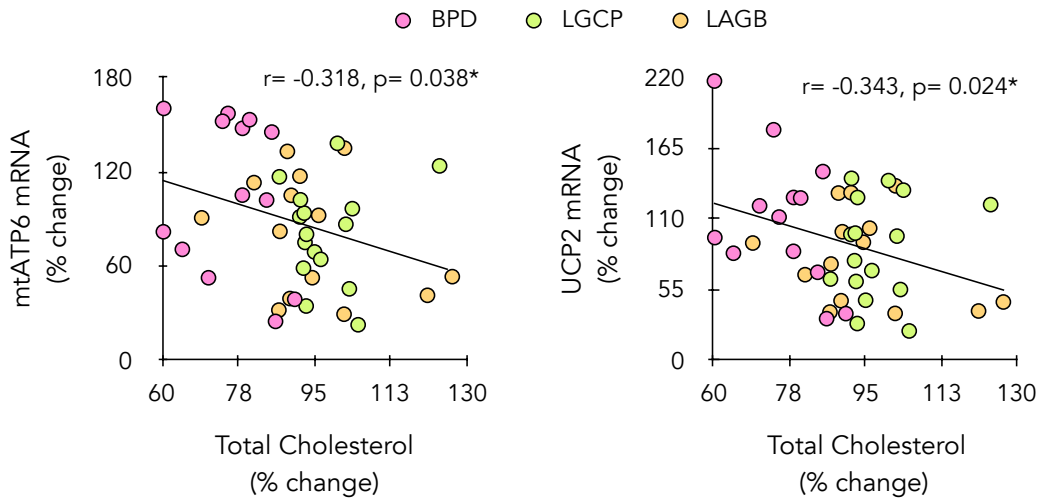

Figure 3.10: Association of total serum cholesterol with adipose mitochondrial genes

Scatter plots of total serum cholesterol correlated against mitochondrial genes mtATP6 (oxidative phosphorylation) and UCP2 (reactive oxygen species clearance). Correlations were calculated using change variables (percentage of pre levels) in the entire patient cohort (n=39), but individual data points are color-coded according to surgical procedure: Bilio-pancreatic diversion (BPD), laparoscopic greater curvature plication (LGCP) or laparoscopic adjustable gastric banding (LAGB). Linear trend line is also shown with Pearson correlation statistic (r) and significance (p).

3.4 Discussion

The present study hypothesized that caloric restriction (as evidenced by weight loss) through bariatric surgery would be accompanied by beneficial effects on adipose tissue mitochondria, supporting systemic metabolic recovery. To investigate this hypothesis, genes controlling a wide range of mitochondrial functions (biogenesis, oxidative phosphorylation, antioxidant, uncoupling, fusion and fission) were investigated. The BPD procedure lead to a tighter control of mitochondrial gene expression than LGCP or LAGB in association with greater weight, lipid and HbA1c reduction. These findings highlighted for the first time that (1) mitochondrial maladaptation may be reversed through bariatric intervention, dependent on (2) the type of procedure (BPD, LGCP and LAGB) which may influence (3) the degree of caloric and nutritional restriction. The BPD procedure which was the only procedure where mitochondrial recovery was evident, was also the surgery to result in the greater improvement of weight loss, HbA1c and dyslipideamia.

Whilst bariatric surgery *per se*, is currently the most effective treatment for severe obesity, associated with substantial and sustained weight loss, coupled with long-term T2DM remission in the majority of cases [271, 174], the type of bariatric surgical intervention given also appears to be an important factor affecting the degree and spectrum of improvements in metabolic parameters. In this present study, weight loss and thus HbA1c improvement rates were greater following the BPD procedure compared with LGCP and LAGB surgeries. These outcomes affirm previous research [174], reporting excess weight loss ranging from 15-25% excess weight loss after LAGB, to 30-40% after BPD/DS, where the highest mean weight loss achieved is also the strongest predictor of T2DM remission [272, 274, 275,

273].

The finding that regulation of mitochondrial genes were significantly improved only in patients who also exhibited the greater metabolic improvements (as is the case of the BPD group), would seem to reinforce the concept that adipose mitochondria play an important role in systemic metabolic health. Following the BPD procedure alone, mitochondrial number was significantly and positively correlated with mRNA expression of most genes assayed, covering a range of mitochondrial (biogenesis, oxidative phosphorylation, uncoupling, antioxidant and quality control) functions, whilst after the LGCP and LAGB surgeries they appeared dysregulated. These mitochondrial differences may have severe functional implications for the adipose tissue at large. The genes MFN2, OPA1, DRP1 and FIS1 together allow the isolation and autophagic elimination of damaged mitochondria [29, 296], and are essential to maintaining mitochondrial quality and function [236]. Furthermore the long-term inhibition of DRP1 and OPA1, which may be induced through nutrient excess [278, 279], may also lead to accumulation of irreversibly damaged mitochondria [29], which may in turn lead to pro-inflammatory cytokine production [283] and impaired insulin signaling [284, 285].

Interestingly, despite similar HbA1c reduction rates between LGCP and BPD (once BMI is accounted for), mitochondrial recovery was evident in BPD alone, with the only measured differential factor being lipidaemic improvement in BPD, though not LGCP. One interpretation of this result would be that mitochondrial recovery is related to diet and specifically caloric restriction, which may ease mitochondrial stress caused by excess nutrient delivery and improve the lipid buffering capacity of adipose depots (evidenced by an improved lipid profile). In accord with this con-

cept, BPD is the only bariatric procedure shown to severely inhibit macronutrient absorption [176, 183], and thus induce the more severe caloric deficit (as evidenced by greater rates of weight loss). Similar mitochondrial benefits have also been reported through hypo-caloric dietary intervention, where some mitochondrial, glucose and lipid metabolism modifications occur after very and moderately low calorie diets [179, 297, 298]. Taken together these data suggest that the severity and duration of the caloric deficit may provide the basis to support mitochondrial recovery, which in human subjects may be better sustained through surgery rather than lifestyle interventions and ultimately lead to the better metabolic recovery.

This study has certain limitations, namely: (1) though subjects of this study did not follow a particular dietary regimen and led a relatively sedentary lifestyle in the period before surgery, these two factors were not controlled either before or after surgery; and (2) despite the prospective study design, it is not possible to clarify in the context of this study whether the observed mitochondrial improvements are the cause or consequence of metabolic recovery, or indeed whether other factors either dependent or independent of weight are at play. Thus, further research is required to clarify these points.

In summary, ensuring that mitochondria are able to cope with the demand of excess nutrients is critical for both functional adipose function and its lipid buffering capacity. Indeed, in conditions of chronic nutrient excess, such as obesity and T2DM, mitochondria become inefficient and dysfunctional. However, these findings suggest that nutrient-induced mitochondrial maladaptation may be reversed through certain bariatric procedures in association with degree of weight loss and dyslipidaemic improvement. Ultimately these data suggest that mitochondrial function

in adipose tissue is closely dependent on overall metabolic health and further understanding of its role during metabolic recovery of adipose tissue may be key in reducing long-term damaging effects on peripheral metabolism.

Chapter 4

Role of Gut-hormone FGF-19 on Adipose Mitochondria Recovery Post Bariatric Surgery

---

4.1 Introduction

A key factor in the development of type-2 diabetes and metabolic syndrome is the inability of adipose tissue to cope with the chronic insult of over-nutrition, whilst maintaining important metabolic and endocrine functions [299, 150]. At the forefront of this challenging environment are mitochondria, major nutrient sensors and metabolic regulators, which are fundamental to adipose tissue function [276, 277]. However, during sustained conditions of chronic nutrient excess, such as obesity and type-2 diabetes, mitochondria appear unable to cope well with this environment, leading to fragmentation, unresponsiveness and dysfunction [287, 236, 280]. This nutrient-induced mitochondrial dysfunction can lead to impaired respiration, lipotoxicity, oxidative species accumulation and inflammation; further exacerbating insulin resistance and type-2 diabetes [281, 283, 284, 285]. Indeed, the importance of adequate mitochondrial function for metabolic health is further highlighted by the observation that mitochondrial DNA mutations often result in diabetic phenotypes [300, 301, 302].

Both insulin resistance and type-2 diabetes status can be reversed through bariatric surgery, with significantly greater success rates than pharmacological, exercise, and diet interventions [271, 273, 174]. Depending on the procedure, bariatric surgery involves a type/degree of gastro-intestinal remodeling, which can lead to reduced stomach volume and nutrient absorption capacity [303, 304]; however, this alone cannot fully explain the profound weight loss and metabolic improvement observed after these surgeries versus medical/lifestyle interventions [178].

Recently, the ileal-derived hormone, fibroblast growth factor 19 (FGF-19), has been identified as a novel enterokine regulator of glucose and lipid homeostasis which

is potentially involved in the metabolic recovery following bariatric surgery [305]. Indeed, rodent studies have shown that mice lacking the receptor required for gut secretion of FGF-19 show significantly impaired weight loss and glucose improvement following bariatric surgery compared with their wild-type counterparts [306]. In addition, direct administration of recombinant FGF-15 (FGF-19 in humans) to obese mice leads to significant weight reduction, principally AT reduction, and reverses dietary and leptin-deficient diabetes [307]. Moreover, in humans, data from clinical studies would seemingly indicate FGF-19 as a cause rather than consequence of type-2 diabetes improvement, given that neither lifestyle interventions nor intense medical management of type-2 diabetes appears to increase circulating FGF-19 levels, despite similar reductions in HbA1c to surgical procedures [308]. Furthermore, there is good clinical evidence that certain bariatric procedures increase serum FGF-19 levels [31, 309, 310]. As such, both human and rodent studies suggest that increased circulating FGF-19 levels may contribute to the underlying mechanisms of metabolic improvement following certain types of bariatric surgery. Beyond the potential effects on white adipose tissue, studies have shown FGF-19 to exert several advantageous effects on various metabolic relevant organs [305]. In the central nervous system, FGF-19 has been associated with lowered brain-hedonistic responses, reduced food intake, improved glycaemic control and enhanced glucose effectiveness [311, 306]. Furthermore, in the liver, FGF-19 has been shown to increase energy expenditure and fatty acid oxidation through raised delivery of fatty acids to the mitochondria [312]. Additionally, in brown adipose tissue, elevated FGF-19 (either through genetic over-expression or systemic administration) can affect the metabolic rate and activity of this highly energy-consuming

tissue [307, 312]. These studies also highlight the importance of mitochondria as a target of FGF-19 [307, 311, 306, 312], although its role in white adipose tissue mitochondria, particularly within the context of type-2 diabetes, remains largely unknown. In Chapter 3, evidence was outlined that suggests that only some bariatric procedures (namely BPD) result in recovery of white adipose mitochondria from severely obese type-2 diabetic individuals. In this present chapter, the hypothesis is investigated that changes in serum FGF-19 levels after bariatric surgery influence this multifactorial recovery and thus impact overall metabolic recovery.

4.2 Methods

Ethics and Study Design

Thirty-nine morbidly obese (BMI>35 Kg/m2), type-2 diabetic, Caucasian women undergoing either bilio-pancreatic diversion (BPD; n=12), laparoscopic greater curvature plication (LGCP; n=15), or laparoscopic adjustable gastric banding (LAGB; n=12) were recruited to participate in this study. Fasted bloods and anthropometric investigations were conducted before (baseline) and following surgery with collection of serum samples and abdominal subcutaneous white adipose tissue (AT) biopsies at both of these time points. Patients on pharmacological treatment with incretin mimetics and/or insulin were not included in this study. For further detail the reader is referred to Chapter 2.

Blood Biochemistry and Anthropometry

All anthropometric and biochemical measurements were performed before and six months after surgery. For detail on blood, adipose tissue sample and other clinical data collection, please see Chapter 2.

RNA isolation and qRT-PCR

Gene expression of mitochondrial genes was assayed through quantitative real-time polymerase chain reaction (qRT-PCR) using subcutaneous white adipose tissue biopsies before and 6 months after bariatric surgery. For detail on primer sequences used in this study the reader is referred to Table 2.1. For further detail please see Chapter 2.

Mitochondrial DNA copy number assay

Mitochondrial (*mtND1*) and nuclear (*BECN1*) gene primers (Table2.2) were used via qRT-PCR to determine relative amounts of mitochondrial to nuclear DNA as a measure of mitochondrial number per adipocyte[266] within subcutaneous white adipose tissue biopsies. For further detail on methods, the reader is referred to Chapter 2.

FGF-19 Serum Levels

For measurement of serum FGF-19 levels (pg/mL), an enzyme-linked immunosorbent assay (ELISA) kit for FGF-19 (Quantikine ELISA, R&D Systems, Minneapolis, MN) was used. All measurements were performed in duplicate according to the manufacturers instructions. This assay has a detection range of 31-544 pg/mL and a coefficient of variation of 4.5% for intra-assay and 5.5 % inter-assay precision.

Statistical Analysis

Statistical analyses were performed using the SPSS 21.0 software. Data are reported as mean $\pm$ standard deviation (SD), unless otherwise specified. Data were examined for normality according to the Shapiro-Wilks criteria. Comparisons between pre- and post-surgery time-points were performed via paired two-tailed t-tests (if parametric) and the Wilcoxon signed ranks test (if non-parametric). For categorical data, Fisher´s exact test was used. Between-group (surgery type) differences were assessed using One-way ANOVA (if parametric) and Kruskal-Wallis test (if non-parametric) using change variables, calculated as percentage change from pre-surgery values [(post/pre) x100]. For Pearson correlation analyses, change

variables [(post/pre) x100] were log-transformed prior to analysis if non-parametric.

4.3 Results

Differential Effect of Bariatric Procedure on Circulating Levels of Gut Hormone FGF-19

Serum levels of gut-hormone FGF-19 were measured before and 6 months after each bariatric procedure, and descriptive statistics for this data are sumarised in Table 4.1.

Table 4.1: Comparisons of surgery-induced changes in serum FGF-19 levels between BPD, LGCP and LAGB bariatric procedures

Bariatric procedure (n)	Percent of patients with increase (%)	Change from pre- to post-surgery (%)†	
		Mean (SD)	Median (IQR)
BPD (12)	58.3	158.90(180.60)	121.72(52.73 to 152.67)
LGCP (15)	73.3	181.32(209.65)	135.41(74.75 to 172.57)
LAGB (12)	16.7	60.03(29.23)*	61.84(43.39 to 72.56)*

*Table shows percentage of patients (%) who exhibited increased serum FGF-19 post-surgery relative to pre-surgery levels. The Wilcoxon signed ranks test was used for within group comparisons of pre and post-surgery levels (*p<0.05). †: The Kruskal-Wallis H test determined there were significant differences in serum FGF-19 between the three surgery types ($\chi 2$=7.655; p=0.022). SD: standard deviation, IQR: interquartile range, BPD: bilio-pancreatic diversion, LGCP: laparoscopic greater curvature plication, LAGB: laparoscopic adjustable gastric banding.*

A wide range in serum FGF-19 concentrations were found both before and after surgery. Pre-surgery levels of FGF-19 between BPD and LGCP cohorts were not significantly different however, they were found to be significantly higher in the LAGB cohort (Figure 4.1**A**). To control for this variability, post-surgery levels were analysed relative to the individual´s pre-surgery readings. The type of bariatric procedure was found to play an important role on whether FGF-19 levels increased or decreased post-surgery (as tested using the Kruskal Wallis H Test, p=0.018). Whilst the BPD and LGCP procedures both seemingly up-regulated FGF-19 levels in circulation in the majority of patients (58% in BPD and 73% in LGCP), the LAGB procedure resulted in their significant down-regulation (Figure 4.1**B**). Only

17% of patients who underwent the LAGB procedure exhibited raised post-surgical serum FGF-19 levels (Figure 4.1**C**). Thus, a step-wise surgery-specific effect on FGF-19 levels was observed (LGCP>BPD>LAGB).

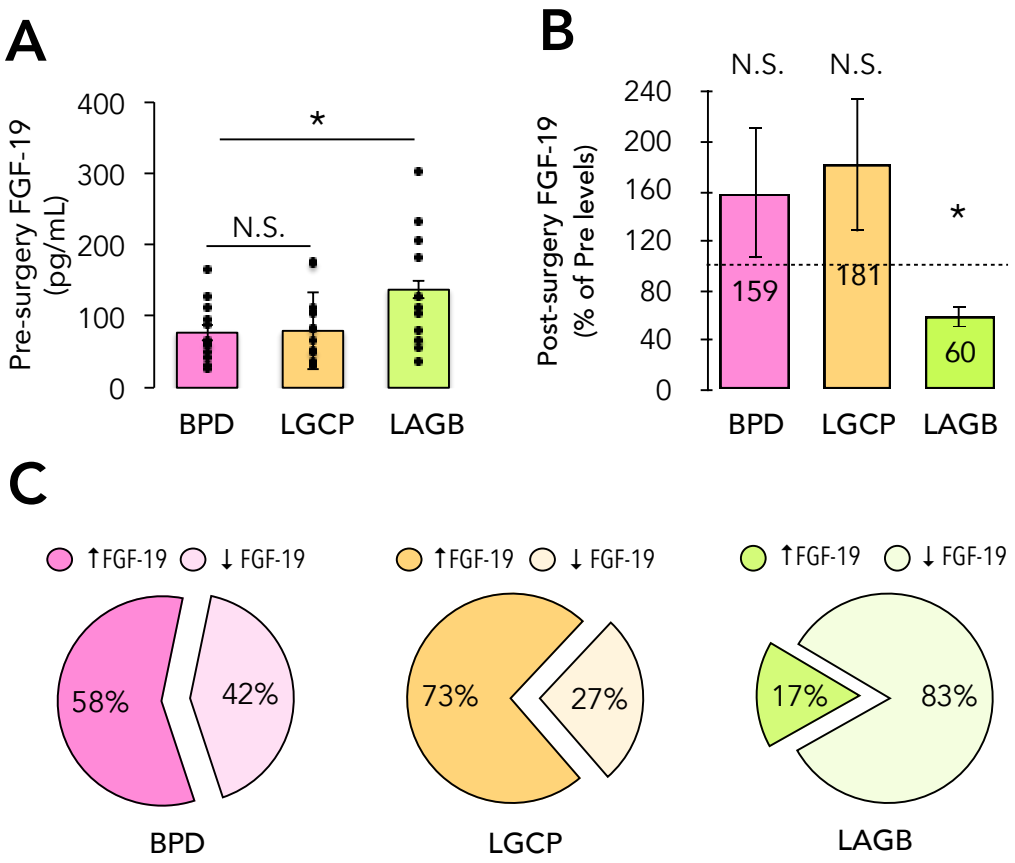

Figure 4.1: Surgery-specific effects on serum FGF-19 concentrations

*Pre- (**A**) and Post-surgery (**B**) serum concentrations of FGF-19 for each surgical procedure: Bilio-pancreatic diversion (BPD), laparoscopic greater curvature plication (LGCP) or laparoscopic adjustable gastric banding (LAGB). Post-surgery data is expressed as percentage of pre-surgical values (shown as dotted line). Pie charts (**C**) show the numerical proportion of FGF-19 increase or decrease for each surgical procedure. Bars represent means ± standard error of the mean, pie chart slices represent percentage of total subjects in each surgical cohort (BPD n=12, LGCP n= 15, LAGB n= 12). Pre-to-post surgical differences were determined via the Wilcoxon signed ranks test (*p<0.05, **p<0.01). The Kruskal-Wallis H test determined there were significant differences in serum FGF-19 between the three surgery types (†p<0.05). N.S. denotes differences shown were not statistically significant (p>0.05).*

Mapping Surgery-Specific Differences in Metabolic Recovery to Serum FGF-19 Levels

In order to ascertain whether FGF-19 may be a contributing factor to the procedure-specific differences in metabolic recovery, the surgery-induced changes in serum FGF-19 were examined against clinical indicators of metabolic health. As shown in Table 4.2, FGF-19 was not associated with any of the surgery-differential clinical variables, such as excess weight loss, BMI, HbA1c and total cholesterol. No association was observed between FGF-19 and age, waist-hip ratio, body fat percentage, glucose, HOMA IR, triglycerides or LDL cholesterol. However, serum FGF-19 levels were significantly associated with insulin, HDL cholesterol and HDL/LDL ratio (Figure 4.2). Higher levels of FGF-19 were also associated with increased serum insulin levels and HDL relative LDL cholesterol across all surgeries; however no clustering on the basis of procedure was evident. These results are therefore consistent with the notion that FGF-19 may participate in metabolic recovery, but does not support the hypothesis that it is involved in modulating superior metabolic outcomes observed with the BPD versus LGCP and LAGB procedures.

Table 4.2: Relationship of circulating FGF-19 levels with clinical indicators of metabolic health

	FGF-19	
	r	p
Age (y)	−0.051	0.556
EWL (%)	0.185	0.259
BMI ($^{Kg}/_{m^2}$)	−0.116	0.481
WHR	−0.060	0.721
Body fat (%)	−0.195	0.241
Glucose ($^{mmol}/_{L}$)	−0.139	0.399
Insulin ($^{pmol}/_{L}$)	0.344	0.032*
HOMA IR	0.084	0.614
HbA1c ($^{mmol}/_{mol}$)	−0.142	0.388
TGL ($^{mmol}/_{L}$)	0.290	0.073
T Chol ($^{mmol}/_{L}$)	0.066	0.688
LDL ($^{mmol}/_{L}$)	−0.044	0.790
HDL ($^{mmol}/_{L}$)	0.399	0.013*
HDL/LDL	0.489	0.002**

*Table shows Pearson´s correlation coefficient (r) and p value significance (p) between serum FGF-19 levels and metabolic variables in the entire patient cohort (n=39). Correlations were calculated using change variables (pre to 6-months post-surgery percentage change). Significant correlations are shown in red. *p<0.05. EWL: excess weight loss, BMI: body mass index, WHR: waist-hip ration, HOMA IR: homeostasis model assessment of insulin resistance, HbA1c: serum glycosylated haemoglobin, TGL: triglycerides, T Chol: total cholesterol, LDL: low-density lipoproteins, HDL: high-density lipoproteins.*

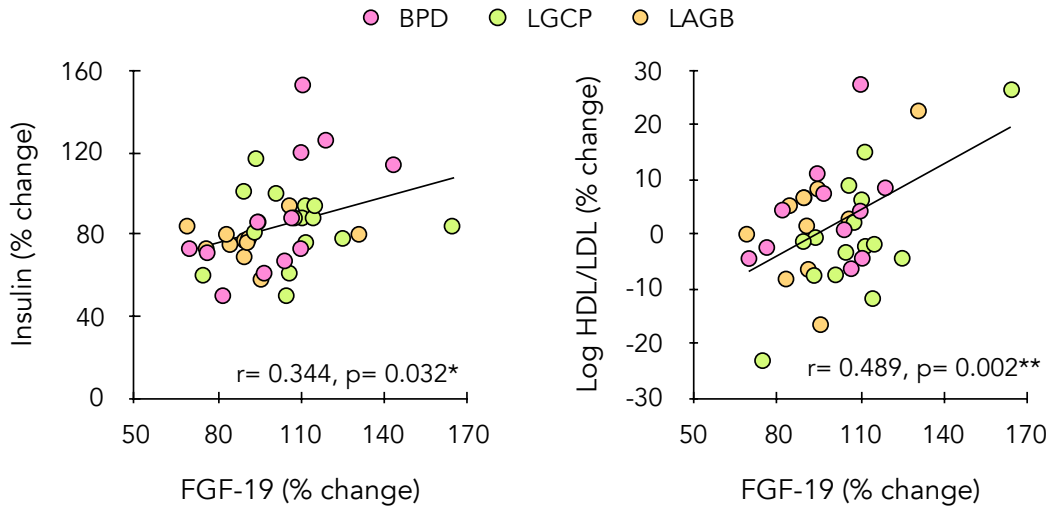

Figure 4.2: Association of serum FGF-19 levels with insulin and HDL/LDL ratio
Scatter plots show correlations of serum FGF-19 against insulin and HDL/LDL ratio. Correlations were calculated using change variables (percentage of pre levels) in the entire patient cohort (n=39), but individual data points are color-coded according to surgical procedure: Biliopancreatic diversion (BPD), laparoscopic greater curvature plication (LGCP) or laparoscopic adjustable gastric banding (LAGB). Linear trend line is also shown with Pearson correlation statistic (r) and significance (p). If non-parametric, variables were log-transformed prior to correlation analysis to improve normality.

Mapping Surgery-Specific Differences in Indicators of Adipose Mitochondrial Functionality to Serum FGF-19 Levels

Next, the question of whether FGF-19 is involved in modulating mitochondrial functionality in the adipose tissue was investigated, and if so, whether surgery-specific changes in FGF-19 may help explain the differential effect also observed in adipose mitochondrial functionality. To evaluate this, the relationship of FGF-19 against mitochondrial number and transcript levels were examined through Pearson correlation analyses. As shown in Table 4.3, no significant association was found between serum FGF-19 levels and any of the mitochondrial genes studied. Interestingly however, FGF-19 levels were significantly and inversely associated with mitochondrial DNA copy number in adipose biopsies (Figure 4.3). Higher levels of FGF-19 were associated with lower levels of mitochondrial number across all surgical cohorts, with no clustering on the basis of type of procedure observed. These results are therefore consistent with the notion that FGF-19 may play a role in modulating adipose mitochondrial function, however no evidence was found to support the hypothesis that FGF-19 is involved in modulating superior mitochondrial outcomes observed with the BPD versus LGCP and LAGB procedures.

Table 4.3: Relationship of circulating FGF-19 levels with indicators of adipose mitochondrial functionality

		FGF-19	
		r	p
	mt number	−0.428	0.014*
Function	PGC1α	−0.140	0.395
	POLG	−0.173	0.294
	TFAM	−0.194	0.288
	mtND6	−0.254	0.119
	SDHA	−0.177	0.282
	COX4I1	−0.234	0.151
	mtATP6	−0.250	0.125
	UCP2	−0.195	0.234
	SOD1	−0.055	0.738
	SOD2	−0.010	0.950
Dynamics	MFN2	−0.118	0.548
	OPA1	−0.027	0.892
	DRP1	0.214	0.283
	FIS1	−0.164	0.406

*Table shows Pearson´s correlation coefficient (r) and p value significance (p) between serum FGF-19 levels and mitochondrial variables in the entire patient cohort (n=39). Correlations were calculated using change variables (pre to 6-months post-surgery percentage change). Significant correlations are shown in red. *p<0.05. mt number: mitochondrial DNA copy number, PGC1α: Peroxisome proliferator-activated receptor gamma coactivator 1-alpha, POLG: mitochondrial DNA polymerase gamma catalytic subunit, TFAM: mitochondrial transcription factor A, mtND6: mitochondrially-encoded NADH dehydrogenase 6, SDHA: Succinate dehydrogenase complex subunit A, COX4I1: Cytochrome c oxidase subunit 4 isoform 1 (complex IV), mtATP6: mitochondria-DNA-encoded ATP synthase subunit 6 (complex V), UCP2: uncoupling protein 2, SOD1: superoxide dismutase 1, SOD2: Superoxide dismutase 2, MFN2: Mitofusin 2; OPA1: mitochondrial dynamin like GTPase; DRP1: Dynamin-1-like protein; FIS1: Mitochondrial fission 1 protein.*

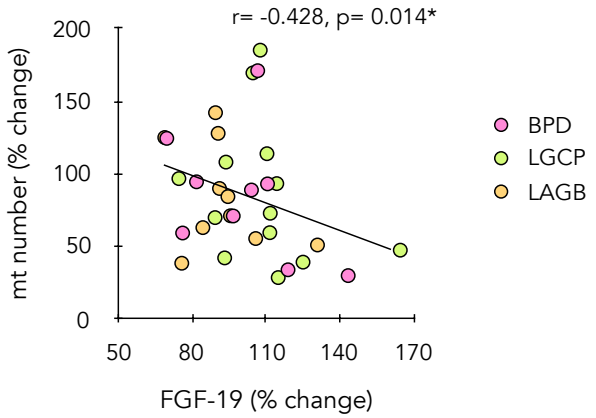

Figure 4.3: Association of serum FGF-19 levels with adipose mitochondrial number
Scatter plot showing correlation between serum FGF-19 and mitochondrial DNA copy number in adipose biopsies. Correlation was calculated using change variables (percentage of pre levels) in the entire patient cohort (n=39), but individual data points are color-coded according to surgical procedure: Bilio-pancreatic diversion (BPD), laparoscopic greater curvature plication (LGCP) or laparoscopic adjustable gastric banding (LAGB). Linear trend line is also shown with Pearson correlation statistic (r) and significance (p).

4.4 Discussion

As outlined in Chapter 3, only one type of bariatric procedure (BPD) was associated with adipose mitochondrial benefits, despite similar rates of weight loss-associated HbA1c improvement, suggesting there may be other factors altered by gut-remodeling specific to each surgery which may be influencing mitochondrial recovery in BPD but not LGCP or LAGB. One likely candidate influencing this dichotomous relationship is Gut-hormone Fibroblast Growth Factor-19 (FGF-19). Therefore, serum FGF-19 levels were measured before and after 3 bariatric procedures (BPD, LGCP and LAGB) and analysed against all anthropometric, biochemical and mitochondrial variables. Our findings confirm for the first time a differential impact between BPD, LGCP and LAGB bariatric procedures on circulating FGF-19 levels, with BPD and LGCP leading to similar significant rises in this hormone, in contrast to the LAGB surgery, which lowered serum FGF-19 levels. Despite these widely ranging effects, circulating FGF-19 was significantly and consistently associated with adipose mitochondrial number across all 3 surgical procedures investigated, adding credence to the notion that FGF-19 may target adipose mitochondrial function to improve metabolic health after bariatric surgery. The finding that FGF-19 levels are inversely correlated with mitochondrial number in AT may be interpreted as a shift towards a less fragmented and more elongated mitochondrial network when FGF-19 levels are raised. This would seem of benefit, given that mitochondrial fragmentation has been associated with apoptosis [313, 314], severely compromised mitochondrial DNA integrity, inefficiency [278, 279], accumulation of reactive oxygen species (ROS) [236], impaired oxygen consumption and ß-oxidation [280, 281], lipotoxic species accumulation [282], pro-

inflammatory cytokine production [283] and impaired insulin signaling [284, 285]. Moreover, fragmentation of muscle mitochondria has been reported in several mouse and human models of obesity and type-2 diabetes [245, 315].

However, it must also be stated that long-term sustained mitochondrial elongation can compromise mitochondrial quality control and function [29], so mitochondrial elongation *per se* is not necessarily indicative of mitochondrial health, and that the cell requires a balance between both fission and fusion processes to maintain mitochondrial quality. As shown in Chapter 3, genes controlling a wide range of mitochondrial functions were tightly correlated with mitochondrial number in BPD patients, whilst in the other surgeries they appeared dysregulated. This finding would support the assertion that BPD improves the control of genes involved in maintaining mitochondrial function to a greater extent than the other two bariatric procedures in this study, and is consistent with a role of serum FGF-19 in mediating a less fragmented and potentially more functional mitochondrial network.

In contrast, in the LGCP group the relationships between mitochondrial number and gene expression followed a significant inverse association, despite similar rise in serum FGF-19 levels compared to BPD. This seemingly paradoxical finding may be better understood within a wider context of additional factors also likely to play a role in mitochondrial recovery [277]. Indeed, the BPD operation (unlike LGCP) produced significantly lower serum lipids levels and nearly twice as much weight loss (30% versus 17%). This is consistent with both previous reports [316], and the notion that these two factors (weight loss and lipid recovery) may have also contributed to the enhanced mitochondrial outcomes observed after BPD versus LGCP. Further in support of this concept, total and HDL cholesterol were the only

biochemical variables (apart from FGF-19) to exhibit a significant association with mitochondrial genes. Decreased cholesterol levels were directly associated with enhanced mRNA expression of complex IV (COX4I1) and V (mtATP6) genes of the electron transport chain. Similar associations were observed with the uncoupling protein 2 (UCP2) gene, which has been implicated in preventing reactive oxygen species accumulation and oxidative stress damage [218].

Interestingly, in the LAGB group (the only study procedure to significantly reduce serum FGF-19 levels), changes in mitochondrial gene expression in AT were (with exception of fusion genes) unrelated to mitochondrial number, suggesting a dysregulation of mitochondrial function in this cohort, potentially resulting from unopposed fusion. Though this bariatric procedure resulted in significant weight loss and general metabolic improvement, the noted HbA1c reduction was significantly less pronounced compared with the other two procedures (even after accounting for BMI), which might be, at least in part, the result of the mitochondrial dysfunction and lower serum FGF-19 levels observed.

Previous studies in mice support the hypothesis that circulating FGF-19 targets white adipose mitochondria to exert metabolic improvements. Mice challenged with a high-fat diet and treated with fexaramine (an intestine-restricted FXR agonist which potently induces intestinal FGF-15, *i.e.* the mouse FGF-19 homologue) exhibited significantly less weight gain, systemic inflammation, and improved glucose homeostasis, with specific effects noted on visceral white adipose tissue, including: reduced activation of inflammatory and lipogenic pathways, browning of white adipocytes, and increased thermogenesis [317]. Though FGF-19 is known to exert several metabolically beneficial effects by its actions in the liver that regulate

glucose and cholesterol production [305], recent evidence in mice further suggests that the improvement of glucose homeostasis after recombinant FGF-15 treatment is likely due to direct signaling in AT and other metabolic relevant organs rather than through the known hepatic effects [318]. Furthermore, previous reports of positive correlations between circulating FGF-19 and adiponectin [319, 320] lend further credence to the role of FGF-19 as a regulator of white adipose tissue endocrine and metabolic function. In accordance with previous research, these findings support the hypothesis that FGF-19 targets white AT and provide evidence for the first time in humans that circulating FGF-19 levels strongly and inversely associate with mitochondrial fragmentation of this tissue.

It should be noted that, this study has certain limitations, namely: 1) though our study subjects did not follow a particular dietary regimen and led a relatively sedentary lifestyle in the period before surgery, these two factors were not controlled either before or after surgery; and 2) despite the prospective study design, it is not possible to clarify in the context of this study the precise mechanism by which each studied surgical procedure alters serum FGF-19 levels, thus further research is required to clarify this point. However, to our knowledge, this is the first study to compare serum FGF-19 levels between these bariatric surgical procedures and to provide evidence of differential mitochondrial and metabolic outcomes based on the type of surgical procedure.

In conclusion, elevated serum FGF-19 levels post-surgery were significantly associated with improved mitochondrial health in AT leading to greater control of mitochondrial gene regulation and overall type-2 diabetes remission. These increased FGF-19 levels were also observed to be surgery-specific with BPD pa-

tients achieving better metabolic health outcomes compared to LGCP and LAGB (BPD>LGCP>LAGB), and highlighting mitochondria in AT as a promising potential target of FGF-19 during diabetic recovery following bariatric surgery.

Chapter 5

Role of Gut-derived LPS on Adipose Mitochondria Recovery Post Bariatric Surgery

---

5.1 Introduction

Chapters 3 and 4 outlined evidence supporting the concept that FGF-19 targets adipose tissue mitochondria, leading to weight loss and metabolic recovery post bariatric surgery. The BPD procedure, which resulted in heightened serum FGF-19 levels, also produced the greater improvements in mitochondrial gene regulation, weight loss and overall type-2 diabetes remission. However, the procedure LGCP also produced similarly heightened serum FGF-19 levels but lacked the corresponding improvements in mitochondrial function. These data raises the question: which surgery-specific factors mediate the differences observed in mitochondrial and metabolic benefit? Gut-derived bacterial lipopolysaccharide (LPS) is a promising target of study for this question, as it is increased in circulation in association with over-nutrition (specifically lipids), has been extensively linked with inflammation and metabolic dysfunction [199, 200, 201, 321] and is likely to be altered by gut-remodeling [322]. Interestingly, a main difference between the two surgeries was greater lipid reduction and weight loss with BPD compared to LGCP or indeed LAGB.

LPS are major outer cell wall components of gram negative bacteria normally present in the gut, which may provide an interesting mechanistic link between the Western diet and metabolic disease (Figure 5.1). Due to their biochemical affinity, LPS are absorbed coupled to chylomicrons, and circulating levels increase in direct relationship with dietary fat absorption [196]. As little as a single high-fat, high-carbohydrate meal can raise serum LPS levels by 50% and generate systemic inflammation [323]. In addition, chronic intake of high-fat, high-carbohydrate meals can increase the gram-negative bacteria sub-population, and thus the gut

LPS load [324, 325, 326, 327, 32]. Therefore, both acute and chronic Western diets can generate systemic inflammation and initiate metabolic disease, through increased LPS absorption. Indeed, direct intravenous administration of LPS to healthy adults has been shown to reduce insulin sensitivity by 30% [328] and several cross-sectional studies have demonstrated that serum LPS levels function as independent predictors of type-2 diabetes incidence [199, 200, 201, 321].

The finding that diabetes rates in people with mitochondrial disease (known as mitochondrial diabetes) are more than four times higher (40%) than the rates in the average population (9%) provides strong evidence that mitochondrial functionality may be intrinsically linked with the pathophysiology of metabolic disease [329, 330, 331, 332, 333]. In addition to respiration and nutrient metabolism, mitochondria are the main cellular source of reactive oxygen species, closely involved in regulating several vital processes including inflammation and apoptosis [334, 294, 281, 283, 152, 335]. Thus, this study hypothesized that heightened LPS may have adverse direct and/or (through inflammation) indirect effects on adipose mitochondria functionality, impacting these tissues´ ability to buffer lipids away from other organs, and contributing to metabolic disease (Figure 5.1). As such, it could be considered that the difference in mitochondrial and metabolic outcomes outlined throughout Chapters 3 and 4 may be explained, at least in part, by differences in serum LPS levels.

It should be stressed that LPS can be difficult to measure reliably in serum because the concentration of (mostly unknown) LPS- neutralizing factors vary from individual to individual [336]. Furthermore, conventional LPS detection methods utilise Limulus Amebocyte Lysate (LAL) which whilst highly sensitive to LPS, can

carry several limitations. Mainly, the LAL-LPS reaction must occur whilst the sample matrix (which contain several inhibitory factors to varying quantities) is present. This limitation can be minimised to some degree by serial dilution and spiking the sample with increasing known amounts of LPS to determine degree of neutralizing factors, heat inactivation steps and the use of glass instead of plastic test tubes [337]. However, these measures are time-consuming and their success can be limited, although procedures can be put in place to minimise these issues. A newer method (EndoLISA®), is based on the recombinant factor C, which is a bacteriophage protein which specifically binds endotoxin onto a microtiter solid phase, allowing the sample matrix (with potentially interfering components) to be removed before the detection reaction takes place. Although not yet tested for use in serum samples, this new method may support a more reliable and less error-prone assessment of LPS than current LAL-based methods.

Therefore, this present chapter (1) compared the specificity and reliability of both methods, in order to use a suitable assay to (2) measure serum LPS levels before and 6-months after 3 bariatric surgeries: BPD, LGCP and LAGB. These set of studies specifically investigated whether BPD would lower serum LPS levels to a greater extent than the other bariatric surgeries, and thereby be associated as a result with superior metabolic and mitochondrial outcomes.

Figure 5.1: Gut-derived LPS links the Western diet with metabolic disease via mitochondrial dysfunction

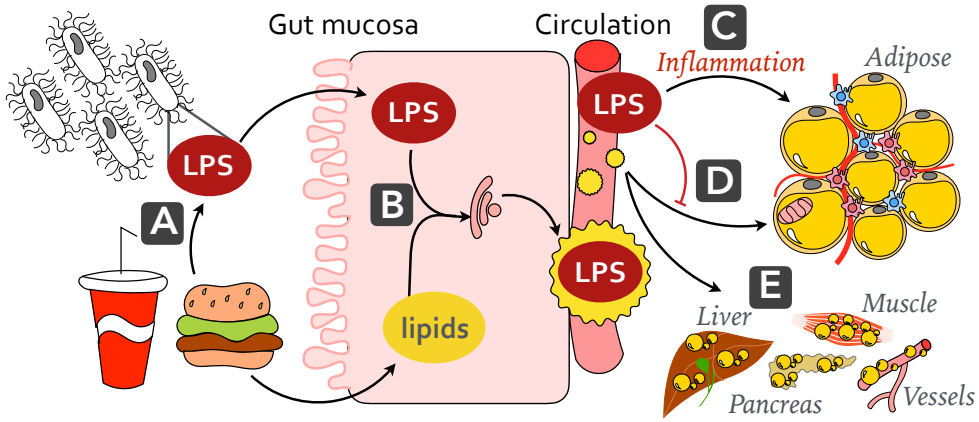

Proposed mechanism by which gut-derived LPS links the Western *diet with metabolic disease via mitochondrial dysfunction. A chronic high-fat, high-carbohydrate diet leads to increased circulating LPS through two main mechanisms: (A) Chronic high-fat high-carbohydrate meals increase gram-negative (LPS-containing) bacterial populations in the gut and (B) lipophilic LPS are coupled, packaged and distributed alongside chylomicrons, so serum LPS levels are directly proportional to degree of chylomycron-dependent fat absorption. (C) Once in circulation, LPS triggers a potent systemic inflammatory response, which may become chronic if* Western *diet is continued. Chronic inflammation is a hallmark of adipocyte dysfunction, insulin resistance and metabolic disease. (D) In the present work, we propose LPS may also generate mitochondrial dysfunction in adipose tissue and compromise the lipid buffering capacity of this organ. (E) Continued energy surplus will then result in ectopic lipid deposition on other metabolic organs, such as liver, pancreas, muscle and blood vessels, initiating systemic metabolic disease.*

5.2 Methods

Ethics and Study Design

Thirty-nine morbidly obese (BMI>35 Kg/m2), type-2 diabetic, Caucasian women undergoing either bilio-pancreatic diversion (BPD; n=12), laparoscopic greater curvature plication (LGCP; n=15), or laparoscopic adjustable gastric banding (LAGB; n=12) were recruited to participate in this study. Fasted bloods and anthropometric investigations were conducted before (baseline) and following surgery with collection of serum samples and abdominal subcutaneous white adipose tissue (AT) biopsies at both of these time points. Patients on pharmacological treatment with incretin mimetics and/or insulin were not included in this study. For further detail the reader is referred to Chapter 2.

Blood Biochemistry and Anthropometry

All anthropometric and biochemical measurements were performed before and six months after surgery. For detail on blood, adipose tissue sample and other clinical data collection, please see Chapter 2.

RNA isolation and qRT-PCR

Gene expression of mitochondrial genes was assayed through quantitative real-time polymerase chain reaction (qRT-PCR) using subcutaneous white adipose tissue biopsies before and 6 months after bariatric surgery. For detail on primer sequences used in this study the reader is referred to Table 2.1. For further detail please see Chapter 2.

Mitochondrial DNA copy number assay

Mitochondrial (*mtND1*) and nuclear (*BECN1*) gene primers (Table2.2) were used via qRT-PCR to determine relative amounts of mitochondrial to nuclear DNA as a measure of mitochondrial number per adipocyte[266] within subcutaneous white adipose tissue biopsies. For further detail on methods, the reader is referred to Chapter 2.

LPS Assay Validation and Quantitation in Serum Levels

For serum lipopolysaccharide (LPS) determination, two methods were compared: the Limulus Amebocyte Lysate (LAL) Kinetic Chromogenic Assay (QCL-1000^{TM}, LONZA) and the EndoLISA® Elisa-based endotoxin detection assay (Hyglos). LPS concentrations of 8 human serum samples $(\mathrm{BMI}{=}21-38\ {}^{\mathrm{kg}}/_{\mathrm{m}^2})$ were determined in parallel with both assays. Samples were run in duplicate according to the manufacturers instructions. Serial sample dilution (from $1:4$ to $1:10$) and appropriate spike and negative controls were utilised to minimise enzyme-inhibitory factors in samples and confirm result validity. Results were calculated, according to manufacturers instructions, based on a LPS standard (*E. Coli* 055:B5) curve ranging from $[4 \text{ to } 0.06\ {}^{\mathrm{EU}}/_{\mathrm{mL}}]$ for the LONZA kit and from $[500 \text{ to } 0.005\ {}^{\mathrm{EU}}/_{\mathrm{mL}}]$ for the EndoLISA.

For bariatric samples, the EndoLISA® Elisa-based endotoxin detection assay (Hyglos) was used to quantify LPS serum levels. A preliminary trial of singlets was run to determine optimal dilution (1:5, 1:10; 1:20), after which samples were run at optimal dilution in duplicate. Results were calculated according to manufacturers instructions, based on a LPS standard (*E. Coli* 055:B5) curve ranging from

$[500 \text{ to } 0.005\,^{\mathrm{EU}}/_{\mathrm{mL}}]$.

Statistical Analysis

Statistical analyses were performed using the SPSS 21.0 software. Data are reported as mean $\pm$ standard deviation (SD), unless otherwise specified. Data were examined for normality according to the Shapiro-Wilks criteria. Comparisons between pre- and post-surgery time-points were performed via paired two-tailed t-tests (if parametric) and the Wilcoxon signed ranks test (if non-parametric). For categorical data, Fisher´s exact test was used. Between-group (surgery type) differences were assessed using One-way ANOVA (if parametric) and Kruskal-Wallis test (if non-parametric) using change variables, calculated as percentage change from pre-surgery values [(post/pre) x100]. For Pearson correlation analyses, change variables [(post/pre) x100] were log-transformed prior to analysis if non-parametric.

5.3 Results

Validation and Optimisation of LPS quantitation in human serum samples

Two methods for the quantitation of circulating LPS levels were validated and compared: Limulus Amebocyte Lysate (LAL) Kinetic Chromogenic Assay (QCL-100^{TM}, LONZA) and the EndoLISA® Elisa-based endotoxin detection assay (Hyglos). To gain a representative picture and given that LPS levels are reported to vary with BMI, eight human serum samples from individuals with a range of BMIs (21-37.5 $^{\mathrm{Kg}}/_{\mathrm{m}^2}$) were used to run the assays. As per the manufacturer´s instructions of the Limulus Amebocyte Lysate (LAL) Kinetic Chromogenic Assay[336], the effect of vessel material (glass vs. plastic) as well as heat inactivation of samples were tested. As shown in Figure 5.2, vessel material did not alter the sensitivity of the LAL assay, whilst heat activation reduced the sensitivity of the assay. Therefore, subsequent LAL assays were run in the absence of heat activation, using validated pyrogen-free polypropylene test tubes.

Next, both assays were run in parallel, with four replicates per sample and the standard curves of each method were compared. The Pearson coefficient of determination (R^2) value was slightly closer to 1 in the EndoLISA, compared with the LAL standard curve (Figure 5.3), indicating a better fit of the EndoLISA data to the suggested linear model. In order to determine assay reliability, two replicates within each sample were spiked with a known amount of LPS (Figure 5.4). Assay reliability was greater with the EndoLISA method, in which more than 50% of the LPS spike was recovered in 6 out of 8 samples (Figure 5.4B). In contrast, spiked

samples in the LAL method showed minimal difference to non-spiked samples (Figure 5.4A). As both assays were tested using the same samples, these differences can not be accounted for by differences in interfering substances present in the sample. Thus, this data would suggest the EndoLISA method to have greater sensitivity in addition to reliability. Figure shows LPS readings via each method side by side. Though higher readings were obtained on average with the LAL method, the EndoLISA method shows more sensitivity to individual variation and may therefore be a better option when between-group differences are subtle.

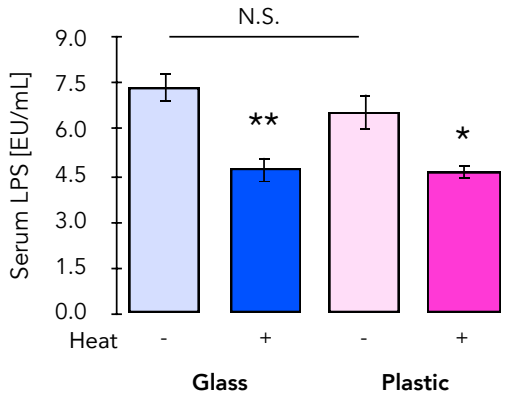

Figure 5.2: Validation of vessel material and heat inactivation for LAL method
*Graph shows the effect of sample heat inactivation and vessel material interference on LPS quantitation via the Limulus Amebocyte Lysate (LAL) kinetic chromogenic method. Data are expressed as endotoxin units per milliliter (EU/mL), and bars represent standard error of the mean. Significant differences were determined via 2-tailed unpaired t-test. *p<0.05, **p<0.01, n=8. N.S. denotes differences shown were not statistically significant.*

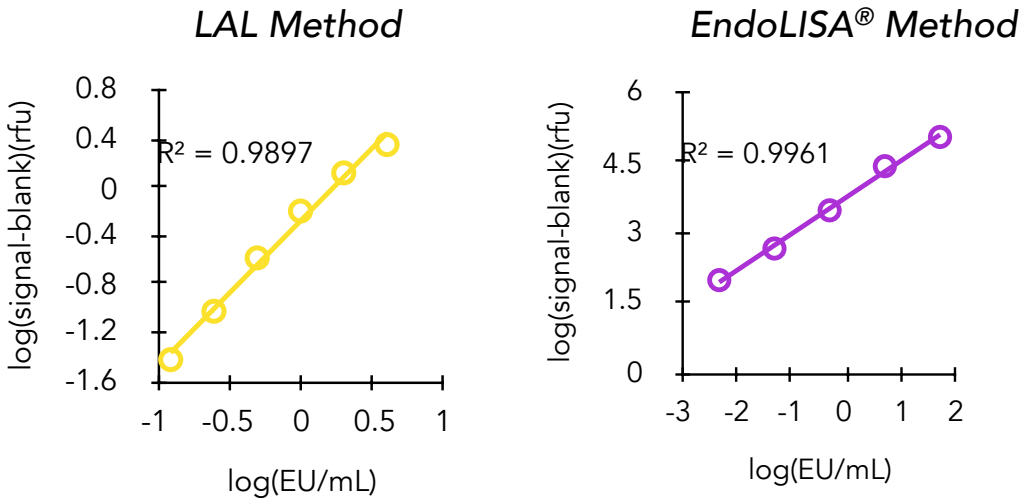

Figure 5.3: Comparison of calibration curves between two methods of LPS quantitation

Graph shows the calibration curve for two LPS quantitation methods: the Limulus Amebocyte Lysate (LAL) kinetic chromogenic Assay (LONZA) and the EndoLISA® Elisa-based endotoxin detection assay (Hyglos). Pearson Coefficient of Determination (R^2) is shown for each linear model.

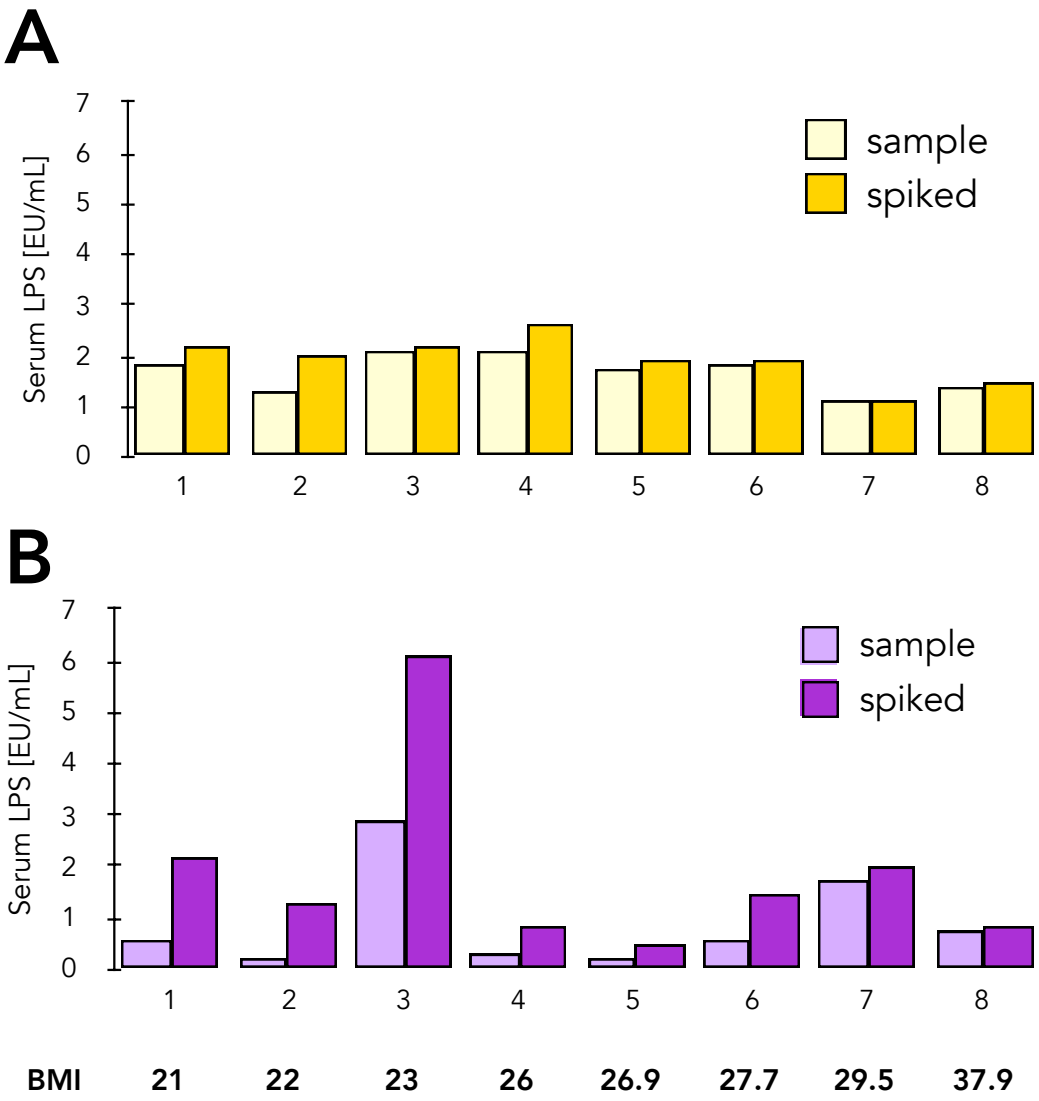

Figure 5.4: Reliability of LAL versus EndoLISA methods

*Eight human serum samples from individuals with a range of BMIs from lean to obese (21-37.5 $^{kg}/_{m^2}$) were used to compare two methods of LPS quantitation: Limulus Amebocyte Lysate (LAL) Kinetic Chromogenic Assay (QCL-1000^{TM}, LONZA) and the EndoLISA® Elisa-based endotoxin detection assay (Hyglos). Graphs display LPS spike recovery with LAL **(A)** and EndoLISA **(B)** methods. Data are expressed as endotoxin units per milliliter (EU/mL), each bar represents reading of one sample without or with LPS spike (darker colour) with corresponding BMI shown below. n=8.*

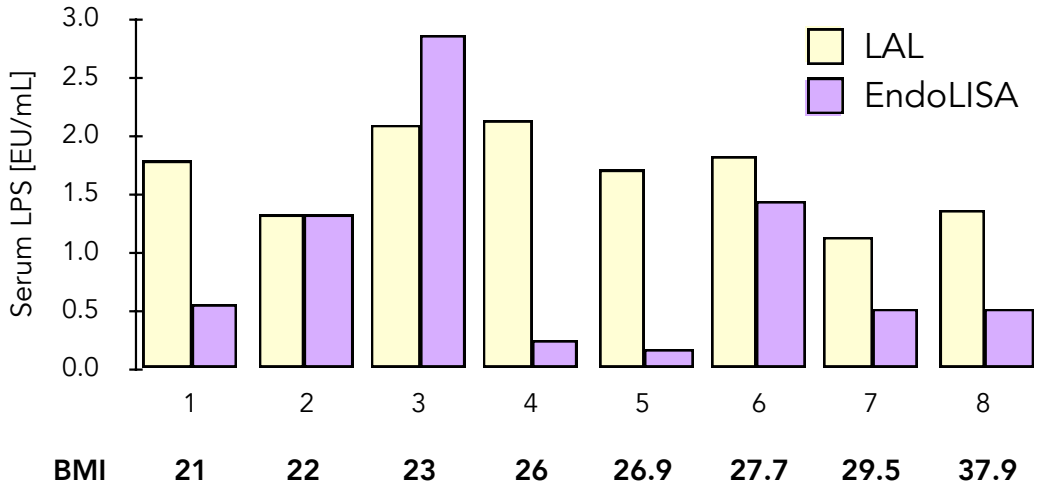

Figure 5.5: Sensitivity of LAL versus EndoLISA methods

LPS levels of eight human serum samples from individuals with a range of BMIs from lean to obese (21-37.5 $\mathrm{kg/m^2}$) measured via two methods: the Limulus Amebocyte Lysate (LAL) Kinetic Chromogenic Assay (QCL-1000^{TM}, LONZA) and the EndoLISA® Elisa-based endotoxin detection assay (Hyglos). Data are expressed as endotoxin units per milliliter (EU/mL), each bar represents reading of one sample, with corresponding BMI shown below.

Effect of Bariatric Surgical Procedure on Circulating LPS Levels

As shown in previous chapters of this thesis, the bariatric procedure BPD resulted in greater improvements in mitochondrial gene regulation, weight loss and overall type-2 diabetes remission, with more moderate improvements also observed after the LGCP, but not the LAGB procedure. To investigate whether circulating levels of bacterial LPS could help explain some of these differences, this chapter next examined the effect of each individual bariatric procedure on endotoxaemia.

Figure 5.6**A** shows serum LPS levels vary substantially between individuals both before and six months after BPD, LGCP or LAGB, and as such no significant differences from pre-to-post surgery were detected within each group. Between groups however, a stepwise trend (BPD<LGCP<LAGB) was detected which was nevertheless non-significant (Figure 5.6**B**). Moreover, all three surgeries resulted

in similar proportion of improvement of metabolic endotoxaemia (approximately 43% on average) (Figure 5.7). Despite this, surgery-specific effects were identified with respect to the degree of LPS improvement (Figure 5.8). When patients who did not achieve endotoxaemic improvement post-surgery (Figure 5.8**A**) were separated from those who did (Figure 5.8**B**), it became apparent that the BPD and LGCP surgeries resulted in substantially greater (approximately 20%) reductions of circulating LPS.

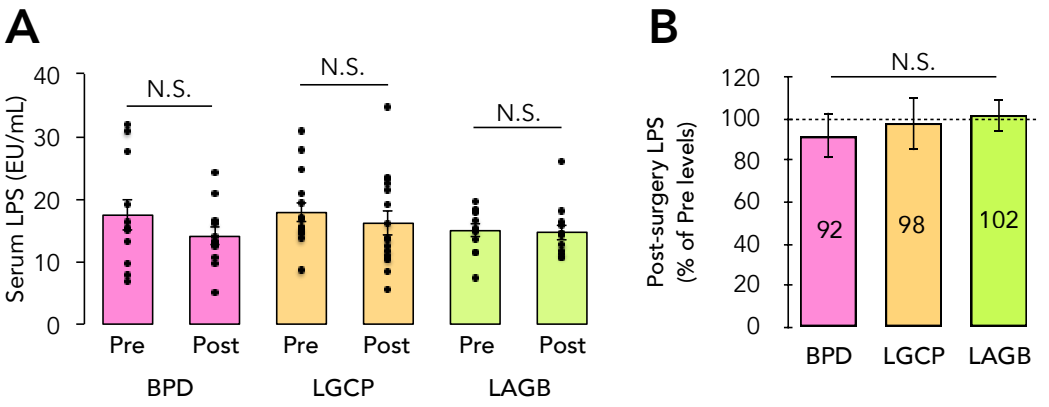

Figure 5.6: Serum LPS levels before and after bariatric surgical intervention
*The EndoLISA® Elisa-based endotoxin detection assay (Hyglos) was used to quantify serum LPS levels before and 6-months after 3 bariatric procedures: Bilio-pancreatic diversion (BPD), laparoscopic greater curvature plication (LGCP) or laparoscopic adjustable gastric banding (LAGB). Data is shown as either $^{\mathrm{EU}}/_{\mathrm{mL}}$ at pre and post surgery **(A)**, or as percentage or pre-surgical levels **(B)**. Dotted line denotes pre levels for each surgery normalised as 100%, bars represent means ± standard error of the mean. Pre-to-post surgical differences were determined via 2-tailed paired t-test (*p<0.05, **p<0.01). One way ANOVA was used to determine differences between surgeries (†p<0.05). N.S. denotes differences shown are not statistically significant (p>0.05).*

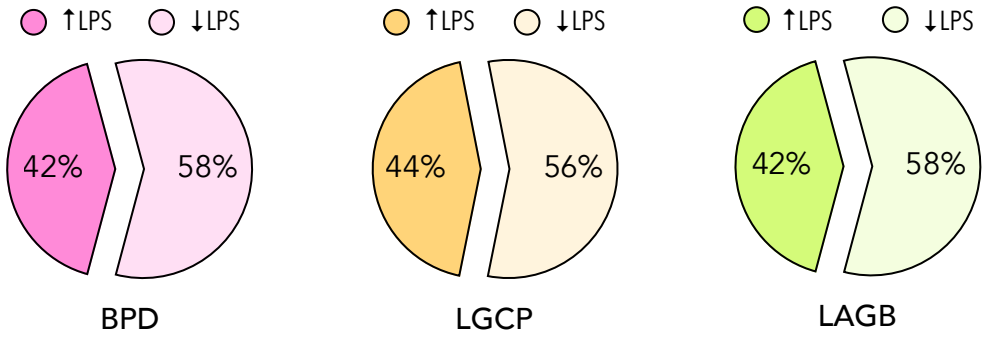

Figure 5.7: Proportion of serum LPS improvement for each surgical procedure
Pie charts showing the numerical proportion of patients with lower LPS post-surgery for each bariatric procedure: Bilio-pancreatic diversion (BPD), laparoscopic greater curvature plication (LGCP) or laparoscopic adjustable gastric banding (LAGB). Proportion is shown as percentage of total subjects in each surgical cohort (BPD n=12, LGCP n= 15, LAGB n= 12).

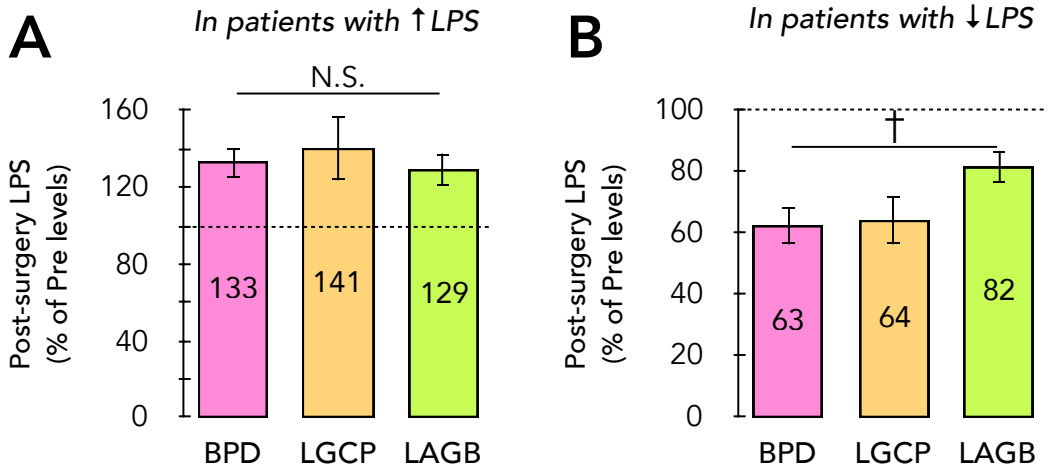

Figure 5.8: Surgery-specific effect on degree of metabolic endotoxaemic recovery
*Each surgical cohort was subdivided by whether or not patients exhibited an improvement in metabolic endotoxaemia (decreased LPS levels). Graphs show surgery-specific effects on serum LPS levels in patients who exhibited raised **(A)** versus lowered **(B)** metabolic endotoxaemia after 3 bariatric procedures: Bilio-pancreatic diversion (BPD), laparoscopic greater curvature plication (LGCP) or laparoscopic adjustable gastric banding (LAGB). Data is expressed as percentage of pre-surgical values (shown as dotted line), and bars represent means ± standard error of the mean. One way ANOVA was used to determine differences between surgeries (†$p<0.05$). N.S. denotes differences shown were not statistically significant ($p>0.05$).*

Mapping Surgery-Specific Differences in Metabolic Recovery to Serum LPS Levels

In order to ascertain whether lower LPS may be a contributing factor to the procedure-specific differences in metabolic recovery, surgery-induced changes in

serum LPS levels were examined against clinical indicators of metabolic health. No statistically significant relationships were identified between LPS and other clinical variables in the patient cohort as a whole. To understand whether the medley of heightened versus lowered serum LPS in post-surgical patients could be masking any association, these relationships were also analysed in each sub-cohort (split by whether or not surgery resulted in endotoxaemic improvement). No statistically significant relationships were identified in those who exhibited lower post-surgery endotoxaemia (Table 5.1). However, in patients who exhibited continued heightened endotoxaemia after surgery however, significant correlations with waist circumference and circulating lipoprotein levels were observed (Table 5.1), which are consistent with previous studies reporting an association between serum LPS and central adiposity.

Table 5.1: Relationship of circulating LPS levels with clinical indicators of metabolic health

	LPS $n = 39$		**↑LPS** $n = 16$		**↓LPS** $n = 23$	
	r	p	r	p	r	p
Age (y)	−0.078	0.637	−0.484	0.058	0.100	0.649
EWL (%)	−0.011	0.945	−0.071	0.795	0.137	0.534
BMI ($^{Kg}/_{m^2}$)	0.028	0.865	0.162	0.549	−0.250	0.250
Waist (cm)	0.122	0.465	0.575	0.025*	−0.070	0.752
WHR	−0.068	0.684	0.096	0.725	−0.339	0.122
Body fat (%)	−0.041	0.813	−0.134	0.648	−0.037	0.871
Glucose ($^{mmol}/_{L}$)	−0.150	0.370	−0.024	0.931	−0.102	0.645
Insulin ($^{pmol}/_{L}$)	−0.130	0.430	−0.032	0.908	−0.054	0.807
HOMA IR	0.191	0.250	0.048	0.861	−0.153	0.496
HbA1c ($^{mmol}/_{mol}$)	0.004	0.981	−0.061	0.829	0.132	0.549
TGL ($^{mmol}/_{L}$)	0.126	0.445	0.126	0.643	0.044	0.842
T Chol ($^{mmol}/_{L}$)	0.022	0.895	−0.178	0.509	0.172	0.432
LDL ($^{mmol}/_{L}$)	−0.123	0.457	−0.348	0.187	−0.103	0.641
HDL ($^{mmol}/_{L}$)	0.122	0.464	0.017	0.952	0.338	0.115
HDL/LDL	0.162	0.337	0.565	0.035*	0.350	0.101

*Table shows Pearson´s correlation coefficient (r) and p value significance (p) between serum LPS levels and metabolic variables in the entire patient cohort (n=39), and sub-cohort of patients with increased (n=16) or decreased (n=23) post-surgery serum LPS. Correlations were calculated using change variables (pre to 6-months post-surgery percentage change). Significant correlations are shown in red. *p<0.05. EWL: excess weight loss, BMI: body mass index, WHR: waist-hip ration, HOMA IR: homeostasis model assessment of insulin resistance, HbA1c: serum glycosylated haemoglobin, TGL: triglycerides, T Chol: total cholesterol, LDL: low-density lipoproteins, HDL: high-density lipoproteins.*

Mapping Surgery-Specific Differences in Indicators of Mitochondrial Functionality to Serum LPS Levels

Next, this study investigated whether LPS may be involved in modulating mitochondrial functionality in the adipose tissue, and whether surgery-specific changes in LPS may help explain the differential effect also observed in adipose mitochondrial functionality. To evaluate this, the relationship of LPS against mitochondrial number and gene transcript levels was examined through Pearson correlation analyses. No significant relationship was noted between LPS and any of the mitochondrial genes studied (Table 5.2). However, serum LPS levels were significantly and

inversely associated with mitochondrial number in adipose biopsies across all surgeries, with no obvious clustering on the basis of surgical procedure *per se* (Figure 5.9**A**). Patients with improved post-surgical LPS levels had significantly greater number of mitochondrial DNA copies in their adipose tissue, than patients who exhibited heightened endotoxaemia (Figure 5.9**B**).

Table 5.2: Relationship of circulating LPS levels with indicators of adipose mitochondrial functionality

		LPS	
		r	p
	mt number	−0.485	0.005*
Function	PGC1α	−0.100	0.540
	POLG	−0.055	0.736
	TFAM	−0.057	0.728
	mtND6	0.043	0.790
	SDHA	−0.097	0.552
	COX4I1	−0.121	0.456
	mtATP6	0.062	0.705
	UCP2	−0.223	0.167
	SOD1	−0.007	0.965
	SOD2	0.008	0.961
Dynamics	MFN2	−0.042	0.832
	OPA1	−0.269	0.166
	DRP1	0.141	0.483
	FIS1	−0.012	0.953

*Table shows Pearson´s correlation coefficient (r) and p value significance (p) between serum LPS levels and mitochondrial variables in the entire patient cohort (n=39). Correlations were calculated using change variables (pre to 6-months post-surgery percentage change). Significant correlations are shown in red. *p<0.05. mt number: mitochondrial DNA copy number, PGC1α: Peroxisome proliferator-activated receptor gamma coactivator 1-alpha, POLG: mitochondrial DNA polymerase gamma catalytic subunit, TFAM: mitochondrial transcription factor A, mtND6: mitochondrially-encoded NADH dehydrogenase 6, SDHA: Succinate dehydrogenase complex subunit A, COX4I1: Cytochrome c oxidase subunit 4 isoform 1 (complex IV), mtATP6: mitochondria-DNA-encoded ATP synthase subunit 6 (complex V), UCP2: uncoupling protein 2, SOD1: superoxide dismutase 1, SOD2: Superoxide dismutase 2, MFN2: Mitofusin 2; OPA1: mitochondrial dynamin like GTPase; DRP1: Dynamin-1-like protein; FIS1: Mitochondrial fission 1 protein.*

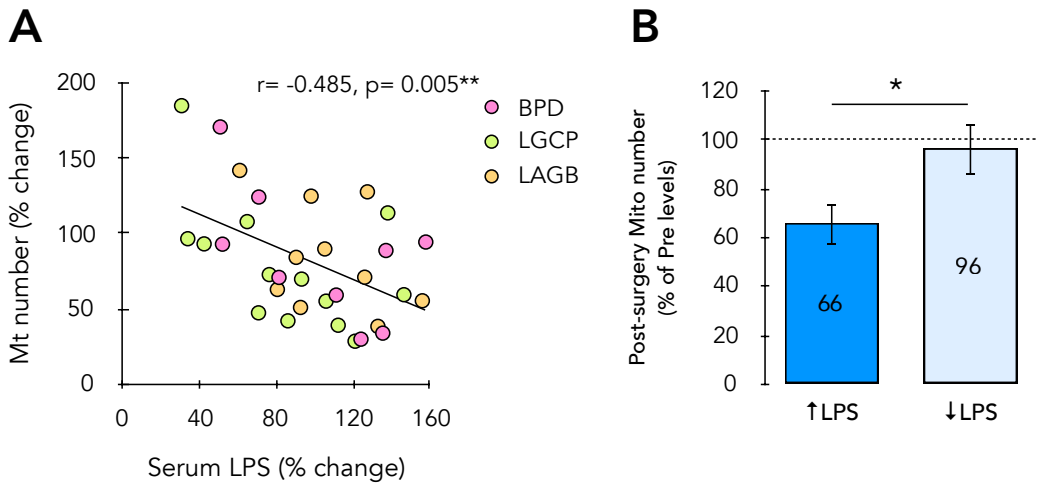

Figure 5.9: Association of serum LPS levels with adipose mitochondrial number
*Scatter plot showing correlation between serum LPS levels and mitochondrial DNA copy number in adipose biopsies (**A**). Correlation was calculated using change variables (percentage of pre levels) in the entire patient cohort (n=39), but individual data points are color-coded according to surgical procedure: Bilio-pancreatic diversion (BPD), laparoscopic greater curvature plication (LGCP) or laparoscopic adjustable gastric banding (LAGB). Linear trend line is also shown with Pearson correlation statistic (r) and significance (p). Post-surgical adipose mitochondrial levels in patients who exhibited an increase (↑LPS) or decrease (↓LPS) of serum LPS levels after surgery (**B**). Data are expressed as percentage to each individual´s pre-surgical levels, bars represent mean ±standard error of the mean. Statistical differences were analysed using a 2-tailed unpaired T-test (*p<0.05).*

5.4 Discussion

In the present chapter, the aim was to (1) optimise the methodology for LPS serum quantification and, (2) to determine whether serum LPS changes post-surgery varied between procedures in a similar manner to mitochondrial improvements, which would support the hypothesis that serum LPS reduction is implicated in adipose mitochondrial recovery after bariatric intervention.

The BPD (and to a lesser-extent the LGCP) procedure resulted in significantly greater reductions of serum LPS than LAGB. This step-wise post-surgery reduction in LPS (BPD>LGCP>LAGB) mimicked the step-wise improvement in mitochondrial gene regulation outlined in Chapter 3. Furthermore, these reductions in LPS levels post surgery were significantly associated with increased numbers of mitochondria in adipose biopsies. Collectively, this data is consistent with the concept that heightened serum LPS contributes to metabolic disease by targeting adipose mitochondria.

Studies on circulating LPS levels post bariatric surgery are limited, and vary substantially based on surgical procedure studied and follow-up duration. Most, however, report decreases to some degree in circulating LPS levels from 90 to 360 days post-surgery. Namely, one study of 15 severely obese individuals with type-2 diabetes undergoing Roux-en-Y gastric bypass (RYGB) reported a significant 20% decrease in circulating LPS levels at 6 months post-surgery [205], whilst another reported significant LPS reductions at 1 year post RYGB or duodenal switch [338]. These reports are consistent with our own findings, where bariatric intervention resulted in a reduction of 20 to 40% depending on the procedure. Despite evidence that LPS levels vary between procedures in the short-term after surgery

[339] however, to our knowledge this is the first study to examine the long-term effects of several bariatric procedures in parallel. Here, these studies demonstrate for the first time that some procedures are more effective than others in lowering serum LPS, and that this difference is associated with enhanced metabolic and mitochondrial benefits.

Recent evidence suggests that between-surgery differences in long-term metabolic benefit are rooted in the degree and type of gastrointestinal remodeling and the resultant changes in gut microbiota composition. This was elegantly demonstrated in a recent study where fecal matter from patients post-RYGB or vertical banded gastroplasty was transplanted to germ-free mice and resulted in significant weight loss, fat deposition and decreased use of carbohydrates as fuel [192]. Within this context, it is conceivable that LPS may be functioning as a communication link between gut and adipose tissue mitochondria to produce this shift in substrate metabolism. Our findings that LPS levels vary depending on surgical procedure in a manner proportional to the degree of mitochondrial improvement is consistent with this notion, however further research is needed to test the direct effect of LPS on mitochondrial functionality.

Chapter 6

Direct Effect of LPS on Human Adipocyte Mitochondrial Function

---

6.1 Introduction

The profound metabolic benefits of bariatric surgery cannot be explained by weight loss alone [176, 179]. Recent findings that fecal transplantation from bariatric subjects to germ-free animals can reproduce weight loss and mimic post-surgical metabolic improvements have bolstered the research potential of gut factors as mediators of obesity and metabolic disease [192]. One such factor is bacterial lipopolysaccharide (LPS). Absorbed alongside dietary lipids, its levels are elevated in obesity, resulting in a low-grade chronic inflammation and insulin resistance [196, 340, 341, 199, 204, 328]. As outlined in previous chapters, reductions in serum LPS after surgery varied substantially based on the bariatric procedure and in direct proportion to the degree of mitochondrial benefit in adipose tissue. Moreover, serum LPS levels were the only circulating factor to show a significant association with mitochondrial number in adipose biopsies. As such, this study hypothesized that heightened circulating LPS levels target adipose mitochondria unfavorably and contribute to insulin resistance and the pathogenesis of metabolic disease.

There are several potential mechanisms by which heightened LPS levels may contribute to mitochondrial dysfunction, which are summarised in Figure 6.1. LPS is a powerful trigger of inflammation, a hallmark of metabolic disease. Studies addressing the molecular link between adipose tissue inflammation and insulin resistance have highlighted the up-regulation of two pathways linking the two: the inhibitor of nuclear factor kappa-B kinase subunit beta/ nuclear factor kappa-light-chain-enhancer of activated B cells (IKKß/NF-κß) and the c-Jun N-terminal kinases (JNK) pathway. Both are triggered either through direct activation of cytokine receptor and its respective pro-inflammatory cytokine; or activation of

toll-like receptors (TLRs) by saturated free fatty acids, lipotoxic species, or indeed LPS [166, 342, 195]. IKKß and JNK are well-established serine kinases that phosphorylate insulin receptor substrate 1 (IRS-1) proteins at serine residues, leading to decreased insulin signaling. Additionally, IKKß activates NF-κß, which further increases inflammation by stimulating the transcription of pro-inflammatory cytokines such as TNF-α and IL-6 [343]. IL-6 induces the expression of suppressors of cytokine signaling proteins (SOCS), which also interfere with insulin signaling [344]. Importantly, inhibition of IKKß and JNK with anti-inflammatory pharmacotherapy or gene knock-out reduces serine phosphorylation of IRS proteins and improves insulin sensitivity [345, 346, 347, 348].

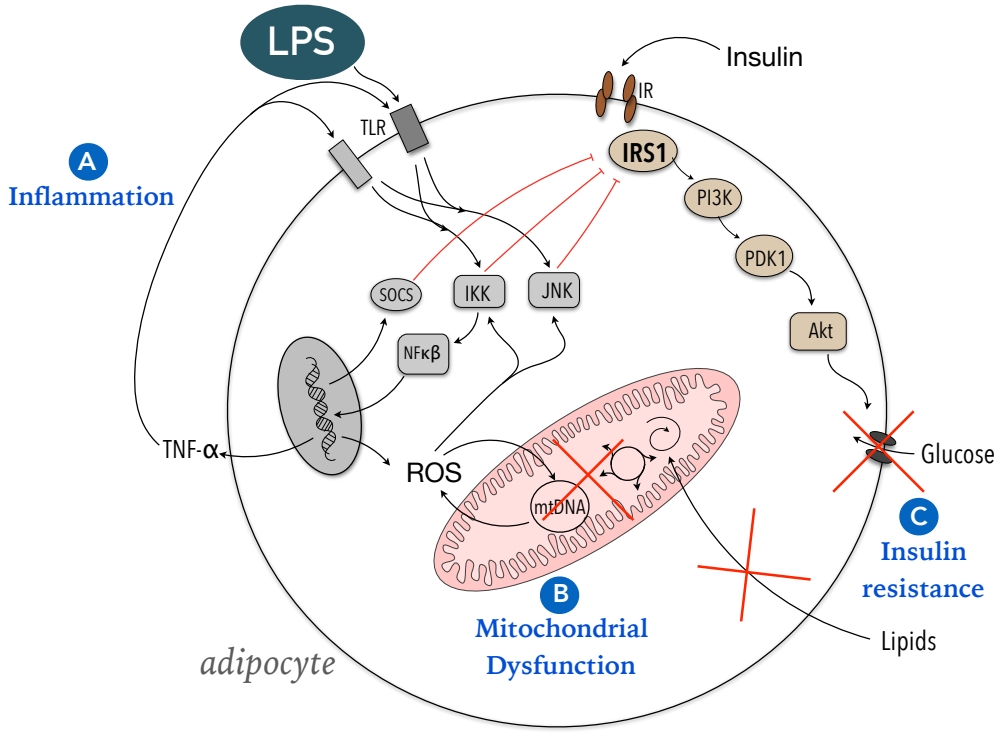

Figure 6.1: **Hypothesis**

Proposed hypothesis for how LPS effect on adipocytes contribute to type-2 diabetes: Heightened LPS after a high-fat, high carbohydrate meal triggers inflammation ***(A),*** *up-regulate IKK/JNK signaling pathways which can directly inhibit insulin signaling through insulin receptor substrate 1 (IRS1). In addition, activation of IKK/NF$\kappa\beta$ leads to transcriptional activation of pro-inflammatory cytokines (such as TNF-α) and reactive oxygen species (ROS) formation, establishing a positive feedback loop and further exacerbating inflammation and oxidative stress. The current work proposes that the accumulation of ROS will lead to mitochondrial DNA damage, bioenergetic inefficiency and mitochondrial dysfunction* ***(B)****, which will add further inflammation and oxidative stress, and ultimately add extra complexity to cellular insulin resistance* ***(C)*** *and have potential adverse consequences on systemic insulin sensitivity via impaired lipid buffering and ectopic fat deposition on non-adipose organs.*

If sustained chronically, the pro-inflammatory environment poses a powerful threat to mitochondrial DNA integrity and organelle functionality. Mitochondrial DNA is thought to be more susceptible to damage than nuclear DNA as in addition to being in closer proximity to ROS (mitochondria are the main source of ROS in the cell) it contains only coding sequences and is not protected by histones [349, 350, 351]. Indeed, several known mitochondrial [288, 352] and nuclear [353] mutations have been associated with detrimental cardio-metabolic phenotypes through impairment

of mitochondrial function [331, 352, 288].

Mitochondrial genes encode 13 protein subunits of the OXPHOS complex including subunit 6 (mt-ND6) of NADH dehydrogenase (complex I) and subunit 6 (mt-ATP6) of ATP synthase (complex V). Nuclear DNA encode all subunits of succinate dehydrogenase (SDHA; complex II) and subunit 4 (COX4) of cytochrome c oxidase (complex IV) as well as proteins involved in mitochondrial DNA replication, transcription, translation, and repair. The expression level of these OXPHOS genes as well as size and shape of mitochondria largely determine oxidative capacity and both morphology and OXPHOS gene expression are closely linked to insulin action [354]. Though studies thus far have described clear evidence of obesity-associated alterations on mitochondrial function in skeletal muscle, the physiological implications of these alterations are yet to be understood, particularly within the context of white adipose tissue dysfunction.

During obesity, white adipose tissue, and the mitochondrial network within this organ are faced with the extreme challenge of metabolising and storing the excess calories as lipids, in order to avoid their harmful deposition in other organs such as liver, pancreas, muscle and blood vessels. Any adverse effects on mitochondrial functionality may have direct consequences on the lipid buffering capacity of white adipose tissue as a whole, and contribute to systemic metabolic disease. As such, the aim of this present chapter was to determine the direct *in vitro* effect of LPS on human adipocyte (1) insulin sensitivity, (2) inflammation, (3) mitochondrial DNA integrity, functionality and morphology and (4) overall energy phenotype in order to determine whether LPS would adversely affect mitochondrial function and adipocyte lipid handling.

6.2 Methods

Human adipocyte culture, differentiation and treatment

Human subcutaneous white adipocyte cell line ChubS7 were grown and differentiated as previously described [269]. Briefly, cells were seeded on to 6-well plates ($0.3\text{x}10^6$) unless otherwise specified, grown to $100\,\%$ confluence and differentiated for 8-10 days in DMEM/F12 with $3\,\%$ FBS and PromoCell Differentiation Supplement Mix (C-39436, PromoCell). After differentiation, cells were allowed to equilibrate in basal media for 12 hours before being treated for 24-72 hours in basal media supplemented with LPS (10 or $100\,^{\mathrm{ng}}/_{\mathrm{mL}}$, *E. Coli* O55:B5, Sigma, L6529), TNFα ($10\,^{\mathrm{ng}}/_{\mathrm{mL}}$, Sigma, H8916) or Insulin ($50\,\mathrm{nM}$, Sigma, I9278). All media were prepared with DMEM/F12 (ThermoFisher Scientific, UK, 11320033) and formulations are shown in Table2.5 in Chapter 2.

2-deoxyglucose uptake

Glucose uptake in differentiated ChubS7 adipocytes was evaluated via cellular incorporation of $[^3\mathrm{H}]$-2-deoxyglucose. Following differentiation and treatment, cells were washed 3 times with warmed PBS and allowed to equilibrate in KRH buffer (containing $0.01\,\%$ BSA, $5\,^{\mathrm{mmol}}/_{\mathrm{L}}$ glucose) at 37ºC for 2.5 hours. Adipocytes were then incubated a further 30 minutes with KRH buffer without glucose and either no (basal control) or $100\,\mu$M insulin. Immediately after, $1\,^{\mu\mathrm{Ci}}/_{\mathrm{mL}}$ $[^3\mathrm{H}]$-2-deoxyglucose (PerkinElmer, NET328A001MC) in KRH buffer at 37ºC was added for a further10 minutes. To finalise the assay, cells were then washed 3 times with ice-cold PBS, lysed and harvested in $200\,\mu$L RIPA buffer and a cell scraper. Radioactivity was

evaluated via scintillation counting of the lysates, diluted 1:4 in β-scintillation fluid (Beta-Plate Scint, PerkinElmer), and a scintillation Counter. Results defined as counts per minute (CPM) were normalised to total protein content and glucose uptake displayed relative to the basal control.

Protein extraction and Western blot

For protein extraction, $100\,\mathrm{mg}$ of frozen human adipose tissue or $1.2\ \mathrm{x}\ 10^6$ cultured adipocytes were homogenised in $200\,\mu$L Phosphosafe^{TM} Extraction Buffer (Novogen®, Merk, Germany). A Bio-Rad detergent compatible protein assay kit (Bio-Rad Laboratories, CA) and nanospectrophotometer (GeneFlow, UK) were used to quantify protein concentrations. As described previously for Western blot analyses [268], 10-20μg of protein were loaded onto a denaturing polyacrylamide gel (GeneFlow, UK), transferred on to a nitrocellulose membrane which was then incubated with a primary antibody diluted in 0.2% I-block PBS-T (IRS1 $1:250$, MT-CO1 $1:1000$, SDHA $1:1000$, ß-Actin $1:1000$) at 4ºC overnight. A chemiluminescence detection system (ECL Plus, GE Healthcare, UK) was used to visualise protein bands, and densitometry was conducted using ImageQuant LAS 4000 Software (GE Healthcare, UK). Equal protein loading was confirmed by examining ß-actin protein expression. Primary antibodies utilised are listed in Table2.4 (Chapter 2).

RNA isolation and qRT-PCR

RNA was extracted from cell lysates containing approximately $1\mathrm{x}10^6$ adipocytes using a column-based isolation method (RNeasy Lipid Tissue Mini Kit; #74804 Qi-

agen, UK) according to manufacturer´s instructions. Samples were digested with DNase I to remove potential genomic DNA contaminants (DNase I kit, #AMP-D1 Sigma-Aldrich). RNA was eluted in 10 µL RNase-free water and 1 µL quantified in duplicate using a spectrophotometer (Nanodrop ND-1000, labtech) at 260 nm absorbancy. Synthesis of cDNA was performed using 1 µg RNA per sample and a Bioline mRNA reverse transcription kit (#BIO-65026) according to the manufacturer´s instructions. Gene expression was assayed through quantitative real-time polymerase chain reaction (qRT-PCR) using ABI 7500 standard sequence detection system (Applied Biosystems, UK). Each reaction was prepared to 25 µL final volume containing Taqman Universal PCR mastermix (#4304437 Applied Biosystems, UK), 1 µL sample cDNA and a specific commercially available Taqman gene expression assay (Applied Biosystems, UK). For detail on primer sequences used in this study the reader is referred to Table 2.1. All samples were assayed in triplicate and multiplexed using 18S (ribosomal RNA) as a pre-optimised control probe. As per the manufacturer´s instructions, reactions were carried out at 50 ºC for 2 minutes, 95 ºC for 10 minutes, and then 40 cycles of 95 ºC for 15 seconds and then 60 ºC for 1 min. For data analysis, a ΔCt was calculated based on the difference between 18S and the target gene. Gene expression was calculated based on the following formula:

$$mRNA\ expression = 2^{-\triangle Ct},\ \text{where}\ \triangle Ct = target\ gene\ Ct - \ 18s\ Ct$$

Endogenous antioxidant activity assays

Activity of endogenous antioxidants SOD and Catalase was evaluated through a colorimetric method, using OxiSelect^{TM} Superoxide Dismutase Activity Assay (STA-340) and OxiSelect^{TM} Catalase Activity Assay (STA-341) Kits (Cell Biolabs). Following adipocyte differentiation and treatment, $\backsim 1.2 \text{ x } 10^6$ adherent cells were washed 3 times with ice-cold PBS, harvested with a cell scraper in $1\,\mathrm{mL}$ of cold Lysis buffer ($10\,\mathrm{mM}$ Tris, pH 7.5, $150\,\mathrm{mM}$ NaCl, $0.1\,\mathrm{mM}$ EDTA). Samples were homogenised, centrifuged and stored at -80ºC until assayed. All assays were conducted within 1 month of sample collection and were conducted in accordance to manufacturers instructions. Absorbance was read using a PheraStar FS microplate reader (BMG Labtech). SOD activity was calculated based on optical density as outlined in the following formula:

$$SOD\ activity\ (inhibition\ \%) = \left[\frac{(Blank_{OD} - Sample_{OD})}{Blank_{OD}}\right]$$

The concentration of active Catalase was determined by interpolation of a catalase standard curve. Optical density at 540nm was plotted on the "x" axis, Catalase (U/mL) on the "y" axis, and a second order polynomial equation was used to determine catalase concentrations as follows:

$$Catalase\ (\mathrm{U/mL}) = 174.01x^2 + 13.678x + 2.7743 \text{ where } x = optical\ density\ (540\,\mathrm{nm})$$

Quantification of total reactive oxygen and nitrogen species

Total reactive oxygen and nitrogen species were evaluated through green fluorescence using OxiSelect^{TM} *in vitro* ROS/RNS Assay Kit (STA-347, Cell Biolabs). Following adipocyte differentiation and treatment, $\backsim 1.2 \text{ x } 10^6$ adherent cells were washed 3 times with ice-cold PBS, flash-frozen in dry-ice and harvested using a cell-scraper. Samples were homogenised in $200\,\mu$L PBS and stored at -80ºC and assayed within 1 month of collection. Assay was conducted according to manufacturers instructions, and fluorescence after 30 minutes was measured using a PheraStar FS microplate reader (BMG Labtech) with a $485/538$ nm filter and $530\,\text{nm}$ cutoff. Total ROS/RNS were calculated by interpolation of a Hydrogen Peroxide standard curve as follows:

$$ROS/RNS \ (\mu\text{M}) = 5354.5x^2 + 1043.3x + 50.496$$

where $x = relative \ flourescence \ units \ (^{485}/_{538})$.

Evaluation of mitochondrial DNA integrity

Total DNA was extracted from cultured cells using DNeasy Blood and Tissue Mini Kit (#69504 Qiagen, UK) in accordance to the manufacturer´s instructions. RNase treatment was performed to eliminate possible RNA contamination. DNA was eluted with 100 µL AE buffer and quantified using a spectrophotometer (Nanodrop ND-1000, Labtech). Evaluation of mitochondrial DNA integrity was performed via qRT-PCR by comparing previously published primers [267] spanning a section of mtDNA susceptible to mutations (where 84% of known mutations occur)

against a section that is not affected by any of the reported large deletions. Real-time PCR of both targets were run using a probe-based duplex qRT-PCR assay on an ABI Prism 7500 thermo cycler (Life Technologies) with the following thermal profile: 95ºC for 10 minutes, followed by 40 cycles of 95ºC for 15s, 55ºC for 15s, and 60ºC for 1 minute. The reaction components consisted of 22.5µL Taqman Universal PCR Mastermix no AmpErase® UNG (Applied Biosystems), each mitochondrial probe at 250nM (Taqman® MGB Probe, ThermoFisher Scientific,UK; shown in Table2.3) with a final reaction volume of 25µL.

Mitochondrial DNA integrity was calculated according to the following published formula [267]:

$$2^{mtDNA_{DR}}, \text{ where } mtDNA_{Deletion\ Ratio} = \frac{(Stable\ Probe\ Ct\ -\ Suceptible\ Probe\ Ct)}{Stable\ Probe\ Ct}$$

Mitochondrial DNA copy number assay

Total DNA was extracted from cell lysates containing approximately $1\text{x}10^6$ adipocytes using DNeasy Blood and Tissue Mini Kit (#69504 Qiagen, UK) in accordance to the manufacturer´s instructions. RNase treatment was performed to eliminate possible RNA contamination. DNA was eluted with 100 µL AE buffer and quantified using a spectrophotometer (Nanodrop ND-1000, Labtech). Relative amounts of mitochondrial DNA copy number were assessed through qPCR in an ABI Prism 7500 thermo cycler (Life Technologies) with the use of iQTM SYBR Green Supermix (#170-8880 BioRad). Mitochondrial (*mtND1*) and nuclear (*BECN1*) gene primers (Table2.2) were used to determine relative amounts of mitochondrial to nuclear DNA [266]. Each sample was measured in triplicate. Mitochondrial number

was calculated based on the following formula:

$$mtDNA\ copy\ number = 2^{\triangle Ct},\ \text{where}\ \triangle Ct = BECN1\ -\ mtND1$$

Analysis of mitochondrial morphology through confocal microscopy

Analysis of the mitochondrial network was performed through live cell imaging using a confocal microscope. ChubS7 cells were seeded on to gelatin-coated 35mm glass bottom culture dishes (MatTek corportation®), grown, differentiated and treated for 24 hours as described above. Upon completion of treatment, basal media was removed, replaced with $100\,\mathrm{nM}$ Mitotracker Red and cells incubated for 20 minutes at 37ºC. Cells were then washed three times with basal media and imaged in HEPES-buffered basal media (pH 7.35) with or without LPS (10 or $100\,{}^{\mathrm{ng}}/_{\mathrm{mL}}$, *E. Coli* O55:B5, Sigma, L6529). The Z system attached to an inverted fluorescence microscope fitted with an F-view-II cooled CCD camera (Olympus) was used to observe cells which were maintained at 37ºC throughout the imaging process. Cells were magnified 40x through an oil objective lens, and a 500 nm excitation filter was used to image the mitochondrial network.

Morphologic assessment of the mitochondrial network was conducted on confocal images using ImageJ (version 1.50i) as described by others [270]. The mitochondrial parameters assessed were mitochondrial area (μm^2) and the degree of branching, as defined by the following equation:

$$BF = \frac{MtP^2}{(4\pi MtA)}$$

where MtP = length of mitochondrial outline (mitochondrial perimeter in μm) and MtA = Area of mitochondria (μm^2). Four independent experiments were conducted and a minimum of 70 images were examined for each experimental group.

Seahorse Cell Mito Stress Test

Respiration and media acidification rate were measured using a Seahorse XF24 Extracellular Flux Analyzer (Seahorse Bioscience, Agilent Technologies). Immortalised human preadipocytes ChubS7 were seeded onto 24-well plates (Seahorse Bioscience, 100850-001) at a density of 10,000 cells/well, grown and differentiated using the standard protocol outlined above, and treated for 24 or 72 hours with or without LPS (10 or $100\,{}^{\mathrm{ng}}/_{\mathrm{mL}}$, *E. Coli* O55:B5, Sigma, L6529). Each experimental group consisted of 5 replicates, with the experiment repeated on at least 2 separate occasions (n=10). The assay was conducted in sterile, unbuffered Assay Media prepared with Seahorse base media (Seahorse Bioscience, 102365-100) at 37ºC (pH 7.4), the formulation of which is listed in Table2.6.

After a calibration step $(30\,\mathrm{min})$ and an equilibration step $(30\,\mathrm{min})$, the assay protocol consisted of 3 cycles of the following steps: mix $(3\,\mathrm{min})$, wait $(2\,\mathrm{min})$, measure $(3\,\mathrm{min})$, which were completed before and after each injection of Oligomycin (Sigma, O4876), FCCP (Sigma, C2920) and combined Rotenone (Sigma, R8875) and Antimycin A (Sigma, A8674). Reagents or vehicle control were injected in the appropriate volume of a tenfold concentrated stock solution to give the following final in-well concentrations: $2\,$μM Oligomycin, $2\,$μM FCCP, $0.5\,$μM Rotenone/Antimycin A. Prior to experiments, reagent concentrations and seeding density were optimised

as per the manufacturers instructions. Oxygen consumption rate (OCR) and extracellular acidification rate (ECAR) were calculated by the WAVE software (Seahorse Bioscience, Agilent Technologies). The basal respiration parameters were calculated from the mean of 3 individual OCR measurements as follows:

$$Basal\ Respiration = Initial\ OCR\ (\mathrm{pmol/L}) - Rotenone\ OCR\ (\mathrm{pmol/L})$$

For OCR and ECAR response to injection of each compound, data was normalised by the basal respiration of each experimental group (shown as percentage of baseline) to account for well-to-well variability in cell number.

Determination of ATP abundance

Immortalised human preadipocytes ChubS7 were seeded onto gelatin-coated 96-well white opaque cell culture plates at a density of 10,000 cells/well. Cells were grown and differentiated according to the standard protocol outlined above, and treated with or without LPS (10 or $100\,\mathrm{ng/mL}$, *E. Coli* O55:B5, Sigma, L6529) for 24 or 72 hours. Bioluminescent determination of ATP abundance was conducted using EnzyLight^{TM} ATP Assay Kit (BioAssay Systems, EATP-100) following the manufacturers instructions for adherent cells. Luminescence was read using a PheraStar FS microplate reader (BMG Labtech), and ATP concentrations determined based on interpolation of a standard curve of known ATP concentrations ranging from $0 - 30\,\mu\mathrm{M}$.

Determination of mitochondrial membrane potential

The dye tetramethylrhodamine ethyl ester perchlorate (TMRE, Sigma, 87917) was used to determine mitochondrial membrane potential. TMRE is a cell-permeant, positive-charged red/orange dye that is readily sequestered by polarised mitochondria (due to their negative charge) in a manner that is directly proportional to their membrane potential. Immortalised human preadipocytes ChubS7 were seeded onto a black opaque 96-well plate, differentiated and treated as described for the ATP abundance assay. Adherent cells were incubated with $300\,\mathrm{nM}$ TMRE (Sigma) diluted in basal media (described in Table2.5) for $30\,\mathrm{min}$ at 37ºC. Cells were then washed 3 times with warm PBS before reading fluorescence with a PheraStar FS microplate reader (BMG Labtech) at $550/590\mathrm{nm}$ excitation/emission immediately and after 10, 20 and 30 minutes. As a positive control for depolarisation, $30\,\mu$M FCCP was added to some cells for $30\,\mathrm{minutes}$, prior to the TMRE incubation step. FCCP is an ionophore which destroys membrane potential, rendering mitochondria unable to accumulate TMRE. For background correction, cells with no TMRE and no FCCP added were used. Membrane potential was calculated using the relative fluorescence signal of samples based on the following formula:

$$Membrane\ Potential\ (\%) = \left[\frac{(LPS\ sample - background)}{(control\ sample - background)}\right] \mathrm{x}\ 100$$

Statistical Analysis

Statistical analyses were performed using the SPSS 21.0 software. Data are reported as mean $\pm$ standard deviation (SD), unless otherwise specified. Data were examined for normality according to the Shapiro-Wilks criteria. Unless otherwise

specified, comparisons between pre- and post-surgery time-points were performed via paired two-tailed t-tests (if parametric) and the Wilcoxon signed ranks test (if non-parametric). For categorical data, Fisher´s exact test was used. Between-group (surgery type) differences were assessed using One-way ANOVA (if parametric) and Kruskal-Wallis test (if non-parametric) using change variables, calculated as percentage change from pre-surgery values [(post/pre) x100]. For Pearson correlation analyses, change variables [(post/pre) x100] were log-transformed prior to analysis if non-parametric.

6.3 Results

LPS administration to human adipocytes directly induced insulin resistance

In order to test the hypothesis that LPS drives adipocyte insulin resistance via mitochondrial dysfunction, the first step was to establish whether *in vitro* LPS administration could directly induce insulin resistance in human subcutaneous adipocytes ChubS7. Therefore, adipocytes were treated with two different doses of LPS and two established *in vitro* models of insulin resistance served as positive controls: chronic TNF-α ($10\,\mathrm{ng/mL}$) and chronic insulin ($50\,\mathrm{nM}$). As shown in Figure 6.2**(A)**, all four treatments successfully resulted in insulin resistance after both 24 and 72 hours, as evidenced by significant reductions in uptake of radio-labelled glucose following an acute dose of insulin ($100\,\mathrm{nM}$) compared with control adipocytes. This functional observation of insulin resistance was accompanied at 24 hours by reduced protein expression of insulin receptor substrate 1 (IRS1), a key first step in the insulin signaling cascade Figure 6.2**(B-C)**. Thus, both low and high doses of LPS resulted in impaired insulin signaling and adipocyte glucose uptake, with stronger effects at 24 hours.

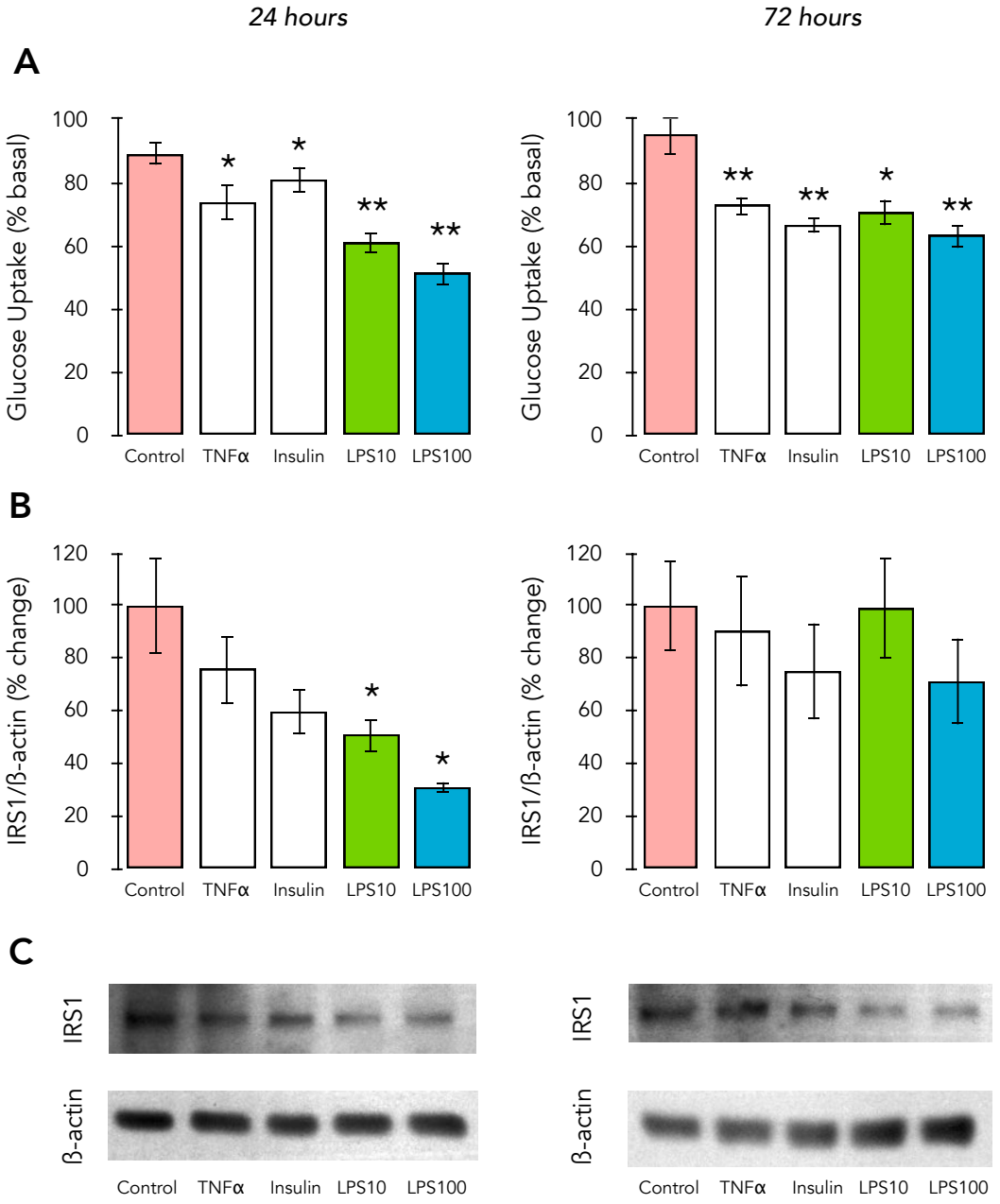

Figure 6.2: **Effect of LPS on Human Adipocyte Insulin Sensitivity**
(A) *Glucose uptake and* ***(B-C)*** *Insulin receptor substrate 1 (IRS1) protein expression in human adipocytes following 24 or 72-hour treatment with* $10\,^{\mathrm{ng}}/_{\mathrm{mL}}$ *TNF-*α*,* $50\,\mathrm{nM}$ *chronic Insulin,* 10 *or* $100\,^{\mathrm{ng}}/_{\mathrm{mL}}$ *LPS.* ***(C)*** *Image of IRS1 and loading control* β*-actin* Western *blot membranes at both time-points. For (A), results are expressed as percentage of basal control; for (B) results are expressed as percentage change from control cells. Bars represent standard error of the mean. *p<0.05, **p<0.01.*

LPS administration up-regulated inflammation and oxidative stress

Next, inflammation and oxidative stress were assessed via measurement of pro-inflammatory cytokine TNF-α, and the combination of total reactive oxygen (ROS) and nitrogen (RNS) species. LPS was a potent inducer of inflammation (particularly at 24 hours), when TNF-α mRNA increased 300-500% in LPS-treated adipocytes relative to control (Figure 6.3**A**). Abundance of total ROS and RNS rose by 50% within 24 hours and 150% within 72 hours of LPS treatment (Figure 6.3**B**). As expected, endogenous antioxidant superoxide dismutase (SOD) also showed a marked increase, both in terms of mRNA transcript levels (400-3000%; Figure 6.3**C**) and activity (30-300%; Figure 6.3**D**). However, the activity of endogenous antioxidant catalase was significantly impaired with LPS treatment, particularly at 24 hours when LPS treatment resulted in an approximately 50-75% decrease (Figure 6.3**E**). Overall, mRNA transcript levels of both TNF-α and SOD2 genes were lower at 72 compared to 24 hours (Figure 6.3**A** and **C**).

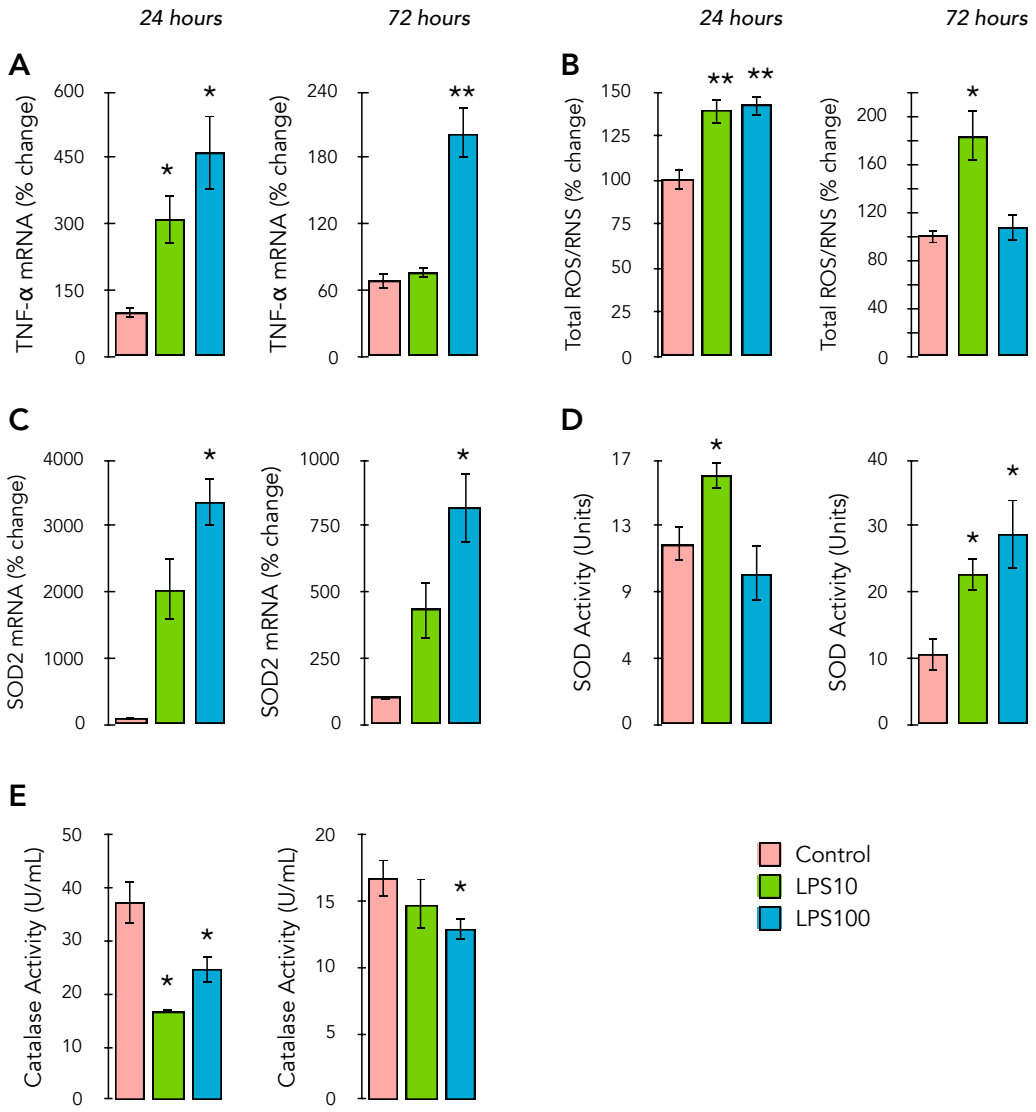

Figure 6.3: **Effect of LPS on Human Adipocyte Inflammation and Oxidative Stress**
(A) *Tumor necrosis factor-alpha (TNF-α) mRNA expression (n= 6),* ***(B)*** *total reactive oxygen (ROS) and nitrogen species (RNS) (n=6),* ***(C)*** *Superoxide dismutase 2 (SOD2) mRNA expression (n=3),* ***(D)*** *SOD activity (n=6), and* ***(E)*** *catalase activity (n=6) in human adipocytes following 24 or 72-hour incubation with 10 or 100 $^{\mathrm{ng}}/_{\mathrm{mL}}$ LPS. Data are expressed as percentage change from control, unless otherwise specified and bars represent standard error of the mean. *p<0.05, **p<0.01.*

LPS administration resulted in mitochondrial DNA deletion, and protein depletion

Given that LPS resulted in increased ROS accumulation and impaired endogenous antioxidant response, the possibility of damage to mitochondrial DNA was

investigated. Briefly, a section of mitochondrial DNA known for its susceptibility to mutations (where 80% of all reported mutations occur) was compared against a stable section (where no mutations have been reported). As shown on Figure 6.4**A**, control adipocytes presented 100% mitochondrial DNA integrity at both 24 and 72 hours. However, adipocyte treatment with LPS produced a mitochondrial DNA deletion of approximately 5% after 24 hours and 10-16% after 72 hours. The damage to mitochondrial DNA was accompanied by adverse effects on mitochondrial protein translation at 24 hours, as evidence by a depletion of mitochondrial protein encoded in mitochondrial DNA versus nuclear DNA-encoded mitochondrial protein (Figure 6.4**B**). Importantly, other cellular stressors (namely, chronic TNFα and insulin) did not produce the same effects on mitochondrial DNA integrity or protein abundance as LPS treatment, suggesting effect on mitochondria may be a specific effect of LPS.

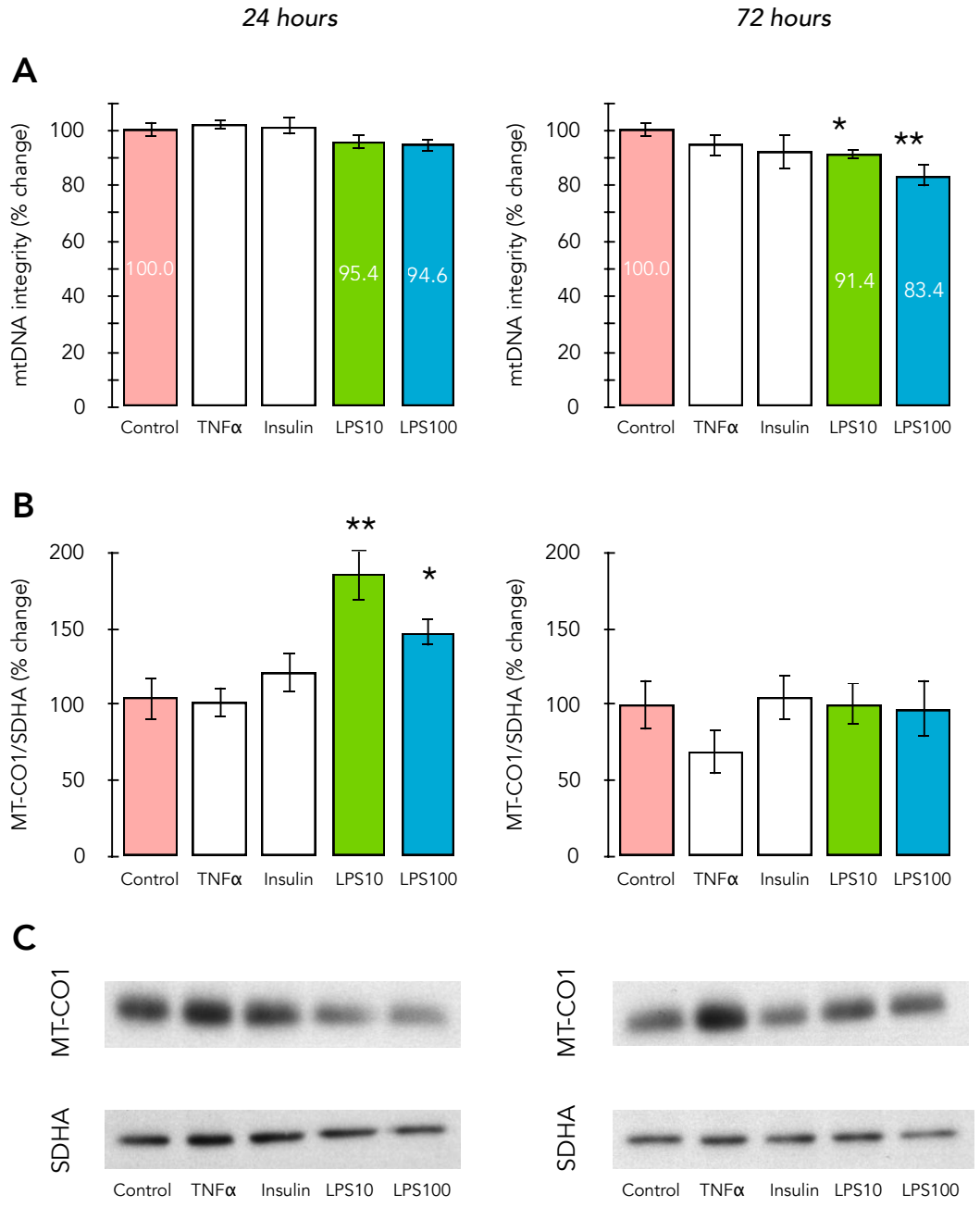

Figure 6.4: **Effect of LPS on Mitochondrial Quality**

*(**A**) Mitochondrial DNA (mtDNA) integrity and **(B)** mitochondrial protein abundance (denoted by mitochondrial MT-CO1 to nuclear SDHA protein ratio) in human adipocytes following a 24 or 72-hour incubation with $10\,^{\mathrm{ng}}/_{\mathrm{mL}}$ TNF-α, $50\,\mathrm{nM}$ chronic Insulin, 10 or $100\,^{\mathrm{ng}}/_{\mathrm{mL}}$ LPS. **(C)** Image of MT-CO1 and SDHA* Western *blot membranes at both time-points. Data are expressed as percentage change from control, and bars represent standard error of the mean. *p<0.05, **p<0.01, n=6.*

LPS administration induced mitochondrial elongation

Assay of mitochondrial DNA copy number revealed a striking 80-95% reduction in mitochondrial number, when adipocytes were treated with LPS for both 24 and 72 hours (Figure 6.5**A**). This finding was further substantiated through confocal imaging analysis, which showed that mitochondrial area in LPS-treated adipocytes was significantly reduced compared with controls (Figure 6.5**B**). Furthermore, the degree of branching in the mitochondrial network was approximately doubled with LPS treatment (Figure 6.5**C**), which is indicative of greater elongation.

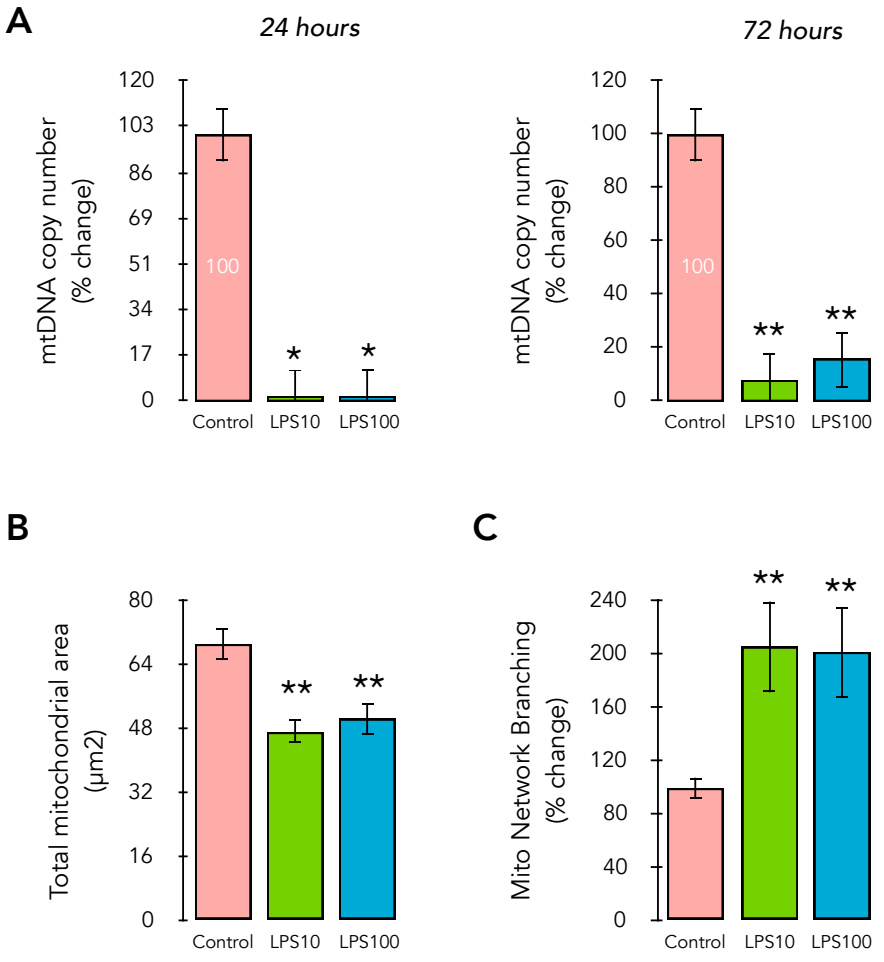

Figure 6.5: **Effect of LPS on Mitochondrial Morphology**
(A) *Mitochondrial DNA copy number in human adipocytes following a 24 or 72-hour incubation with* 10 *or* $100\,^{\mathrm{ng}}/_{\mathrm{mL}}$ *LPS (n=6).* ***(B)*** *Total mitochondrial area (µm*^{2}*) and* ***(C)*** *Degree of mitochondrial network branching calculated through confocal microscopy analysis (n=70). Unless otherwise specified, data are expressed as percentage change from control, and bars represent standard error of the mean. *p<0.05, **p<0.01.*

Shown in Figure 6.6 are three representative confocal images for each experimental group. These confocal images highlight the high abundance of mitochondria, forming a wide mitochondrial network within adipocytes. Indeed in many cases, mitochondria encircle lipid droplets either partially or completely (indicated by white arrowheads), further evidence of the important functional link between these two cellular structures.

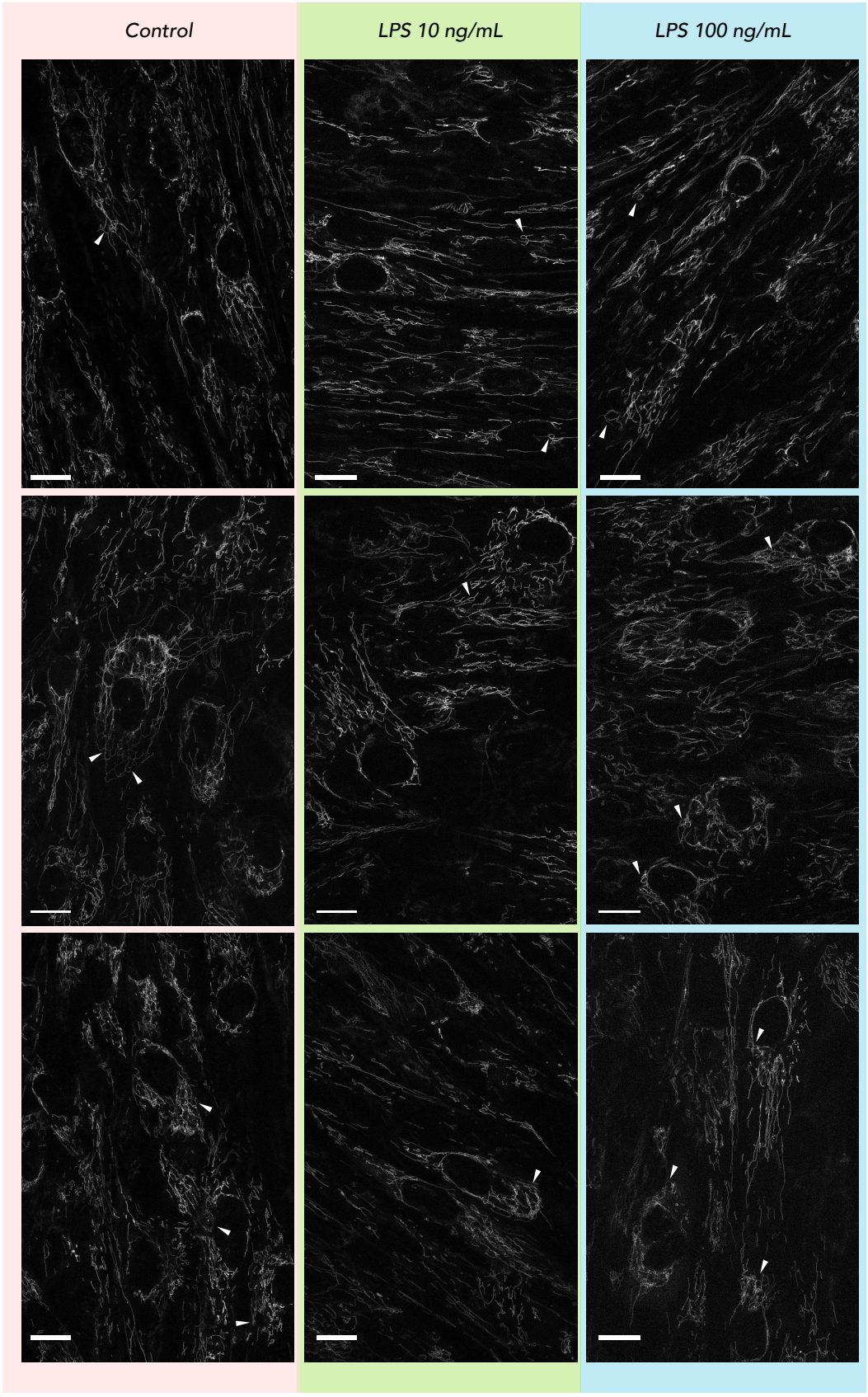

Figure 6.6: Confocal Microscopies of Adipocytes treated with or without LPS
Representative confocal images of control (left panel) and LPS-treated adipocytes (middle and right panel). Images are shown at 40x magnification, scale bar represents $10\,\mu m$*. Arrowheads indicate where lipid droplets are clearly evident within the mitochondrial network.*

LPS administration impaired mitochondrial efficiency, leading to a greater reliance on glucose as an energy substrate

To understand the implications of LPS treatment on mitochondrial function, a Seahorse extracellular flux analyzer was used to measure basal oxygen consumption rate (OCR) and extracellular acidification rate (ECAR) as indicators of aerobic and anaerobic respiration, respectively. As shown in Figure 6.7**A**, 24 hours of LPS treatment did not significantly alter OCR, but up-regulated glycolysis, indicated by increased ECAR (Figure 6.7**B**). Despite the increased respiration with LPS treatment, ATP production was significantly reduced at both 24 and 72 hours (Figure 6.7**C**), resulting in significantly impaired bioenergetic efficiency (Figure 6.7**D**). Interestingly, mitochondrial membrane potential was unaffected by LPS treatment (Figure 6.7**E**), indicating reduced efficiency was not related to mitochondrial uncoupling.

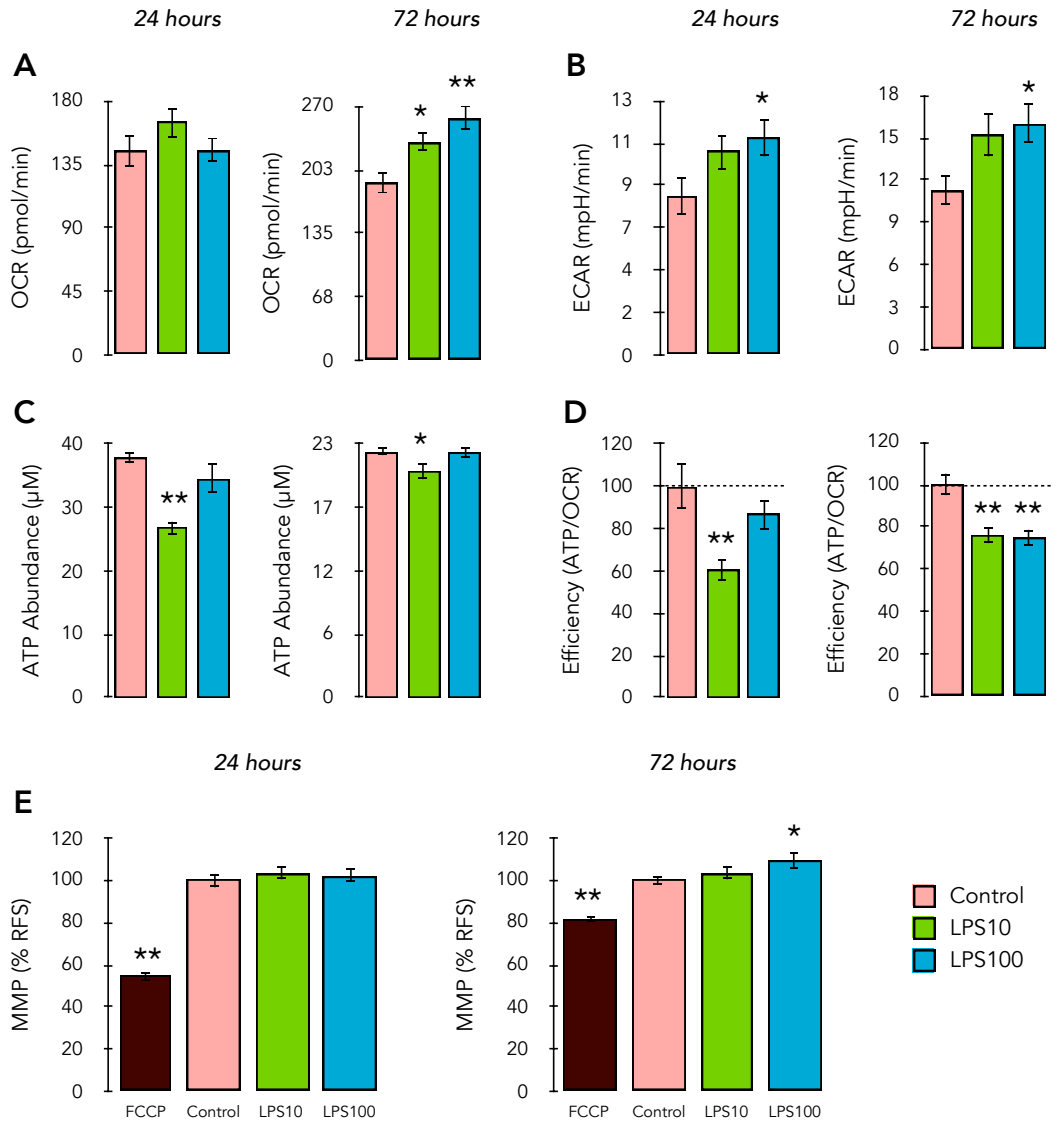

Figure 6.7: **Effect of LPS on Basal Mitochondrial Bioenergetics**
(A) *Basal oxygen consumption rate (OCR),* ***(B)*** *Basal extracellular acidification rate (ECAR),* ***(C)*** *ATP abundance,* ***(D)*** *basal bioenergetic efficiency (ATP/ mitochondrial OCR), and* ***(E)*** *mitochondrial membrane potential (MMP; expressed as relative flourescence signal) in human adipocytes following a 24 or 72-hour incubation with* 10 *or* $100\,^{\mathrm{ng}}/_{\mathrm{mL}}$ *LPS (n=10). Data are expressed as percentage change from control, unless otherwise specified and bars represent standard error of the mean. *p<0.05, **p<0.01.*

LPS administration reduced cellular metabolic flexibility under stress

Given that obesity represents a chronic stress to adipocytes, it became necessary to understand the implications of LPS treatment when adipocyte mitochondria

are under stress. Therefore, a Seahorse Mito Stress Test was performed after LPS treatment. Briefly, this test consists of the successive delivery of 3 compounds which systematically shut down different components of the electron transport chain. The compound oligomycin inhibits ATP synthase, the ionophore FCCP disrupts the mitochondrial membrane potential, and Rotenone/Antimycin A inhibit complex I action, effectively arresting all mitochondrial respiration. With each additional compound, the cell must increase its reliance on glycolysis to meet ATP demand and sustain life. As shown in Figure 6.8, that is indeed the case for control cells, where each compound addition during the stress test results in increased ECAR. However, with LPS treatment, adipocytes are unable to sustain the high glycolytic rate, indicating an impaired metabolic flexibility under stress. Figure 6.9, indicates adipocytes do not alter their aerobic respiration (OCR) to cope with decreasing glycolysis. The net result of LPS treatment is a shift towards increased glycolysis in basal conditions, but impaired glycolytic capacity under stress (Figure 6.10). This shift in energy phenotype of adipocytes is indicative of greater reliance on glucose rather than lipids as an energy substrate, which may further exacerbate the stress of over-nutrition.

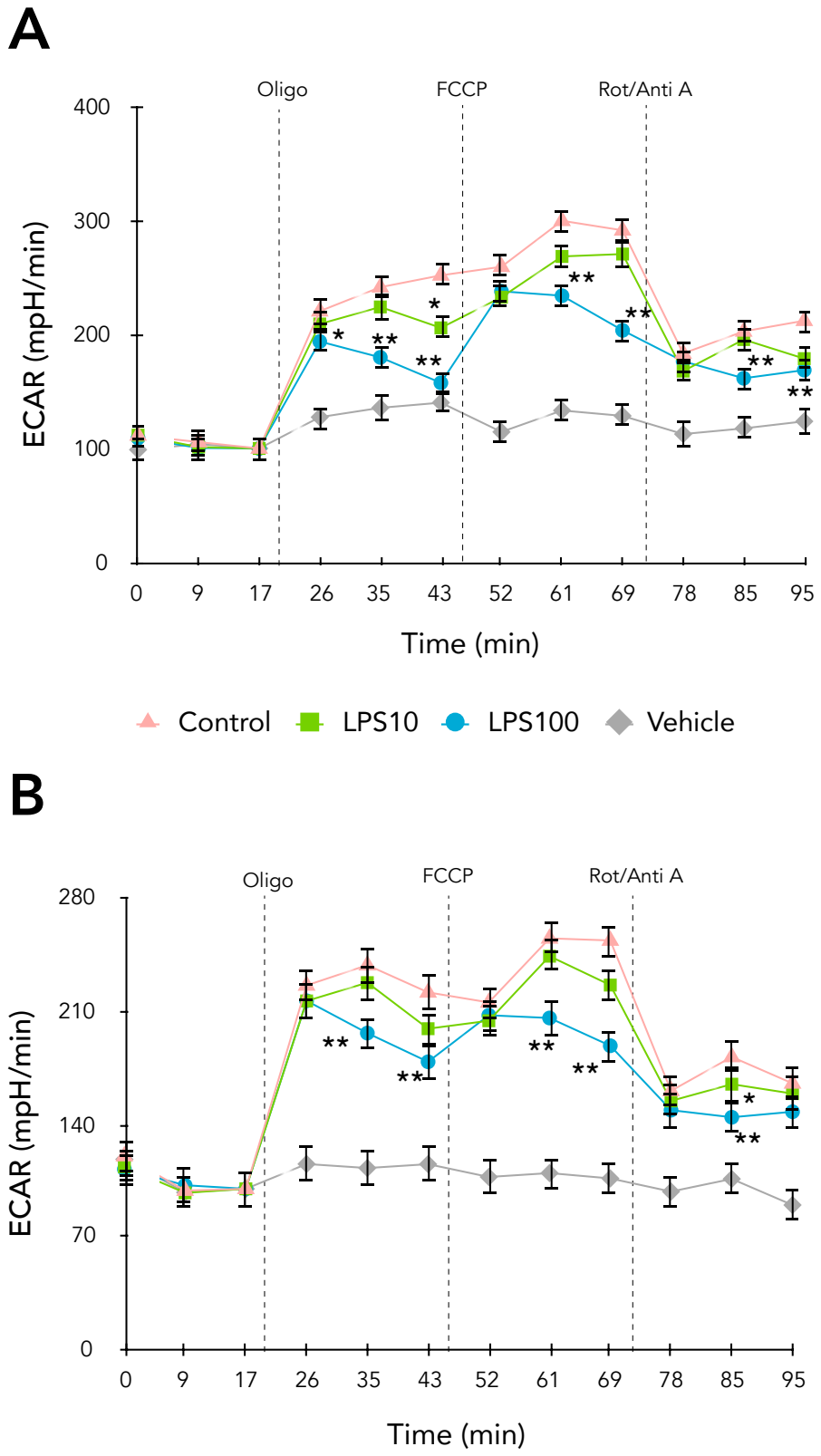

Figure 6.8: Effect of LPS on glycolytic capacity under stress

*Time-lapse of glycolytic capacity as measured by extracellular acidification rate (ECAR) of the media during a seahorse mitochondria stress test performed after a 24-hour **(A)** or 72-hour **(B)** incubation with 10 or 100 $^{ng}/_{mL}$ LPS (n=10). Values were normalised to basal levels of each experimental group to account for inter-well cell number variability. Error bars represent standard error of the mean. *p<0.05, **p<0.01.*

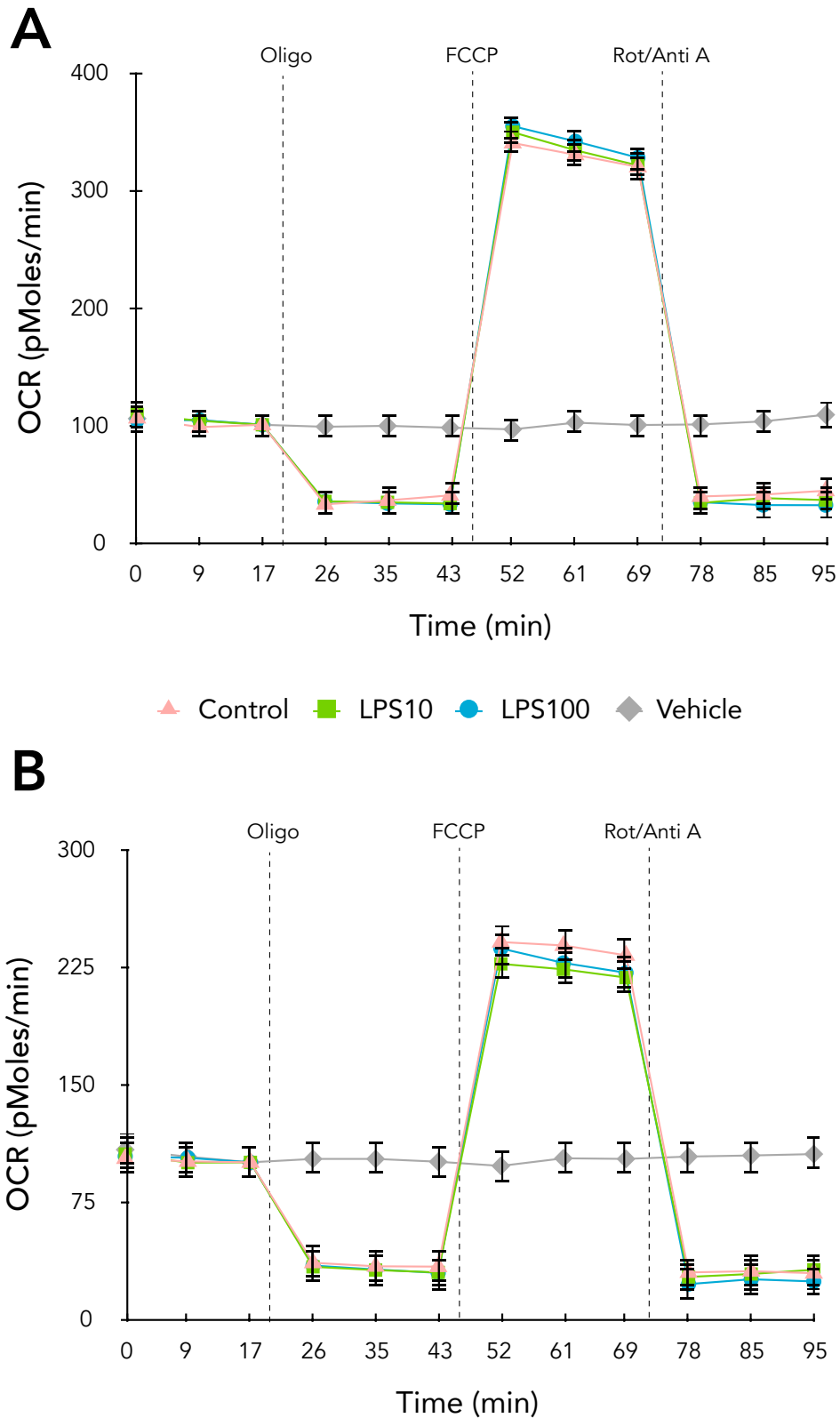

Figure 6.9: Effect of LPS on aerobic capacity under stress

*Time-lapse of aerobic capacity as measured by oxygen consumption rate (OCR) during a seahorse mitochondria stress test performed after a 24-hour **(A)** or 72-hour **(B)** incubation with 10 or 100 $^{ng}/_{mL}$ LPS (n=10). Values were normalised to basal levels of each experimental group to account for inter-well cell number variability. Error bars represent standard error of the mean. *p<0.05, **p<0.01.*

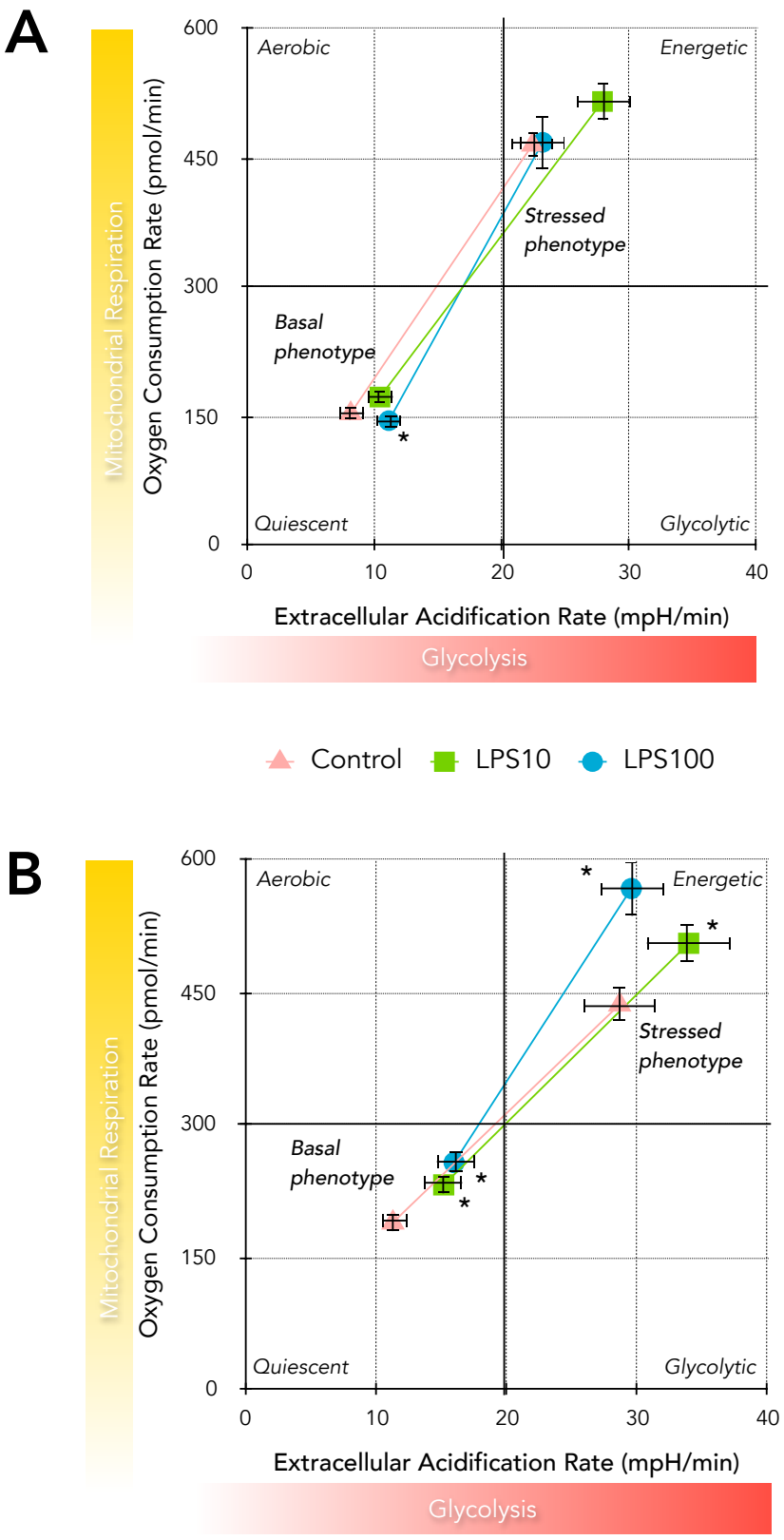

Figure 6.10: Effect of LPS on energy phenotype of the adipocyte

*Energy phenotype mapping of control vs. LPS-treated adipocytes assessed after 24-hour **(A)** or 72-hour **(B)** treatments in both, basal and stressed conditions. Error bars represent standard error of the mean. *p<0.05, **p<0.01.*

6.4 Discussion

In this present chapter, it was hypothesized that surgery-specific changes in serum concentrations of gut-derived bacterial LPS may modulate the differential metabolic and mitochondrial outcomes observed between bariatric surgical procedures (outlined in previous chapters). Thus, human subcutaneous adipocytes were treated with LPS to test the direct effect on mitochondrial function and insulin sensitivity. These novel studies demonstrate that increased circulating LPS levels (often present as a result of a Western diet), when delivered *in vitro,* can directly trigger mitochondrial damage, and a dysfunctional switch of energy substrate from lipids towards glucose, potentially impairing the lipid buffering capacity of adipose tissue. The key finding of this study was that incubation of adipocytes with LPS induced a switch in metabolic phenotype: from primarily reliant on oxidative phosphorylation for energy requirements to greater reliance on glycolysis. The relevance of this finding is tied to the implication that reliance on glucose instead of lipids as a fuel will impair the lipid buffering capacity of adipose tissue, leading to lipid spill-over and deposition in other organs such as liver, pancreas, blood vessels and skeletal muscle. The ectopic deposition of fat in organs other than adipose tissue is known to initiate systemic insulin resistance [282, 150]. Thus, lowering LPS levels in circulation (either through diet, pharmacotherapy and/or bariatric surgery) may have therapeutic potential, and warrant further investigation.

The switch in fuel preference resulted in reduced bioenergetic efficiency, which could not be explained by mitochondrial membrane potential or uncoupling action (as both were unaltered). However, LPS resulted in sustained conditions of inflammation and oxidative stress in tandem with deletion of mitochondrial DNA,

protein depletion and dramatic morphological alterations. Sustained mitochondrial elongation and/or conditions of high oxidative stress are known to compromise mitochondrial DNA quality [281, 236], and in this instance either through defective protein translation, redox signaling or some other unknown mechanism resulted in the metabolic phenotype observed.

This study has some limitations, namely, an *in vitro* study design which, though selected because it would minimise interference of confounders, does not necessarily reflect the phenomenon as it would occur *in vivo*. Recent evidence from germ-free animals have shown that the interaction of the microbiota with diet and metabolic health is enormously complex, and can vary with species, genetic background, diet, physiological and pathological state [30]. Further research is required to elucidate this interaction, and specifically the relationship between LPS and adipose mitochondria.

In conclusion, this study provides direct, novel evidence, that a Western diet is linked with impaired adipose tissue metabolism through gut-derived LPS, which modulates mitochondrial dysfunction and may initiate and/or exacerbate the metabolic syndrome. These findings are consistent with the initial hypothesis that surgery-specific differences in mitochondrial outcomes may be due, at least in part, to divergence in serum LPS concentrations. Nevertheless, many other factors (including compliance with dietary and lifestyle advice) may also play a role in both serum LPS levels and metabolic outcomes after bariatric surgery, and should not be discounted, particularly as reduction of LPS levels alone, is unlikely to be sufficient to counteract all other adverse factors from an unhealthy diet and lifestyle to provide significant metabolic benefit. Thus, in the next (and final) chapter of

this thesis, the impact of environmental factors on bariatric surgical outcomes are explored in greater detail.

Chapter 7

Environmental Factors Influencing Bariatric Outcomes of a Specialist Weight Management Service: Lessons from a Clinical Audit

---

7.1 Introduction

The purpose of this chapter was to examine the pathophysiology of obesity through a clinical perspective, and to explore the environmental barriers to its successful resolution. Despite the fact that bariatric surgery has been shown to result in significant and profound weight loss, significant weight regain is seen in in 10-20% of patients after all of the most commonly performed procedures: Roux-en-Y gastric bypass, vertical sleeve gastrectomy and laparoscopic adjustable gastric banding [355, 356]. Since weight recidivism can have significant detrimental effects on the person´s metabolic health and quality of life, it is paramount to understand the factors involved.

A recent systematic review has highlighted diet and behaviour/psychology as the most common reasons for weight regain following bariatric surgery (in approximately 25% and 20% of cases, respectively) [173, 357]. Indeed, dietary non-compliance may cause a 50% excess weight regain in as little as 3 months [358], and poor diet quality, inappropriate food choices and lack of nutritional counseling were shown to predict weight regain post-surgery [359]. In addition, the presence of a psychiatric diagnosis [360], greater impulsivity and binge-eating behaviour [144], lack of psychological follow-up [361], and "food grazing" behaviours [362, 363] are all positively associated with weight regain post-bariatric surgery. Thus, engagement and compliance with medical, dietetic and lifestyle advice is an important component of successful long-term post-operative weight management [173].

During the course of these studies, data was collected as part of an audit in the Tier 3 and 4 specialist weight management service at University Hospitals Coventry and Warwickshire NHS Trust. This specialist service offers an integrated medical and

surgical management of complex and severe obesity, with a wide and diverse multidisciplinary team which includes Endocrinology, Nursing, Dietetics, Psychology and Surgery (please see acknowledgements section). To ensure patient safety and maximal outcomes, the National Institute for Health and Care Excellence (NICE) guidelines state that bariatric surgery should be considered only if an individual meets all of the following criteria [1]:

- A BMI of ≥ 40 or between $35 - 40$ with a significant co-morbidity is present which could be improved with weight loss.
- All appropriate non-surgical methods have been tried and failed
- Has had or will have intensive pre and post-operative multi-disciplinary management and support (including psychological and dietetic)
- Generally fit for surgery and anaesthesia
- Patient commitment to long-term follow-up
- Bariatric surgery is the treatment of choice for individuals with a BMI > 50

In the UHCW bariatric service, two additional criteria were enforced: a minimum 12-month engagement with the medical pathway and at least 5% excess weight loss and maintenance before the day of surgery.

Thus, in this audit the following research questions were investigated: (1) how effective is this Tier 3 and 4 service on weight loss and glycaemic outcomes, (2) how effective are the current UHCW surgical criteria at predicting post-surgical outcomes, and (3) what impact does the degree of multidisciplinary support have on patient outcomes?

7.2 Methods

Audit Rationale and Description

The aim of this study was to evaluate local weight loss and glycaemic control outcomes of the service´s own patient population and to identify specific barriers or strategies which may help improve patient outcomes. In particular, evidence for the validity of the current surgical criteria was investigated. The audit population was comprised of 100 morbidly obese patients who started and completed both medical and surgical service pathways of the Warwickshire Institute for the Study of Diabetes, Endocrinology, and Metabolism (WISDEM), University Hospitals Coventry and Warwickshire NHS Trust (UHCW) between 2011 and 2016. All patients underwent the same sleeve gastrectomy procedure and were followed-up for 18 months post-surgery. All data included in this audit was prospectively collected, and retrospectively collated from the electronic clinical results reporting system and patient appointment booking system. Data collected was limited to Age, Height and Weight at start, day of surgery, then 3, 6, 9, 12 and 18 months post-surgery. Starting type-2 diabetes status, and serum HbA1c levels at day of surgery, and 1 year post-surgery were also collected. Pre-surgery clinic attendance information was collected for a sub-cohort of 55 patients for whom complete data was available and included: total appointments with Medical doctor, Dietitian, Psychologist, and Surgeon as well as duration of time spent on the medical pathway.

Statistical Analysis

All statistical analyses were performed using IBM SPSS Statistics Version 22. Excess weight loss was calculated as percentage of excess weight, using an ideal body weight corresponding to BMI of 25. Data were analysed for normality and log-transformed if non-parametric. Correlations were analysed using bivariate Pearson correlation analyses. Unless otherwise stated, differences between 2 groups were analysed using 2-tailed independent samples T-test and One-way ANOVA for more than 2 groups. A p value of <0.05 was considered as statistically significant.

7.3 Results

Description of the Service Pathway

The integrated medical and surgical pathways for the specialist weight management service at the Warwickshire Institute for the Study of Diabetes, Endocrinology and Metabolism (WISDEM) are shown in Figure 7.1. All patients are seen by a Dietitian, Medical Endocrinologist, and Psychologist for an initial assessment at the start of the medical pathway, after which they are followed up regularly (approximately every 3 months) by a Dietitian, and based on medical need by a Medical endocrinologist (approximately every 6 months for those patients with a comorbidity or other medical need relevant to cardio-vascular disease risk management). Depending on need, there is some limited availability for psychological treatment. Once the patient has met the surgical criteria, the MDT make a joint decision on surgical candidacy, and the patient is then invited to attend a group education session on the surgical options available, and pre and post-surgical advice. After this point, they are seen by a surgeon in clinic and placed on the surgery waiting list. Post-surgically, patients are followed-up at 3, 6, 9, 12, and 18 months by either a Dietitian or Bariatric Nurse and at 12 and 24 months by a medical endocrinologist before being discharged to the care of their GP at 24 months.

Effect of Service Pathway on Weight Loss and Glycaemic Control

Table 7.1 shows the starting demographics of the audit population, split by T2DM status. Of the total audit population (n=100), fourty-five had been diagnosed with

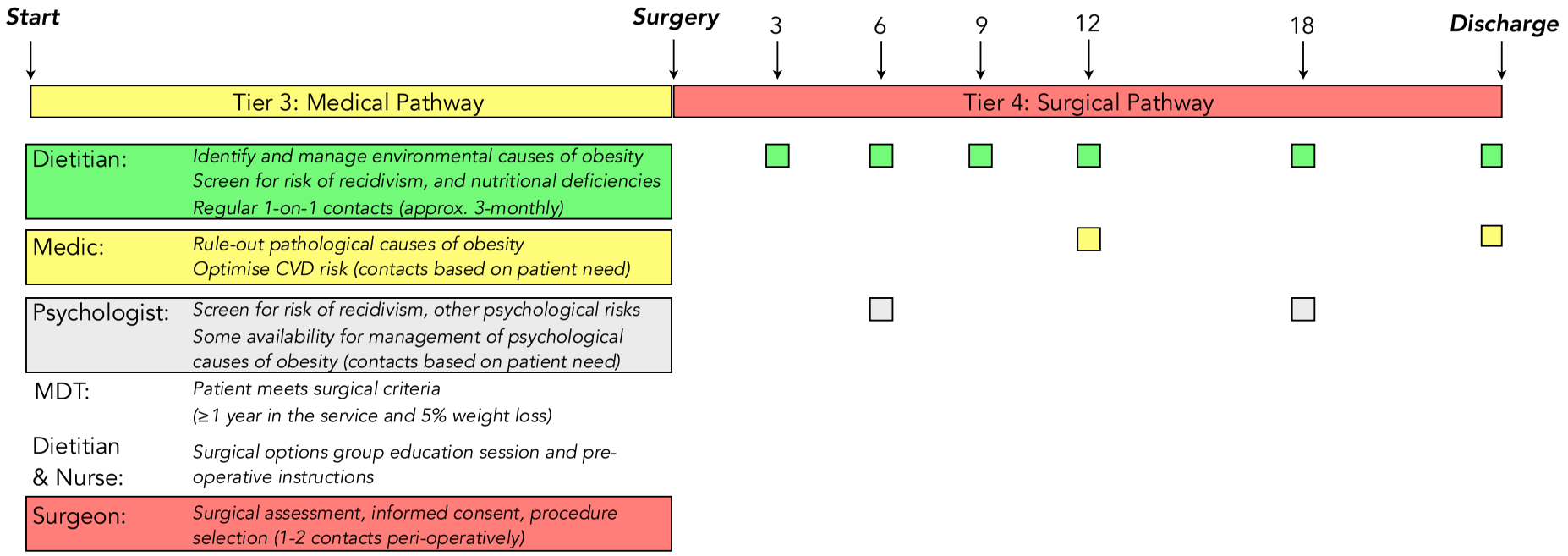

Figure 7.1: Diagram of the integrated medical and surgical service pathways

Diagram of the integrated medical and surgical bariatric pathways at the Warwickshire Institute for the Study of Diabetes, Endocrinology and Metabolism (WISDEM) in the University Hospitals Coventry and Warwickshire NHS Trust (UHCW). Numbers indicated in surgical pathway correspond to timeline in months post-surgery, whilst coloured boxes denote clinical contacts between the patient, and a Dietitian, medical Endocrinologist and Psychologist. CVD: cardio-vascular disease.

type-2 diabetes mellitus (T2DM) prior to their first appointment, whilst fifty-five had not (Figure 7.2). The two sub-cohorts did not differ significantly in either age, BMI or excess weight.

Table 7.1: Starting demographics of non-diabetic and diabetic cohorts

	Non T2DM $n = 55$		T2DM $n = 45$		Non T2DM vs. T2DM
	Mean±SD	Min-Max	Mean±SD	Min-Max	p value
Age (y)	46.3 ± 9.33	$23 - 65$	48.1 ± 10.2	$26 - 67$	0.371
Height (m)	1.65 ± 0.09	$1.51 - 1.91$	1.68 ± 0.08	$1.52 - 1.91$	0.078
Weight (Kg)	146.6 ± 20.0	$108.4 - 201.2$	147.0 ± 23.9	$112.0 - 225.0$	0.917
BMI (Kg/m^2)	53.4 ± 6.30	$40.4 - 72.1$	51.5 ± 5.96	$40.3 - 64.1$	0.119
IBW (Kg)	78.8 ± 7.79	$57.1 - 91.0$	71.4 ± 7.47	$57.8 - 91.2$	0.084
Excess Weight (Kg)	77.8 ± 17.1	$42.8 - 131.5$	75.6 ± 19.6	$50.28 - 133.8$	0.556
Excess Weight ($\% \; of \; IBW$)	213.9 ± 24.9	$161.6 - 288.6$	205.8 ± 23.8	$161.3 - 256.3$	0.100

Data are means ± standard deviation. Statistical differences between non-diabetic and diabetic cohorts were determined via 2-tailed independent T-tests, and significance p value shown in right-most column. BMI: body mass index, IBW: ideal body weight (calculated if BMI was 25).

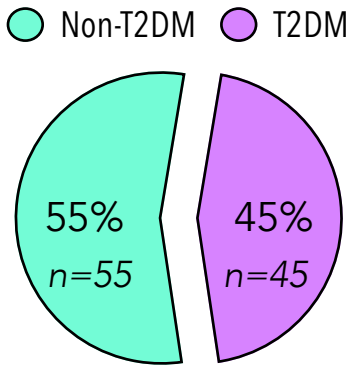

Figure 7.2: Starting proportion of type-2 diabetes in the patient cohort
Pie chart showing numerical proportion of patients with a diagnosis of type-2 diabetes mellitus (T2DM) prior to their start in the specialist weight management service.

Figure 7.3 shows the BMI, total body weight and excess weight loss up to the day of surgery. Both non-T2DM and T2DM patients lost a significant amount of weight during this time (20% of their excess weight on average). Though non-T2DM patients lost 2% extra (approximately 4 Kg) than the T2DM group, this difference was not statistically significant.

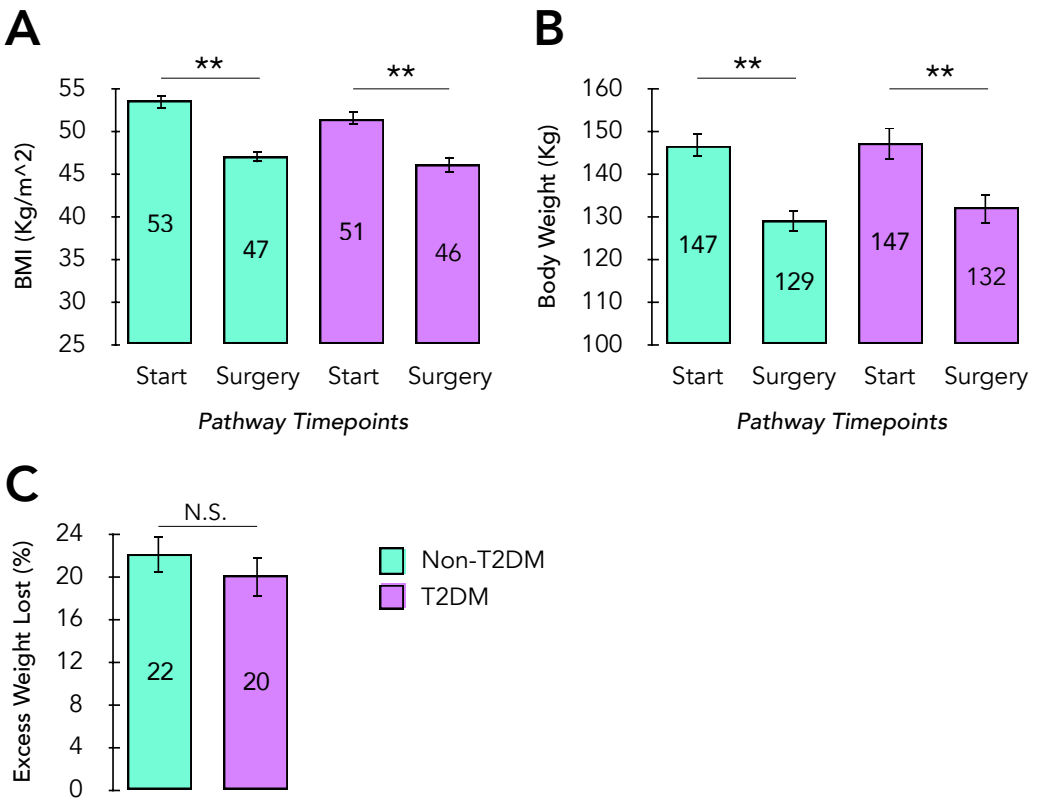

Figure 7.3: Effect of the medical pathway on obesity

*Indicators of obesity taken at the beginning (first appointment) and end (surgery day) of the medical pathway for both non-diabetic and diabetic cohorts. Charts show (**A**) BMI, (**B**) total body weight, and (**C**) body weight lost by the day of surgery (expressed as percentage of excess weight). Bars represent means ± standard error of the mean. Statistical differences between start and day of surgery were analysed using 2-tailed paired t-test, *p<0.05; **p<0.01. Statistical differences between non-T2DM and T2DM cohorts were determined via 2-tailed independent samples t-test. †p<0.05; ††p<0.01.*

In terms of glycaemic control, Figure 7.4 shows the proportion of patients who achieved serum HbA1c targets of less than $48^{\text{mmol}}/_{\text{mol}}$ by the day of surgery. As expected, all but one non-T2DM patients had serum HbA1c levels well below $48^{\text{mmol}}/_{\text{mol}}$ (on average $38.5 \pm 4.5^{\text{mmol}}/_{\text{mol}}$), whilst the majority (68%) of T2DM patients had sub-optimal glycaemic control (on average $60.0 \pm 2.14^{\text{mmol}}/_{\text{mol}}$).

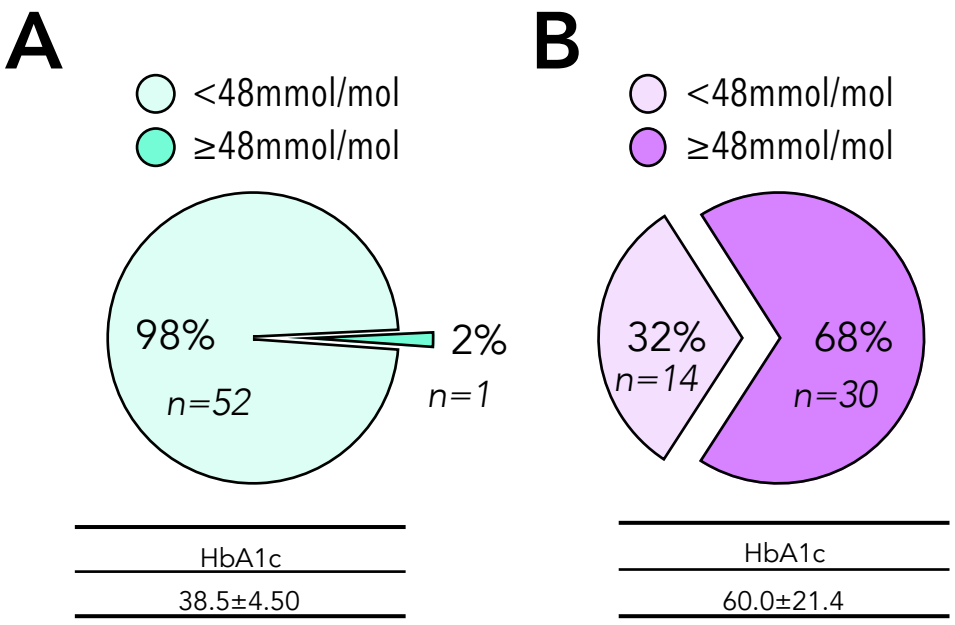

Figure 7.4: Proportion of patients who achieved glycaemic control before surgery
*Pie charts showing numerical proportion of patients who achieved target HbA1c of <48mmol/mol by the end of the medical pathway (day of surgery). Independent charts are shown for (**A**) non-T2DM and (**B**) T2DM cohorts. Serum HbA1c levels (means ±standard deviation) are shown below for each cohort.*

Figure 7.5 shows the trend of weight loss throughout the service pathway. Significant reductions in BMI were observed at every follow-up contact up until one year post-surgery, after which (18 months) this trend reached an apparent plateau (Figure 7.5**A**). Indeed, an average of approximately 2-4% of excess weight was regained between 12 and 18 months post-surgery (Figure 7.5**B**). This trend was not significantly different between T2DM and non-T2DM groups.

In terms of timing, as shown in Figure 7.6, much of the weight loss (approximately 34%) occurred prior to surgery during the medical pathway, and peaked shortly after surgery, with an additional 37% lost within the first 3 months post-surgery. The initial weight loss pre-surgery was slightly reduced in T2DM (32%) compared with non-T2DM patients (36%), however this difference was not statistically significant (p=0.307).

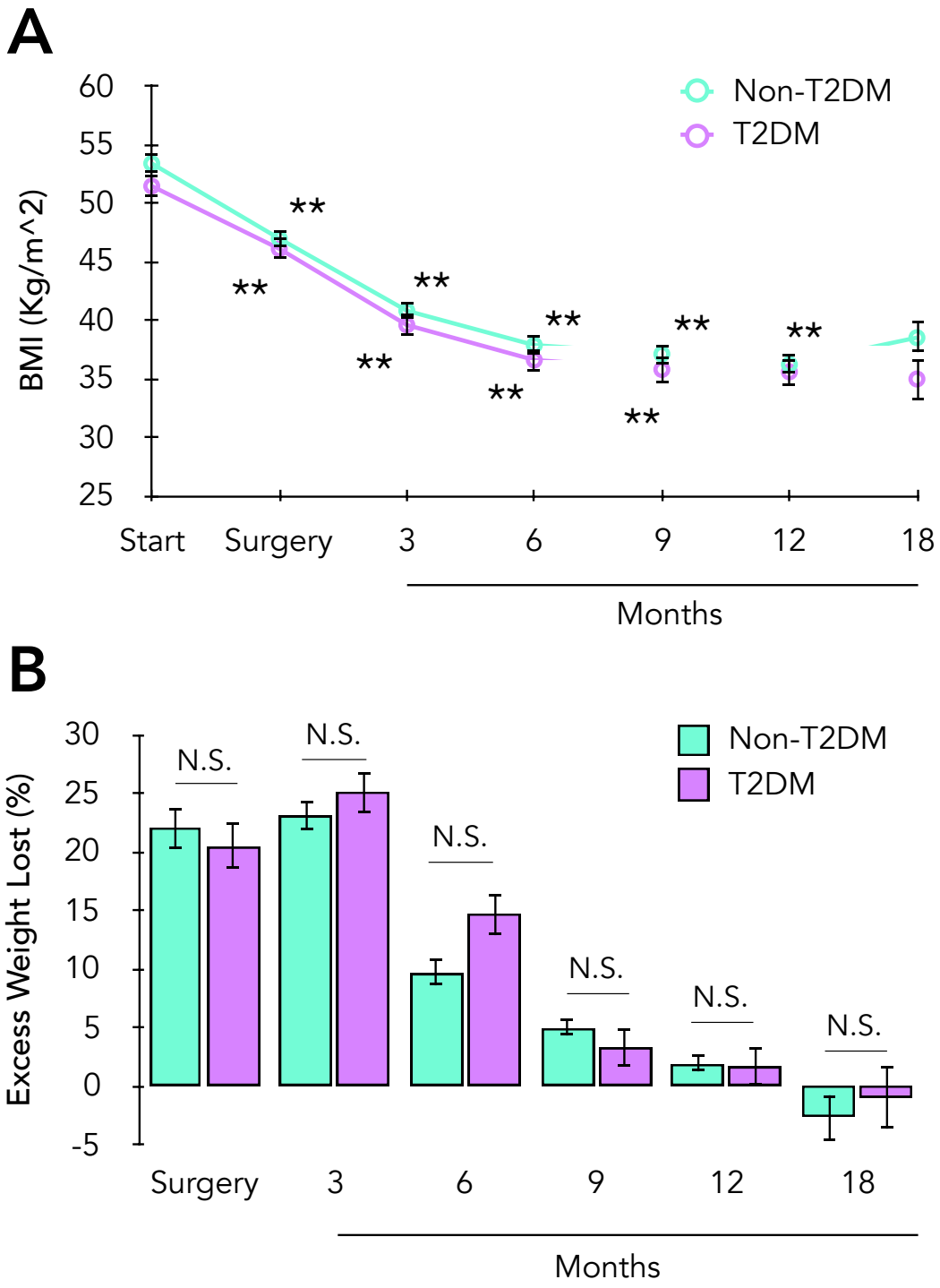

Figure 7.5: Trend of weight loss throughout the service pathway

*Mean BMI (**A**) and excess weight loss (**B**) for non-T2DM and T2DM cohorts from beginning to end of the service pathway. Error bars represent standard error of the mean. Statistical differences from one contact to the next were analysed using 2-tailed paired t-test, *p<0.05; **p<0.01. Statistical differences between non-T2DM and T2DM cohorts were determined via 2-tailed independent samples t-test. †p<0.05; ††p<0.01. N.S. denotes differences are not statistically significant.*

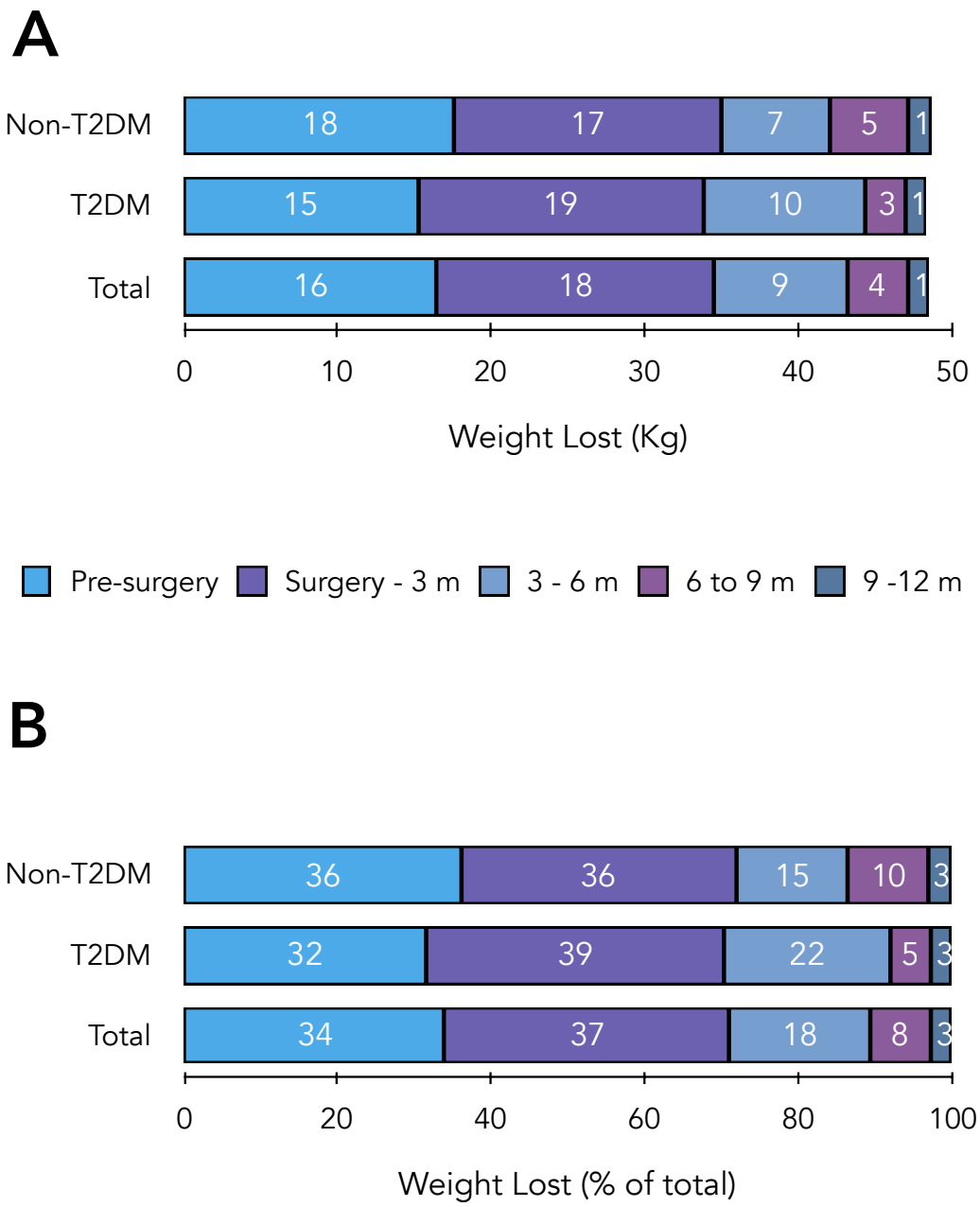

Figure 7.6: Timing of weight loss between patient contacts

*Distribution of weight lost in (**A**) Kg and (**B**) as percentage of total weight loss between each patient contact of the service pathway, for non-T2DM (n=55), T2DM (n=45) patient cohorts and the combined total (n=100).*

Figure 7.7 summarises the net effect of the service on weight loss. On average patients lost nearly 50 Kg, with a minimal regain (1 to 3 Kg) by the final follow-up appointment (Figure 7.7**A**). However, the extent of weight loss varied widely from one individual to the next. Figure 7.7**B** shows this distribution for the total patient cohort (n=100), as well as non-T2DM (n=45) and T2DM cohorts (n=55). In all

cohorts and sub-cohorts, the most frequent result was a loss of 50 to 74% of excess weight (an outcome achieved by 45 to 56% of patients). Around 30% of patients lost between 25 and 49% of their excess weight, and around 17% lost more than 75% of their excess weight. Finally, only 2% of patients achieved less than 25% excess weight loss. The final weight loss outcomes, though slightly less robust for the T2DM group did not differ significantly between sub-cohorts.

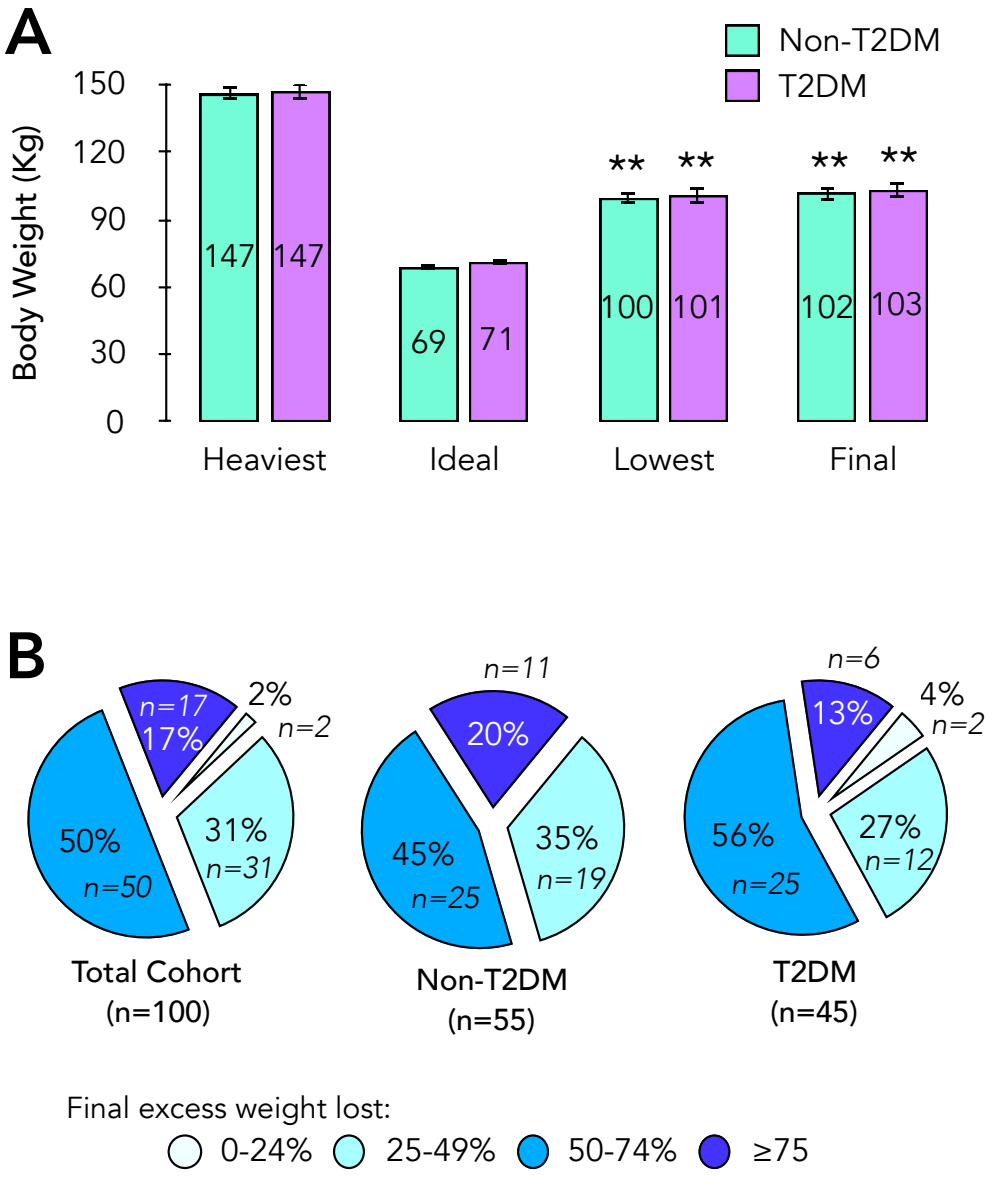

Figure 7.7: Summary of achieved weight loss

(A)*Summary of changes in body weight from heaviest to final weight recorded. Ideal and lowest body weight are included for reference. Bars represent means ± standard error of the mean. Statistical differences between heaviest and lowest or last weight were analysed using a 2-tailed paired t-test, *p<0.05; **p<0.01. (**B**) Pie charts showing the proportion of weight loss success in the combined total, non-T2DM and T2DM cohorts. Categories represent varying degrees of weight loss (expressed as a percentage of individual excess weight).*

Figure 7.8 summarises the net effect of the service pathway on glycaemic control (as evidenced by serum HbA1c levels). As expected, T2DM individuals had higher levels at both pre and post-surgery than non-T2DM patients, however, both patient groups achieved significantly lower HbA1c levels at 12 months post-surgery (Figure 7.8**A**). This reduction was nevertheless significantly greater in T2DM patients,

who exhibited a 20% serum HbA1c reduction on average, whilst a 10% reduction was observed in the non-T2DM group (Figure 7.8**B**). In contrast to only 30% of T2DM patients who met HbA1c targets ($< 48^{\mathrm{mmol}/\mathrm{mol}}$) before surgery, at one year post-surgery 65% of T2DM patients had met this target (Figure 7.8**C**). Medication information was not collected for this audit, so it is unclear whether this constituted true remission, or simply better medical management.

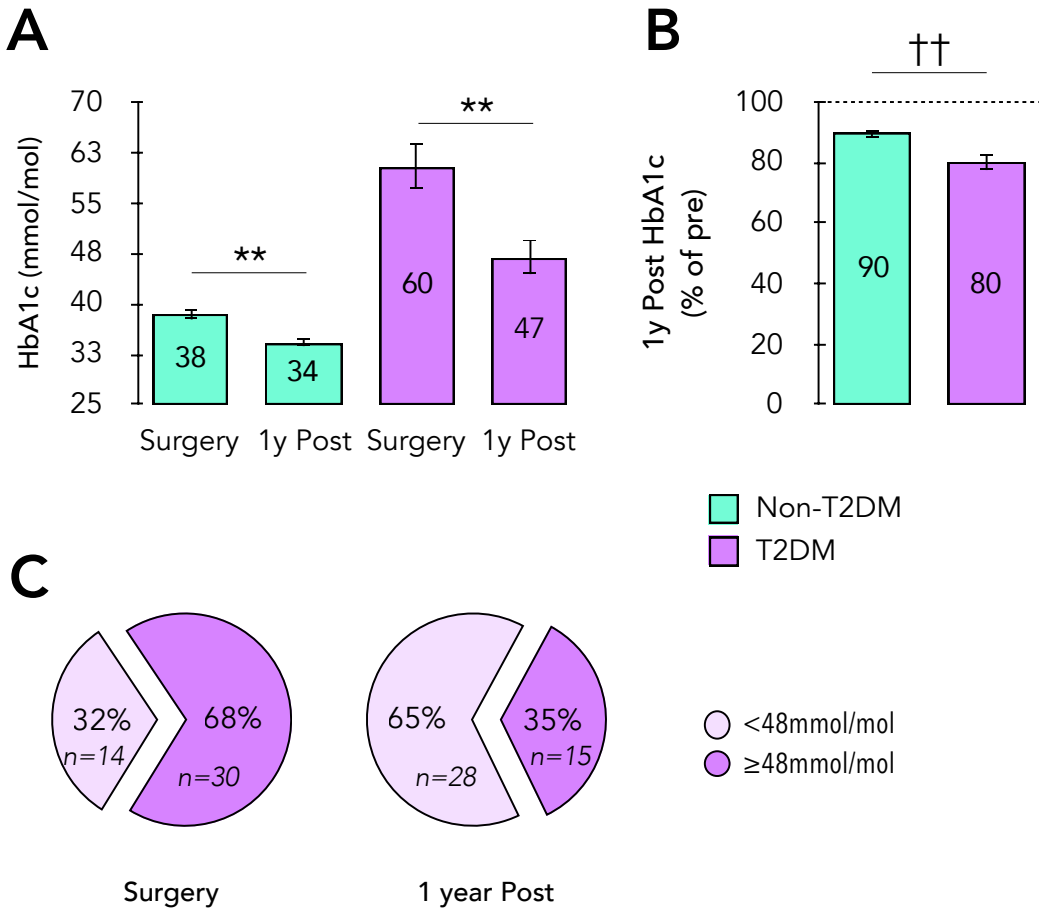

Figure 7.8: Summary of achieved glycaemic control

(A)*Serum HbA1c levels at time of and 1 year post-surgery in non-T2DM and T2DM cohorts. (**B**) Comparison of surgery-induced changes (expressed as percentage of peri-operative values) in serum HbA1c between non and T2DM cohorts. (**C**) Pie charts showing the proportion of patients who achieved HbA1c targets at the time of and 1 year post-surgery in the T2DM cohort. Bars represent means ± standard error of the mean. Statistical differences between pre and post-surgery were analysed using a 2-tailed paired t-test, *p<0.05; **p<0.01. Statistical differences between non-T2DM and T2DM cohorts were determined via 2-tailed independent samples t-test. †p<0.05; ††p<0.01.*

Pre-Surgery 5% Weight Loss as an Indicator of Compliance and Post-Surgical Outcomes

In the UHCW specialist weight management service, one of the criterion for bariatric surgical candidacy is that the patients lose 5% of their excess weight before surgery. The rationale for this criterion is that it is an indicator of dietetic and lifestyle compliance (more objective than self-reported information) and will allow the multidisciplinary team to select those patients who are most likely to benefit from surgery.

As 5% excess weight loss is a criterion for surgery, a very small minority of the audit population (6%) did not meet this target. The majority of patients (47%) lost well above the target (>20%) by the day of surgery, followed by 27% who lost between 10 and 20% excess weight, and 20% who lost between 6 and 10% excess weight prior to surgery (Figure7.9).

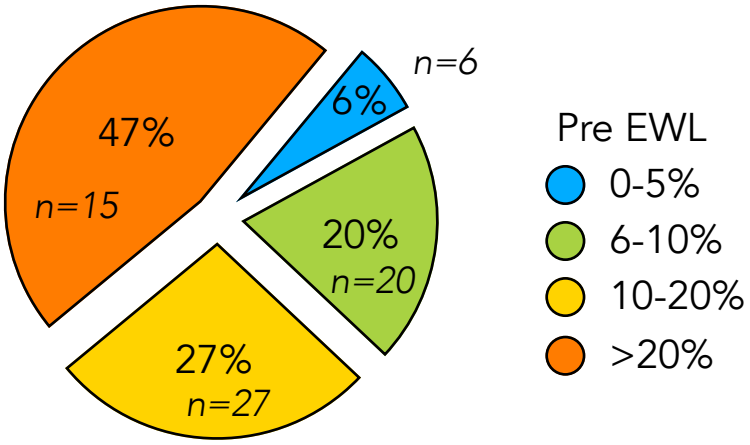

Pre Excess Weight Loss (%)	
mean±SD	21.4±12.7
median	19.9
mode	20.0
min-max	0-57.5

Figure 7.9: Excess weight loss pre-surgery

Pie chart depicting patient distribution across increasing categories of pre-surgical weight loss (as % of excess weight). Descriptive statistics for pre-surgical excess weight loss (EWL) are shown below the chart.

Next, Pearson correlation analyses were used to examine the relationship between pre-surgical weight loss and post-surgery weight loss and T2DM outcomes. As shown in Table 7.2, pre-surgical weight loss was significantly and positively associated with post-surgical weight loss, namely that occurring within the first 3 months post-operation (coincidentally the period with fastest weight loss), the maximal weight loss and the final weight loss achieved. Importantly, pre-surgical weight loss was also significantly and inversely associated with post-surgical glycaemic control (as evidenced by HbA1c at 12 months after surgery).

Table 7.2: Relationship of pre-surgery weight loss to post-surgical outcomes

	Pre-surgery EWL (%)	
	Pearson´s r	p value
Post EWL (Surgery to 3m)	−0.622	0.0000002**
Post EWL (3m to 6m)	−0.022	0.850
Post EWL (6m to 9m)	−0.168	0.185
Post EWL (9m to 12m)	−0.068	0.631
Post EWL (12m to 18m)	0.099	0.596
Post Maximum EWL (%)	0.512	0.0000004**
Post Final EWL (%)	0.475	0.000003**
Pre HbA1c (mmol/mol)	−0.126	0.214
1 year Post HbA1c (mmol/mol)	−0.246	0.016*
1 year Post HbA1c (% of pre)	−0.050	0.630

*Table shows Pearson´s correlation coefficient (r) and p value significance (p) between pre-surgical excess weight loss (EWL) and post-surgical weight loss and glycaemic outcomes. Significant correlations are shown in red. *p<0.05, **p<0.01, n=100. EWL: weight loss expressed as percentage of excess weight.*

The association of pre-surgical weight loss with final post-operation excess weight loss and HbA1c are shown in greater detail as scatterplots on Figure 7.10. Interestingly, past the limit of 30% pre-surgery weight loss, the associated improvement in HbA1c appears to reach a plateau (Figure 7.10**B**).

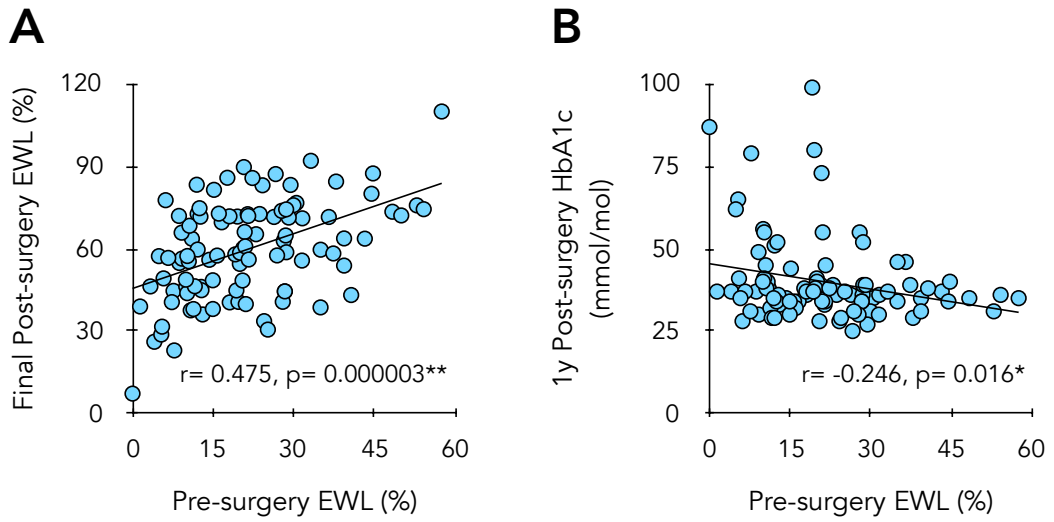

Figure 7.10: Association of pre-surgical weight loss with post-surgical outcomes
*Scatter plots showing correlation between pre-surgical excess weight loss and **(A)** final post-operative weight loss outcomes and **(B)** glycaemic control. EWL: weight loss expressed as percentage of excess weight. n=100.*

The trend in BMI throughout the service pathway in different categories of pre-

surgery excess weight loss is shown in Figure 7.11. The BMI of patients who did not achieve the 5% weight loss target was significantly higher no just at the start, but also throughout the pathway. Furthermore, they exhibited significant weight regain, back to nearly the same BMI as pre-surgery. Interestingly, past the minimum 5%, there was no significant difference in BMI between patients who lost 10%, 20% or greater than 20%, indicating the enhanced outcomes in those who lost more than 5% may be the result of greater compliance with dietetic and lifestyle advice, rather than the weight loss *per se*.

This observation was mirrored in T2DM outcomes as well. As shown in Figure 7.12, patients who lost more than 5% of their excess weight prior to surgery had significantly lower levels of serum HbA1c on the day of surgery as well as 1 year post-operation. However, this advantage was not significantly greater with further weight loss, further supporting the notion that this gain is the result of lifestyle and dietetic compliance in these individuals rather than a function of the weight loss itself.

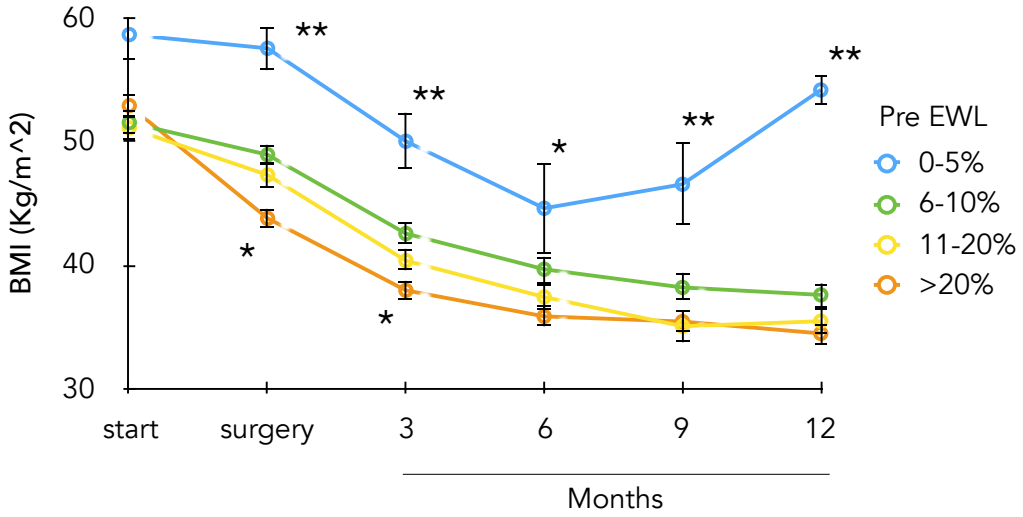

Figure 7.11: Effect of 5% weight loss target achievement on BMI throughout the service pathway

*Mean BMI trend from beginning to end of the service pathway for sub-cohorts split on the basis of pre-surgical excess weight loss (EWL). Error bars represent standard error of the mean. Statistical differences shown in figure represent comparison between categories of EWL and were analysed using one-way ANOVA, *p<0.05; **p<0.01, n=100.*

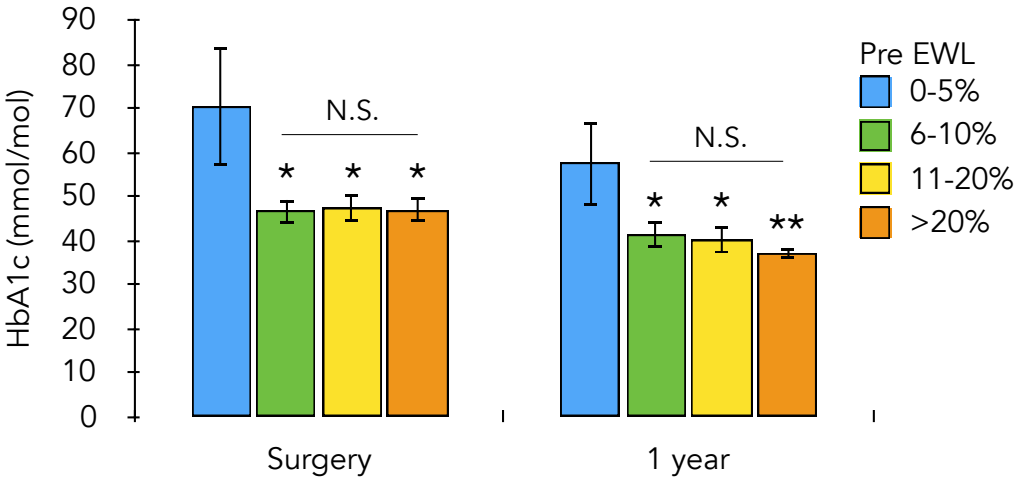

Figure 7.12: Effect of 5% weight loss target achievement on glycaemic control

*Serum HbA1c levels at time of and 1 year post-surgery in sub-cohorts split on the basis of pre-surgical excess weight loss (EWL). Bars represent means ± standard error of the mean. Statistical differences between EWL categories were analysed using one-way ANOVA, *p<0.05; **p<0.01. N.S. denotes differences shown are not statistically significant.*

1-Year Duration in Medical Pathway as an Indicator of Patient Engagement and Post-Surgical Outcomes

In the specialist weight management service, one of the criterion for bariatric surgical candidacy is a minimum 1-year duration in the service. The rationale is that this is an indicator of engagement with the service, which will maximise weight loss outcomes, whilst minimise risk of complications. Therefore, we investigated whether duration on the medical pathway (prior to progression to surgery) had a direct association with weight loss or glycaemic control in the local patient population. Figure 7.13 shows how duration on the medical pathway is distributed in the audit population. The greater proportion of patients audited (49%) progressed to surgery within the second year of being in the service, whilst 31% did so within the third year. A very small minority (12%) took longer than three years and 8% took less than one year. The most frequent duration (mode) was just under 2 years.

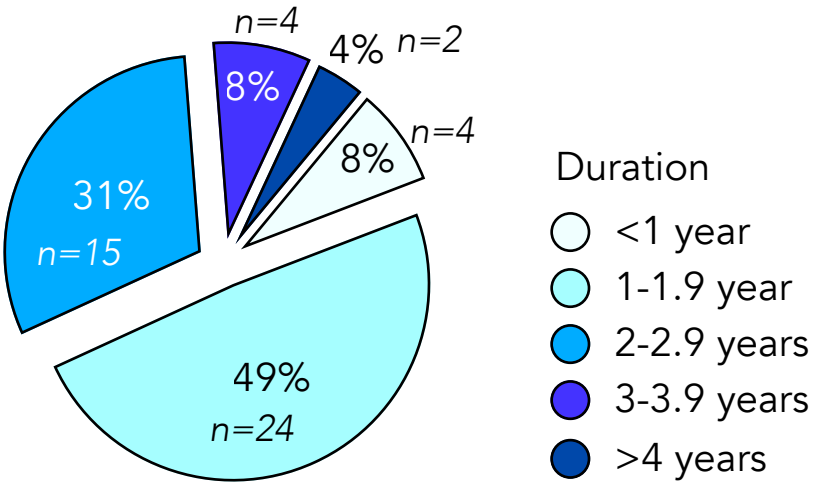

Duration (y)	
mean±SD	2.04±0.925
median	1.85
mode	1.90
min-max	0.7-5.10

Figure 7.13: Duration of the medical pathway

Pie chart depicting patient distribution across increasing categories of duration on the medical pathway (starting from their first appointment to the date of surgery), from less than 1 year to more than 4 years. Descriptive statistics (in years) of duration are shown below the chart.

Next, Pearson correlation analyses were carried out to ascertain whether duration of the medical pathway was associated with weight loss and glycaemic control outcomes post-surgery. As shown on Table 7.3, no association was found between duration of the medical pathway and either weight loss or serum HbA1c concentrations at any point in the pre or post-surgical period.

Table 7.3: Relationship of duration of the medical pathway with surgical outcomes

	Duration (y)	
	Pearson´s r	p value
Pre-surgery EWL (%)	0.023	0.874
Post EWL (Surgery to 3m)	−0.092	0.538
Post EWL (3m to 6m)	−0.082	0.630
Post EWL (6m to 9m)	−0.107	0.580
Post EWL (9m to 12m)	0.099	0.637
Post EWL (12m to 18m)	0.204	0.505
Post Maximum EWL (%)	−0.033	0.820
Post Final EWL (%)	0.002	0.989
Pre HbA1c (mmol/mol)	0.027	0.854
1 year Post HbA1c (mmol/mol)	−0.130	0.384
1 year Post HbA1c (% of pre)	−0.106	0.478

*Table shows Pearson´s correlation coefficient (r) and p value significance (p) between medical pathway duration (y) and indicators of weight loss and glycaemic control throughout the service pathway. Correlations were calculated in the sub-cohort of patients where attendance data was available (n=49). Significant correlations are shown in red. *p<0.05. EWL: weight loss expressed as percentage of excess weight.*

Clinic Attendance Record During Medical Pathway as an Indicator of Patient Engagement and Post-Surgical Outcomes

Given that duration on the medical pathway was not a good indicator of post-surgical outcomes in the audit population, we next tested the potential of clinic attendance record ("did not attend" instances) as a substitute indicator of patient engagement.

In order to ascertain whether attendance record was associated with weight loss and T2DM outcomes, we analysed these relationships via Pearson correlation analyses. The total number of instances in which patients failed to attend any multidisciplinary appointment within the medical pathway was significantly and inversely associated with both pre and post-surgical excess weight loss (Figure 7.14). In terms of glycaemic control, no such association was found either with pre or post-surgical

HbA1c levels ($r = 0.097$, $p = 0.497$ and $r = 0.049$, $p = 0.733$, respectively).

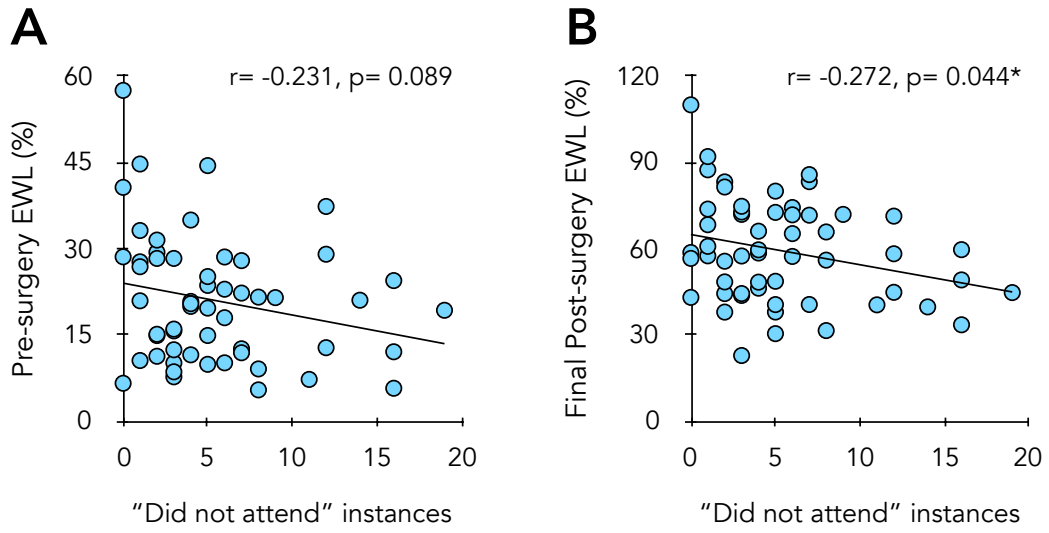

Figure 7.14: Impact of patient engagement on pre and post surgical weight loss success

Scatter plots showing correlation between instances of failure to attend clinic appointments during the medical pathway and ***(A)*** *pre-surgery and* ***(B)*** *final post-surgery excess weight loss (%). EWL: weight loss expressed as percentage of excess weight. Correlations were calculated in the sub-cohort of patients where attendance data was available (n=55).*

Having established that lack of clinic attendance was associated with poorer weight loss outcomes, this study next focused on determining which individuals were at higher risk of not engaging. In order to address this point Pearson correlation analyses were performed between starting demographics and absence rates. As shown in Table 7.4, starting weight and BMI were significantly and positively correlated with absences throughout the medical pathway. Figure 7.15 shows this association in greater detail, whereby patients with more than seven total absences recorded, had significantly higher weight than those with fewer and two. Importantly, this trend continued throughout the pathway, with patients who had fewer than two absences achieving a significantly lower weight than those with greater than two absences. Thus, it is possible that targeting heavier patients with more intensive follow-up may help maximise patient engagement and therefore

post-surgical outcomes.

Table 7.4: Relationship between starting demographics and absence rates

	"Did not attend" instances	
	Pearson´s r	p value
Age (years)	-0.203	0.137
Starting Weight (Kg)	0.344	0.010*
Starting BMI ($\mathrm{Kg/m^2}$)	0.272	0.044*

*Table shows Pearson´s correlation coefficient (r) and p value significance (p) between total instances in which a patient did not attend a clinic appointment pre-surgery, and starting demographics collected. Significant correlations are shown in red. *p<0.05, **p<0.01, n=100.*

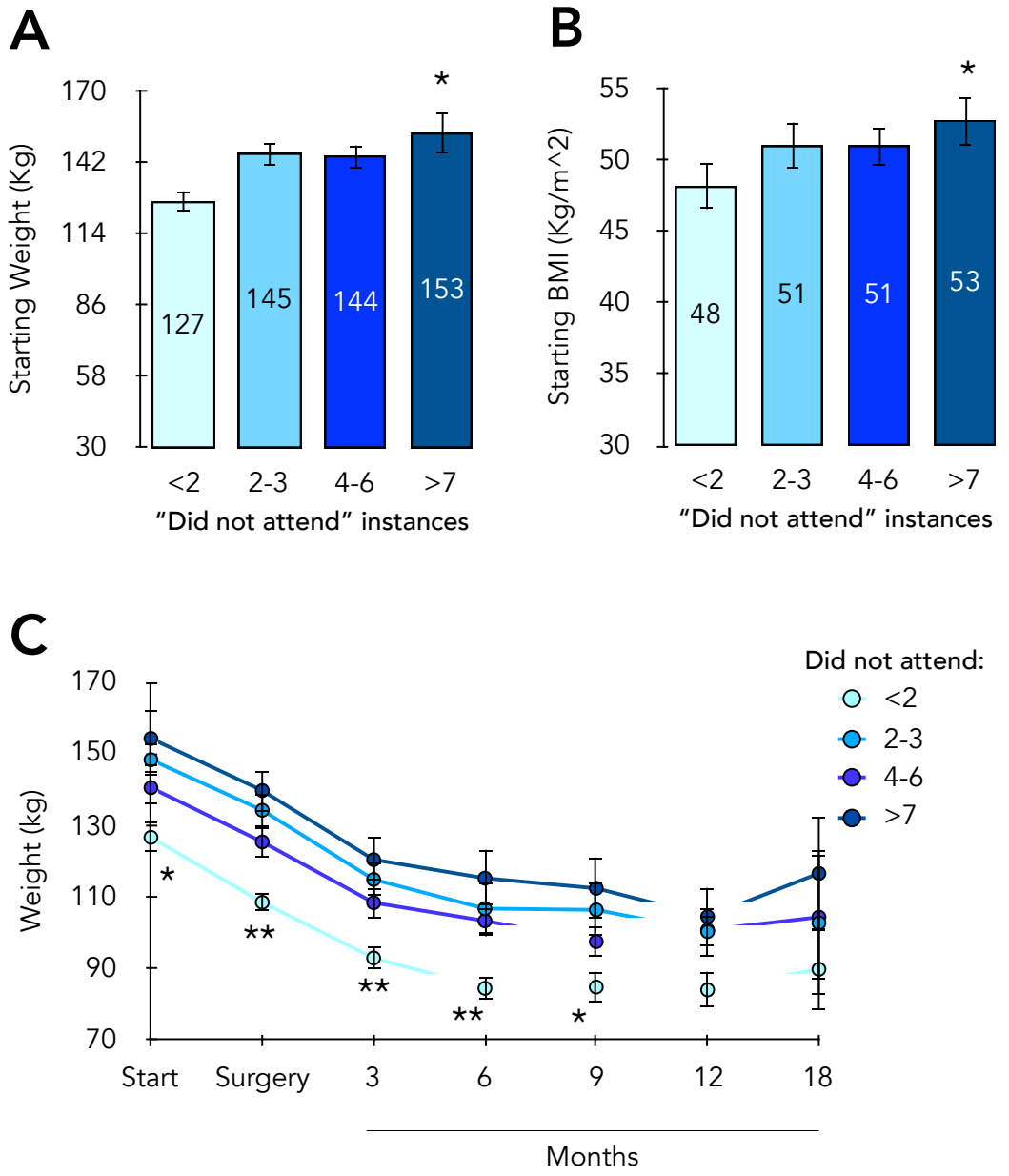

Figure 7.15: Impact of obesity severity on patient engagement throughout the medical pathway

*Association of **(A)** weight and (**B**) BMI to "did not attend" instances at the start and **(C)** throughout the medical pathway. Data represent means ± standard error of the mean and correspond to the sub-cohort of patients where attendance information was available (n=55). Statistical differences between "did not attend" categories were analysed via one-way ANOVA, *p<0.05; **p<0.01.*

Role of Multidisciplinary Support on Patient Attendance and Weight Trajectory

Since appropriate specialist multidisciplinary support has been reported to play a critical role in preventing post-surgical weight recidivism, this study next examined the relationship between degree of multidisciplinary support and clinic attendance record in the audit population.

Figure 7.16 describes the amount, intensity and distribution of patient contacts by each discipline involved in the specialist weight management service on the audit population. On average, patients saw a dietitian seven times, a psychologist twice, a medical Endocrinologist four times and a surgeon once in total by the end of the medical pathway. Dietetic contacts ranged in intensity from monthly to 6-monthly, with the largest majority (38%) seeing a dietitian every 3 months (Figure 7.16**C**). Psychology contacts ranged in intensity from nil to every 6 months, with the majority of patients (58%) seeing a psychologist once per year (Figure 7.16**D**). Medical Endocrinologist contacts ranged in intensity from every three months to once only, with the largest majority (33%) being seen by a medical Endocrinologist once per year (Figure 7.16**E**). In general surgery clinic contacts were once only for the majority of patients (89%) once they had met the surgical criteria and been cleared by the multidisciplinary team to progress to the surgical pathway (Figure 7.16**F**).

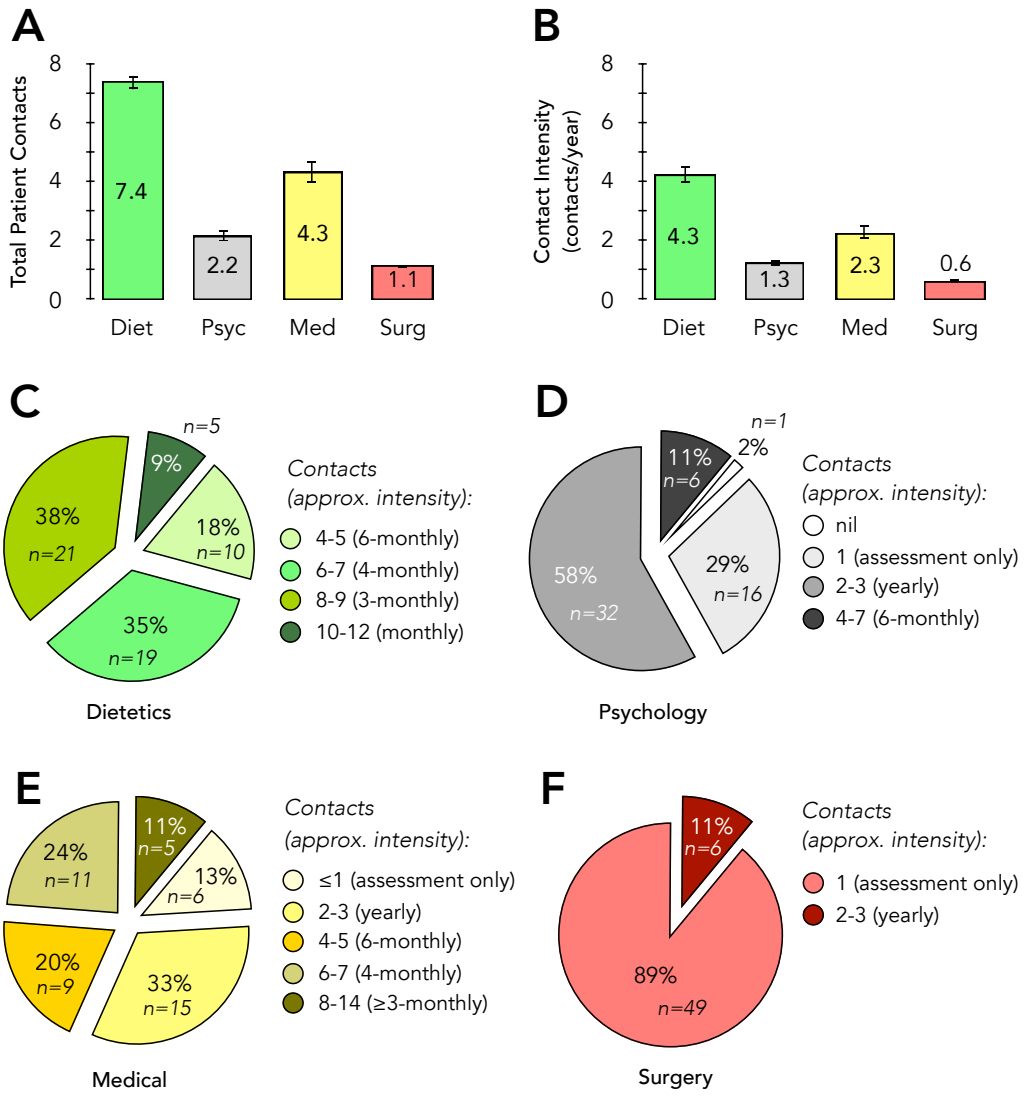

Figure 7.16: Patient contacts during the medical pathway by discipline
*(**A**) Total patient contacts and (**B**) contact intensity of each discipline (Dietetics, Psychology, Endocrinology, and Surgery) during the medical pathway. Bars represent means ± standard error of the mean. **(C-F)** Pie charts showing the proportionality of patient contacts for each discipline. Data correspond to the sub-cohort of patients where attendance information was available (n=55).*

Figure 7.17 details the relationship of absence rate against total contacts for each discipline, whilst Figure 7.18 shows the same absence rate against contact intensity (contacts/year). Though no relationships were evident when considering total contacts, significant associations emerged if considering contact intensity. Interestingly, increased contact intensity was only associated with decreased absences in disciplines that target and support the removal of environmental contributors to

obesity (Dietetics and Psychology). A positive correlation was found between total medical Endocrinologist contacts and absence rate, though this is perhaps more an indicator that medical appointments are often offered as a result of medical need, and patients who are ill are likely less able to attend appointments. Indeed, this association was no longer present when examining contact intensity.

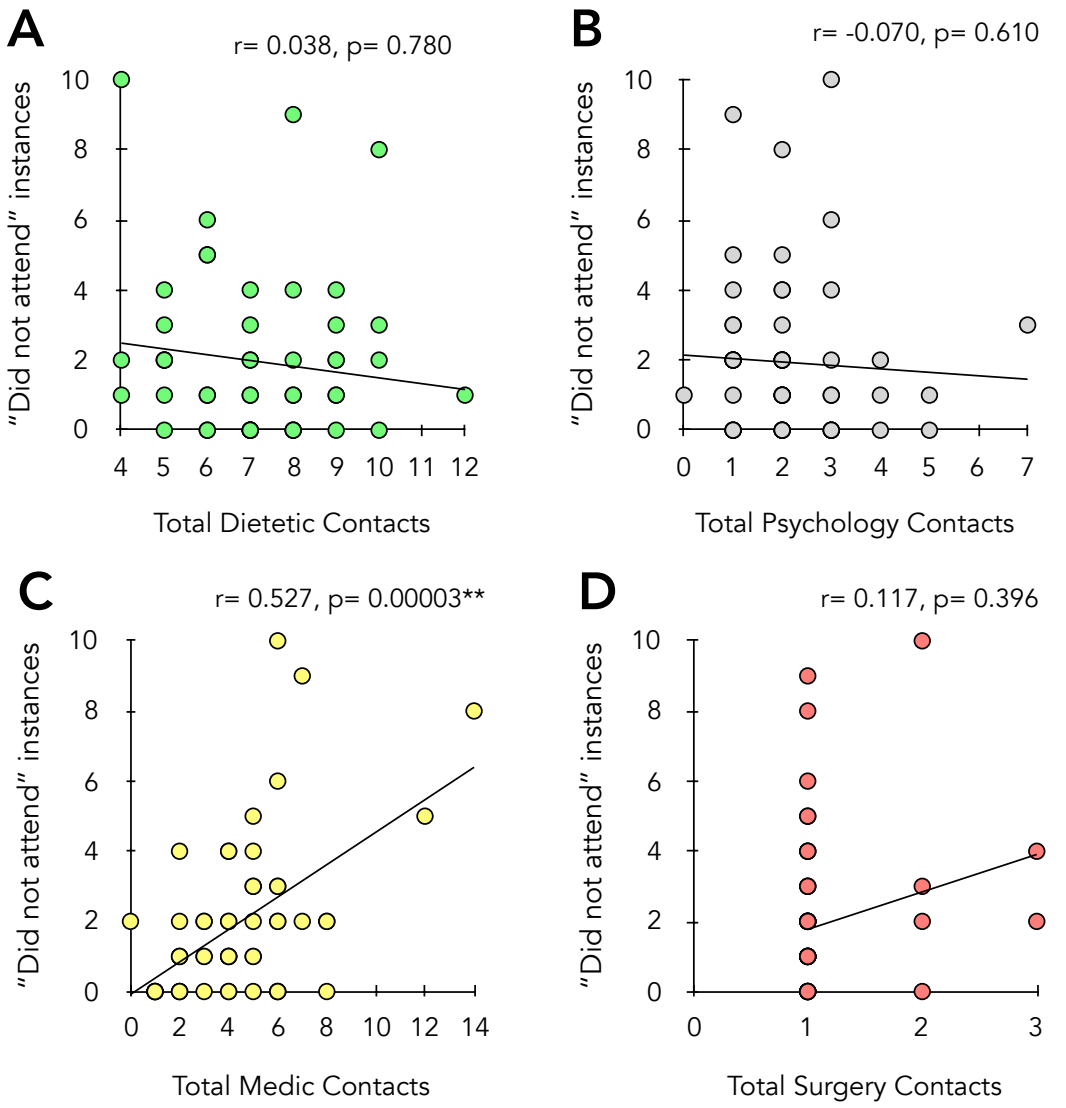

Figure 7.17: Impact of total MDT contacts on patient engagement

Scatter plots showing relationship between instances of "did not attend" clinic appointment and total patient contacts during the medical pathway for each discipline: ***(A)*** *Dietetic,* ***(B)*** *Psychology,* ***(C)*** *Endocrinology and* ***(D)*** *Surgery. Correlations were calculated in the sub-cohort of patients where attendance data was available (n=55).*

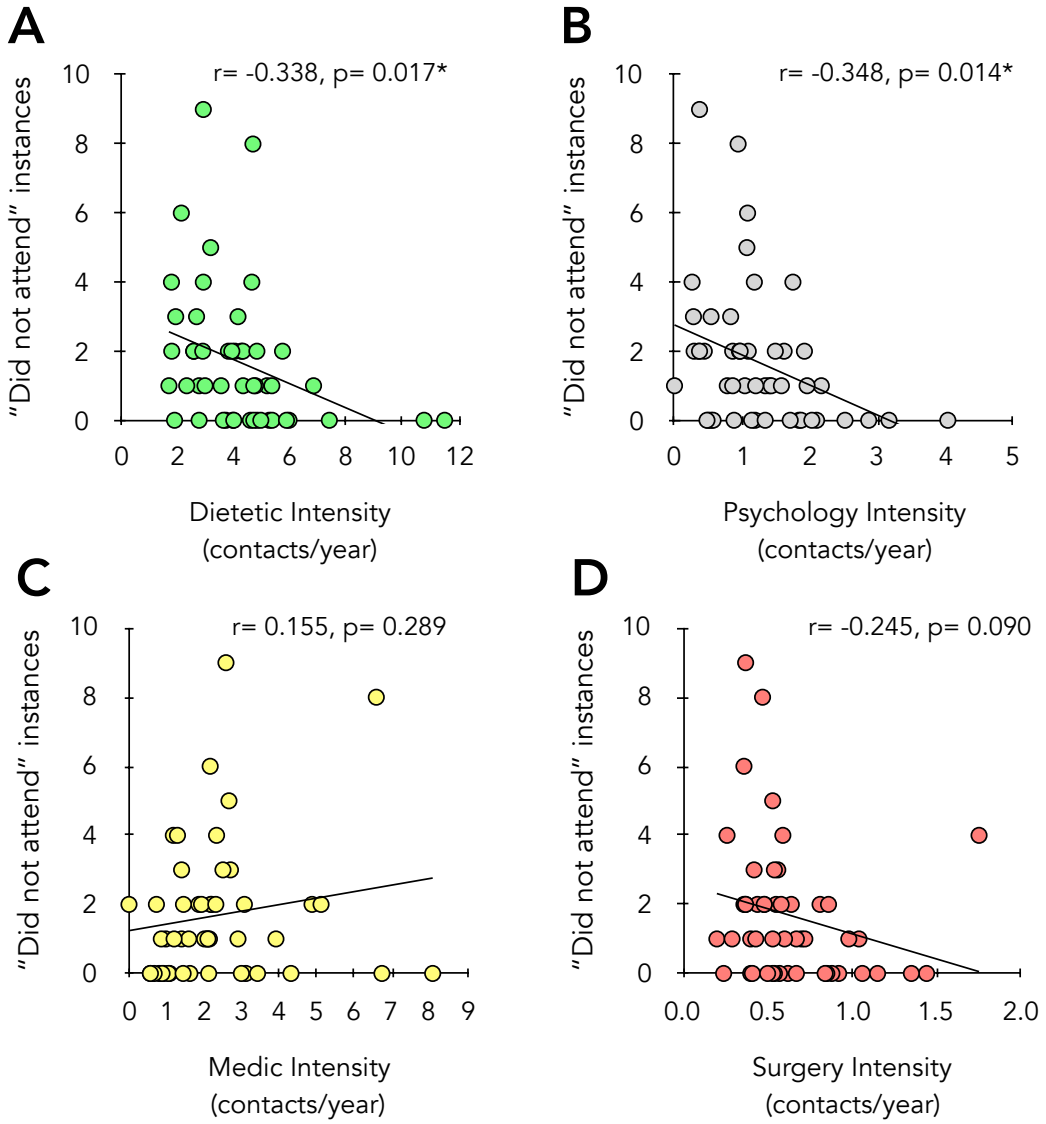

Figure 7.18: Impact of MDT contact intensity on patient engagement

Scatter plots showing relationship between instances of "did not attend" clinic appointment and intensity of patient contacts during the medical pathway for each discipline: ***(A)*** *Dietetic,* ***(B)*** *Psychology,* ***(C)*** *Endocrinology and* ***(D)*** *Surgery. Correlations were calculated in the sub-cohort of patients where attendance data was available (n=55).*

7.4 Discussion

Despite the well-recognised challenge that is long-term maintenance of weight loss and glycaemic control (even after bariatric surgery), there is no clear consensus on which environmental factors are responsible. Recent evidence have highlighted a complex multi-factorial relationship involving dietetic, psychological and physiological issues which alter satiety, food choice, eating behaviours and metabolic health [173]. In the present chapter, these issues were examined through a clinical audit of a joint tier 3 and 4 bariatric specialist service. The main finding of this study, was that environmental factors, namely dietetic compliance (evidenced by pre-surgical weight loss) and patient engagement (evidenced by clinic attendance record) were the principal factors associated with enhanced post-surgical weight loss outcomes, with dietetic compliance also associated with further benefits for post-surgical glycaemic control. This study also identified patients with larger starting BMI to be at higher risk of poor engagement, and that more frequent appointments may prove protective against this.

The finding that patients with higher starting BMI were at significantly higher risk of not attending appointments and poorer post-surgical outcomes is consistent with the findings of a previous study from the same bariatric centre, where pre-surgery BMI was negatively associated with quality of life [364]. Both studies highlight that even within the specialised umbrella of morbid obesity, one-size does not necessarily fit all, and the availability of tailored, holistic support throughout the service pathway is critical to patient benefit.

Another key finding of this audit was the inverse association between appointment frequency of some disciplines and missed appointments. Failure of patients

to attend appointments does not just result in poorer weight loss outcomes as demonstrated in this chapter, but also according to a 2013 estimate cost the NHS up to £225 million annually [365]. The implication that patient engagement rates and healthcare costs may be modifiable through more frequent appointments targeted towards higher BMI patients warrants serious consideration as a service development strategy.

It is also worth noting that patents with lower BMI at the start engaged better, and achieved better weight outcomes than those with higher BMI. Whilst it may be possible to enhance outcomes in individuals with high BMI through intense and long-term multi-disciplinary support, this data also highlights that weight loss interventions are more effective at lower BMI. Given that though the fastest growing obesity category is that of morbid obesity [366], it may very well be more cost-effective to invest resources in preventing patients from attaining morbid obesity in the first place. However, currently provision of tier 2 and 3 weight management does not reflect the alarming rise in obesity prevalence [367].

This audit had certain limitations, namely: (1) due to the need to confine the boundaries of the research question, medication, gender and other clinical information were not collected, (2) given the retrospective approach, dietary, lifestyle and psychological data was not readily available, and (3) though significant correlations were identified, due to the study design, causation could not be determined.

In conclusion, dietetic compliance and patient engagement were critical to post-surgical weight loss and glycaemic control. Higher frequency of Dietetic and Psychology appointments were significantly associated with enhanced patient engagement, whilst a larger starting BMI was associated with reduced engagement and

poorer overall post-surgical weight outcomes. Taken together, this data supports the notion that a holistic, intense and patient-tailored approach is critical to maximising patient benefit. Patients with larger BMI are likely to require more intense support, and achieve more modest outcomes, thus adequate provision of prevention services is crucial to resolving the obesity crisis.

General Discussion and Conclusions

The obesity pandemic is expected to continue to rise exponentially despite current efforts to curb it [3]. In the UK, the current strategy has been to prioritise treatment based on risk of metabolic co-morbidities [1], whilst treatment and/or prevention of obesity itself remains largely ignored or limited to behaviour change strategies which social marketing research have been shown to be ineffective (such as public information campaigns) [121, 122].

Whilst considerable effort has been devoted to obesity research, this has been heavily biased towards the pathophysiology and treatment of metabolic disease, whilst research into effective lifestyle interventions for obesity treatment are limited [103, 142, 104, 97, 106]. Evidence from obesity area research largely supports the notion that neurobehavioural changes in physiology (affecting appetite, satiety and food choices) underly most genetic causes of obesity, and strongly suggest any genetic predispositions are likely to contribute to obesity in much the same way [14, 368, 12, 19, 369]. Evidence from developmental, social, psychological and other sciences indicate that human behaviour is largely shaped by interaction with the environment [124, 126, 370, 128, 21, 22, 121]. In recent history, changes in food production, availability, and marketing have significantly manipulated global food choices, and cultural practices, especially in the socially, medically and economically vulnerable [105, 54, 88, 34, 92, 46, 5]. Thus, there is great need to integrate the environmental with the physiological determinants of health in order to produce meaningful improvements to the obesity epidemic. The aim of the present thesis was to approach this subject translationally in order to integrate and advance our understanding of this subject.

From the basic research perspective, the aim was to investigate the potential role

of emerging novel molecular mediators of metabolic recovery following bariatric surgical intervention. The enterokine FGF-19 has been recently implicated in this process by the finding that mice lacking the receptor for FGF-19 secretion show significantly impaired weight loss and glycaemic control after bariatric surgery [306]. The evidence in this thesis demonstrates for the first time a differential effect of bariatric surgical procedure on serum FGF-19 levels in tandem with metabolic and mitochondrial improvements. Though not all surgeries which resulted in increased serum FGF-19 levels produced evidence of mitochondrial improvements, a significant association between FGF-19 levels and adipose mitochondrial number was observed across all surgeries, highlighting the mitochondrial network as a potential target of this novel gut hormone.

Another mechanism for metabolic recovery following bariatric surgery, which was investigated in this thesis, focused on circulating levels of gut-derived bacterial lipopolysaccharide (LPS). Recent evidence suggests that surgery-specific differences in metabolic benefit may be the result of changes in gut microbiota that arise from the type and extent of gastro-intestinal remodeling. In particular, a recent study transplanted fecal matter from post-surgical patients on to germ-free mice fed a high-fat diet, resulting in significant weight loss, and reduced fat deposition and decreased use of carbohydrates as fuel versus animals transplanted with fecal matter from control patients [192]. In this thesis, it was hypothesized that LPS may be involved in the cross-talk between intestinal remodeling and metabolic fuel partitioning in adipose mitochondria. Here, this study shows for the first time, that LPS levels were significantly different between surgical procedures, and correlated significantly with reduced mitochondrial number in adipose tissue. Direct

administration of LPS to adipocytes resulted in mitochondrial DNA damage, and a functional shift towards carbohydrates versus lipid as a fuel source. Taken together, the findings outlined in this study support our hypothesis and highlight LPS as a novel link between a Western diet and impaired adipose tissue functionality, with potential implications for systemic lipid toxicity and metabolic disease.

From the clinical perspective, the aim of this thesis was to examine the environmental barriers to successful weight loss and metabolic recovery, both before and after bariatric surgery. The collective evidence to date suggests that the main reason bariatric surgery has so far been more effective than non-surgical interventions is grounded in its ability to avoid triggering many of the mechanisms seen with the latter, which defend energy stores and promote weight regain [8, 9, 10, 11, 176]. However, some weight recidivism is still commonly seen even with bariatric interventions, with dietary and psychological factors highlighted as the most common reasons [357, 358, 359, 173]. The results from the clinical audit of a Tier 3 and 4 bariatric service are consistent with this notion. Whilst the majority of patients lost more than 50% of their excess weight by the end of surgical pathway (18 months post surgery), there was substantial variability in the extent of weight loss achieved between individuals. The main factors associated with weight loss success were dietetic compliance (evidenced by pre-surgical weight loss) and patient engagement (evidence by clinic attendance record). Patients with larger starting BMI and less frequent dietetic or psychology appointments were at higher risk of poorer outcomes, further substantiating the argument that patient-tailored holistic support addressing the environmental as well as the physiological determinants of health are crucial to achieving maximal weight loss and patient benefit.

In conclusion, the evidence set out in this thesis (and by previous studies) overwhelmingly supports the notion that obesity is the result of a complex, multifactorial interaction with an obesogenic environment. Great gains have been made in our understanding of the physiological mechanisms leading to obesity and metabolic disease. In particular, the key fact that most obesity-associated monogenetic mutations target hypothalamic pathways (controlling hunger, satiety and food intake) has reframed our understanding of obesity from a metabolic to a neurobehavioural origin. Further understanding of how the obesogenic environment disrupts molecular mechanisms that control food choice will be critical for the development of more effective treatments. Gut-derived factors such as bacterial LPS, the enterokine FGF-19 and other promising research targets may hold further insight into the mechanism of metabolic recovery, which may be enhanced through multidisciplinary holistic treatment. However, any intervention which seeks to target metabolic disease, food choice or behaviour without seeking to also alter the environment is at a strong disadvantage for success. Therefore, there is great need to collaborate across disciplines, in order to gain an accurate perspective of the causes and solutions to the obesity pandemic.

Appendix 1: WISDEM Staff

Table 7.5: Warwickshire Institute for the Study of Diabetes, Endocrinology and Metabolism Staff (2011-2016)

Prof. Harpal Randeva	(WISDEM Clinical Director, Consultant Endocrinologist)
Mr. Vinod Menon	(Consultant Surgeon)
Mr. FT Lam	(Divisional Medical Director)
Mr. Matthew Venus	(Consultant Plastic Surgeon)
Mr. Ian Fraser	(Consultant Surgeon)
Mrs. Jenny Abraham	(Specialist Bariatric Nurse)
Ms. Joanne Wood	(Bariatric Coordinator)
Prof. Sudhesh Kumar	(Professor of Medicine, Diabetes and Metabolism)
Dr. Tom Barber	(Associate Professor of Endocrinology)
Prof. Grigorios Kaltsas	(Consultant Endocrinologist)
Dr. Milan Piya	(Consultant Endocrinologist)
Dr. Vidhya Jahagirdar	(ST7 Endocrinology and Diabetes)
Dr. Hassan Kahal	(NIHR Clinical Lecturer)
Dr. Hema Venkataraman	(ST3 Endocrinology and Diabetes)
Dr. Daniel Border	(ST2 Acute Internal Medicine)
Dr. Georgios Dimitriadis	(Clinical Research Fellow)
Dr. Helen Miller	(Clinical Psychologist)
Dr. David Kendrick	(Clinical Psychologist)
Dr. Emma Shuttlewood	(Bariatric Clinical Psychologist)
Miss Neha Shah	(Specialist Bariatric Dietitian)
Mrs. Olga Sutton	(Senior Dietitian)
Mrs. Louise Halder	(Senior Bariatric Dietitian)
Mrs Margaret Bosworth	(Assistant Therapist)
Ms Wendy Clayton	(Diabetes Specialist Nurse)
Ms Wendy Goodwin	(Diabetes Specialist Nurse)
Dr. Narendra Reddy	(NIHR Clinical Lecturer)
Dr. Saboor Aftab	(NIHR Clinical Lecturer)
Dr. Umar Shariff	(Registrar)
Dr. Aruna Munasinghe	(Clinical Fellow)
Dr. Shameen Jaunoo	(Clinical Fellow)
Dr. Peng Cheun Lau	(Clinical Fellow)

Appendix 2: List of Formal Presentations during PhD Studies (2014-2017)

Dates	June 30^{th}, 2017
Conference	Surgical Research Forum
Venue	University Hospital Coventry and Warwickshire
Presentation	Factors influencing metabolic recovery after bariatric surgery: lessons from the UHCW service (ORAL)

Dates	June 10^{th}, 2017
Conference	American Diabetes Association 17th Annual Scientific Sessions
Venue	San Diego, CA, USA
Presentation	Gut Hormone FGF-19 Modulates Adipose Mitochondrial Function and Type-2 Diabetes Recovery Following Bariatric Surgery (Mod POSTER)

Dates	April $18^{th} - 21^{st}$, 2017
Conference	Scandinavian Society for Atherosclerosis Research
Venue	Copenhagen, Denmark
Presentation	Gut-derived bacterial LPS links western diet with adipocyte dysfunction through mitochondrial damage (**BEST POSTER AWARD**)

Dates	March 30^{th}, 2017
Conference	Warwick Medical School Research Network Symposium
Venue	Arden House, Westwood Campus, University of Warwick
Presentation	Effective Treatment of Obesity: Lessons from a Bariatric Service (ORAL)

Dates	December 9^{th}, 2016
Conference	43rd Adipose Tissue Discussion Group
Venue	Merton College, Oxford University
Presentation	Gut-derived bacterial LPS drive mitochondrial dysfunction, inflammation and insulin resistance in human adipocytes (**2nd BEST POSTER AWARD**)

Dates	November $7^{th} - 9^{th}$, 2016
Conference	British Society for Endocrinology BES Annual Meeting
Venue	Brighton, UK
Presentation	Metabolic Endotoxaemia Impairs Mitochondrial Respiration and Insulin Sensitivity in Human Adipocytes (POSTER). **Short-listed for Early Career Endocrinologist Award** Endocrine Abstracts 44 P179. DOI:10.1530/endoabs.44.P179

Dates	October $24^{th} - 25^{th}$, 2016
Conference	World Mitochondria Society 7th Annual Meeting
Venue	Maritim ProArte Hotel, Berlin, Germany
Presentation	Contribution of Gut-derived Bacterial LPS to Mitochondrial Dysfunction, Oxidative Stress and Inflammation in Human Adipocytes (ORAL) JWMS 2(2) page 5 DOI:10.18143/JWMS_v2i2

Dates	September $7^{th} - 10^{th}$, 2016
Conference	17th International Congress of Dietetics Associations
Venue	Granada, Spain
Presentation	The fat benefits of Nutrient Malabsorption in Obese Patients with Type-2 Diabetes (ORAL). Rev Esp Nutr Hum Diet 20(1) O-070 DOI:10.14306/renhyd

Dates	March 31^{st}, 2016
Conference	Midlands Academy of Medical Sciences Research Festival
Venue	Leicester, UK
Presentation	Obesity-induced Mitochondrial Dysfunction in T2DM Women is Resolved with Malabsorptive but not Restrictive Bariatric Surgery (POSTER)

Dates	February $15^{th} - 19^{th}$, 2016
Conference	Obesity and Adipose Tissue Biology Keystone Symposia
Venue	Fairmont Banff Springs, Banff, Canada
Presentation	Malabsorptive Bariatric Surgery Resolves Obesity-induced Mitochondrial Maladaptation in Subcutaneous Adipose Tissue of Obese T2DM women (POSTER) P-2052

Dates	November $2^{nd} - 4^{th}$, 2015
Conference	British Society for Endocrinology BES Annual Meeting
Venue	Edinburgh, Scotland
Presentation	Evidence for Improved Mitochondrial Efficiency in Adipose Tissue of T2DM women after malabsorptive but not restrictive bariatric surgery (POSTER) Endocrine Abstracts 38 P199 DOI:10.1530/endoabs.38.P199

Dates	December 15^{th}, 2014
Conference	41st Adipose Tissue Discussion Group
Venue	University of East Anglia, Norwich, UK
Presentation	Evidence for Improved Regulation of Mitochondrial Biogenesis in Abdominal Subcutaneous Adipose Tissue of Obese T2DM women Undergoing Bariatric Surgery (POSTER)

Bibliography

[1] Barry P, Batterham RL, Blakemore A, Clare K, Connell C, Holt R, et al.. Obesity: identification, assessment and management | Guidance and guidelines GC189 | NICE. National Institute for Health and Care Excellence (NICE); 2014. Available from: https://www.nice.org.uk/guidance/cg189.

[2] The Organisation for Economic Co-operation and Development. Obesity Update. The Organisation for Economic Co-operation and Development; 2014.

[3] Organisation for Economic Co-operation and Development (OECD). Obesity Update. Organisation for Economic Co-operation and Development (OECD); 2017. Available from: www.oecd.org/health/obesity-update.htm.

[4] Di Angelantonio E, Bhupathiraju SN, Wormser D, Gao P, Kaptoge S, de Gonzalez AB, et al. Body-mass index and all-cause mortality: individual-participant-data meta-analysis of 239 prospective studies in four continents. Lancet. 2017;388(10046):776–786.

[5] Mary Ea. Adult Obesity and Type 2 Diabetes About Public Health England; 2014.

[6] Baker C, editor. Briefing Paper: Obesity Statistics. House of Commons Library; 2017.

[7] Butland B, Jebb S, Kopelman P, McPherson K, Thomas S, Mardell J, et al. Foresight Tackling Obesities: Future Choices – Project report. Gov Off Sci. 2007;p. 1–161.

[8] Rosenbaum M, Hirsch J, Murphy E, Leibel RL. Effects of changes in body weight on carbohydrate metabolism, catecholamine excretion, and thyroid function. Am J Clin Nutr. 2000;71(6):1421–1432.

[9] Rosenbaum M, Vandenborne K, Goldsmith R, Simoneau JA, Heymsfield S, Joanisse DR, et al. Effects of experimental weight perturbation on skeletal muscle work efficiency in human subjects. Am J Physiol - Regul Integr Comp Physiol. 2003;285(1):R183–R192.

[10] Chaston TB, Dixon JB, O'Brien PE. Changes in fat-free mass during significant weight loss: a systematic review. Int J Obes. 2006;.

[11] Rosenbaum M, Hirsch J, Gallagher DA, Leibel RL. Long-term persistence of adaptive thermogenesis in subjects who have maintained a reduced body weight. Am J Clin Nutr. 2008;88(4):906–912.

[12] Farooqi IS, O'Rahilly S. Genetic factors in human obesity. Obes Rev. 2007;8 Suppl 1(7-8):37–40.

[13] Maes HHM, Neale MC, Eaves LJ. Genetic and environmental factors in relative body weight and human adiposity; 1997.

[14] O'Rahilly S, Farooqi IS. Genetics of obesity. Philos Trans R Soc Lond B Biol Sci. 2006;361(1471):1095–105.

[15] Stern JH, Rutkowski JM, Scherer PE. Adiponectin, Leptin, and Fatty Acids in the Maintenance of Metabolic Homeostasis through Adipose Tissue Crosstalk. Cell Metab. 2016;23(5):770–784.

[16] Zhang Y, Proenca R, Maffei M, Barone M, Leopold L, Friedman JM. Positional cloning of the mouse obese gene and its human homologue. Nature. 1994 dec;372(6505):425–432.

[17] Halaas JL, Gajiwala KS, Maffei M, Cohen SL, Chait BT, Rabinowitz D, et al. Weight reducing effects of the plasma protein encoded by the Obese gene. Science. 1995;269(5223):543–546.

[18] Myers MG, Cowley MA, Munzberg H. Mechanisms of Leptin Action and Leptin Resistance. Annu Rev Physiol. 2008;70(1):537–556.

[19] Sumithran P, Prendergast LA, Delbridge E, Purcell K, Shulkes A, Kriketos A, et al. Long-Term Persistence of Hormonal Adaptations to Weight Loss. Obstet Gynecol Surv. 2012;67(2):91–92.

[20] Guyenet SJ, Schwartz MW. Clinical review: Regulation of food intake, energy balance, and body fat mass: implications for the pathogenesis and treatment of obesity. J Clin Endocrinol Metab. 2012;97(3):745–755.

[21] Lattimore P, Maxwell L. Cognitive load, stress, and disinhibited eating. Eat Behav. 2004;5(4):315–324.

[22] Maio GR, Haddock GG, Jarman HL. Social psychological factors in tackling obesity; 2007.

[23] Fuhrer D, Zysset S, Stumvoll M. Brain Activity in Hunger and Satiety: An Exploratory Visually Stimulated fMRI Study. Obesity. 2008;16(5):945–950.

[24] Haase L, Cerf-Ducastel B, Murphy C. Cortical activation in response to pure taste stimuli during the physiological states of hunger and satiety. Neuroimage. 2009;44(3):1008–1021.

[25] Benelam B. Satiation, satiety and their effects on eating behaviour. Nutr Bull. 2009;34(2):126–173.

[26] Llewellyn CH, Trzaskowski M, van Jaarsveld CHM, Plomin R, Wardle J. Satiety Mechanisms in Genetic Risk of Obesity. JAMA Pediatr. 2014;168(4):338.

[27] Leibel RL, Rosenbaum M, Hirsch J. Changes in Energy Expenditure Resulting from Altered Body Weight. N Engl J Med. 1995;332(10):621–628.

[28] Schulz LO, Schoeller DA. A compilation of total daily energy expenditures and body weights in healthy adults. Am J Clin Nutr. 1994 nov;60(5):676–81.

[29] Twig G, Elorza A, Molina AJA, Mohamed H, Wikstrom JD, Walzer G, et al. Fission and selective fusion govern mitochondrial segregation and elimination by autophagy. EMBO J. 2008;27(2):433–446.

[30] Turnbaugh PJ, Ridaura VK, Faith JJ, Rey FE, Knight R, Gordon JI. The effect of diet on the human gut microbiome: a metagenomic analysis in humanized gnotobiotic mice. Sci Transl Med. 2009 nov;1(6):6ra14.

[31] Pournaras DJ, Osborne A, Hawkins SC, Mahon D, Ghatei MA, Bloom SR, et al. The gut hormone response following roux-en-Y gastric bypass: Cross-sectional and prospective study. Obes Surg. 2010;20(1):56–60.

[32] Pendyala S, Walker JM, Holt PR. A High-Fat Diet Is Associated With Endotoxemia That Originates From the Gut. Gastroenterology. 2012 may;142(5):1100–1101.e2.

[33] Oike H. Modulation of circadian clocks by nutrients and food factors. Biosci Biotechnol Biochem. 2017 may;81(5):863–870.

[34] Swinburn BA, Sacks G, Hall KD, McPherson K, Finegood DT, Moodie ML, et al. The global obesity pandemic: Shaped by global drivers and local environments. Lancet. 2011;378(9793):804–814.

[35] Ludwig DS, Peterson KE, Gortmaker SL. Relation between consumption of sugar-sweetened drinks and childhood obesity: A prospective, observational analysis. Lancet. 2001;357(9255):505–508.

[36] Levy P, Fried M, Santini F, Finer N. The comparative effects of bariatric surgery on weight and type 2 diabetes. Obes Surg. 2007;17(9):1248–1256.

[37] Carter P, Gray LJ, Troughton J, Khunti K, Davies MJ. Fruit and vegetable intake and incidence of type 2 diabetes mellitus: systematic review and meta-analysis. BMJ. 2010;341:c4229.

[38] Oyebode O, Gordon-Dseagu V, Walker A, Mindell JS. Fruit and vegetable consumption and all-cause, cancer and CVD mortality: analysis of Health

Survey for England data. J Epidemiol Community Health. 2014;68(9):856–862.

[39] Canella DS, Levy RB, Martins APB, Claro RM, Moubarac JC, Baraldi LG, et al. Ultra-processed food products and obesity in Brazilian households (2008-2009). PLoS One. 2014;9(3).

[40] Popkin BM, Adair LS, Ng SW. Global nutrition transition and the pandemic of obesity in developing countries. Nutr Rev. 2012;70(1):3–21.

[41] Rouhani MH, Salehi-Abargouei A, Surkan PJ, Azadbakht L. Is there a relationship between red or processed meat intake and obesity? A systematic review and meta-analysis of observational studies; 2014.

[42] Moubarac JC, Martins APB, Claro RM, Levy RB, Cannon G, Monteiro CA. Consumption of ultra-processed foods and likely impact on human health. Evidence from Canada. Public Health Nutr. 2013;16(12):2240–8.

[43] Juul F, Hemmingsson E. Trends in consumption of ultra-processed foods and obesity in Sweden between 1960 and 2010. Public Health Nutr. 2015;18(17):3096–3107.

[44] Abete I, Romaguera D, Vieira AR, Lopez de Munain A, Norat T. Association between total, processed, red and white meat consumption and all-cause, CVD and IHD mortality: a meta-analysis of cohort studies. Br J Nutr. 2014;112(05):762–775.

[45] Pan A, Sun Q, Bernstein AM, Schulze MB, Manson JE, Willett WC, et al. Red meat consumption and risk of type 2 diabetes: 3 cohorts of US adults and an updated meta-analysis. Am J Clin Nutr. 2011;94(4):1088–96.

[46] Monteiro CA, Moubarac JC, Cannon G, Ng SW, Popkin B. Ultra-processed products are becoming dominant in the global food system. Obes Rev. 2013;14(S2):21–28.

[47] McLaughlin C, Tarasuk V, Kreiger N. An examination of at-home food preparation activity among low-income, food-insecure women; 2003.

[48] Yan J, Liu L, Zhu Y, Huang G, Wang PP. The association between breastfeeding and childhood obesity: A meta-analysis; 2016.

[49] Horta BL, de Mola CL, Victora CG. Long-term consequences of breastfeeding on cholesterol, obesity, systolic blood pressure, and type-2 diabetes: systematic review and meta-analysis. Acta Paediatr. 2015;p. n/a–n/a.

[50] Ventura AK, Worobey J. Early influences on the development of food preferences. Curr Biol. 2013;23(9).

[51] Harris KC, Kuramoto LK, Schulzer M, Retallack JE. Effect of school-based physical activity interventions on body mass index in children: a meta-analysis. CMAJ. 2009 mar;180(7):719–26.

[52] Cesa CC, Sbruzzi G, Ribeiro RA, Barbiero SM, de Oliveira Petkowicz R, Eibel B, et al. Physical activity and cardiovascular risk factors in children: meta-analysis of randomized clinical trials. Prev Med (Baltim). 2014 dec;69:54–62.

[53] Metcalf BS, Voss LD, Hosking J, Jeffery AN, Wilkin TJ. Physical activity at the government-recommended level and obesity-related health outcomes: a longitudinal study (Early Bird 37). Arch Dis Child. 2008 sep;93(9):772–777.

[54] Davis B, Carpenter C. Proximity of fast-food restaurants to schools and adolescent obesity. Am J Public Health. 2009 mar;99(3):505–10.

[55] Carter FA, Jansen A. Improving psychological treatment for obesity. Which eating behaviours should we target? Appetite. 2012 jun;58(3):1063–1069.

[56] Berkowitz RI, Fabricatore AN. Obesity, Psychiatric Status, and Psychiatric Medications. Psychiatr Clin North Am. 2011 dec;34(4):747–764.

[57] Istvan J, Zavela K, Weidner G. Body weight and psychological distress in NHANES I. Int J Obes Relat Metab Disord. 1992;16(12):999–1003.

[58] Carpenter KM, Hasin DS, Allison DB, Faith MS. Relationships between obesity and DSM-IV major depressive disorder, suicide ideation, and suicide attempts: Results from a general population study. Am J Public Health. 2000;90(2):251–257.

[59] Onyike CU, Crum RM, Lee HB, Lyketsos CG, Eaton WW. Is Obesity Associated with Major Depression? Results from the Third National Health and Nutrition Examination Survey. Am J Epidemiol. 2003;158(12):1139–1147.

[60] Wadden TA, Womble LG, Stunkard AJ, Anderson DA. Psychosocial consequences of obesity and weight loss.; 2002.

[61] Goodman E, Whitaker RC. A prospective study of the role of depression in the development and persistence of adolescent obesity. Pediatrics. 2002;110(3):497–504.

[62] Roberts RE, Deleger S, Strawbridge WJ. Prospective association between obesity and depression: Evidence from the Alameda County Study. Int J Obes. 2003;27(4):514–521.

[63] Tajik E, Zulkefli NAM, Baharom A, Minhat HS, Latiff LA. Contributing factors of obesity among stressed adolescents. Electron physician. 2014;6(1):771–8.

[64] Staffieri JR. A study of social stereotype of body image in children. J Pers Soc Psychol. 1967 sep;7(1):101–4.

[65] Cramer P, Steinwert T. Thin is good, fat is bad: How early does it begin? J Appl Dev Psychol. 1998;19(3):429–451.

[66] Puhl R, Brownell KD. Bias, Discrimination, and Obesity. Obes Res. 2001;9(12):788–805.

[67] Hebl MR, Mannix LM. The weight of obesity in evaluating others: a mere proximity effect. Pers Soc Psychol Bull. 2003 jan;29(1):28–38.

[68] Harris JE, Hamaday V, Mochan E. Osteopathic family physicians' attitudes, knowledge, and self-reported practices regarding obesity. J Am Osteopath Assoc. 1999;99(7):358–365.

[69] Schwartz MB, Chambliss HO, Brownell KD, Blair SN, Billington C. Weight Bias among Health Professionals Specializing in Obesity. Obes Res. 2003;11(9):1033–1039.

[70] Doll Ha, Petersen SE, Stewart-Brown SL. Obesity and physical and emotional well-being: associations between body mass index, chronic illness, and the physical and mental components of the SF-36 questionnaire. Obes Res. 2000;8(2):160–170.

[71] Fontaine KR, Cheskin LJ, Barofsky I. Health-related quality of life in obese persons seeking treatment. J Fam Pract. 1996;43(3):265–70.

[72] Kolotkin RL, Crosby RD, Williams GR. Health-related quality of life varies among obese subgroups. Obes Res. 2002;10(8):748–756.

[73] Dixon JB, Dixon ME, O'Brien PE. Depression in Association With Severe Obesity. Arch Intern Med. 2003 sep;163(17):2058.

[74] American Psychiatric Association. Diagnostic and Statistical Manual of Mental Disorders; 2013.

[75] Matza LS, Revicki DA, Davidson JR, Stewart JW. Depression With Atypical Features in the National Comorbidity Survey. Arch Gen Psychiatry. 2003 aug;60(8):817.

[76] Stunkard AJ, Fernstrom MH, Price A, Frank E, Kupfer DJ. Direction of weight change in recurrent depression. Consistency across episodes. Arch Gen Psychiatry. 1990;47(9):857–60.

[77] Fagiolini A, Frank E, Houck PR, Mallinger AG, Swartz HA, Buysse DJ, et al. Prevalence of obesity and weight change during treatment in patients with bipolar I disorder. J Clin Psychiatry. 2002;63(6):528–533.

[78] McElroy SL, Keck PE. Obesity in bipolar disorder: An overview; 2012.

[79] Fagiolini A, Kupfer DJ, Houck PR, Novick DM, Frank E. Obesity as a correlate of outcome in patients with bipolar I disorder. Am J Psychiatry. 2003;160(1):112–117.

[80] Allison DB, Fontaine KR, Heo M, Mentore JL, Cappelleri JC, Chandler LP, et al. The distribution of body mass index among individuals with and without schizophrenia. J Clin Psychiatry. 1999;60(4):215–220.

[81] Homel P, Casey D, Allison DB. Changes in body mass index for individuals with and without schizophrenia, 1987-1996. Schizophr Res. 2002 jun;55(3):277–84.

[82] Marder SR, Essock SM, Miller AL, Buchanan RW, Casey DE, Davis JM, et al. Physical health monitoring of patients with schizophrenia. Am J Psychiatry. 2004;161(8):1334–49.

[83] Newman SC, Bland RC. Mortality in a cohort of patients with schizophrenia: a record linkage study. Can J Psychiatry-Revue Can Psychiatr. 1991;36(4):239–245.

[84] Allison DB, Mentore JL, Heo M, Chandler LP, Cappelleri JC, Infante MC, et al. Antipsychotic-induced weight gain: A comprehensive research synthesis. Am J Psychiatry. 1999;156(11):1686–1696.

[85] American Diabetes Association, American Psychiatric Association, American Association of Clinical Endocrinologist, North American Association for the study of Obesity. Consensus development conference on antipsychotic drugs and obesity and diabetes. Diabetes Care. 2004;27(2):597–601.

[86] Fava M. Weight gain and antidepressants. J Clin Psychiatry. 2000;61(SUPPL. 11):37–41.

[87] Hemmingsson E, Johansson K, Reynisdottir S. Effects of childhood abuse on adult obesity: a systematic review and meta-analysis. Obes Rev. 2014 nov;15(11):882–893.

[88] Fraser LK, Edwards KL, Cade J, Clarke GP. The geography of fast food outlets: A review; 2010.

[89] Drewnowski A. Obesity, diets, and social inequalities. In: Nutr. Rev.. vol. 67; 2009. .

[90] Guthman J. Weighing In: Obesity, Food Justice, and the Limits of Capitalism. United States Department of Agriculture; 2011.

[91] Stuckler D, Nestle M. Big food, food systems, and global health. PLoS Med. 2012;9(6):7.

[92] Moodie R, Stuckler D, Monteiro C, Sheron N, Neal B, Thamarangsi T, et al. Profits and pandemics: Prevention of harmful effects of tobacco, alcohol, and ultra-processed food and drink industries. Lancet. 2013;381(9867):670–679.

[93] Sanchez S, Casilli AA. Status and use of food products with health claim (FPHC) in the USA, Japan and France an anthropological perspective. Food Qual Prefer. 2008;19(8):682–691.

[94] Booth S. Food Politics: How the Food Industry Influences Nutrition and Health. Crit Public Health. 2003;13(2):187–188.

[95] Burgoine T, Forouhi NG, Griffin SJ, Wareham NJ, Monsivais P. Associations between exposure to takeaway food outlets, takeaway food consumption, and body weight in Cambridgeshire, UK: population based, cross sectional study. BMJ. 2014;348(mar13 5):g1464–g1464.

[96] Public Health England. Child Obesity :: Public Health England Obesity Knowledge and Intelligence team; 2015.

[97] Ebbeling CB, Pawlak DB, Ludwig DS. Childhood obesity: Public-health crisis, common sense cure. In: Lancet. vol. 360; 2002. p. 473–482.

[98] Moholdt T, Wisløff U, Lydersen S, Nauman J. Current physical activity guidelines for health are insufficient to mitigate long-term weight gain: more data in the fitness versus fatness debate (The HUNT study, Norway). Br J Sports Med. 2014 oct;48(20):1489–1496.

[99] Lee IM, Djoussé L, Sesso HD, Wang L, Buring JE. Physical Activity and Weight Gain Prevention. JAMA. 2010 mar;303(12):1173.

[100] Hankinson AL, Daviglus ML, Bouchard C, Carnethon M, Lewis CE, Schreiner PJ, et al. Maintaining a High Physical Activity Level Over 20 Years and Weight Gain. JAMA. 2010 dec;304(23):2603.

[101] Richardson CR, Newton TL, Abraham JJ, Sen A, Jimbo M, Swartz AM. A Meta-Analysis of Pedometer-Based Walking Interventions and Weight Loss. Ann Fam Med. 2008 jan;6(1):69–77.

[102] Handschin C, Spiegelman B. The role of exercise and PGC1 in inflammation and chronic disease. Nature. 2008;454(7203):463–469.

[103] Stice E, Shaw H, Marti CN. A meta-analytic review of obesity prevention programs for children and adolescents: The skinny on interventions that work. Psychol Bull. 2006;132(5):667–691.

[104] Doak CM, Visscher TLS, Renders CM, Seidell JC. The prevention of overweight and obesity in children and adolescents: a review of interventions and programmes. Obes Rev. 2006;7(1):111–36.

[105] White M. Food access and obesity; 2007.

[106] Lehnert T, Sonntag D, Konnopka A, Riedel-Heller S, König HH. The long-term cost-effectiveness of obesity prevention interventions: Systematic literature review. Obes Rev. 2012;13(6):537–553.

[107] Borys JM, Le Bodo Y, Jebb SA, Seidell JC, Summerbell C, Richard D, et al. EPODE approach for childhood obesity prevention: Methods, progress and international development. Obes Rev. 2012;13(4):299–315.

[108] Knowler WC, Barrett-Connor E, Fowler SE, Hamman RF, Lachin JM, Walker EA, et al. Reduction in the incidence of type 2 diabetes with lifestyle intervention or metformin. N Engl J Med. 2002;346(6):393–403.

[109] Lindstrom J, Ilanne-Parikka P, Peltonen M, Aunola S, Eriksson JG, Hemio K K, et al. Sustained reduction in the incidence of type 2 diabetes by lifestyle intervention: follow-up of the Finnish Diabetes Prevention Study. Lancet. 2006;368(9548):1673–1679.

[110] Lindstrom J, Ilanne-Parikka P, Peltonen M, Aunola S, Eriksson JG, Hemio K, et al. Sustained reduction in the incidence of type 2 diabetes by lifestyle intervention: follow-up of the Finnish Diabetes Prevention Study. Lancet. 2008;368(9548):1673–1679.

[111] Heistaro S, Laatikainen T, Vartiainen E, Puska P, Anttiuutela, Pokusajeva S, et al. Self-reported health in the Republic of Karelia, Russia and in North Karelia, Finland in 1992. Eur J Public Health. 2001;11(1):74–80.

[112] Puska P. Successful prevention of non-communicable diseases: 25 year experiences with North Karelia Project in Finland. Public Heal Med. 2002;4(1):5–7.

[113] Pekka Puska, Erkki Vartiainen, Tiina Laatikainen, Pekka Jousilahti MPe. The North Karelia Proje: From North Karelia To National Action. Natl Med J India. 2009;11(4):187–8.

[114] Puska P, Vartiainen E, Nissinen A, Laatikainen T, Jousilahti P. Background, Principles, Implementation, and General Experiences of the North Karelia Project. Glob Heart. 2016;11(2):173–178.

[115] Randolph W, Viswanath K. Lessons Learned from Public Health Mass Media Campaigns: Marketing Health in a Crowded Media World. Annu Rev Public Health. 2004;25(1):419–437.

[116] Emery SL, Szczypka G, Powell LM, Chaloupka FJ. Public Health Obesity-Related TV Advertising. Lessons Learned from Tobacco. Am J Prev Med. 2007;33(4 SUPPL.).

[117] Blouin C, Dubé L. Global health diplomacy for obesity prevention: Lessons from tobacco control. J Public Health Policy. 2010;31(2):244–55.

[118] Hawkes C. Agro-food industry growth and obesity in China: What role for regulating food advertising and promotion and nutrition labelling? In: Obes. Rev.. vol. 9; 2008. p. 151–161.

[119] Harris JL, Pomeranz JL, Lobstein T, Brownell KD. A Crisis in the Marketplace: How Food Marketing Contributes to Childhood Obesity and What Can Be Done. Annu Rev Public Health. 2009;30(1):211–225.

[120] Brownell KD. Thinking forward: The quicksand of appeasing the food industry. PLoS Med. 2012;9(7).

[121] Rayner M. Social marketing: How might this contribute to tackling obesity?; 2007.

[122] Stead M, Hastings G, McDermott L. The meaning, effectiveness and future of social marketing; 2007.

[123] Fisher JD, Fisher WA. Changing AIDS-risk behavior. Psychol Bull. 1992;111(3):455–474.

[124] Suomi SJ. Early determinants of behaviour: evidence from primate studies. Br Med Bull. 1997;53(1):170–184.

[125] Kruglanski A, Higgins E. Social psychology: Handbook of basic principles. Soc Psychol Handb Basic Princ. 2007;p. 334–352.

[126] Bamberg S, Moser G. Twenty years after Hines, Hungerford, and Tomera: A new meta-analysis of psycho-social determinants of pro-environmental behaviour. J Environ Psychol. 2007;27(1):14–25.

[127] Fiske ST, Gilbert DT, Lindzey G. Handbook of Social Psychology. vol. 2. Lavoisier; 2010.

[128] Jackson T. Motivating Sustainable Consumption - A review of evidence on consumer behaviour and behavioural change; 2005. January.

[129] Dhar R, Wertenbroch K. Self-Signaling and the Costs and Benefits of Temptation in Consumer Choice. J Mark Res. 2012;49(1):15–25.

[130] Baumeister RF, Newman LS. Self-regulation of cognitive inference and decision processes. Personal Soc Psychol Bull. 1994;20(1):3–19.

[131] Metcalfe J, Mischel W. A hot/cool-system analysis of delay of gratification: Dynamics of willpower. Psychol Rev. 1999;106(1):3–19.

[132] Magen E, Kim B, Dweck CS, Gross JJ, McClure SM. Behavioral and neural correlates of increased self-control in the absence of increased willpower. Proc Natl Acad Sci. 2014;111(27):9786–9791.

[133] Kruglanski AW, Webster DM. Motivated closing of the mind: "Seizing" and "freezing.". Psychol Rev. 1996;103(2):263–283.

[134] Wood W, Quinn JM, Kashy DA. Habits in everyday life: Thought, emotion, and action. J Pers Soc Psychol. 2002;83(6):1281–1297.

[135] Ruiter RAC, Abraham C, Kok G. Scary warnings and rational precautions: A review of the psychology of fear appeals. Psychol Health. 2001;16(6):613–630.

[136] Das EHHJ, de Wit JBF, Stroebe W. Fear appeals motivate acceptance of action recommendations: evidence for a positive bias in the processing of persuasive messages. Personal Soc Psychol Bull. 2003;29(5):650–664.

[137] Buchwald H, Estok R, Fahrbach K, Banel D, Jensen MD, Pories WJ, et al. Weight and type 2 diabetes after bariatric surgery: systematic review and meta-analysis. Am J Med. 2009;122(3):248–256 e5.

[138] Hess DWS, Hess DWS, Oakley RS. The biliopancreatic diversion with the duodenal switch: results beyond 10 years. Obes Surg. 2005;15(3):408–16.

[139] O'Brien PE, McPhail T, Chaston TB, Dixon JB. Systematic review of medium-term weight loss after bariatric operations. Obes Surg. 2006;16(8):1032–1040.

[140] Bikman BT, Zheng D, Pories WJ, Chapman W, Pender JR, Bowden RC, et al. Mechanism for Improved Insulin Sensitivity after Gastric Bypass Surgery. J Clin Endocrinol Metab. 2008 dec;93(12):4656–4663.

[141] Martins C, Strømmen M, Stavne Oa, Nossum R, Mårvik R, Kulseng B. Bariatric surgery versus lifestyle interventions for morbid obesity–changes in body weight, risk factors and comorbidities at 1 year. Obes Surg. 2011;21(7):841–849.

[142] Cannon CP, Kumar A. Treatment of overweight and obesity: Lifestyle, pharmacologic, and surgical options. Clin Cornerstone. 2009;9(4):55–71.

[143] Lang T, Rayner G. Overcoming policy cacophony on obesity: An ecological public health framework for policymakers. Obes Rev. 2007;8(SUPPL. 1):165–181.

[144] Van Hout GCM, Van Oudheusden I, Van Heck GL. Psychological profile of the morbidly obese. Obes Surg. 2004;14(5):579–588.

[145] Hubert HB, Feinleib M, McNamara PM, Castelli WP. Obesity as an independent risk factor for cardiovascular disease: a 26- year follow-up of participants in the Framingham Heart Study. Circulation. 1983;67(5):968–977.

[146] Kopelman PG. Obesity as a medical problem. Nature. 2000;404(6778):635–643.

[147] Vucenik I, Stains JP. Obesity and cancer risk: Evidence, mechanisms, and recommendations. Ann N Y Acad Sci. 2012;1271(1):37–43.

[148] Zhang X, Wu WKK, Yu J. Obesity and Cancer. Obesity. 2016;p. 211–220.

[149] Zhang P, Zhang X, Brown J, Vistisen D, Sicree R, Shaw J, et al. Global healthcare expenditure on diabetes for 2010 and 2030. Diabetes Res Clin Pract. 2010;87(3):293–301.

[150] Dennedy MC, Vidal-Puig A. Review Article: An Adipocentric View of the Metabolic Syndrome and Cardiovascular Disease. Curr Cardiovasc Risk Rep. 2014;8(3):1–9.

[151] Itani SI, Ruderman NB, Schmieder F, Boden G. Lipid-Induced Insulin Resistance in Human Muscle Is Associated With Changes in Diacylglycerol, Protein Kinase C, and I B- . Diabetes. 2002;51(7):2005–2011.

[152] Kim JA, Wei Y, Sowers JR. Role of mitochondrial dysfunction in insulin resistance. Circ Res. 2008;102(4):401–414.

[153] Arner P, Bernard S, Salehpour M, Possnert G, Liebl J, Steier P, et al. Dynamics of human adipose lipid turnover in health and metabolic disease. Nature. 2011 sep;478(7367):110–113.

[154] Bays HE, Toth PP, Kris-Etherton PM, Abate N, Aronne LJ, Brown WV, et al. Obesity, adiposity, and dyslipidemia: A consensus statement from the National Lipid Association. J Clin Lipidol. 2013;7(4):304–383.

[155] Imbeault P, Lemieux S, Prud'homme D, Tremblay A, Nadeau A, Després JP, et al. Relationship of visceral adipose tissue to metabolic risk factors for coronary heart disease: is there a contribution of subcutaneous fat cell hypertrophy? Metabolism. 1999;48(3):355–62.

[156] Michaud A, Drolet R, Noel S, Paris G, Tchernof A. Visceral fat accumulation is an indicator of adipose tissue macrophage infiltration in women. Metabolism. 2012;61(5):689–698.

[157] Zhang Y, Marsboom G, Toth PT, Rehman J. Mitochondrial Respiration Regulates Adipogenic Differentiation of Human Mesenchymal Stem Cells. PLoS One. 2013;8(10).

[158] Harman-Boehm I, Bluher M, Redel H, Sion-Vardy N, Ovadia S, Avinoach E, et al. Macrophage infiltration into omental versus subcutaneous fat across different populations: Effect of regional adiposity and the comorbidities of obesity. J Clin Endocrinol Metab. 2007;92(6):2240–2247.

[159] Chistiakov DA, Sobenin IA, Revin VV, Orekhov AN, Bobryshev YV. Mitochondrial aging and age-related dysfunction of mitochondria. Biomed Res Int. 2014;2014.

[160] Park S, Kim H, Lee J, Yoon K, Chang M, Park S. The age-dependent induction of apoptosis-inducing factor (AIF) in the human semitendinosus skeletal muscle. Cell Mol Biol Lett. 2010;15(1):1–12.

[161] Marzetti E, Leeuwenburgh C. Skeletal muscle apoptosis, sarcopenia and frailty at old age. Exp Gerontol. 2006;41(12):1234–1238.

[162] Parker VER, Savage DB, O'Rahilly S, Semple RK. Mechanistic insights into insulin resistance in the genetic era. Diabet Med. 2011;28(12):1476–1486.

[163] Gandotra S, Le Dour C, Bottomley W, Cervera P, Giral P, Reznik Y, et al. Perilipin deficiency and autosomal dominant partial lipodystrophy. N Engl J Med. 2011;364(8):740–748.

[164] Votruba SB, Mattison RS, Dumesic DA, Koutsari C, Jensen MD. Meal fatty acid uptake in visceral fat in women. Diabetes. 2007;56(10):2589–2597.

[165] McQuaid SE, Humphreys SM, Hodson L, Fielding BA, Karpe F, Frayn KN. Femoral adipose tissue may accumulate the fat that has been recycled as VLDL and nonesterified fatty acids. Diabetes. 2010;59(10):2465–2473.

[166] Donath MY, Shoelson SE. Type 2 diabetes as an inflammatory disease. Nat Rev Immunol. 2011;11(2):98–107.

[167] Prieur X, Mok CYL, Velagapudi VR, Nuñez V, Fuentes L, Montaner D, et al. Differential lipid partitioning between adipocytes and tissue macrophages modulates macrophage lipotoxicity and M2/M1 polarization in obese mice. Diabetes. 2011;60(3):797–809.

[168] Weisberg SP, McCann D, Desai M, Rosenbaum M, Leibel RL, Ferrante AW. Obesity is associated with macrophage accumulation in adipose tissue. J Clin Invest. 2003;112(12):1796–1808.

[169] Weisberg SP, Hunter D, Huber R, Lemieux J, Slaymaker S, Vaddi K, et al. CCR2 modulates inflammatory and metabolic effects of high-fat feeding. J Clin Invest. 2006;116(1):115–124.

[170] Harte AL, Tripathi G, Piya MK, Barber TM, Clapham JC, Al-Daghri N, et al. NFkappaB as a potent regulator of inflammation in human adipose tissue, influenced by depot, adiposity, T2DM status, and TNFalpha. Obesity. 2013 nov;21(11):2322–2330.

[171] Dahlman I, Forsgren M, Sjögren A, Nordström EA, Kaaman M, Näslund E, et al. Downregulation of electron transport chain genes in visceral adipose tissue in type 2 diabetes independent of obesity and possibly involving tumor necrosis factor-α. Diabetes. 2006;55(6):1792–1799.

[172] Pories WJ, MacDonald KG, Morgan EJ, Sinha MK, Dohm GL, Swanson MS, et al. Surgical treatment of obesity and its effect on diabetes: 10-y follow-up. Am J Clin Nutr. 1992;55(SUPPL. 2).

[173] Karmali S, Brar B, Shi X, Sharma AM, de Gara C, Birch DW. Weight Recidivism Post-Bariatric Surgery: A Systematic Review. Obes Surg. 2013 nov;23(11):1922–1933.

[174] Sjöström L. Review of the key results from the Swedish Obese Subjects (SOS) trial - a prospective controlled intervention study of bariatric surgery. J Intern Med. 2013 mar;273(3):219–34.

[175] Shankar P, Boylan M, Sriram K. Micronutrient deficiencies after bariatric surgery. Nutrition. 2010;26(11-12):1031–1037.

[176] Dixon JB, Lambert EA, Lambert GW. Neuroendocrine adaptations to bariatric surgery. Mol Cell Endocrinol. 2015;418:143–152.

[177] Cummings DE. Endocrine mechanisms mediating remission of diabetes after gastric bypass surgery. Int J Obes. 2009;33:S33–S40.

[178] Batterham RL, Cummings DE. Mechanisms of diabetes improvement following bariatric/metabolic surgery. Diabetes Care. 2016;39(6):893–901.

[179] Knop FK, Taylor R. Mechanism of Metabolic Advantages After Bariatric Surgery: It's all gastrointestinal factors versus it's all food restriction. Diabetes Care. 2013 aug;36(Supplement_2):S287–S291.

[180] Ochner CN, Kwok Y, Conceição E, Pantazatos SP, Puma LM, Carnell S, et al. Selective Reduction in Neural Responses to High Calorie Foods Following Gastric Bypass Surgery. Ann Surg. 2011;253(3):502–507.

[181] Olbers T, Bjorkman S, Lindroos A, Maleckas A, Lonn L, Sjostrom L, et al. Body composition, dietary intake, and energy expenditure after laparoscopic

Roux-en-Y gastric bypass and laparoscopic vertical banded gastroplasty: a randomized clinical trial. Ann Surg. 2012;(5):715–722.

[182] Ye J, Hao Z, Mumphrey MB, Townsend RL, Patterson LM, Stylopoulos N, et al. GLP-1 receptor signaling is not required for reduced body weight after RYGB in rodents. AJP Regul Integr Comp Physiol. 2014;306(5):R352–R362.

[183] Miras AD, le Roux CW. Mechanisms underlying weight loss after bariatric surgery. Nat Rev Gastroenterol Hepatol. 2013;10(10):575–84.

[184] Dixon AFR, Dixon JB, O'Brien PE. Laparoscopic adjustable gastric banding induces prolonged satiety: A randomized blind crossover study. J Clin Endocrinol Metab. 2005;90(2):813–819.

[185] le Roux CW, Aylwin SJB, Batterham RL, Borg CM, Coyle F, Prasad V, et al. Gut hormone profiles following bariatric surgery favor an anorectic state, facilitate weight loss, and improve metabolic parameters. Ann Surg. 2006;243(1):108–14.

[186] Laferrère B, Teixeira J, McGinty J, Tran H, Egger JR, Colarusso A, et al. Effect of weight loss by gastric bypass surgery versus hypocaloric diet on glucose and incretin levels in patients with type 2 diabetes. J Clin Endocrinol Metab. 2008;93(7):2479–85.

[187] Anderson B, Switzer NJ, Almamar A, Shi X, Birch DW, Karmali S. The impact of laparoscopic sleeve gastrectomy on plasma ghrelin levels: A systematic review. Obes Surg. 2013;23(9):1476–1480.

[188] Chambers AP, Kirchner H, Wilson-Perez HE, Willency JA, Hale JE, Gaylinn BD, et al. The effects of vertical sleeve gastrectomy in rodents are ghrelin independent. Gastroenterology. 2013;144(1):50–52.

[189] McFarlane MR, Brown MS, Goldstein JL, Zhao TJ. Induced ablation of ghrelin cells in adult mice does not decrease food intake, body weight, or response to high-fat diet. Cell Metab. 2014;20(1):54–60.

[190] Kohli R, Bradley D, Setchell KD, Eagon JC, Abumrad N, Klein S. Weight loss induced by Roux-en-Y gastric bypass but not laparoscopic adjustable gastric banding increases circulating bile acids. J Clin Endocrinol Metab. 2013;98(4).

[191] Haeusler RA, Astiarraga B, Camastra S, Accili D, Ferrannini E. Human insulin resistance is associated with increased plasma levels of 12alpha-hydroxylated bile acids. Diabetes. 2013;62(12):4184–4191.

[192] Tremaroli V, Karlsson F, Werling M, Ståhlman M, Kovatcheva-Datchary P, Olbers T, et al. Roux-en-Y Gastric Bypass and Vertical Banded Gastroplasty Induce Long-Term Changes on the Human Gut Microbiome Contributing to Fat Mass Regulation. Cell Metab. 2015 aug;22(2):228–238.

[193] Ghanim H, Abuaysheh S, Sia CL, Korzeniewski K, Chaudhuri A, Fernandez-Real JM, et al. Increase in plasma endotoxin concentrations and the expression of toll-like receptors and suppressor of cytokine signaling-3 in mononuclear cells after a high-fat, high-carbohydrate meal: Implications for insulin resistance. Diabetes Care. 2009;32(12):2281–2287.

[194] Ghanim H, Sia CL, Upadhyay M, Korzeniewski K, Viswanathan P, Abuaysheh S, et al. Orange juice neutralizes the proinflammatory effect of a high-fat, high-carbohydrate meal and prevents endotoxin increase and toll-like receptor expression. Am J Clin Nutr. 2010;91(4):940–949.

[195] Triantafilou M, Triantafilou K. Lipopolysaccharide recognition: CD14, TLRs and the LPS-activation cluster; 2002.

[196] Creely SJ, McTernan PG, Kusminski CM, Fisher FM, Da Silva NF, Khanolkar M, et al. Lipopolysaccharide activates an innate immune system response in human adipose tissue in obesity and type 2 diabetes. Am J Physiol Endocrinol Metab. 2007;292(3):E740–E747.

[197] Ouchi N, Parker JL, Lugus JJ, Walsh K. Adipokines in inflammation and metabolic disease. Nat Rev Immunol. 2011;11(2):85–97.

[198] Cani PD, Amar J, Iglesias MA, Poggi M, Knauf C, Bastelica D, et al. Original Article. Diabetes. 2007;56(July):1761–1772.

[199] Dixon AN, Valsamakis G, Hanif MW, Field A, Boutsiadis A, Harte A, et al. Effect of the orlistat on serum endotoxin lipopolysaccharide and adipocytokines in South Asian individuals with impaired glucose tolerance. Int J Clin Pract. 2008 jun;62(7):1124–1129.

[200] Al-Attas OS, Al-Daghri NM, Al-Rubeaan K, da Silva NF, Sabico SL, Kumar S, et al. Changes in endotoxin levels in T2DM subjects on anti-diabetic therapies. Cardiovasc Diabetol. 2009;8(1):20.

[201] Harte AL, da Silva NF, Creely SJ, McGee KC, Billyard T, Youssef-Elabd EM, et al. Elevated endotoxin levels in non-alcoholic fatty liver disease. J Inflamm. 2010;7(1):15.

[202] Pussinen PJ, Havulinna AS, Lehto M, Sundvall J, Salomaa V. Endotoxemia is associated with an increased risk of incident diabetes. Diabetes Care. 2011;34(2):392–397.

[203] Piya MK, McTernan PG, Kumar S. Adipokine inflammation and insulin resistance: The role of glucose, lipids and endotoxin. J Endocrinol. 2013;216(1).

[204] Harte AL, Varma MC, Tripathi G, Mcgee KC, Al-Daghri NM, Al-Attas OS, et al. High fat intake leads to acute postprandial exposure to circulating endotoxin in type 2 diabetic subjects. Diabetes Care. 2012;35(2):375–382.

[205] Monte SV, Caruana JA, Ghanim H, Sia CL, Korzeniewski K, Schentag JJ, et al. Reduction in endotoxemia, oxidative and inflammatory stress, and insulin resistance after Roux-en-Y gastric bypass surgery in patients with morbid obesity and type 2 diabetes mellitus. Surgery. 2012;151(4):587–593.

[206] Mithieux G, Misery P, Magnan C, Pillot B, Gautier-Stein A, Bernard C, et al. Portal sensing of intestinal gluconeogenesis is a mechanistic link in the diminution of food intake induced by diet protein. Cell Metab. 2005;2(5):321–329.

[207] Mithieux G. Nutrient control of energy homeostasis via gut-brain neural circuits. Neuroendocrinology. 2014;100:89–94.

[208] Mithieux G. Metabolic effects of portal vein sensing. Diabetes, Obes Metab. 2014;16:56–60.

[209] Delaere F, Akaoka H, De Vadder F, Duchampt A, Mithieux G. Portal glucose influences the sensory, cortical and reward systems in rats. Eur J Neurosci. 2013 nov;38(10):3476–86.

[210] Trung VN, Yamamoto H, Yamaguchi T, Murata S, Aimi Y, Kuwahara A, et al. Intact neural system of the portal vein is important for maintaining normal glucose metabolism by regulating glucagon-like peptide-1 and insulin sensitivity. Peptides. 2014;52:38–43.

[211] Hayes MT, Foo J, Besic V, Tychinskaya Y, Stubbs RS. Is intestinal gluconeogenesis a key factor in the early changes in glucose homeostasis following gastric bypass? Obes Surg. 2011;21(6):759–762.

[212] Colles SL, Dixon JB, O'Brien PE. Hunger control and regular physical activity facilitate weight loss after laparoscopic adjustable gastric banding. Obes Surg. 2008;18(7):833–840.

[213] Favretti F, Segato G, Ashton D, Busetto L, De Luca M, Mazza M, et al. Laparoscopic adjustable gastric banding in 1,791 consecutive obese patients: 12-Year results. Obes Surg. 2007;17(2):168–175.

[214] Spector AC. Linking gustatory neurobiology to behavior in vertebrates. Neurosci Biobehav Rev. 2000;24(4):391–416.

[215] Bueter M, Löwenstein C, Olbers T, Wang M, Cluny NL, Bloom SR, et al. Gastric Bypass Increases Energy Expenditure in Rats. Gastroenterology. 2010;138(5).

[216] Brand MD, Nicholls DG. Assessing mitochondrial dysfunction in cells. Biochem J. 2011;435(2):297–312.

[217] Brehm A, Krssak M, Schmid AI, Nowotny P, Waldhausl W, Roden M. Increased lipid availability impairs insulin-stimulated ATP synthesis in human skeletal muscle. Diabetes. 2006;55(1):136–140.

[218] Arsenijevic D, Onuma H, Pecqueur C, Raimbault S, Manning BS, Miroux B, et al. Disruption of the uncoupling protein-2 gene in mice reveals a role in immunity and reactive oxygen species production. Nat Genet. 2000;26(4):435–439.

[219] Kozak LP. Genetic variation in brown fat activity and body weight regulation in mice: Lessons for human studies. Biochim Biophys Acta - Mol Basis Dis. 2014;1842(3):370–376. Available from: http://dx.doi.org/10.1016/j.bbadis.2013.04.025.

[220] Wu Z, Puigserver P, Andersson U, Zhang C, Adelmant G, Mootha V, et al. Mechanisms controlling mitochondrial biogenesis and respiration through the thermogenic coactivator PGC-1. Cell. 1999;98(1):115–124.

[221] West IC. Radicals and oxidative stress in diabetes. Diabet Med. 2000;17(3):171–180.

[222] Rosen P, Nawroth PP, King G, Moller W, Tritschler HJ, Packer L. The role of oxidative stress in the onset and progression of diabetes and its complications: a summary of a Congress Series sponsored by UNESCO-MCBN, the American Diabetes Association and the German Diabetes Society. Diabetes Metab Res Rev. 2001;17(3):189–212.

[223] Evans JL, Maddux BA, Goldfine ID. The Molecular Basis for Oxidative Stress-Induced Insulin Resistance. Antioxid Redox Signal. 2005;7(7-8):1040–1052.

[224] Rachana, Thakur S, Basu S. Oxidative stress and diabetes. Free Radicals Hum Heal Dis. 2015;p. 241–257.

[225] Morino K, Petersen KF, Dufour S, Befroy D, Frattini J, Shatzkes N, et al. Reduced mitochondrial density and increased IRS-1 serine phosphorylation in muscle of insulin-resistant offspring of type 2 diabetic parents. J Clin Invest. 2005;115(12):3587–3593.

[226] Nishikawa T, Araki E. Impact of Mitochondrial ROS Production in the Pathogenesis of Diabetes Mellitus and Its Complications. Antioxid Redox Signal. 2006;0(0):061221112325010.

[227] Lee KU, Lee IK, Han J, Song DK, Kim YM, Song HS, et al. Effects of recombinant adenovirus-mediated uncoupling protein 2 overexpression on endothelial function and apoptosis. Circ Res. 2005;96(11):1200–1207.

[228] Clapham JC, Arch JRS, Chapman H, Haynes A, Lister C, Moore GBT, et al. Mice overexpressing human uncoupling protein-3 in skeletal muscle are hyperphagic and lean. Nature. 2000;406(6794):415–418.

[229] Brand MD, Pamplona R, Portero-Otin M, Requena JR, Roebuck SJ, Buckingham JA, et al. Oxidative damage and phospholipid fatty acyl composition in skeletal muscle mitochondria from mice underexpressing or overexpressing uncoupling protein 3. Biochem J. 2002;368(Pt 2):597–603.

[230] Rudich A, Tirosh A, Potashnik R, Khamaisi M, Bashan N. Lipoic acid protects against oxidative stress induced impairment in insulin stimulation of protein kinase B and glucose transport in 3T3-L1 adipocytes. Diabetologia. 1999;42(8):949–957.

[231] Cleasby ME, Dzamko N, Hegarty BD, Cooney GJ, Kraegen EW, Ye JM. Metformin prevents the development of acute lipid-induced insulin resistance in the rat through altered hepatic signaling mechanisms. Diabetes. 2004;53(12):3258–3266.

[232] Zou MH, Kirkpatrick SS, Davis BJ, Nelson JS, Wiles WG, Schlattner U, et al. Activation of the AMP-activated protein kinase by the anti-diabetic drug metformin in vivo. Role of mitochondrial reactive nitrogen species. J Biol Chem. 2004;279(42):43940–43951.

[233] Bogacka I, Xie H, Bray Ga, Smith SR. Pioglitazone Induces Mitochondrial Biogenesis in Human Subcutaneous Adipose Tissue In Vivo. Diabetes. 2005;54(5):1392–1399.

[234] Puigserver P, Wu Z, Park CW, Graves R, Wright M, Spiegelman BM. A cold-inducible coactivator of nuclear receptors linked to adaptive thermogenesis. Cell. 1998 mar;92(6):829–39.

[235] Duncan JG, Fong JL, Medeiros DM, Finck BN, Kelly DP. Insulin-resistant heart exhibits a mitochondrial biogenic response driven by the peroxisome proliferator-activated receptor-alpha/PGC-1alpha gene regulatory pathway. Circulation. 2007;115(7):909–917.

[236] Liesa M, Shirihai OS. Mitochondrial dynamics in the regulation of nutrient utilization and energy expenditure. Cell Metab. 2013;17(4):491–506.

[237] Jheng HF, Tsai PJ, Guo SM, Kuo LH, Chang CS, Su IJ, et al. Mitochondrial Fission Contributes to Mitochondrial Dysfunction and Insulin Resistance in Skeletal Muscle. Mol Cell Biol. 2012;32(2):309–319.

[238] Westwick JK, Bielawska AE, Dbaibo G, Hannun YA, Brenner DA. Ceramide activates the stress-activated protein kinases. J Biol Chem. 1995;270(39):22689–22692.

[239] Yu C, Chen Y, Cline GW, Zhang D, Zong H, Wang Y, et al. Mechanism by which fatty acids inhibit insulin activation of insulin receptor substrate-1 (IRS-1)-associated phosphatidylinositol 3-kinase activity in muscle. J Biol Chem. 2002 dec;277(52):50230–6.

[240] Gao Z, Zhang X, Zuberi A, Hwang D, Quon MJ, Lefevre M, et al. Inhibition of insulin sensitivity by free fatty acids requires activation of multiple serine kinases in 3T3-L1 adipocytes. Mol Endocrinol. 2004;18(8):2024–2034.

[241] Savage DB, Petersen KF, Shulman GI. Disordered Lipid Metabolism and the Pathogenesis of Insulin Resistance. Physiol Rev. 2007;87(2):507–520.

[242] Schenk S, Saberi M, Olefsky JM. Insulin sensitivity: Modulation by nutrients and inflammation; 2008.

[243] Frisard M, Ravussin E. Energy metabolism and oxidative stress: impact on the metabolic syndrome and the aging process. Endocrine. 2006;29(1):27–32.

[244] Mogensen M, Sahlin K, Fernstro M, Glintborg D, Vind BF, Beck-nielsen H, et al. Mitochondrial respiration is decreased in skeletal muscle of patients with type 2 diabetes. Diabetes. 2007;56(6):1592–1599.

[245] Kelley DE, He J, Menshikova EV, Ritov VB. Dysfunction of Mitochondria in Human Skeletal Muscle in Type 2 Diabetes. Diabetes. 2002;51(October).

[246] Ritov VB, Menshikova EV, He J, Ferrell RE, Goodpaster BH, Kelley DE. Deficiency of subsarcolemmal mitochondria in obesity and type 2 diabetes. Diabetes. 2005;54(1):8–14.

[247] Stump CS, Short KR, Bigelow ML, Schimke JM, Nair KS. Effect of insulin on human skeletal muscle mitochondrial ATP production, protein synthesis, and mRNA transcripts. Proc Natl Acad Sci. 2003;100(13):7996–8001.

[248] Ling C, Poulsen P, Carlsson E, Ridderstråle M, Almgren P, Wojtaszewski J, et al. Multiple environmental and genetic factors influence skeletal muscle PGC-1alpha and PGC-1beta gene expression in twins. J Clin Invest. 2004;114(10):1518–26.

[249] Handschin C, Spiegelman BM. Peroxisome proliferator-activated receptor gamma coactivator 1 coactivators, energy homeostasis, and metabolism. Endocr Rev. 2006;27(7):728–735.

[250] Austin S, St-Pierre J. PGC1alpha and mitochondrial metabolism: emerging concepts and relevance in ageing and neurodegenerative disorders. J Cell Sci. 2012;125(Pt 21):4963–4971. Available from: http://www.ncbi.nlm.nih.gov/pubmed/23277535.

[251] Hayashi T, Hirshman MF, Kurth EJ, Winder WW, Goodyear LJ. Evidence for 5' AMP-activated protein kinase mediation of the effect of muscle contraction on glucose transport. Diabetes. 1998;47(8):1369–1373.

[252] Yoon JC, Puigserver P, Chen G, Donovan J, Wu Z, Rhee J, et al. Control of hepatic gluconeogenesis through the transcriptional coactivator PGC-1. Nature. 2001;413(6852):131–138.

[253] Finck BN, Kelly DP. PGC-1 coactivators: inducible regulators of energy metabolism in health and disease. J Clin Invest. 2006 mar;116(3):615–622.

[254] Jager SS, Handschin CC, St-Pierre JJ, Spiegelman BMBM. AMP-activated protein kinase (AMPK) action in skeletal muscle via direct phosphorylation of PGC-1alpha. Pnas. 2007;104(29):12017–12022.

[255] Patti ME, Butte AJ, Crunkhorn S, Cusi K, Berria R, Kashyap S, et al. Coordinated reduction of genes of oxidative metabolism in humans with insulin resistance and diabetes: Potential role of PGC1 and NRF1. Proc Natl Acad Sci U S A. 2003;100(14):8466–71.

[256] Kukidome D, Nishikawa T, Sonoda K, Imoto K, Fujisawa K, Yano M, et al. Activation of AMP-activated protein kinase reduces hyperglycemia-induced mitochondrial reactive oxygen species production and promotes mitochondrial biogenesis in human umbilical vein endothelial cells. Diabetes. 2006;55(1):120–127.

[257] Short KR, Vittone JL, Bigelow ML, Proctor DN, Rizza RA, Coenen-Schimke JM, et al. Impact of aerobic exercise training on age-related changes in insulin sensitivity and muscle oxidative capacity. Diabetes. 2003;52(8):1888–1896.

[258] Toledo FGS, Menshikova EV, Ritov VB, Azuma K, Radikova Z, DeLany J, et al. Effects of physical activity and weight loss on skeletal muscle mitochondria and relationship with glucose control in type 2 diabetes. Diabetes. 2007;56(8):2142–2147.

[259] Lopez-Lluch G, Hunt N, Jones B, Zhu M, Jamieson H, Hilmer S, et al. Calorie restriction induces mitochondrial biogenesis and bioenergetic efficiency. Proc Natl Acad Sci. 2006;103(6):1768–1773.

[260] Guarente L. Sirtuins as potential targets for metabolic syndrome. Nature. 2006;444(7121):868–874.

[261] St-Pierre J, Lin J, Krauss S, Tarr PT, Yang R, Newgard CB, et al. Bioenergetic analysis of peroxisome proliferator-activated receptor gamma coactivators 1alpha and 1beta (PGC-1alpha and PGC-1beta) in muscle cells. J Biol Chem. 2003;278(29):26597–603.

[262] Wenz T, Rossi SG, Rotundo RL, Spiegelman BM, Moraes CT. Increased muscle PGC-1 expression protects from sarcopenia and metabolic disease during aging. Proc Natl Acad Sci. 2009;106(48):20405–20410.

[263] Hoeks J, Arany Z, Phielix E, Moonen-Kornips E, Hesselink MKC, Schrauwen P. Enhanced lipid-but not carbohydrate-supported mitochondrial respiration in skeletal muscle of PGC-1alpha overexpressing mice. J Cell Physiol. 2012;227(3):1026–1033.

[264] Matthews DR, Hosker JP, Rudenski aS, Naylor Ba, Treacher DF, Turner RC. Homeostasis model assessment: insulin resistance and beta-cell function from fasting plasma glucose and insulin concentrations in man. Diabetologia. 1985;28(7):412–419.

[265] Friedewald WT, Levy RI, Fredrickson DS. Estimation of the concentration of low-density lipoprotein cholesterol in plasma, without use of the preparative ultracentrifuge. Clin Chem. 1972;18(6):499–502.

[266] Hsieh CJ, Weng SW, Liou CW, Lin TK, Chen JB, Tiao MM, et al. Tissue-specific differences in mitochondrial DNA content in type 2 diabetes. Diabetes Res Clin Pract. 2011;92(1):106–10.

[267] Phillips NR, Sprouse ML, Roby RK. Simultaneous quantification of mitochondrial DNA copy number and deletion ratio: a multiplex real-time PCR assay. Sci Rep. 2014;4:3887.

[268] Alhusaini S, McGee K, Schisano B, Harte A, McTernan P, Kumar S, et al. Lipopolysaccharide, high glucose and saturated fatty acids induce endoplas-

mic reticulum stress in cultured primary human adipocytes: Salicylate alleviates this stress. Biochem Biophys Res Commun. 2010;397(3):472–478.

[269] Darimont C, Zbinden I, Avanti O, Leone-Vautravers P, Giusti V, Burckhardt P, et al. Reconstitution of telomerase activity combined with HPV-E7 expression allow human preadipocytes to preserve their differentiation capacity after immortalization. Cell Death Differ. 2003;10(9):1025–1031.

[270] Mortiboys H, Thomas KJ, Koopman WJH, Klaffke S, Abou-Sleiman P, Olpin S, et al. Mitochondrial function and morphology are impaired in parkin-mutant fibroblasts. Ann Neurol. 2008;64(5):555–565.

[271] Sjöström L, Lindroos AK, Peltonen M, Torgerson J, Bouchard C, Carlsson B, et al. Lifestyle, diabetes, and cardiovascular risk factors 10 years after bariatric surgery. N Engl J Med. 2004 dec;351(26):2683–93.

[272] Dixon JB, O'Brien PE, Playfair J, Chapman L, Schachter LM, Skinner S, et al. Adjustable gastric banding and conventional therapy for type 2 diabetes: a randomized controlled trial. JAMA. 2008;299(3):316–23.

[273] Schauer PR, Kashyap SR, Wolski K, Brethauer SA, Kirwan JP, Pothier CE, et al. Bariatric surgery versus intensive medical therapy in obese patients with diabetes. N Engl J Med. 2012;366(17):1567–76.

[274] Bradley D, Conte C, Mittendorfer B, Eagon JC, Varela JE, Fabbrini E, et al. Gastric bypass and banding equally improve insulin sensitivity and β cell function. J Clin Invest. 2012;122(12):4667–4674.

[275] Arterburn DE, Bogart A, Sherwood NE, Sidney S, Coleman KJ, Haneuse S, et al. A multisite study of long-term remission and relapse of type 2 diabetes mellitus following gastric bypass. Obes Surg. 2013;23(1):93–102.

[276] Corkey BE, Shirihai O. Metabolic master regulators: Sharing information among multiple systems. Trends Endocrinol Metab. 2012;23(12):594–601.

[277] Kusminski CM, Scherer PE. Mitochondrial dysfunction in white adipose tissue. Trends Endocrinol Metab. 2012;23(9):435–443.

[278] Las G, Serada SB, Wikstrom JD, Twig G, Shirihai OS. Fatty acids suppress autophagic turnover in ß-cells. J Biol Chem. 2011;286(49):42534–42544.

[279] Molina AJ, Wikstrom JD, Wikstrom JD, Stiles L, Stiles L, Las G, et al. Mitochondrial Networking Protects Beta Cells from Nutrient Induced Apoptosis. Diabetes. 2009;58(October):2303–2315.

[280] Choo HJ, Kim JH, Kwon OB, Lee CS, Mun JY, Han SS, et al. Mitochondria are impaired in the adipocytes of type 2 diabetic mice. Diabetologia. 2006;49(4):784–791.

[281] Wang T, Si Y, Shirihai OS, Si H, Schultz V, Corkey RF, et al. Respiration in adipocytes is inhibited by reactive oxygen species. Obesity (Silver Spring). 2010;18(8):1493–1502.

[282] Brookheart RT, Michel CI, Schaffer JE. As a Matter of Fat. Cell Metab. 2009;10(1):9–12.

[283] Lin Y, Berg AH, Iyengar P, Lam TKT, Giacca A, Combs TP, et al. The hyperglycemia-induced inflammatory response in adipocytes: The role of reactive oxygen species. J Biol Chem. 2005;280(6):4617–4626.

[284] Koves TR, Ussher JR, Noland RC, Slentz D, Mosedale M, Ilkayeva O, et al. Mitochondrial Overload and Incomplete Fatty Acid Oxidation Contribute to Skeletal Muscle Insulin Resistance. Cell Metab. 2008;7(1):45–56.

[285] Houstis N, Rosen ED, Lander ES. Reactive oxygen species have a causal role in multiple forms of insulin resistance. Nature. 2006;440(7086):944–948.

[286] Heinonen S, Buzkova J, Muniandy M, Kaksonen R, Ollikainen M, Ismail K, et al. Impaired mitochondrial biogenesis in adipose tissue in acquired obesity. Diabetes. 2015;64(9):3135–3145.

[287] Yin X, Lanza IR, Swain JM, Sarr MG, Nair KS, Jensen MD. Adipocyte mitochondrial function is reduced in human obesity independent of fat cell size. J Clin Endocrinol Metab. 2014 feb;99(2):E209–16.

[288] Wilson FH, Hariri A, Farhi A, Zhao H, Petersen KF, Toka HR, et al. A cluster of metabolic defects caused by mutation in a mitochondrial tRNA. Science. 2004 nov;306(5699):1190–4.

[289] Szendroedi J, Schmid AI, Meyerspeer M, Cervin C, Kacerovsky M, Smekal G, et al. Impaired Mitochondrial Function and Insulin Resistance of Skeletal Muscle in Mitochondrial Diabetes. Diabetes Care. 2009;32(4):677–679.

[290] Pietilainen KH, Naukkarinen J, Rissanen A, Saharinen J, Ellonen P, Ker??nen H, et al. Global transcript profiles of fat in monozygotic twins discordant for BMI: Pathways behind acquired obesity. PLoS Med. 2008;5(3):0472–0483.

[291] Vernochet C, Damilano F, Mourier A, Bezy O, Mori MA, Smyth G, et al. Adipose tissue mitochondrial dysfunction triggers a lipodystrophic syndrome with insulin resistance, hepatosteatosis, and cardiovascular complications. FASEB J. 2014 oct;28(10):4408–19.

[292] Wang CH, Wang CC, Huang HC, Wei YH. Mitochondrial dysfunction leads to impairment of insulin sensitivity and adiponectin secretion in adipocytes. FEBS J. 2013 feb;280(4):1039–50.

[293] Enos RT, Velázquez KT, Murphy EA. Insight into the impact of dietary saturated fat on tissue-specific cellular processes underlying obesity-related diseases. J Nutr Biochem. 2014 jun;25(6):600–12.

[294] Paglialunga S, Ludzki A, Root-McCaig J, Holloway GP. In adipose tissue, increased mitochondrial emission of reactive oxygen species is important for short-term high-fat diet-induced insulin resistance in mice. Diabetologia. 2015 may;58(5):1071–80.

[295] Wang PW, Kuo HM, Huang HT, Chang AYW, Weng SW, Tai MH, et al. Biphasic response of mitochondrial biogenesis to oxidative stress in visceral fat of diet-induced obesity mice. Antioxid Redox Signal. 2014 jun;20(16):2572–88.

[296] Ishihara N, Fujita Y, Oka T, Mihara K. Regulation of mitochondrial morphology through proteolytic cleavage of OPA1. EMBO J. 2006;25(13):2966–2977.

[297] Lim EL, Hollingsworth KG, Aribisala BS, Chen MJ, Mathers JC, Taylor R. Reversal of type 2 diabetes: normalisation of beta cell function in association with decreased pancreas and liver triacylglycerol. Diabetologia. 2011 oct;54(10):2506–2514.

[298] Viguerie N, Vidal H, Arner P, Holst C, Verdich C, Avizou S, et al. Adipose tissue gene expression in obese subjects during low-fat and high-fat hypocaloric diets. Diabetologia. 2005 jan;48(1):123–131.

[299] Gibby JT, Njeru DK, Cvetko ST, Merrill RM, Bikman BT, Gibby WA. Volumetric analysis of central body fat accurately predicts incidence of diabetes and hypertension in adults. BMC Obes. 2015;2:10.

[300] Zhou MC, Min R, Ji JJ, Zhang S, Tong AL, Xu Jp, et al. Analysis of association among clinical features and shorter leukocyte telomere length in mitochondrial diabetes with m.3243A>G mitochondrial DNA mutation. BMC Med Genet. 2015;16(1):92.

[301] Loo JH, Trejaut JA, Yen JC, Chen ZS, Ng WM, Huang CY, et al. Mitochondrial DNA association study of type 2 diabetes with or without ischemic stroke in Taiwan. BMC Res Notes. 2014;7:223.

[302] Scharfe C, Lu HHS, Neuenburg JK, Allen EA, Li GC, Klopstock T, et al. Mapping Gene Associations in Human Mitochondria using Clinical Disease Phenotypes. PLoS Comput Biol. 2009;5(4).

[303] Yang J, Wang C, Cao G, Yang W, Yu S, Zhai H, et al. Long-term effects of laparoscopic sleeve gastrectomy versus roux-en-Y gastric bypass for the treatment of Chinese type 2 diabetes mellitus patients with body mass index 28-35 kg/m(2). BMC Surg. 2015 jul;15:88.

[304] Våge V, Sande VA, Mellgren G, Laukeland C, Behme J, Andersen JR. Changes in obesity-related diseases and biochemical variables after laparoscopic sleeve gastrectomy: a two-year follow-up study. BMC Surg. 2014 dec;14(1):8.

[305] Kyrou I, Weickert MO, Gharanei S, Randeva HS, Tan BK. Fibroblast growth factors: new insights, new targets in the management of diabetes. Minerva Endocrinol. 2016;.

[306] Ryan KK, Tremaroli V, Clemmensen C, Kovatcheva-Datchary P, Myronovych A, Karns R, et al. FXR is a molecular target for the effects of vertical sleeve gastrectomy. Nature. 2014 mar;509(7499):183–188.

[307] Fu L, John LM, Adams SH, Yu XX, Tomlinson E, Renz M, et al. Fibroblast growth factor 19 increases metabolic rate and reverses dietary and leptin-deficient diabetes. Endocrinology. 2004;145(6):2594–2603.

[308] Sachdev S, Wang Q, Billington C, Connett J, Ahmed L, Inabnet W, et al. FGF 19 and Bile Acids Increase Following Roux-en-Y Gastric Bypass but Not After Medical Management in Patients with Type 2 Diabetes. Obes Surg. 2016;26(5):957–965.

[309] Gerhard GS, Styer AM, Wood GC, Roesch SL, Petrick AT, Gabrielsen J, et al. A role for fibroblast growth factor 19 and bile acids in diabetes remission after Roux-en-y gastric bypass. Diabetes Care. 2013;36(7):1859–1864.

[310] Jansen PLM, van Werven J, Aarts E, Berends F, Janssen I, Stoker J, et al. Alterations of hormonally active fibroblast growth factors after Roux-en-Y gastric bypass surgery. Dig Dis. 2011;29(1):48–51.

[311] Morton GJ, Matsen ME, Bracy DP, Meek TH, Nguyen HT, Stefanovski D, et al. FGF19 action in the brain induces insulin-independent glucose lowering. J Clin Invest. 2013 nov;123(11):4799–4808.

[312] Tomlinson E, Fu L, John L, Hultgren B, Huang X, Renz M, et al. Transgenic mice expressing human fibroblast growth factor-19 display increased metabolic rate and decreased adiposity. Endocrinology. 2002;143(5):1741–1747.

[313] Lee YJ, Jeong SY, Mariusz K, Smith CL, Youle RJ. Roles of the Mammalian Mitochondrial Fission and Fusion Mediator Fis1, Drp1, and Opa1 and Apoptosis. Mol Biol Cell. 2004;15(1):5001–5011.

[314] Frank S, Gaume B, Bergmann-Leitner ES, Leitner WW, Robert EG, Catez F, et al. The Role of Dynamin-Related Protein 1, a Mediator of Mitochondrial Fission, in Apoptosis. Dev Cell. 2001;1(4):515–525.

[315] Bach D, Pich S, Soriano FX, Vega N, Baumgartner B, Oriola J, et al. Mitofusin-2 determines mitochondrial network architecture and mitochondrial metabolism: A novel regulatory mechanism altered in obesity. J Biol Chem. 2003;278(19):17190–17197.

[316] Vila M, Ruíz O, Belmonte M, Riesco M, Barceló A, Perez G, et al. Changes in lipid profile and insulin resistance in obese patients after Scopinaro biliopancreatic diversion. Obes Surg. 2009;19(3):299–306.

[317] Fang S, Suh JM, Reilly SM, Yu E, Osborn O, Lackey D, et al. Intestinal FXR agonism promotes adipose tissue browning and reduces obesity and insulin resistance. Nat Med. 2015;21(August 2014):159–65.

[318] Wu X, Ge H, Lemon B, Weiszmann J, Gupte J, Hawkins N, et al. Selective activation of FGFR4 by an FGF19 variant does not improve glucose metabolism in ob/ob mice. Proc Natl Acad Sci U S A. 2009;106(34):14379–84.

[319] Reiche M, Bachmann A, Lossner U, Bluher M, Stumvoll M, Fasshauer M. Fibroblast growth factor 19 serum levels: relation to renal function and metabolic parameters. Horm Metab Res. 2010;42(3):178–181.

[320] Mráz M, Lacinová Z, Kaválková P, Haluzíková D, Trachta P, Drápalová J, et al. Serum concentrations of fibroblast growth factor 19 in patients with obesity and type 2 diabetes mellitus: The influence of acute hyperinsulinemia, very-low calorie diet and PPAR-gamma agonist treatment. Physiol Res. 2011;60(4):627–636.

[321] Wiesner P, Choi SH, Almazan F, Benner C, Huang W, Diehl CJ, et al. Low doses of lipopolysaccharide and minimally oxidized low-density lipoprotein cooperatively activate macrophages via nuclear factor kappa B and activator protein-1: possible mechanism for acceleration of atherosclerosis by subclinical endotoxemia. Circ Res. 2010 jul;107(1):56–65.

[322] Tuomi K, Logomarsino JV. Bacterial Lipopolysaccharide, Lipopolysaccharide-Binding Protein, and Other Inflammatory Markers in Obesity and After Bariatric Surgery. Metab Syndr Relat Disord. 2016 aug;14(6):279–288.

[323] Erridge C, Attina T, Spickett C, Webb DJ. A high-fat meal induces low-grade endotoxemia: evidence of a novel mechanism of postprandial inflammation. Am J Clin Nutr. 2007;86(5):1286–1292.

[324] Hildebrandt MA, Hoffmann C, Sherrill-Mix SA, Keilbaugh SA, Hamady M, Chen YY, et al. High-Fat Diet Determines the Composition of the Murine Gut Microbiome Independently of Obesity. Gastroenterology. 2009 nov;137(5):1716–1724.e2.

[325] Hrncir T, Stepankova R, Kozakova H, Hudcovic T, Tlaskalova-Hogenova H. Gut microbiota and lipopolysaccharide content of the diet influence development of regulatory T cells: studies in germ-free mice. BMC Immunol. 2008;9(1):65.

[326] Licht TR, Hansen M, Poulsen M, Dragsted LO. Dietary carbohydrate source influences molecular fingerprints of the rat faecal microbiota. BMC Microbiol. 2006;6(1471-2180 (Electronic)):98.

[327] Moreira APB, Texeira TFS, Ferreira AB, do Carmo Gouveia Peluzio M, de Cássia Gonçalves Alfenas R. Influence of a high-fat diet on gut microbiota, intestinal permeability and metabolic endotoxaemia. Br J Nutr. 2012 sep;108(05):801–809.

[328] Mehta NN, McGillicuddy FC, Anderson PD, Hinkle CC, Shah R, Pruscino L, et al. Experimental Endotoxemia Induces Adipose Inflammation and Insulin Resistance in Humans. Diabetes. 2010 jan;59(1):172–181.

[329] Walker JM. Mitochondrial Disorders. vol. 837; 2012. Available from: http://link.springer.com/10.1007/978-1-61779-504-6.

[330] Guariguata L, Whiting DR, Hambleton I, Beagley J, Linnenkamp U, Shaw JE. Global estimates of diabetes prevalence for 2013 and projections for 2035. Diabetes Res Clin Pract. 2014 feb;103(2):137–149.

[331] Maassen JA, 't Hart LM, van Essen E, Heine RJ, Nijpels G, Jahangir Tafrechi RS, et al. Mitochondrial Diabetes: Molecular Mechanisms and Clinical Presentation. Diabetes. 2004 feb;53(Supplement 1):S103–S109.

[332] van den Ouweland JMW, Lemkes HHPJ, Ruitenbeek W, Sandkuijl LA, de Vijlder MF, Struyvenberg PAA, et al. Mutation in mitochondrial tRNALeu(UUR) gene in a large pedigree with maternally transmitted type II diabetes mellitus and deafness. Nat Genet. 1992 aug;1(5):368–371.

[333] Vidal-Puig AJ, Hart LMt, van Essen E, Heine RJ, Nijpels G, Tafrechi RSJ, et al. Uncoupling expectations. Nat Genet. 2000 dec;26(4):387–8.

[334] Sorriento D, Pascale AV, Finelli R, Carillo AL, Annunziata R, Trimarco B, et al. Targeting mitochondria as therapeutic strategy for metabolic disorders. Sci World J. 2014;2014.

[335] West AP, Shadel GS, Ghosh S. Mitochondria in innate immune responses. Nat Rev Immunol. 2011;11(6):389–402.

[336] Dawson ME. Interference with the LAL test and How to Address It. LAL Update. 2005;22(3):1–6.

[337] Williams KL. Endotoxins : pyrogens, LAL testing and depyrogenation. Informa Healthcare; 2007.

[338] Trøseid M, Nestvold TK, Rudi K, Thoresen H, Nielsen EW, Lappegård KT. Plasma Lipopolysaccharide Is Closely Associated With Glycemic Control and Abdominal Obesity. Diabetes Care. 2013 July;36(11).

[339] Clemente-Postigo M, Roca-Rodriguez MDM, Camargo A, Oca??a-Wilhelmi L, Cardona F, Tinahones FJ. Lipopolysaccharide and lipopolysaccharide-binding protein levels and their relationship to early metabolic improvement after bariatric surgery. Surg Obes Relat Dis. 2015;11(4):933–939.

[340] Guerville M, Boudry G. Gastro-intestinal and hepatic mechanisms limiting the entry and dissemination of lipopolysaccharide into the systemic circulation. Am J Physiol - Gastrointest Liver Physiol. 2016;311(1):ajpgi.00098.2016.

[341] Tomita M, Ohkubo R, Hayashi M. Lipopolysaccharide transport system across colonic epithelial cells in normal and infective rat. Drug Metab Pharmacokinet. 2004;19(1):33–40.

[342] Maloney E, Sweet IR, Hockenbery DM, Pham M, Rizzo NO, Tateya S, et al. Activation of NF- B by Palmitate in Endothelial Cells: A Key Role for NADPH Oxidase-Derived Superoxide in Response to TLR4 Activation. Arterioscler Thromb Vasc Biol. 2009 sep;29(9):1370–1375.

[343] Shoelson SE, Lee J, Yuan M. Inflammation and the IKKβ/IκB/NF-κB axis in obesity- and diet-induced insulin resistance. Int J Obes. 2003;27(S3):S49–S52.

[344] Howard JK, Cave BJ, Oksanen LJ, Tzameli I, Bjørbæk C, Flier JS. Enhanced leptin sensitivity and attenuation of diet-induced obesity in mice with haploinsufficiency of Socs3. Nat Med. 2004;10(7):734–738.

[345] Cai D, Yuan M, Frantz DF, Melendez PA, Hansen L, Lee J, et al. Local and systemic insulin resistance resulting from hepatic activation of IKK-beta and NF-kappaB. Nat Med. 2005;11(2):183–90.

[346] Hirosumi J, Tuncman G, Chang L, Gorgun CZ, Uysal KT, Maeda K, et al. A central role for JNK in obesity and insulin resistance. Nature. 2002;420(6913):333–336.

[347] Kim JK, Kim YJ, Fillmore JJ, Chen Y, Moore I, Lee J, et al. Prevention of fat-induced insulin resistance by salicylate. J Clin Invest. 2001;108(3):437–446.

[348] Yuan M, Konstantopoulos N, Lee J, Hansen L, Li ZW, Karin M, et al. Reversal of obesity- and diet-induced insulin resistance with salicylates or targeted disruption of Ikkbeta. Science. 2001;293(5535):1673–7.

[349] Harper ME, Bevilacqua L, Hagopian K, Weindruch R, Ramsey JJ. Ageing, oxidative stress, and mitochondrial uncoupling. Acta Physiol Scand. 2004;182(4):321–31.

[350] Park CB, Larsson NG. Mitochondrial DNA mutations in disease and aging. J Cell Biol. 2011;193(5):809–818.

[351] Wallace DC. A mitochondrial paradigm for degenerative diseases and ageing. Novartis Found Symp. 2001;235:247–63; discussion 263–6.

[352] He M, Rutledge SL, Kelly DR, Palmer CA, Murdoch G, Majumder N, et al. A new genetic disorder in mitochondrial fatty acid beta-oxidation: ACAD9 deficiency. Am J Hum Genet. 2007;81(1):87–103.

[353] Muller YL, Bogardus C, Pedersen O, Baier L. A Gly482Ser missense mutation in the peroxisome proliferator-activated receptor ?? coactivator-1 is associated with altered lipid oxidation and early insulin secretion in Pima Indians. Diabetes. 2003;52(3):895–898.

[354] Petersen KF, Befroy D, Dufour S, Dziura J, Ariyan C, Rothman DL, et al. Mitochondrial Dysfunction in the Elderly: Possible Role in Insulin Resistance. Science (80-). 2003;300(5622):1140–1142. Available from: http://www.sciencemag.org/content/300/5622/1140.abstract.

[355] Gracia JA, Martínez M, Elia M, Aguilella V, Royo P, Jiménez A, et al. Obesity surgery results depending on technique performed: Long-term outcome. Obes Surg. 2009;19(4):432–438.

[356] Sjöström CD, Lissner L, Wedel H, Sjöström L. Reduction in incidence of diabetes, hypertension and lipid disturbances after intentional weight loss induced by bariatric surgery: the SOS Intervention Study. Obes Res. 1999 sep;7(5):477–84.

[357] Thompson CC, Slattery J, Bundga ME, Lautz DB. Peroral endoscopic reduction of dilated gastrojejunal anastomosis after Roux-en-Y gastric bypass: A possible new option for patients with weight regain. Surg Endosc Other Interv Tech. 2006;20(11):1744–1748.

[358] Faria SL, De Oliveira Kelly E, Lins RD, Faria OP. Nutritional management of weight regain after bariatric surgery. Obes Surg. 2010;20(2):135–139.

[359] Kofman MD, Lent MR, Swencionis C. Maladaptive eating patterns, quality of life, and weight outcomes following gastric bypass: results of an Internet survey. Obesity (Silver Spring). 2010 oct;18(10):1938–43.

[360] Kinzl JF, Schrattenecker M, Traweger C, Mattesich M, Fiala M, Biebl W. Psychosocial predictors of weight loss after bariatric surgery. Obes Surg. 2006;16(12):1609–1614.

[361] Magro DO, Geloneze B, Delfini R, Pareja BC, Callejas F, Pareja JC. Long-term weight regain after gastric bypass: A 5-year prospective study. Obes Surg. 2008;18(6):648–651.

[362] Saunders R. "Grazing": A High-Risk Behavior. Obes Surg. 2004;14(1):98–102.

[363] Colles SL, Dixon JB, O'Brien PE. Grazing and Loss of Control Related to Eating: Two High-risk Factors Following Bariatric Surgery. Obesity. 2008;16(3):615–622.

[364] Saboor Aftab SA, Halder L, Piya MK, Reddy N, Fraser I, Menon V, et al. Predictors of weight loss at 1 year after laparoscopic adjustable gastric banding and the role of presurgical quality of life. Obes Surg. 2014;24(6):885–890.

[365] by the Comptroller R, General A. NHS waiting times for elective care in England. https://www.nao.org.uk/report/nhs-waiting-times-elective-care-england-2/; 2014.

[366] Digital N. Health Survey for England 2015; 2016. Available from: http://www.content.digital.nhs.uk/catalogue/PUB22610.

[367] Public Health England. National Mapping of Weight Management Services. 2015521. PHE publications; 2015. Available from: https://www.gov.uk/government/publications/weight-management-services-national-mapping [cited 25 May 2017].

[368] Murphy KG, Bloom SR. Gut hormones and the regulation of energy homeostasis. Nature. 2006;444(7121):854–859.

[369] Harrold JA, Dovey TM, Blundell JE, Halford JCG. CNS regulation of appetite. Neuropharmacology. 2012;63(1):3–17.

[370] Delamater. Handbook of social psychology. J Appl Psychol. 2006;39(5):384–385.